GEOPHYSICAL
PROSPECTING FOR OIL

GEOPHYSICAL
PROSPECTING FOR OIL

GEOPHYSICAL
PROSPECTING FOR OIL

BY

L. L. NETTLETON

Geophysicist, Gulf Research and Development Company,
Pittsburgh, Pa., Advisory Professor of Physics.
University of Pittsburgh

FIRST EDITION
SIXTH IMPRESSION

McGRAW-HILL BOOK COMPANY, INC.
NEW YORK AND LONDON
1940

PREFACE

Within the last twelve years there has grown up a voluminous periodical literature on geophysics as applied to prospecting for oil. However, no single source gives a connected presentation of the principles and practice of modern oil prospecting by geophysical methods. It is primarily to supply such a source that this work has been attempted.

The present work is intended for the student or lay reader rather than the geophysical specialist. Therefore, the fundamentals and basic ideas of most of the material included are available in the periodical or other geophysical literature of the present time or are quite generally known to practicing exploration geophysicists. The selection and emphasis of subject matter have been governed by practical aspects based on the writer's experience and active participation in the application of geophysical methods to prospecting for oil through most of the period of their active development. The work will have fulfilled its purpose if the general reader or student finds a presentation of the modern methods used in prospecting for oil that will enable him to understand the basis of geophysical maps and results and to judge their meaning and the reliance (or lack of it) that may be placed upon them. Also, it is believed that the material will serve as a convenient and useful reference work for professional geophysicists. Furthermore, it is hoped that it may introduce a certain degree of uniformity in notation and nomenclature which has been lacking in the periodical literature.

The book is the outgrowth of a course of lectures given for several years at the University of Pittsburgh, chiefly for students in petroleum geology and petroleum engineering. It is thus designed for those with a geological rather than a physical background. However, physical fundamentals of geophysical prospecting have been emphasized throughout. Mathematics has not been avoided or suppressed, but an attempt has been made to supplement the equations with written explanations to help clarify their meaning.

The work would hardly have been possible without the material help that has been generously given by many members of the staff of the Geophysical Section of the Gulf Research Laboratory. Various parts of the manuscript have been read by individuals particularly familiar with the subject matter. It is a pleasure to acknowledge the help thus given by James Affleck, Thomas Bardeen, Milton Dobrin, C. H. Dresbach, L. W. Gardner, S. Hammer, G. B. Lamb, M. Muskat, B. Perkins, Jr., O. F. Ritzmann, W. B. Robinson, C. A. Swartz, V. V. Vacquier, and R. D. Wyckoff. Special acknowledgment is due to T. A. Elkins, who read most of the manuscript and provided part of the bibliography, to W. L. Dowler, who made all the drawings, and to Elmina Lewis for all the stenographic work. Finally, I wish to express my appreciation to Dr. Paul D. Foote, director of the Gulf Research Laboratory, for his interest and for the stenographic and other facilities provided by the laboratory and to him and Dr. E. A. Eckhardt for permission to undertake this work.

<div align="right">L. L. Nettleton.</div>

Gulf Research and Development Company,
   Pittsburgh, Pa.,
     July, 1940.

CONTENTS

PART II. MAGNETIC METHOD

CHAPTER VIII

CHAPTER IX

CHAPTER X

PART III. SEISMIC METHODS

PART IV. ELECTRICAL AND MISCELLANEOUS
METHODS AND MEASUREMENTS IN DRILL HOLES

PART V. GEOPHYSICAL INTERPRETATION

GEOPHYSICAL PROSPECTING FOR OIL

INTRODUCTION

In its struggle to keep up with the ever increasing demand for its products, the oil industry is putting forth great efforts and enormous sums of money in finding new oil reserves. The present rate of consumption of crude oil would exhaust the present known and proven reserves in the United States in ten to fifteen years.[1] To insure its operation in the not very distant future, the American oil industry must find new oil supplies fast enough to keep up with the billion barrels per year that are used up.

Within the last fifteen years, the various methods of geophysical prospecting have come to be an increasingly important part of the exploration branch of all the large and many of the smaller American oil companies. The intensive search for new oil reserves has, to a large extent, tested those prospects which are evident from the surface. In recent years the search has been carried into areas where underground oil prospects have no visible surface expressions whatever. Their detection depends on artificial means for peering below the surface to see what the nature and attitude of the rocks may be. The various forms of geophysical prospecting are the tools for such seeing. Our vision is imperfect at best and often is extremely hazy, so that different means may be called in to try to see the same picture. Also,

[1] Alexander Deussen, Discoveries, *Geophysics*, vol. 3, No. 3, p. 177, July, 1938.

A Special Committee of the American Petroleum Institute, Petroleum Production and Supply, *Bull. Am. Assoc. Petroleum Geologists*, vol. 20, pp. 1–14, 1936.

L. C. Snider and B. T. Brooks, Probable Petroleum Shortage in the United States and Methods for Its Alleviation, *Bull. Am. Assoc. Petroleum Geologists*, vol. 20, pp. 15–50, 1936.

the oil itself, which is our real objective, is still quite invisible. However, a very little light is extremely useful to one otherwise completely blind. Geophysical prospecting has proven valuable in the search for oil and is almost certain to be relied upon more and more to find the oil that will run the automobiles and airplanes beyond 1950.

Geophysical prospecting does not find oil. It searches for the geological conditions that are commonly associated with the accumulation of oil. So far, geophysical science has not found a method of measuring or detecting at a distance any property of oil, as such, that will indicate its presence directly, under great thicknesses of intervening rock.[1]

THE ACCUMULATION OF OIL

Geologists have known since comparatively early in the history of the oil industry that the accumulation of oil occurs under certain rather restricted underground conditions. An oil "pool" is not an open underground lake but is a porous rock, more or less saturated with oil. Hence a "reservoir rock"—usually a porous sandstone or limestone—is required. Oil will not accumulate unless there is a place for it to come from. Hence, there must be "source rocks"—usually shale beds containing organic matter. Oil would not be held in a particular place unless there were something to prevent its further migration from that place. Hence there must be an impervious "cap rock" above the reservoir rock.

The oil indigenous to the source rocks is not sufficiently concentrated to make an oil pool. The required accumulation necessitates migration of oil through porous rocks and some irregularity of the rocks which will arrest the migration in a comparatively local area.

The spaces between the grains of porous rocks are practically never void but are filled with fluid which may be oil, gas, or water, either separate or mixed. As the fluids migrate through the porous rocks, the lighter ones tend to rise through and float on the heavier ones. If a trap of some kind exists within which the migrating fluids accumulate, they will tend to separate

---

[1] A development that may prove an exception to this statement has been tried in the field very recently;

according to their relative densities, the lightest (gas) at the top, the oil next, and the heaviest (water) below.[1]

Traps that cause the local accumulation of oil are the result of a variety of geologic processes and rock deformations (Fig. 1).

(a)

(b)

(c)
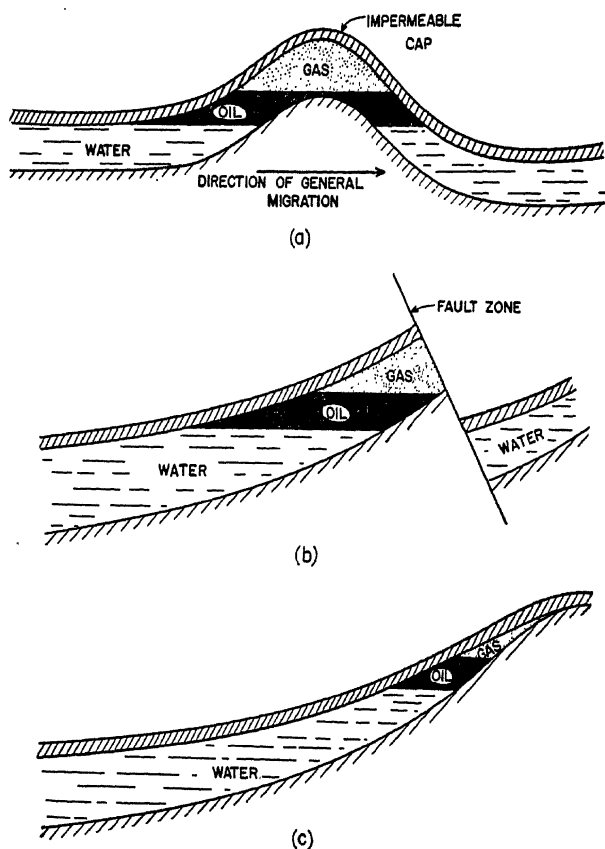
Fig. 1.—Different ways in which structure may control oil accumulation. (*After Muskat.*)

Such deformations are usually called "structures." To serve as a trap it is generally considered necessary that the structure be "closed." This means that a contour on the cap rock or its

---

[1] For a brief discussion of the fundamentals of the origin and accumulation of oil and gas, see M. Muskat, "The Flow of Homogeneous Fluids through Porous Media," McGraw-Hill Book Company, Inc., (New York,) pp. 43–54, 1937.

equivalent is closed about a point from which the dip is downward in all directions. A simple structural dome may be considered as an upside-down bowl under which oil and gas accumulate over water, much as gas is collected over water with an inverted beaker in some simple chemical experiments.

When the requirements of source rock, reservoir rock, and cap rock are present in a general region, the area underlain by any suitable trap or closed structure may have a fair to high probability of being a potential oil field. Where the geologic movement that causes a trap is of such a nature or occurred at such a geologic time that the rocks at the surface are affected, the presence of underground conditions favorable for the accumulation of oil may be inferred from a study of the nature and attitude of the surface rocks, *i.e.*, by surface geologic mapping. However, in many cases, geologic deposits have been laid down subsequent to the geologic movement that caused the structure so that there is absolutely no visible surface evidence of its presence. The problem and the *raison d'être* of geophysical prospecting are the finding of such buried structures.

There are many kinds of geologic disturbances or conditions that may form closed structures which are possible traps for the accumulation of oil. The means by which buried structures may be detected and the relative difficulty of their detection depend on the nature of the geologic disturbances forming the traps and the physical properties of the rocks involved. Also, the depth of the buried structure below the surface is always an important consideration.

GEOPHYSICAL METHODS OF PROSPECTING

Any conceivable property or process that could be measured or carried out at the surface and that would be affected by the nature or attitude of rocks (or by oil itself) through a cover of hundreds to many thousands of feet of intervening rocks might be made the basis of a method of geophysical prospecting. Many principles have been suggested and tried (including some that are purely psychic[1]), but practically all the geophysical search for oil depends on a very few basic physical principles. A brief outline of these principles follows:

[1] L. W. Blau, Black Magic in Geophysical Prospecting, *Geophysics*, vol. 1, No. 1, p. 1, January, 1936.

Gravitational Methods.—All gravitational methods are based on the measurement at the surface of small variations in the gravitational field. Small differences or distortions in the gravitational field from point to point over the surface of the earth are caused by any lateral variation in the distribution of mass in the earth's crust. Therefore, if geologic movements involve rocks of differing density, the resulting irregularity in mass distribution will make a corresponding variation in the intensity of gravity and in the space rate of change of gravity at the surface. Sensitive instruments are used to measure either the relative value of gravity or its space derivatives. The measured variation in gravity is interpreted in terms of probable mass distributions below the surface, which in turn are the basis for inferences as to probable geologic conditions and the presence or absence of traps favorable for the accumulation of oil.

Magnetic Methods.—Magnetic methods are based on the measurements at the surface of small variations in the magnetic field. The magnetic field is affected by any variation in the distribution of magnetized (or polarized) rocks. Most sedimentary rocks are nearly nonmagnetic, but the underlying igneous or basement rocks are slightly magnetic. Therefore, if geologic movement involves these magnetic rocks, the resulting irregularities will cause corresponding variations in the intensity of the magnetic field at the surface. A sensitive magnetometer is used to measure the relative values of magnetic intensity (usually the vertical component only). The measured variation is interpreted in terms of the probable distribution of magnetic material below the surface, which in turn is the basis for inferences as to the probable geologic conditions and the presence or absence of structure favorable for the accumulation of oil.

Seismic Methods.—Seismic methods are based on the measurement of travel times of artificial elastic waves. Such waves, set up by explosives at or near the surface, travel in all directions from the source or shot point. Waves having paths in certain directions are refracted or reflected so that they come back to the surface. Sensitive seismic detectors, set on the surface at various distances from the shot point and connected to an oscillograph, record the ground movement on a photographic tape on which the instant of explosion also is shown. By measurements on this tape, the travel times from shot point to

detector are determined. These travel times depend on the nature of the rocks penetrated and the corresponding speed of wave travel and on the existence of discontinuities in velocity or density which determine points of reflection or refraction below the surface. In many cases, such seismic records show reflected waves which give very definite information as to the depth to certain discontinuities in the lithologic character of the rock series. Under favorable conditions a certain geologic bed may be mapped very accurately by reflected seismic waves even though it may be many thousands of feet deep. In another application of the seismic method the depths of different beds and their characteristic wave speeds may be determined by the travel times of waves that have been refracted through those beds. Under favorable conditions, seismic methods may give information that can be interpreted quite simply and directly in terms of geologic conditions. Under less favorable conditions the detection of reflected or refracted waves or their interpretation in terms of definite geologic conditions may be uncertain and leave many unanswered questions.

Electrical Methods and Measurements in Wells.—A variety of electrical methods depends on making electrical or electromagnetic measurements, at the surface, of the effects of artificial or natural currents in the earth. Such measurements are affected by the electrical conductivity of the earth at a depth that depends on the lateral spread of the conductors or electrodes by which the currents are set up. Changes with depth in electrical quantities so measured are interpreted in terms of the depth to lithologic discontinuities which affect the electrical characteristics of the rocks. Several electrical methods have been developed and used extensively in the search for minerals at comparatively shallow depths. However, they are little used by the oil industry in the search for geologic structure on account of their lack of penetration to sufficient depth.

The application of the electrical methods to measurements in wells is of great interest and importance to the oil industry. Measurements are made at the surface of the current and potential to a set of electrodes lowered into the well. Such measurements serve to detect the presence and vertical position of oil and gas with considerable certainty and precision and also are used for correlations of strata. Other measurements essentially

electrical in character, are made in wells and give information on temperature, source of fluids, etc., which may answer important questions in regard to the processes taking place far below the surface.

The different methods may serve quite different purposes in a general geophysical campaign for the exploration of a large area. For instance, a general preliminary, or reconnaissance, survey of a large area may be made by gravity or magnetic methods. The interesting indications from such a survey then can be tested by the much more expensive, but often more certain, seismic method. In this way the more expensive method is concentrated on the areas that have higher probabilities of yielding favorable structural possibilities.

COST OF GEOPHYSICAL SURVEYS

The cost of geophysical surveys varies enormously, depending on the method used, the detail with which an area is covered, and the physical difficulties of transportation. It is impossible to give even a rough estimate of cost per unit area because of its enormous range under different circumstances. The ratio of cost per square mile between, say, a reconnaissance gravity survey in an area of easy transportation and a detailed seismograph survey in a difficult marsh might easily be 1 to 1,000.

In terms of cost per party month, a magnetic party is cheapest, costing $1,000 or more per month; a gravity (gravimeter or torsion balance) party comes next, costing $2,000 to $4,000 per month; and a seismic party is most expensive, costing $7,000 to $15,000 per month. However, a gravity party might cover several hundred square miles per month, and a seismograph party might work for a month on only a few or, in extreme cases, on only 1 sq. mile—hence the enormous range in cost per unit area covered.

In general, rapid reconnaissance exploration is cheap but gives only general and often indefinite information. Detailed and definite information is expensive. In well-planned exploration work, the results, in terms of amount and certainty of the subsurface information obtained, are more or less proportional to the cost.

PART I
GRAVITATIONAL METHODS

CHAPTER I

FUNDAMENTAL PRINCIPLES AND UNITS

GRAVITATIONAL ACCELERATION

The law of universal gravitation was conceived by Newton from a study of Kepler's empirical laws of the motion of the planets. To explain these motions, Newton deduced the law that every particle of matter exerts a force of attraction on every other particle that is proportional to the masses and inversely proportional to the square of the distance between them; *i.e.*,

$$F = \gamma \frac{m_1 m_2}{r^2} \tag{1}$$

where F is the force between two particles of mass m_1 and m_2, r is the distance between them, and γ is a constant with dimensions $L^3 M^{-1} T^{-2}$ and a numerical value depending on the units used.

We all know that a body on the earth has weight. The weight of a body is the force acting on it due to the gravitational attraction of the earth. If we consider the body as one of the masses, say m_1, in Eq. (1) the force (weight) is the attraction on this body of another body (m_2) which is the whole earth (which we may consider as concentrated at its center) at a distance r, the radius of the earth.

The force acting on the body m_1 also may be considered as defined by Newton's second law of motion; *i.e.*, $F = m_1 a$, where a is the acceleration that would be caused by the gravitational attraction of the earth if the body were allowed to fall. Thus the force on the body m_1 is exactly the same as if it were being accelerated at a rate

$$a = \frac{F}{m_1} = \gamma \frac{m_2}{r^2} \tag{2}$$

Thus the attraction of the earth may be considered as a force per unit mass and therefore as exactly equivalent to an acceleration. Therefore, we often speak of the "acceleration" of gravity

rather than the "force" of gravity, and the concept of acceleration rather than force will be used throughout this book.

Without reference to the earth we may consider that the gravitational field at a point O (Fig. 2) which is associated with any elemental particle of matter of mass dm at point P is equivalent to an acceleration of magnitude.

$$a = \gamma \frac{dm}{r^2}$$

directed toward the elemental particle dm.

The component of this acceleration in any other direction Z, making an angle φ with the line $\overline{OP}$, is

FIG. 2.—Gravitational attraction.
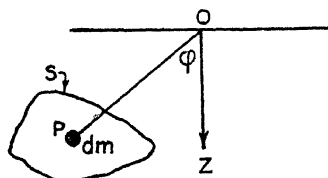
$$a_z = \gamma \frac{dm}{r^2} \cos \varphi \qquad (3)$$

Finally, the component of acceleration at O in the direction Z due to a continuous body S is the sum of the effects of all particles dm within the body, or is

$$(a_z)_s = \gamma \int_S \frac{dm}{r^2} \cos \varphi \qquad (4)$$

where the integration is carried out over the body S.

THE GRAVITATIONAL CONSTANT

The constant γ of the foregoing section is one of the fundamental constants of nature. It cannot be determined from astronomical observational data such as led Newton to the general law expressed by Eq. (1). However, if all the quantities in Eq. (1) except γ can be measured experimentally, the value of γ then can be calculated.

The earliest workers in this field were interested primarily in Δ, the density of the earth, rather than the gravitational constant γ. However, the two quantities are closely related so that the determination of one evaluates the other. This may be shown as follows:

If we assume the earth to be a sphere of mass M and radius R, the gravitational acceleration g at its surface [from Eq. (2)] is

$$g = \frac{\gamma M}{R^2} = \frac{\gamma}{R^2}\left(\frac{4}{3}\pi R^3 \Delta\right) = \frac{4\pi R}{3}(\gamma \Delta) \qquad (5)$$

$$\gamma\Delta = \frac{3g}{4\pi R}^{1} \qquad (5a)$$

Thus, if g and R are known, the determination of γ and Δ are equivalent problems, as the measurement of either determines the other.

Probably the earliest attempt to evaluate Δ was made by Bouguer, a French geodesist, in about 1740. He attempted to measure the deviations of a plumb line produced by the gravitational attraction of a high mountain in Peru. This deviation is a measure of the relative attractions of the earth and the mountain. From an estimate of the shape and density of the mountain mass, the density of the earth could be computed. Bouguer's value was much too large because of the effect, unknown at that time, of isostatic compensation. Other experiments based on the same principle were made later in Great Britain and gave approximately correct values for the earth's density.
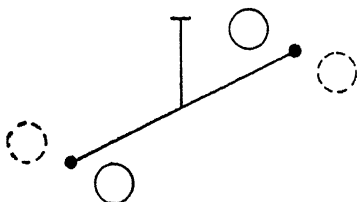
FIG. 3.—Principle of the Cavendish balance.

The earliest direct laboratory measurement of Δ was made by Cavendish in England in 1797 and 1798, using an apparatus suggested by Rev. John Mitchell. In principle, the commonly called "Cavendish experiment" consists of measuring the deflection of a horizontal beam, carrying two small weights, which is produced by the gravitational attraction of two larger weights. One method, shown in Fig. 3, consists of interchanging the positions of the large weights, as indicated by their dotted positions, and measuring the resulting rotation of the beam. From the torsion constant of the suspending fiber and the length of the beam (or the period of torsional vibration of the suspended system), the force of attraction between the masses is computed. Then, if the distances between the weights and their masses are

---

[1] Since only gravitational forces are considered, this expression applies to a nonrotating earth so that the value of g used must be the total value at the surface plus the normal outward component of centrifugal acceleration.

known, all the quantities in Eq. (2) except γ are measured, and it can be computed, and hence Δ can be determined by Eq. (5a).

Boys in 1889 made a careful determination of γ by a modified Cavendish balance.[1]   He used a balance with a very short beam and with the weights suspended at different heights so as to separate them enough to permit each of the large weights to act appreciably on only one of the smaller weights.

Probably the most accurate value of γ is that measured by Heyl,[2] using a modification of the Cavendish balance in which times of oscillation are measured.

Many other measurements of γ and Δ have been made by various modifications of the Cavendish torsion balance or by special applications of the ordinary balance.   The history of the principal measurements is summarized in the following table.

MEASUREMENTS OF γ OR Δ[1]

Name	Year	Method	γ $(10^{-8}$ c.g.s. units)	Δ (g./cc.³)
Cavendish...........	1797–1798	Torsion balance	6.754	5.448
Baily...............	1841–1842	Torsion balance	......	5.674
Reich..............	1837	Torsion balance	......	5.49
Reich..............	1849	Torsion balance	......	5.58
Cornu and Baille....	1870	Torsion balance	......	5.56
Boys...............	1895	Torsion balance	6.6576	5.5270
Braun..............	1896	Torsion balance	6.6579	5.5275
Wilsing............	1886	Metronome balance	6.596	5.579
Von Joly...........	1878–1881	Common balance	6.465	5.692
Eötvös.............	1896	Torsion balance	6.65	5.53
Richarz and Krigar-Menzel...........	1898	Common balance	6.684	5.505
Burgess.............	1899	Buoyant torsion balance	6.64	5.55
Poynting...........	....	Ordinary balance	6.6984	5.4934
Heyl[2].............	1930	Torsion balance	6.670	
Zahradnicek[3].......	1932	Resonance	6.659	

[1] Tabulated mostly from Poynting and Thompson, 1927, pp. 36–44, and Boys, 1923.
[2] Heyl, 1930.
[3] See Champion and Davy, 1937, pp. 38–41.

[1] See Champion and Davy, 1937, pp. 33–43.
[2] Heyl, 1930.

The value for γ in c.g.s. units is the attraction in dynes between two (spherical) masses of 1 g. each, when their centers are separated by a distance of 1 cm.

As a convenient and easily remembered close approximation, useful in connection with quantitative gravity calculations,

$$\gamma = \frac{200}{3} \cdot 10^{-9} \text{ c.g.s. unit}[1] \tag{6}$$

This value (*i.e.*, $\gamma = 66.67 \cdot 10^{-9}$) will be used for numerical calculations in this book.

UNIT OF ACCELERATION

In most textbooks on physics, no special name has been generally used for the unit of acceleration. However, the name "gal"[2] (after Galileo) is commonly used in the literature of geophysical prospecting. Thus:

$$1 \text{ gal} = 1 \text{ cm./sec./sec.}$$

Since the gal is a rather large unit in terms of the magnitudes usually of interest in geophysical prospecting, the milligal (abbreviated mg.) is more commonly used; *i.e.*,

$$1 \text{ mg.} = 1 \text{ milligal} = 0.001 \text{ gal} = 0.001 \text{ cm./sec./sec.} \tag{7}$$

Since the normal gravitational acceleration at the surface of the earth is about 980 gals, 1 mg. is approximately 1 part in a million of the normal gravity of the earth.

---

[1] The factor 10^{-9} rather than the more usual 10^{-8} is used here because the torsion balance quantities are also usually expressed in 10^{-9} c.g.s. unit, and the two factors conveniently cancel each other in many equations (see p. 82 below).

[2] Apparently the first use of the word "gal" was in German geophysical literature in about 1926. Since then it has been gradually accepted and is now used quite generally in German, American, and other geophysical literature.

CHAPTER II

GRAVITY OF THE EARTH

All gravity measurements necessarily are made in the gravitational field of the earth. Therefore, a knowledge of this field is required so that proper allowance for it may be made in reducing any kind of gravity measurement to a form useful for indicating geologic structure.[1]

VARIATION OF GRAVITY WITH LATITUDE

The earth is not a perfect sphere. To a rather close approximation, its shape is that of a *perfect* fluid for which a balance is maintained between the gravitational forces tending to make it spherical and the centrifugal forces of rotation tending to flatten it. As a result of this balance the equatorial radius is about 21 km. greater than the polar radius. Because of this flattening, the acceleration of gravity is distinctly less at the equator than at the poles for two reasons: (1) At the equator the surface is farther from the center of mass, making the attraction smaller, and (2) at the equator the centrifugal acceleration, which is outward and therefore opposite to the gravitational acceleration, is a maximum. The total difference in gravity between the equator and the poles is about 5 gals.

The exact shape of the earth has been a matter of great interest and scientific study since the time of Newton.[2] It can be derived from certain geodetic and astronomic measurements and also from a study of the variation of gravity over the surface, together with a knowledge of the radius of the earth.[3]

---

[1] A detailed account of the corrections mentioned in this section is given in Hubbert and Melton, 1928.

[2] For a very readable history of such studies see Lambert, 1936.

[3] This is shown by Clairaut's fundamental theorem, which may be written (to second-order approximation)

$$f = \tfrac{5}{2}C - \beta$$

where f is the flattening of the earth expressed in terms of the equatorial

The shape of the earth is expressed in terms of the dimensions of an ideal *spheroid* of reference. The dimensions usually given are the equatorial and polar radii a and b, respectively, or the equatorial radius together with the flattening; *i.e.*,

$$f = \frac{a - b}{a}$$

When the spheroid is determined from gravity measurements, a gravity formula giving the variation of gravity with latitude also is determined (by Clairaut's theorem, see note, page 16).

Gravity Formulas.—Several slightly different spheroids and corresponding gravity formulas have been determined from time to time as the amount and precision of gravity and geodetic information have increased. Those which are of greatest interest with regard to the reduction of gravity surveys are:

Helmert's[1] 1901 *Formula:*

$$g_0 = 978.030(1 + 0.005302 \sin^2 \varphi - 0.000007 \sin^2 2\varphi) \quad (8)$$

which corresponds to $a = 6,378,200$ meters, $b = 6,356,818$ meters, $1/f = 298.2$. This formula has been used extensively in connection with older gravity surveys and also for calculating the "normal gradient" for torsion balance surveys (see page 90 below).

---

radius a and the polar radius b as

$$f = \frac{a - b}{a}$$

C is the ratio of the centrifugal acceleration to the gravitational acceleration g_e at the equator; *i.e.*, $C = a\omega^2/g_e$ where ω is the angular velocity of rotation of the earth; β is the coefficient in the equation $g_0 = g_e(1 + \beta \sin^2 \varphi)$, in which g_0 is the gravity at latitude φ. β also can be expressed in terms of the gravity g_e at the equator and g_p at the poles as

$$\beta = \frac{g_p - g_e}{g_e}$$

The values of g_e and β are determined from an adjustment of gravity values determined at points widely distributed over the surface of the earth. From the values so determined and the equatorial radius, the flattening, which defines a spheroid giving the shape of the earth, can be calculated.

[1] Helmert, 1910, pp. 89-96.

The 1917 *U.S. Coast and Geodetic Survey Formula:*[1]

$$g_0 = 978.039(1 + 0.005294 \sin^2 \varphi - 0.000007 \sin^2 2\varphi) \quad (9)$$

The constants for this formula were based on the adjustment of 216 gravity values in the United States, 42 in Canada, 17 in Europe, and 73 in India. This formula has been used for the reduction of extensive gravity surveys made in the United States by the U.S. Coast and Geodetic Survey.

The corresponding value for $1/f$ is 297.4.

The 1930 *"International Formula":*[2]

$$g_0 = 978.049(1 + 0.0052884 \sin^2 \varphi - 0.0000059 \sin^2 2\varphi) \quad (10)$$

which corresponds to $a = 6{,}378{,}388$ meters, $b = 6{,}356{,}909$ meters, $1/f = 297.0$.

This formula has been adopted by an international geodetic commission and now is commonly used for the reduction of gravity measurements. A table of values of "normal" gravity, calculated[3] from this formula, is given in Appendix I (page 139).

The Normal Spheroid and the Geoid.—If the earth were a perfect fluid with no lateral variations in density, its surface would correspond to the ideal, or so-called normal, spheroid represented by the gravity formula. This would be a level surface, and the direction of gravity everywhere would be perpendicular to this surface. Actually, the earth is not uniform, and there are departures of the level surface from the normal, or reference, spheroid. The actual level surface may be considered as that of the oceans (if free from disturbing tidal and wind forces), and the oceans as extended across land areas by cutting imaginary deep canals down to sea level. The level surface so defined is the "geoid." An ordinary spirit level indicates a surface parallel to the geoid (and a plumb line gives a direction normal to the geoid). The actual level surface is deformed or warped by the irregularities in density within the earth and the topographic irregularities of its surface. Evidence for this warping of the geoid is given by small deviations of the plumb, or vertical, from the direction it should have if it were perpendicular to the normal spheroid. These deviations are

[1] Bowie, 1917, p. 134.
[2] Cassinis, Doré, and Vallarin, 1937.
[3] Lambert and Darling, 1931.

determined by certain geodetic and astronomic measurements. The plumb line tends to be deviated toward an area of excess mass, such as a continent (Fig. 4), and away from an area of deficiency of mass, such as an ocean. This deviation of the vertical causes a corresponding warping of the geoid upward over continental areas and downward over ocean areas. The deviations of the vertical are very small (seconds or fractions of seconds of arc), and the corresponding elevations and depressions of the geoid above and below the reference or normal spheroid are quite small. For instance, Hosmer[1] gives a map that shows the elevation of the geoid from the spheroid in the Rocky Mountains to be about 40 meters. In addition to such large-scale warping
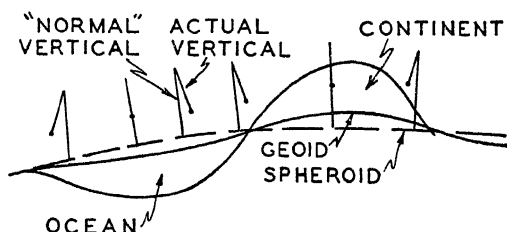
Fɪɢ. 4.—The normal spheroid, the geoid, and the deflection of the vertical.

and deformation of the geoid, or level surface, smaller deformations are produced by local irregularities of mass distribution and are of interest in connection with geophysical prospecting. They will be considered below in the discussion of the torsion balance (page 83).

The principal interest of the foregoing in connection with gravitational prospecting is the variation of gravity with latitude. This variation is so large that careful corrections must be made to remove this normal latitude effect before measured gravity or torsion balance quantities can be used for geophysical mapping. The manner of making these corrections is discussed later (pages 51 and 90 below).

VARIATION OF GRAVITY WITH ELEVATION (FREE-AIR EFFECT)

Gravity varies with elevation because a point at a higher elevation is farther away from the center of the earth and therefore has a lower gravitational acceleration than one at a lower

[1] Hosmer, 1930, p. 244.

elevation. The rate of this normal vertical variation, or the "vertical gradient," of gravity can be calculated quite accurately from the gravity formula and the radius of the earth. The value so calculated (by any of the gravity formulas) is

$$g_h = g_0 - 0.0003086h \tag{11}$$

where g_h is the value of gravity in gals at a height h in meters and g_0 is its value at a reference level, commonly sea level.

The variations of the vertical gradient with latitude (only 0.2 per cent from equator to pole) and with elevation (only 0.3 per cent from sea level to 10 km.) are too small to require attention in the reduction of any gravity measurements for geophysical prospecting. Therefore, we may consider the normal vertical gradient as constant[1] and with a value of

$$-0.3086 \text{ mg./meter} \qquad \text{or} \qquad -0.09406 \text{ mg./ft.} \tag{12}$$

If a proper correction for this elevation effect were not made, a gravity map would be strongly affected by differences in elevation between different points of measurement. Therefore, a correction for the elevation is always made before mapping gravity measurements made for gravitational prospecting.

The simple correction for elevations, using the constant given above, is called the "free-air" correction, because it is calculated as if the elevated point of measurement were suspended free in the air and without any regard for the effect of the attraction of the mass of matter between the elevation of the point of measurement and the reference elevation.

VARIATION OF GRAVITY WITH ATTRACTION OF SURFACE MATERIAL (BOUGUER EFFECT)

Suppose that two gravity stations are at different elevations, such as points A and B (Fig. 5), and we wish to calculate what

---

[1] Direct measurements of the vertical gradient of gravity were attempted in the past by very careful weighings with sensitive balances by means that permitted changing the vertical positions of the masses used. Practically all such measurements contained systematic errors which gave values lower than the theoretical value. A review of these measurements and a new series of experiments made by direct measurements of gravity at different elevations in high buildings were described recently by Hammer, 1938. His results indicate an actual variation in the vertical gradient of the order of ±1 per cent from the theoretical value. These variations are almost

their gravity difference would be if they were made at the same level (say the level of A). If we simply correct station B to the elevation of A by the free-air correction discussed above, we have taken no account of the attraction at B of the mass of material below B which would not be present if B were at the same level as A. The correction for the attraction of this material is commonly called the "Bouguer[1] correction."

If the topography is fairly flat, the attraction of material under the point B is given quite closely as that of an infinite

Fig. 5.—The Bouguer gravity effect.

slab of thickness h and density σ. The attraction of such a slab for $\gamma = 66.67 \times 10^{-9}$ is

$$\left.\begin{array}{l} 0.04185\sigma h \text{ (mg. per meter)} \\ \\ 0.01276\sigma h \text{ (mg. per ft.)} \end{array}\right\} \qquad (12a)$$

or

The Bouguer effect under station B tends to increase the gravity and therefore is always opposite to the free-air effect (which would decrease the gravity at B relative to that at the lower point A). Thus the free-air and Bouguer corrections are always opposite in sign.

In calculating corrections to gravity stations the free-air and Bouguer corrections commonly are combined into a single factor (which depends on the density σ of the surface rocks within the range of the topography). The combined elevation correction is made to sea level or some other reference level.

If the topography is irregular, the correction for the attraction of the material is much more complicated, and the attraction of

certainly caused by local irregularities of mass distribution in the earth's crust in the vicinity of the point of measurement.

[1] Bouguer was a French mathematician and geodesist. He made pendulum measurements in the high mountains of Peru in 1735 to 1743 and first made corrections for the effect that now bears his name in connection with the reduction of these measurements.

all excess masses (such as M, Fig. 5) above the plane of the station (or mass deficiencies from voids below the plane of the station) must be taken into account. Such corrections are usually called "terrain corrections." A more detailed discussion of them and of methods for their calculation is given below (page 144).

CHAPTER III

DIRECT GRAVITY-MEASURING INSTRUMENTS

Measurements of the magnitude of the earth's gravitational acceleration have been made since the time of Newton. The early measurements were accurate enough to show that gravity varies with latitude and with elevation. However, the demands of geophysical prospecting require that differences in gravity be measured to a precision several orders of magnitude higher than any of these early measurements. In fact, simple calculations show[1] that the gravity effects which may be expected from moderate geologic structure are of the order of a few milligals to as little as a few tenths of a milligal. Thus, to be effective as a means of geophysical prospecting, gravity differences must be measured to 1 part in a million or better, and a precision of 0.1 mg. is required for accurate measurement of small features.

Three quite different type instruments for gravity measurement are used in geophysical prospecting. Historically, the first gravity instrument used by the oil industry was the torsion balance which measures rates of change of gravity rather than gravity itself. It was first used in the United States late in 1922[2] and is still being utilized a little. The next was the pendulum. It had been used in Europe, America, and other countries in the scientific and geodetic investigations of gravity for two centuries, but the precision and speed of operation required for geophysical prospecting were first reached in about 1929. Its most extensive use was by the Gulf Oil Corporation, which made many thousand pendulum stations in 1930 to 1935. The most recent type of instrument is the static gravity meter, or gravimeter, which was first used for geophysical prospecting in the United States in about 1932. In the last three years several different types of gravimeter have been developed and have proved quite satisfactory. At the present time (1940) the

[1] See p. 105 below.
[2] Barton, 1929a, p. 475.

gravimeter has almost completely displaced the torsion balance and promises to be the most important type of gravity instrument in the future.

GRAVIMETERS

· In principle a gravimeter is simply an extremely sensitive weighing device. The weight or force of gravitational attraction on a constant mass will vary with any variation in the gravitational field so that, if means are provided for detecting small enough differences in weight, the corresponding differences in gravity can be measured.

Several different types of apparatus have been suggested and built for gravity exploration. However, the only ones so far that have been reasonably successfully employed in the field in geophysical prospecting are essentially a mass supported by a spring.

It may seem simple to hang a mass on a spring and measure the changes in weight produced by changes in gravity. However, let us consider the sensitivity requirements. To be useful in geophysical prospecting, it is necessary to detect differences in gravity at least as small as 1 mg. and preferably as small as 0.1 mg. or even a few hundredths of a milligal. To measure a gravity difference of 0.1 mg. means measuring 1 part in 10 million of total gravity. Suppose that we hang a mass on a spring and the spring is stretched about 1 ft., or 30 cm. This stretch results from the total force of gravity acting on the mass. A change in gravity of 1 part in 10 million will produce a change in length or movement of the weight of 30×10^{-7} cm. Now, one of the most sensitive methods of measuring small changes in length is an interferometer which will measure lengths of the order of one wave length of light which is about 5×10^{-5} cm. The changes in length in the spring that it is required to measure in a gravimeter are only about $\frac{1}{10}$ wave length of light and therefore are beyond the range of a simple interferometer.

TYPES OF GRAVIMETERS

On the basis of the means used for the measurement of these very small changes in the length of a spring, gravimeters may be divided into two types: (1) the stable type, which uses a system to give a high order of optical or mechanical magnification so that

the change in position of a weight or associated property, resulting from a change in gravity, is measured directly; or (2) the unstable type, which uses a moving system which approaches a point of instability so that small changes in gravity produce relatively large motions. Usually, stable type instruments give readings that vary linearly with gravity over a wide range, whereas unstable types have a more limited range or have a nonlinear calibration or are used as null instruments.

For a stable gravimeter, *i.e.*, one having a simple weight on a spring, the total elongation of the spring is

$$d = \frac{mg}{c}$$

where c is the spring constant, or force for unit elongation, and m is the suspended mass.

The period of the same system vibrating in simple harmonic motion is

$$T = 2\pi \sqrt{\frac{m}{c}}$$

From these two equations,

$$d = \frac{gT^2}{4\pi^2}$$

and the elongation Δd, due to a change in gravity Δg, is

$$\Delta d = \Delta g \, \frac{T^2}{4\pi^2}$$

Thus, for a simple or stable gravimeter, the sensitivity is proportional to the square of the period.

The same consideration can be applied to unstable type instruments. All such instruments contain an element that contributes a force in the same direction as the deflecting force being measured and, therefore, in the opposite direction to the ordinary restoring force. Therefore if C is the spring constant for the restoring, or "stabilizing," force and C' is the constant for the opposite, or "labilizing," force, the net restoring force is $C - C'$, and the period is

$$T' = 2\pi \sqrt{\frac{m}{C - C'}}$$

Thus, the more nearly equal the stabilizing and labilizing forces are the more sensitive is the instrument, until the point of instability is reached where $C = C'$ and the period becomes infinite.

All gravimeters that are made sensitive enough to detect changes of gravity to the order of 1 part in 10 million are also apt to be affected by other things than gravity. Thus, most gravimeters have a thermostat and are kept at nearly constant temperature. They are more or less sensitive to changes in level, to magnetic effects, and to seismic effects which may result from very small tremors of the earth's surface. If not sealed, they are sensitive to variations of barometric pressure.

A number of different gravimeters have been developed and are being applied at the present time[1] in routine geophysical prospecting. For the most part, the mechanical details of their construction and operation are not disclosed. However, the general operating principles of a number of instruments have been made public. A brief description of such instruments, classified according to whether stable or unstable, follows.
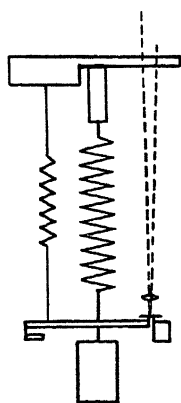
FIG. 6.—Principle of the Hartley gravimeter.

STABLE TYPE GRAVIMETERS

Hartley Gravimeter.—One of the earliest descriptions of an instrument designed for commercial geophysical exploration is that by Hartley[2] (Fig. 6). This instrument consists of a mass suspended on a spring. The position of the mass with respect to the surrounding case is determined by an optical lever. In Hartley's instrument the ratio of the motion of the spot of light reflected from the optical lever to the motion of the suspended weight was about 60,000. In practice the instrument is read by compensating for the variation of gravity by a small auxiliary spring which brings the suspended system back to a fixed reference position. Apparently, this instrument could detect gravity differences of about 1 mg. It apparently has never been used

[1] For a table of gravimeters in operation, see Steinmann, 1938, p. 62. For theory and description of several gravimeters, see Heiland, 1939.
[2] Hartley, 1932.

extensively in actual fieldwork, perhaps because of the death of its inventor.

Boliden (Lindblad-Malmquist) Electrical Gravimeter.[1]—This instrument has a moving system suspended on a pair of bowed springs (Fig. 7). The moving system carries plates at its two ends, each plate being one side of an electrical condenser. One of these condensers serves to measure the position of the moving system by the well-known principle of the "ultramicrometer"; *i.e.*, the condenser is part of an oscillating electric circuit the frequency of oscillation of which is sensitive to the capacity of the condenser and therefore to the distance between the plates. The other serves as the means by which a force is applied that balances a small part of the force of gravitational attraction. For each measurement the balancing force is adjusted to bring the moving system to a fixed reference position, the device being used as a null instrument. It is claimed that the instrument can detect gravity differences to about 0.01 mg.; but as used in the field, various sources of error reduce the practical sensitivity to about 0.1 mg. It was designed for use in mining exploration, and the

FIG. 7.—Principle of the Boliden electrical gravimeter.

degree to which it has been applied for oil exploration is not known.

Gulf (Hoyt) Gravimeter.[2]—This instrument (Fig. 8) does not measure directly the change of length of a spring due to changes in gravity but measures rather the rotation of the spring associated with its elongation. By winding the spring from a flat ribbon the amount of angular rotation associated with a given elongation is greatly increased over that which results from a spring wound with round wire. The spring carries a weight provided with electromagnetic damping vanes, and underneath the weight is a mirror which hangs close by a fixed mirror. The mirrors are partially silvered so that light passing through them is reflected back and forth a number of times. Images formed from these reflections are read in a micrometer eye piece at the top of the instrument. Thus the ultimate reading is changed from measur-

[1] Hedstrom, 1938.
[2] Hoyt, 1938*a*, 1938*b*, 1938*c*.

ing a small length to measuring a small angle.   The magnitude of
the angular change resulting from a given change of gravity is pro-

portional to the order of the reflec-
tion which is read in the eye piece.
By reading from the sixth to the
tenth reflection it is possible to
detect differences in gravity to
0.01 mg.   The drift of the instru-
ment is quite regular so that
gravity differences can be read
reliably to considerably better
than 0.1 mg.[1]   The instrument is
somewhat sensitive to temperature
and therefore is provided with
thermal insulation and a thermo-
regulator so that the temperature
is kept constant to around 0.1°C.

FIG. 8.—Working principle and
external view of the Gulf (Hoyt)
gravimeter.
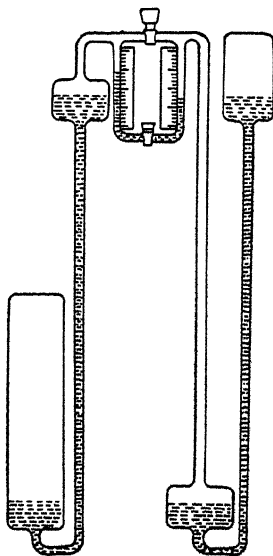
FIG. 9.—Principle of the
Haalck gas gravimeter.

This instrument has been in use in the field by the Gulf Oil

[1] Eckhardt, 1936.

Corporation for several years, and many thousands of stations made which, from repeat observations and other information, have a probable error of 0.05 mg. or better.

Haalck Gas Gravimeter.[1]—In this instrument the "spring" is a volume of gas compressed by the weight of a column of mercury. Two vessels containing the gas are connected to each other
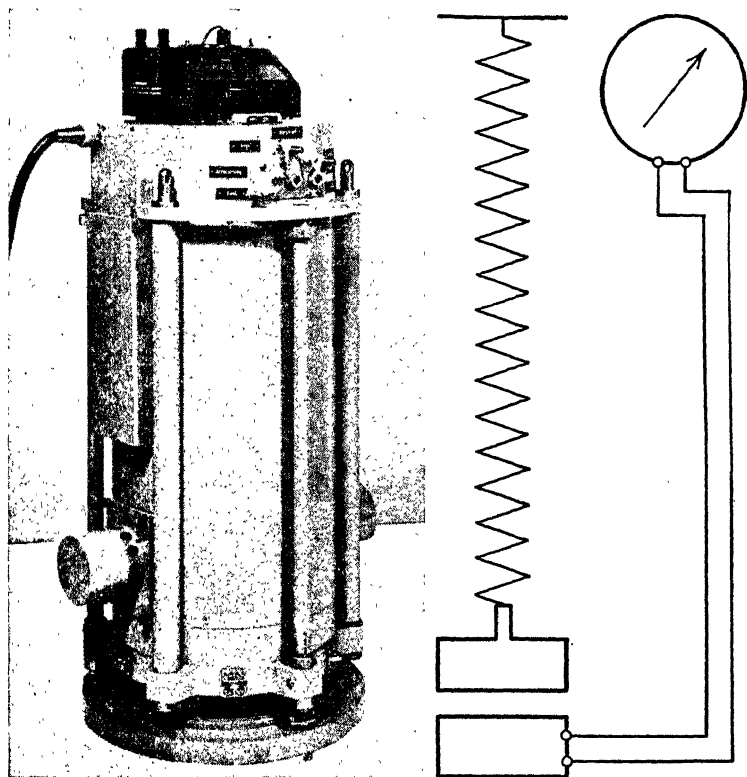
Fig. 10.—Schematic diagram of working principle and external view of the Askania (Graf) gravimeter. (*Photograph courtesy American Askania Co.*)

through a tube containing a mercury column (Fig. 9). The mercury column terminates in two enlarged parts where the mercury surface comes in contact with a light fluid. The difference in pressure in the two vessels is proportional to σgh, where h is the vertical difference in height between the two mercury surfaces. A change in gravity produces a small dif-

[1] Haalck, 1934, pp. 30–32.

ference in the height h, which, in turn, produces a motion in opposite directions of the meniscus surfaces of the light liquid. This motion is amplified in the ratio of the area of the mercury surface to the cross-sectional area of the capillary. As constructed, the two vessels are closely associated and are, in effect, interlaced with each other to insure equality of temperature. The instrument is kept in an ice bath for temperature control. It has a precision of about 1 mg.[1] which is hardly sufficient for commercial prospecting. It has been used for measurements in moving boats on rivers in Germany and may be useful for certain types of gravity measurement where the highest precision is not required.

Askania Gravimeter (by Graf).[2]—This instrument (Fig. 10) has recently appeared on the market and is offered for sale (price $11,600). The exact details are not yet available. However, the instrument is said to consist of a freely hanging weight on a spring and apparently uses an electrical method for detecting the very small changes in the length of the spring. It is claimed to measure gravity differences to 0.1 mg. and to have a range of 1,600 mg., over which the scale is linear. The instrument uses a thermostat. The moving system is sealed so that no barometric correction is necessary. The instrument weighs about 125 lb. It is carried in a truck with a special spring suspension, and readings are made with the instrument in the truck.

UNSTABLE TYPE GRAVIMETERS

Holweck-Lejay Pendulum.[3]—This instrument is not strictly a static gravimeter since it depends on measurement of the period of a pendulum. However, the pendulum is inverted, the mass being at the upper end of a flat spring (Fig. 11). The elastic constant of the spring and the size and shape of the mass are adjusted in such a way that the system approaches instability and the period becomes very sensitive to small changes in gravity.[4] The ratio of change in period to change in gravity is many times greater than for an ordinary pendulum so that differences in gravity can be detected by time measurements

[1] Haalck, 1938, pp. 285–316.

[2] Graf, 1938.

[3] Holweck-Lejay, 1930.

[4] Hoskinson, 1936.

which are much less accurate and correspondingly faster than those required for an ordinary gravity pendulum. This instrument apparently has an accuracy of 1 to 2 mg.[1] It has been used considerably in large-scale government gravity surveys, particularly in France and China, but has had little if any commercial use in the United States.

Ising Gravimeter.[2]—This is one of the oldest of the gravimeters and was described nearly twenty years ago.[3] The fundamental principle of the instrument is very similar to that of the Holweck-Lejay pendulum, although the two developments apparently were quite independent.

The essential feature of the Ising instrument is a small rod r (Fig. 12a) which stands vertically on a quartz torsion fiber a when the instrument is level. The instrument as a whole is tilted through a small angle φ (Fig. 12b). The resulting deflection of the rod is through an angle x, which may be much larger than φ and will depend on the force of gravity acting on the equivalent mass m at a distance r from the axis of rotation (*i.e.*, the horizontal torsion fiber). Measurements are made by tilting
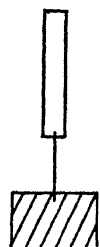
Fig. 11.—Principle of the Holweck-Lejay inverted pendulum.
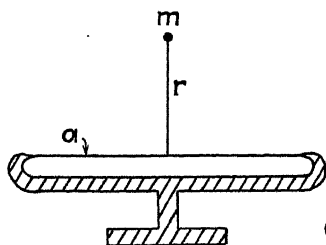
Fig 12a.
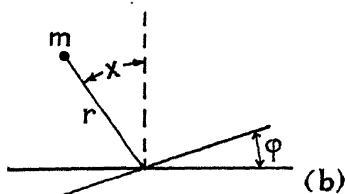
Fig. 12b.

Fig. 12a.—Cross section of the Ising gravimeter parallel to torsion fiber.

Fig. 12b.—Cross section of the Ising gravimeter perpendicular to the torsion fiber, showing the inclination of the instrument φ and the resulting angular deflection x of the moving system.

the instrument successively to one side and the other by a known angle φ and measuring the resulting angular deflections x. The instrument depends on the very stable elastic properties of the

[1] Steinmann, 1938, p. 62.

[2] Ising, 1937a.

[3] See Ising, 1937b, which contains a translation from the Swedish of the original paper, Ising, 1918.

quartz fiber, and therefore it is claimed to have no drift. However, the temperature coefficient of elasticity of fused quartz is about 10^{-4} per degree centigrade, so the temperature must be controlled very closely. This is done by surrounding the working parts by two ice-filled containers, one inside the other, so that the temperature is that of melting ice. A reading requires about 30 min. time, and a precision of about 0.5 mg. is claimed. The instrument has been used for some geophysical surveys in Denmark.

Humble (Truman) Gravimeter.—This is one of the practical field gravimeters and has been used in the field by the Humble Oil and Refining Company and the Carter Oil Company. It has been described by Bryan.[1] In this instrument the mass (Fig. 13) is carried horizontally on a hinged triangular member connected to two springs. The line of action of one of these springs is almost through the point of support which makes an unstable system. By careful adjustment of the geometry of the system and the tensions of the springs, the entire system approaches a critical point where the equilibrium becomes unstable. As this point is approached more and more closely, the sensitivity increases. This instrument apparently measures gravity differences to about 0.2 mg.
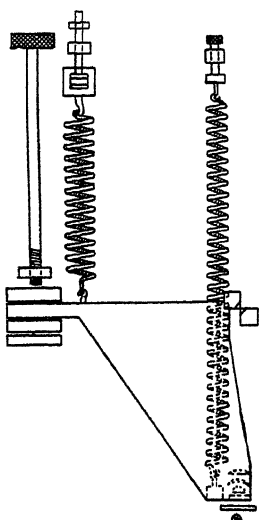
FIG. 13.—Principle of the Humble (Truman) gravimeter.

The Thyssen Gravimeter.—This instrument has had quite extensive application in Germany and other foreign countries and a limited application in the United States. A schematic description of its internal construction has been published by Heiland.[2] From the patent[3] descriptions it is of the unstable type. The sensitivity depends on the angle between the arm carrying the mass (Fig. 14) and the arm to which the spring is attached together

[1] Bryan, 1937.
[2] Heiland, 1939, p. 22.
[3] Thyssen, 1938a.

with the tension on the spring. By a proper adjustment of these relations, the instrument can be made very sensitive to changes in weight of the mass. As used, the instrument has a double moving system.[1] This is designed to decrease the high level sensitivity which is inherent in the single moving system.

FIG. 14.—Principle of the Thyssen gravimeter.

It is stated[2] that 80 Thyssen gravimeters are in use. Most of these apparently are outside the United States. From its operating characteristics[3] this instrument apparently is capable of measuring gravity differences with a probable error of about 0.2[4] to 0.3 mg.[5] It is interesting that this instrument is constructed in such a way that temperature effects are compensated, as it does not use a thermostat.

FIG. 15.—Principle of the torsion gravimeter of Tomaschek and Schaffernicht.

The Gravimeter of Tomaschek and Schaffernicht.[6]—This instrument has been developed primarily for a stationary application in the measurement of the small-time changes in gravity which are responsible for the tide-producing forces.[7] The essential principle of the instrument is a mass the weight of which is partially supported on a spiral spring and partially on a pair of crossed fibers (Fig. 15).

By a proper adjustment of the position and tension of the fibers, together with the torsion in the spring, the instrument can be placed in a critical condition such that a comparatively small change in gravity

[1] Heiland, 1939, p. 22.
[2] Steinmann, 1938, p. 62.
[3] Schleusener, 1935.
[4] Lubiger, 1938.
[5] v. Thyssen, 1938b.
[6] Tomaschek, 1937.
[7] It has been stated (Tomaschek, 1937, p. 179) that the Thyssen gravimeter is of this type. There appears to be nothing in the published litera-

produces a relatively large rotation of the suspended system. The change in length is not measured directly, but rather the angular rotation that is produced.

The Mott-Smith Gravimeter.[1]—This instrument consists essentially of a horizontal quartz fiber (Fig. 16) carrying a horizontal weight arm which is connected to "labilizer" fiber which passes through the line of the horizontal fiber and is attached to a spring. The weight arm carries a vertical index the position of which is measured by a microscope. The adjustment of the torsion of the fiber and the tension in the labilizer fiber is such that their effects on the moving system are nearly balanced so that a

Fɪɢ. 16.—Moving system of the Mott-Smith gravimeter.

small change in gravitational attraction on the weight arm produces a relatively large movement of it and of the index arm. The essential parts of the instrument are all made of fused quartz fused together so that the entire moving system may be considered a continuous piece of fused quartz. The instrument is quite small. The torsion fiber is about $1\frac{1}{2}$ in. long and 0.002 in. in diameter. The weight arm and pointer are each about 1 in. long. The labilizing fiber is about 2 in. long and 0.0005 in. in diameter. The instrument is mounted in an airtight box about 2 in. deep and 5 in. in diameter which in turn is in a liquid thermostat which keeps a constant temperature to about 0.001°C. Fused quartz should have very stable elastic properties, and the

---

ture to show definitely whether this or the principle shown in the Thyssen patents is actually used in the field instrument.

[1] Mott-Smith, 1938.

produces a relatively large rotation of the suspended system. The change in length is not measured directly, but rather the angular rotation that is produced.

The Mott-Smith Gravimeter.[1]—This instrument consists essentially of a horizontal quartz fiber (Fig. 16) carrying a horizontal weight arm which is connected to "labilizer" fiber which passes through the line of the horizontal fiber and is attached to a spring. The weight arm carries a vertical index the position of which is measured by a microscope. The adjustment of the torsion of the fiber and the tension in the labilizer fiber is such that their effects on the moving system are nearly balanced so that a

FIG. 16.—Moving system of the Mott-Smith gravimeter.

small change in gravitational attraction on the weight arm produces a relatively large movement of it and of the index arm. The essential parts of the instrument are all made of fused quartz fused together so that the entire moving system may be considered a continuous piece of fused quartz. The instrument is quite small. The torsion fiber is about $1\frac{1}{2}$ in. long and 0.002 in. in diameter. The weight arm and pointer are each about 1 in. long. The labilizing fiber is about 2 in. long and 0.0005 in. in diameter. The instrument is mounted in an airtight box about 2 in. deep and 5 in. in diameter which in turn is in a liquid thermostat which keeps a constant temperature to about 0.001°C. Fused quartz should have very stable elastic properties, and the

ture to show definitely whether this or the principle shown in the Thyssen patents is actually used in the field instrument.

[1] Mott-Smith, 1938.

operating characteristics[1] of the instrument indicate a very regular drift and stability such that gravity measurements can be made to better than 0.1 mg. It is stated[2] that 18 of these instruments are in use.

The Brown Gravimeter.[3]—The moving system of this gravimeter is a torsion pendulum consisting of a horizontal bar suspended on two wires (Fig. 17). The wires are twisted in the same direction until the axis of the bar is nearly perpendicular to the line between the supports at the upper ends of the two wires. This twist of the wires exerts a force opposite to the gravitational stabilizing force, and the system approaches an unstable condition as the position with the bar axis perpendicular to the support axis is approached. As used in the field, the instrument is adjusted closely enough to instability so that its torsional period is from 20 to 40 sec. It is claimed that this gravimeter is read in the field to 0.03 mg. and that it has a probable error of a single observation of 0 065 mg.
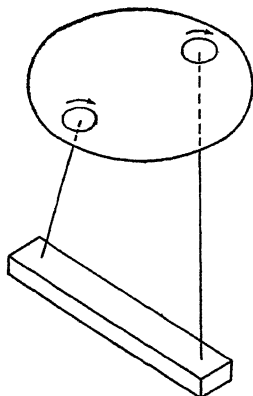
Fig. 17.—Principle of the Brown gravimeter.

The Wright Gravimeter.[4]—The moving system of this instrument is a horizontal coiled spring with an "hourglass" shape (Fig. 18). At the center, or constricted, part of the spring is a small "boom," or staff, carrying a small weight at its outer end. The spring is mounted within a cylinder which is rotatable on a horizontal axis. As the spring is rotated, the boom is raised against gravitational attraction. As it nears a horizontal position, it approaches a condition of instability. A reading of a scale on the rotating cylinder is made when it is adjusted to bring the boom to a fixed reference position near but just below the instability point. Then the cylinder is rotated back past the point where the boom hangs vertically downward and until it reaches another reference point, near but just below the insta-

[1] Mott-Smith, 1937.
[2] Steinmann, 1938, p. 62.
[3] Brown, 1939.
[4] Wright and England, 1938.

bility point on the opposite side. The total number of turns and fraction of a turn through which the cylinder is rotated to carry the boom from one reference point to the other is a measure of the gravitational attraction on the weight. The angle can be read to 10 sec. Therefore with a total rotation of 1,400 deg. (four turns), differences in angle and in gravity can be read to 1 part in 10^6.

On account of elastic hysteresis of the spring, it is necessary to take the readings according to a definite time schedule. This instrument is particularly susceptible to hysteresis difficulties because the stress in the spring is reversed for each reading. On the other hand, it has no detectable zero shift or drift and
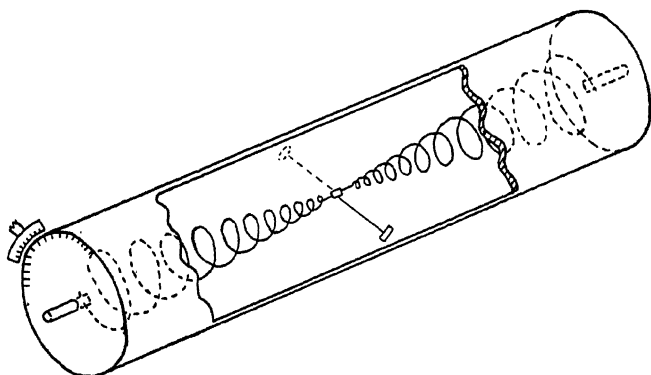
Fig. 18.—Principle of the Wright gravimeter.

therefore may be more suitable for carrying gravity differences over long distances when readings at fixed points for drift determinations could not be made.

This instrument has been developed at the Geophysical Laboratory at Washington over a number of years. It is claimed that a new model, recently completed, gives repeated readings that agree within 1 mg.

DRIFT, OR TIME VARIATION, OF GRAVIMETERS

Apparently practically all gravimeters sensitive enough for commercial geophysical prospecting have a certain amount of drift, or time variation. This results from the fact that whatever means are used to measure the very small elongations of a spring or spring system, due to small changes in gravity, also will

measure small changes from other causes. Even under well-controlled surroundings a spring and the associated mounting and connections are not perfectly stable, and either slow or abrupt changes occur which are larger than those due to the small gravity differences that are being measured. These changes are called the "drift," and the fieldwork must be conducted in such a way that this drift can be taken into account.

Commonly the instrument is returned several times a day to a reference station. A curve (Fig. 19) is plotted of the readings at this station. This curve presumably is that which the instrument would have if continuous readings were made at the same
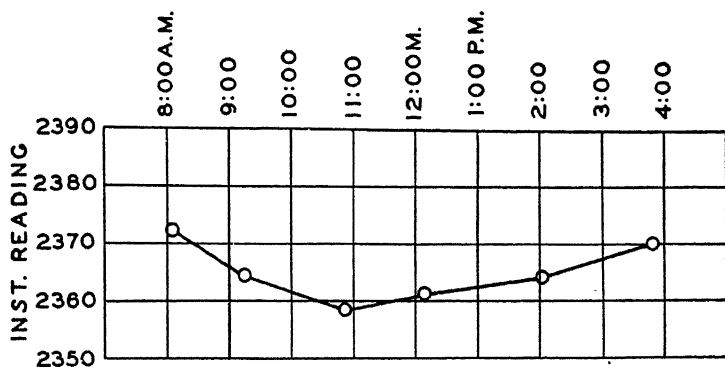
FIG. 19.—A gravimeter drift curve (Gulf gravimeter). One unit of the "instrument reading" scale is approximately 0.01 mg.

point. Readings at other stations are then referred to this curve; *i.e.*, the difference of the reading at a station from the value interpolated along the drift curve at the corresponding time gives the number of instrument scale divisions due to the gravity difference between the reference point and the station. This scale division difference is then converted to a gravity difference from the calibration data of the instrument.

It is not necessary that the drift readings be made at the same station if other points with previously established gravity values are more convenient. The readings can be reduced to what they would have been at a single reference point or base station by properly taking into account the established gravity differences between bases.

¹ Mott-Smith, 1937; Barton and White, 1937.

The frequency with which drift observations must be made depends on the stability of the instrument.   If the drift curve is quite regular and nearly linear, three or four drift station observations per day may be sufficient.   For very accurate work it may be necessary to take drift readings as frequently as once per hour or to consider each station a drift station for the next station made (the "loop" method of observation described below).

FIELD OPERATION OF GRAVIMETERS

The details of the field methods used for gravimeter surveys depend on the characteristics of

Fig. 20.—Sequence of "looping" gravimeter observations.

the instrument used and on the technical policies of the operating company.   Commonly a net of base stations is set out in advance to which other stations are

MEASUREMENT OF BASE STATION GRAVITY DIFFERENCES
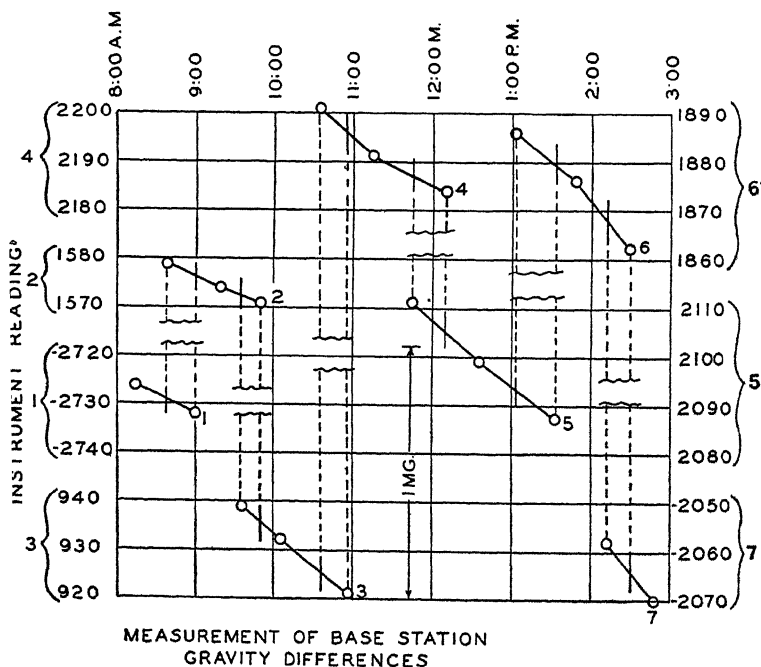
Fig. 21.—Drift curves for "loop" gravimeter observations.

referred.   The bases may be set out by "looping" (Fig. 20), *i.e.*, by an observation, say, at station 1, ahead to station

2, looping back to 1, then on to 2 again, then on to 3, back to 2, ahead to 3, on ahead to 4, etc.   Thus, the successive observations at the same station are, in effect, short segments of a drift curve to which the next station is referred (Fig. 21).   The average differences between these curves give the scale division differ-
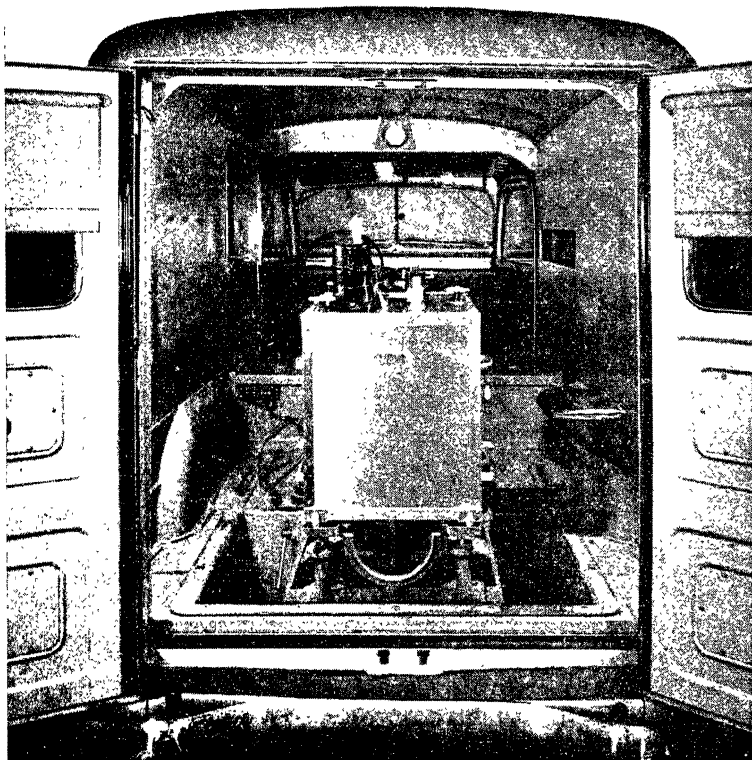
Fig. 22.—Mott-Smith gravimeter in truck.   (*Courtesy L. M. Mott-Smith.*)

ences between the successive stations.   Closed traverses of such loops may be set out so that the accuracy of the work may be checked by the closure errors.   Modern gravimeters can carry closures of many miles or several tens of miles with closure errors of only a few tenths of a milligal.[1]

In some cases, traverses of gravimeter stations may be connected to pendulum stations.   A large government gravity

[1] See Mott-Smith, 1937; Barton and White, 1937.

survey in Germany was made by setting out a primary control of pendulum stations and filling in with gravimeter and torsion balance[1] stations. In this country there is an extensive net of gravity stations set out by the U.S. Coast and Geodetic Survey.[2] Most of these can be depended on to a probable error of about 1 or 2 mg. and can often serve as useful checks on gravimeter gravity differences, especially over long distances.

Commonly, gravimeter stations are laid out along roads, and the survey then consists of lines of stations at intervals of $\frac{1}{2}$ to 2 miles on roads that may be 1 to several miles apart. In areas where there is a regular grid of roads, such as section-line roads, stations may be set out in a regular grid of, say, a station on each section corner or each quarter section corner or on a grid 2 miles on a side, etc. Some instruments (such as Mott-Smith and Humble) make their observations on a tripod let down through the floor of the truck (see Fig. 22) and therefore are confined to stations at points that may be reached by truck. However, gravimeters may be and have been adapted to transportation by whatever means are available, from fast motor trucks to boats of various kinds, piroques, wagons, marsh buggies, and mules, and finally carried by hand in areas not accessible by any other means (Fig. 23).

For most gravimeters used in commercial exploration, the actual time of setting up and reading the instrument is only a few (1 to 10) minutes. Commonly the instrument crew consists of one observer and a helper. They take the instrument to previously located and marked stations and make all the necessary observations for determining the gravity differences. The associated surveying required for mapping the station locations and reducing the gravity values (see Chap. IV) is done by a separate crew. Usually the surveying crew required is considerably larger than the instrument crew, and the cost of the surveying may be as much as or several times more than the cost of the gravity observations themselves.

The program of fieldwork always must be laid out with the drift curve of the instrument in mind. For most instruments reliable observations cannot be made unless the instrument is

---

[1] Barsch, 1937.

[2] Bowie, 1917; Bowie, 1924.
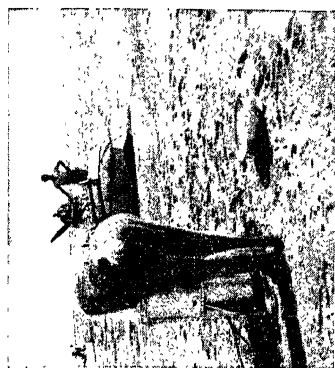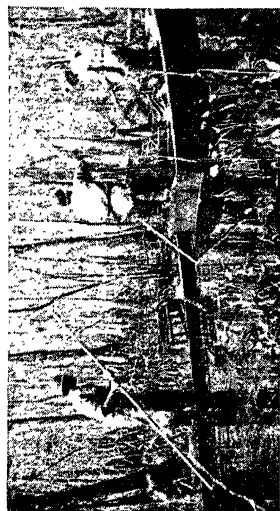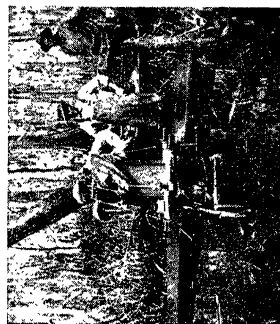
Fig. 23.—Gravimeters in the field showing operations under a variety of transportation conditions. (a) Gravimeter at a marsh station; (b) gravimeter being unloaded from a marsh buggy; (c) gravimeter station on a beach, using air-boat transportation; (d) carrying a gravimeter through cypress swamp; (e) gravimeter transportation by piroque; (f) gravimeter station in dense cypress swamp.

returned to a check point of some kind in a time of, at most, a few hours. In areas where motor cars or trucks can be used, this is not a serious restriction, for a reference point, even if it is several miles away, can be reached in a short time. Where travel is difficult and slow, the required drift observations impose an onerous but necessary restriction on the rate at which field stations may be made.

If stations at wide intervals for primary control are desired, it should be possible to make them by using an airplane to carry the instrument, provided an instrument is available with a sufficiently wide range of reading (50 to 100 mg.). The mode of operation probably would be essentially the same as the looping described above, except that the stations presumably could be 50 to 100 miles apart. With the large gravity differences which would be encountered, the precision probably would be limited by the accuracy of calibration.

Calibration of Gravimeters.—The instrumental observations with a gravimeter give figures in instrument scale divisions. These figures must be changed to gravity units (milligals) through a calibration curve, or constant, which must be determined experimentally. Several methods have been used to calibrate gravimeters.

Probably the most common method[1] is that of taking observations at different heights in tall buildings. The theoretical rate of change of gravity with elevation [Eq. (11), page 20] is used to calculate the gravity change. Small corrections are necessary for the mass of the building and particularly for the basement excavation and for surrounding topography, if quite rugged.[2] It has been pointed out[3] that the actual value of the vertical gradient may vary by about ± 1 per cent from the theoretical value because of local mass irregularities in the earth's crust, so this method of calibration is subject to unknown errors of this magnitude.

Another possible method is the use of a small known mass which can be lowered on to the moving system to apply a known force. This should be particularly useful on an unstable type instrument for which the calibration may be variable.

[1] See Bryan, 1937, p. 304.
[2] Hammer, 1938, pp. 73–74.
[3] Hammer, 1938, p. 80.

The most direct method of calibration is to take instrument readings at points between which the gravity difference has been measured with a pendulum.[1] However, the required precision of pendulum measurements is difficult to achieve, as the gravity differences should be known to considerably better than 1 per cent if the method is to have any advantage over the simpler method of depending on the vertical gradient of gravity (*i.e.*, making measurements at different elevations in buildings). If the calibration gravity difference is, say, 40 mg., this difference should be known to about 0.1 mg. which is a difficult but not impossible requirement for a pendulum. A proposal for a cooperative program to set out a series of pendulum stations for this purpose has been made[2] but has not yet been carried out.

THE GRAVITY PENDULUM

Measurements of gravity with pendulums have been used to a comparatively limited extent for commercial geophysical prospecting but have been quite extensively used for geodetic and other scientific purposes.

Gravity measurement with a pendulum depends on the fact that the period of a freely swinging pendulum is inversely proportional to the square root of the gravitational acceleration. If the physical dimensions of a pendulum are held constant and the period can be measured sufficiently accurately, small changes in the period will indicate small changes in gravity. The period may be measured by comparing the pendulum with an accurate chronometer, the rate of which is independent of small variations in gravity.[3] The period also may be measured by simultaneously comparing the period of a "base pendulum," kept at a fixed reference point, with that of a "field pendulum" which is set up at the field station, the two pendulums being connected by telegraphy or radio. The latter method is the one used for geophysical prospecting.

This comparison of pendulums has been done in two ways: (1) by the coincidence method[4] in which the individual swings of two

[1] Poynting and Thomson, 1927, p. 27.

[2] Eckhardt, 1938.

[3] This method is discussed in detail by Haalck, 1934, pp. 21–27.

[4] This is described briefly by Haalck, 1934, pp. 27–28, and in detail by Berroth, 1927.

pendulums or of a pendulum and a chronometer are compared continuously and the time measured in which one pendulum gains or loses an integral number of half swings or (2) by the phase position method[1] by which the phase positions of the two pendulums are compared with a simultaneous time mark at the beginning and again at the end of a run. Either method, of course, requires telegraph or radio connection between the base and field pendulums.

Theory of Pendulum Measurements.—The measurements, by either method of comparison, give the number of swings of the two pendulums over identical time intervals. The following indicates briefly how gravity differences may be derived from these swings.

The period of a physical pendulum may be written as

$$T = 2\pi \sqrt{\frac{I}{mgh}} \tag{13}$$

where I = moment of inertia about the knife-edge.

m = total mass of the pendulum.

h = distance from the knife-edge to the center of gravity.

g = acceleration of gravity.

Let us consider two pendulums A and B of which A is the reference, or base station, pendulum and B is the moving, or field, pendulum. We shall compare the periods of these two. First when they are side by side at the base station, the periods of the two pendulums are

$$\left. \begin{aligned} T_A &= 2\pi \sqrt{\frac{I_A}{m_A g h_A}} = \frac{K_A}{\sqrt{g}} \\ T_B &= 2\pi \sqrt{\frac{I_B}{m_B g h_B}} = \frac{K_B}{\sqrt{g}} \end{aligned} \right\} \tag{14}$$

where K_A and K_B are constants which are fixed by the physical dimensions of pendulums A and B, respectively. The number of swings, S_A and S_B, of the two pendulums in a time interval t are determined with the two pendulums at the base. Then with

---

[1] This method is described in detail by Bullard, 1933. In the measurements described in Horsfield and Bullard, 1937, the reference pendulum was in England and the field pendulum in Africa, the time marks being supplied by recording commercial radio-telegraph signals.

pendulum A at the base and pendulum B in the field, the numbers of swings S'_A and S'_B are determined in another time interval t'. Let the value of gravity at base and field stations be g_b and g_f, respectively.

For the first run with pendulums A and B at the base:

$$S_A = \frac{t}{T_A}; \qquad S_B = \frac{t}{T_B} \tag{15}$$

$$\frac{S_B}{S_A} = \frac{T_A}{T_B} = \frac{K_A/\sqrt{g_b}}{K_B/\sqrt{g_b}} = \frac{K_A}{K_B} = R \tag{16}$$

For the second run with pendulum A at the base and pendulum B in the field, the period of pendulum A remains T_A, but that of pendulum B changes to T'_B. The swings in the new time interval t' are

$$S'_A = \frac{t'}{T_A}; \qquad S'_B = \frac{t'}{T'_B} \tag{17}$$

$$\frac{S'_B}{S'_A} = \frac{T_A}{T'_B} = \frac{K_A/\sqrt{g_b}}{K_B/\sqrt{g_f}} = \frac{K_A}{K_B}\sqrt{\frac{g_f}{g_b}} \tag{18}$$

Substituting for K_A/K_B from Eq. (16);

$$\frac{S'_B}{S'_A} = \frac{S_B}{S_A}\sqrt{\frac{g_f}{g_b}} \tag{19}$$

$$\sqrt{\frac{g_f}{g_b}} = \frac{S'_B S_A}{S'_A S_B} \tag{20}$$

If we let

$$S_B = S_A(1 + E); \qquad S'_B = S'_A(1 + E'); \qquad g_f = g_b + \Delta g$$

or

$$\frac{S_B}{S_A} = 1 + E; \qquad \frac{S'_B}{S'_A} = 1 + E'; \qquad \frac{g_f}{g_b} = 1 + \frac{\Delta g}{g_b};$$

$$\sqrt{\frac{g_f}{g_b}} = \sqrt{1 + \frac{\Delta g}{g_b}}$$

Then Eq. (20) becomes

$$\sqrt{1 + \frac{\Delta g}{g_b}} = \frac{1 + E'}{1 + E} = (1 + E')(1 - E + E^2 - E^3 + \cdots)$$
$$= 1 + (E' - E) \text{ approximately}$$

and

$$1 + \frac{\Delta g}{g_b} = 1 + 2(E' - E) \text{ approximately.} \tag{21}$$

Since the gravity differences measured will seldom be more than around 100 mg., $\Delta g/g_b$ will be of the order 10^{-4} or less, so that the approximations used above are very close and will not introduce errors of more than a few hundredths of a milligal.

Finally, we may write

$$\frac{\Delta g}{g_b} = 2(E' - E)$$

$$= 2\left(\frac{S_B'}{S_A'} - \frac{S_B}{S_A}\right) = 2\,\Delta R \tag{22}$$

$$\Delta g = 2g_b\,\Delta R \tag{22a}$$

where ΔR is the difference in swing ratios resulting from the difference in gravity. Thus, we see that the pendulum measures directly the ratio of the difference in gravity between two points to the gravity at the base station. Equation (22) shows that the precision of the timing required, *i.e.*, the precision of determination of ΔR, must be twice as great as the desired precision of determination of gravity. Thus, if Δg is to be determined to 0.2 mg., $\Delta g/g_b$ is about 2×10^{-7}, and the time measurements on which the swing ratios are based must be made to 1 part in 10 million.

Pendulum Field Apparatus.—The following is a brief description of the pendulum apparatus as developed by the Gulf Oil Corporation (Fig. 24).

Each unit consists of two pendulums in a single case. The periods of the two pendulums are carefully adjusted so that throughout a normal run of up to 1 hr. the total number of swings will be within a small fraction of one swing of the same. The pendulums are started swinging in opposite phases, and because of the equality of the periods this phase relation is maintained throughout the run. The primary purpose of this arrangement is to eliminate sway of the case which would result from the reaction of a single pendulum on the case. With a double pendulum the forces tending to cause sway from the two pendulums are equal and opposite and compensate each other. Amplitude corrections are eliminated by always starting the pendulums with the same amplitude. The decrement is quite constant so that the final amplitude also is the same from one run to another. Electrostatic disturbances are eliminated by use of a small amount of radioactive material in the case which renders the

residual atmosphere conducting and dissipates any electrical charge on the pendulums. Also, it is the practice in field operations to use two complete sets of apparatus so that at each station two independent values of gravity are determined.

The pendulum itself consists of a fused quartz bar which is carefully designed as a "minimum pendulum."[1] The bar is carried by a quartz knife-edge resting on a solid pyrex glass flat. The pendulum period (complete cycle) is about 0.9 sec. The motion of the pendulum is recorded by a beam of light reflected from a mirror surface polished on the upper end of the quartz bar.
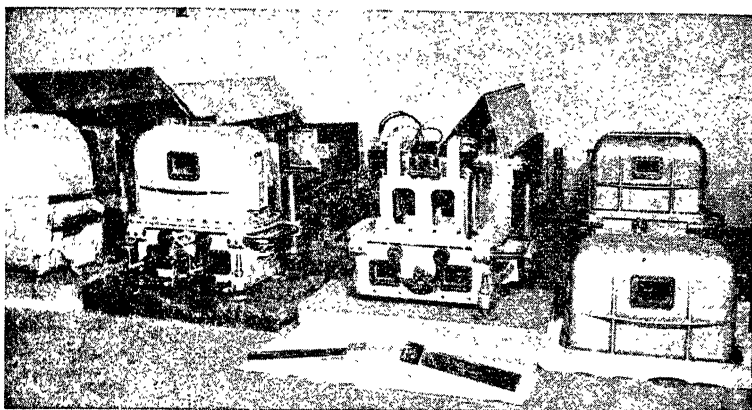
Fig. 24.—Field pendulum apparatus. Apparatus on left with case closed, showing starting mechanism with amplitude setting device. Recording apparatus in rear with film holder and camera at rear of recorder. Apparatus on right with cover of case removed to show pendulum support and clamping mechanism. At extreme left, a partial view of case with insulating cover. In the foreground, a pair of fused quartz pendulums.

The pendulums are mounted in a vacuum-tight cast-aluminum case. Clamping, starting, and stopping of the pendulums are all done from the outside through vacuum-tight stuffing boxes without disturbing the vacuum. The cases are tight enough so that a vacuum of 0.1 mm. of Hg can be maintained for months without pumping out. The pendulum case is surrounded by a net of electric heating wires and is covered on the outside with a thick eiderdown blanket. This permits maintaining the case at a constant temperature, the heating power being supplied by auto-

[1] A "minimum pendulum" is proportioned so that its period is a minimum. For a physical pendulum, oscillating about a knife-edge at E, at a

mobile storage batteries and controlled by a thermostat mounted
on the metal case.   The temperature is kept constant to about
0.1°C.

The recording apparatus contains a small lamp to serve as a
light source from which a beam of light passes into the pendulum
case.   This beam is divided into two beams, each of which is
reflected four times from the faces of the two pendulums and a
set of fixed mirrors.   Finally, the two reflected beams are
returned to the recorder where they fall on a moving photo-
graphic tape.   The tape also records light reflected from two
oscillograph elements.   One of these is used for recording the
radio time signal sent out from the base station, and the other
for recording reference time marks which are controlled by a
tuning fork with a period of about 500 cycles per second.

A tape is run out on the base and the field pendulums simul-
taneously, and the same time signal is recorded on these two

---

distance S from the center of gravity G, the reduced length l, or length of the
equivalent simple pendulum (Fig. 25), is

$$l = \frac{K_0 + S^2 M}{SM}$$

where K_0 is the moment of inertia about the center of gravity and M is the
total mass.

FIG. 25.

The period of the pendulum is a minimum when

$$\frac{dl}{dS} = 0$$

or when

$$S_0 = \frac{K_0}{M}$$

which also gives

$$l = 2S_0$$
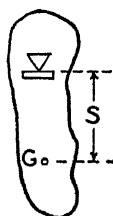
Thus, a minimum pendulum is so proportioned that the distance from the
knife-edge to the center of gravity is half the length of the equivalent simple
pendulum.   The advantage of a minimum pendulum for an invariable
pendulum is that small changes in the distance S will not change the priod.
Thus, a minimum pendulum is much less sensitive to wear of the knife-edge
or slight movement of the knife-edge with respect to the pendulum itself
than is the more common simple pendulum with a heavy weight on a rela-
tively long staff.

For more complete theory and design of minimum pendulums, see Meisser,
1930.

tapes. The transits of the beams of light reflected from the pendulums also are recorded on the tape. The phase position of the pendulums with respect to the time signal is determined by careful measurements of time difference from the time signal to the adjacent transits of the pendulum across the center of the tape, this time between successive transits being measured by the 500-cycle tuning-fork records. The same process is repeated at the end of the run. Thus, the relative phase positions of the two pendulums with respect to identical time signals at the beginning and end of the run are determined. The periods of the pendulums are known closely enough so that the number of whole swings in the run can be determined from the number of seconds (measured with a chronometer) between the starting and ending time signals. Thus, the measurements give, for each pendulum, the total number of swings and fractions of a swing in the precisely identical time interval (*i.e.*, S_A and S_B if the run is at the base, or S'_A and S'_B if one pendulum is in the field), and the ratios of these numbers give ΔR, which gives the gravity difference, as indicated by Eq. (22) above. The time measurements can be made to about one ten-thousandth of a second. Since the total run is usually $\frac{1}{2}$ hr., or 1,800 sec., the time measurements are made to better than 1 part in 10 million. Actually, in routine field pendulum operations, gravity determinations are made regularly to a precision of about 1 in 4 million.

Pendulum Field Operations.—Pendulum field operations as conducted by the Gulf Oil Corporation were carried out as follows:

The field pendulums were compared with the base pendulums at the beginning and the end of each day's work [determination of base ratio R, Eq. (16)]. This gave good control on any small changes that might take place in the periods of the pendulums. The two sets of equipment in two trucks then went to the field station and were set up. Two-way radio communication was established, so that when the field operator was ready he reported back to the base station. The base and field pendulums were then started swinging, and a radio time signal code was sent from the base station. About 1 sec. before the final time signal, the camera motor that moves the photographic tape through the camera was started. The tape was run for 3 or 4 sec., during

which time the time signal and several transits of the pendulum were recorded. The pendulums were then left swinging undisturbed for $\frac{1}{2}$ or 1 hr. (usually $\frac{1}{2}$ hr.). At the end of this time radio communication was again established, and the same process of recording the time signal and several transits of the pendulum repeated.

The photographic records of the runs were kept in light-tight collectors and taken to the field office. An office staff there developed the records and read the tapes to determine the swing numbers and calculate the gravity differences.

A field party could set up the pendulum apparatus in about 10 or 15 min. time after arriving at the station site. The total time at the station (for a half-hour run), including setting up, making the run, taking down the equipment, and loading the truck was around 1 hr. A common output was three to five stations per day. In part of the work a double set of field equipment was used. The operations of the two separate field units were synchronized by radio communication so that the same base station run was used for the two separate field outfits.

In addition to the pendulum operators, a pendulum field party included surveyors to determine the positions and elevations of the stations. Also a crew of tape readers was required, as there was considerable labor in making the necessary measurements on the tapes for determining the total swings of the pendulums. A crew for a pendulum party using two field units was around 25′ men.

CHAPTER IV

REDUCTION OF GRAVITY OBSERVATIONS

The final field results of gravimeter or pendulum measurements are the gravity differences between an arbitrary reference point and a series of field stations. Before being useful as possible indications of subsurface conditions, these observed gravity differences must be corrected for various large influences on the measured values, for which the causes are accurately known and which would completely mask the desired effects if they were not removed. These necessary corrections are always three and sometimes four: (1) latitude correction, (2) free-air correction, (3) Bouguer correction, and (sometimes) (4) terrain corrections.

LATITUDE CORRECTION

The latitude correction takes account of the increase of gravity from equator to pole as discussed in detail above (page 16). Usually the correction is made to an arbitrary base latitude. The basis of the correction is one of the various gravity formulas. If a survey is of rather limited extent and is not to be connected in to another survey, it may be sufficient to use a constant and calculate the correction as the distance in miles (or kilometers) from the reference latitude multiplied by this constant. The constant K can be derived from the gravity formula[1] of the type

$$g_0 = A(1 + B \sin^2 \varphi - C \sin^2 2\varphi) \tag{23}$$

as,

$$K = \frac{dg_0}{dx} = \frac{dg_0}{r \, d\varphi} \tag{24}$$

for $dx = r \, d\varphi$ where r is the radius of the earth. From Eqs. (23) and (24)

$$K = \frac{1}{r} \frac{dg_0}{d\varphi} = \frac{A}{r} (B \sin 2\varphi - 2C \sin 4\varphi) \tag{25}$$

[1] See Eqs. (8), (9), and (10).

From this formula, we can compute the value of K for any given latitude by inserting the values of A, B, and C from the gravity formula. For the international formula [Eq. (10) above] the values are

$$A = 978.049; \quad B = 0.0052884; \quad C = 0.0000059$$

For the radius r we can use the mean radius of the earth; *i.e.*, $(a + b)/2 = 6,368,000$ meters. Inserting these numerical values in Eq. (15), neglecting C, which is too small to have an appreciable effect,

$$K = 0.8122 \sin 2\varphi \text{ (mg./km.)} \qquad (26)$$
$$= 1.307 \sin 2\varphi \text{ (mg./mile)}$$

Values of K for several latitudes are tabulated below and also are shown by the curve (Fig. 26)

Latitude φ, degrees	K, mg./mile	K, mg./km.
0	0	0
10	0.447	0.278
20	0.840	0.522
30	1.132	0.703
40	1.287	0.800
50	1.287	0 800
60	1.132	0 703
70	0.840	0.522
80	0.447	0.278
90	0	0

If gravity surveys are more extensive or are to be tied in to other surveys, the gradual departure of any constant value of K from its true value leads to irregularities. Therefore, it is better to use a correction based on gravity differences derived directly from the gravity formula. This can be done by use of a table giving gravity differences from the base latitude. The table of gravity values computed from the International Gravity Formula (Appendix I) is a very convenient base for the construction of such tables. If the latitude of stations is expressed in degrees and minutes, the correction tables can be made accordingly, preferably using gravity differences from a reference latitude within the general area of the survey (to avoid carrying large

numbers). The table also can be made up in terms of miles (or kilometers) from the reference latitude.[1] In either case, the latitude correction is made simply by reading from the table the value corresponding with the latitude or distance that describes the north-south coordinate of the station location and subtracting this latitude correction from the measured gravity value.

From the values of K, above, it is evident that the latitude correction for intermediate latitudes is of the order of 1 mg. per mile. Therefore, if gravity measurements are made to, say, 0.1 mg. or better, and if all the precision of the observation is
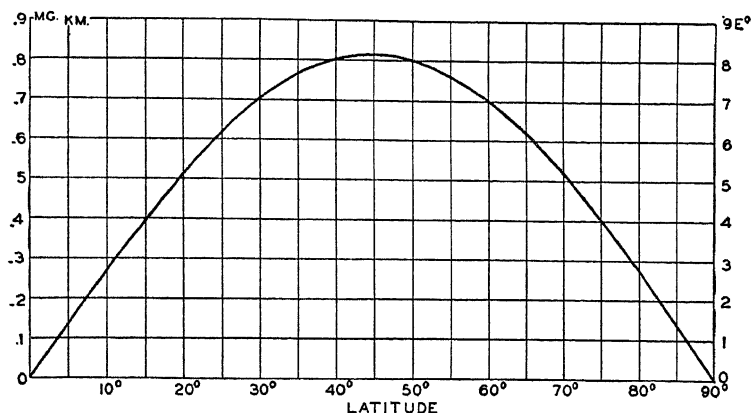
Fig. 26.—The normal gradient of gravity. Scale on left in milligals per kilometer. Scale on right in Eötvös units (see pp. 82 and 90).

preserved in the reductions, it is evident that the north-south position of the station must be known to better than 0.1 mile. This means that an accurate gravity survey demands good mapping of the stations. If reliable maps are available, such as the U.S. Coast and Geodetic Survey topographic sheets, accurately controlled aerial maps, or a dependable or checked township and section grid, the stations may be spotted on such maps and the latitudes determined with sufficient precision to make the corrections. If such maps are not available, sufficient surveying must be done to locate the stations within the precision required. Commonly this consists of a survey by plane table and stadia.

[1] *U.S. Coast and Geodetic Survey, Special Pub. 5*, 6th ed., 1935, gives very convenient tables for the conversion of latitude or longitude differences into miles or kilometers.

In some cases automobile speedometers (preferably with a special odometer reading to 0.01 mile) are used to locate stations along roads. This must be done very carefully if the positions are given accurately enough to preserve a precision of less than 0.1 mg. in the reductions. However, by careful checking of the speedometer, control of tire air pressure, etc., quite satisfactory results may be obtained in this way, especially if the roads are straight over relatively long distances (several miles or more).

ELEVATION CORRECTIONS

The corrections to gravity values which must be made on account of differences in elevation take care of two effects: (1) the free-air correction and (2) the Bouguer correction.

Free-air Correction.—This correction takes care of the vertical decrease of the gravity with increase of elevation which was considered above (page 20). As pointed out there, this variation amounts to

$$-0.3086 \text{ mg./meter} \quad \text{or} \quad -0.09406 \text{ mg./ft.}$$

The correction may be made to any arbitrary reference or datum level that is convenient, such as the elevation of a base station for a survey, or may be made to sea level. Since a station at a relatively higher elevation has a lower gravity (because it is farther away from the center of the earth), the correction must be *added* to stations at a *higher* elevation and must be *subtracted* from stations at a *lower* elevation than the reference level.

The Bouguer Correction.—This correction takes care of the attraction of the material between a reference elevation and that of the individual station. The term "Bouguer correction" is used here in a restricted sense to designate the correction for the attraction as approximated by considering the material as an infinite horizontal slab. The gravity attraction for a point on the surface of such a slab [Eq. (12a), page 21] is

$$0.04185\sigma h \text{ (mg./meter)}$$

or

$$0.01276\sigma h \text{ (mg./ft.)}$$

If a given station is *higher* than the reference elevation, its gravity value is *increased* because of the attraction of the slab

of material between it and the reference level. If the station is *lower* than the reference elevation, its gravity value is *decreased* because of the lack of attraction of the absent material between it and the reference level. Therefore, the Bouguer correction is always opposite in sign to the free-air correction.

Since both the free-air and the Bouguer corrections are simple constants, multiplied by the elevation differences, it is common practice to combine the two effects into a single constant. The values of this constant for different densities are given in the following table:

TOTAL OR COMBINED ELEVATION CORRECTIONS

Density	Mg./meter	Mg./ft.
1.6	0.2416	0.07364
1.7	0.2375	0.07237
1.8	0.2333	0.07109
1.9	0.2291	0.06982
2.0	0.2249	0.06954
2.1	0.2207	0.06826
2.2	0.2165	0 06599
2.3	0.2123	0.06471
2.4	0.2082	0.06344
2.5	0.2040	0.06216
2 6	0.1998	0.06088
2.7	0 1956	0.05960

From the magnitudes of the elevation corrections it is evident that elevations of gravity stations must be known to about 1 ft. if the elevation correction is to be accurate to less than 0.1 mg. Usually it is necessary to determine the elevation of each station, as elevation contour maps of sufficient accuracy are seldom, if ever, available. In some cases aneroid barometers have been used for determining elevations; but the accuracy attainable by such methods is not sufficient to make corrections to 0.1 mg., as good aneroids carefully used have probable errors of a few feet. Entirely aside from the precision of the barometer itself, it has been shown that horizontal variations in the air pressure make uncertainties of elevation of about 1 ft. over distances of only a few miles.[1] Therefore, a good gravimeter survey is

[1] Vacquier, 1937.

usually accompanied by leveling which gives the elevations of stations to a fraction of a foot.

TERRAIN CORRECTIONS

The free-air and Bouguer corrections as outlined above are adequate if the topography in the vicinity of the station is reasonably flat. However, if there are considerable differences in elevation, particularly rather close to the station, these local irregularities of topography will have appreciable effects and must be taken into account for accurate reduction of the gravity values.[1]

The terrain correction requires some sort of survey to determine the irregularities around the station. If topographic maps such as the usual U. S. Coast and Geodetic Survey maps at a scale of 1 to 62,500 and a contour interval of 20 ft. are available, these can be used for making the corrections unless the station is very close to a sharp topographic feature, in which case the detail of these maps may not be sufficient for points within about 200 ft. of the station. If no maps are available, it is necessary to make some sort of special survey to determine approximately the topography in the vicinity of the station.

To make the corrections the topography is divided up into a series of zones and compartments which are defined by circles and radial lines. The size of the compartments increases rapidly with the distance away from the station. Tables are prepared that give, for each zone, the attraction, as a function of the average elevation with respect to the station, of a single compartment in that zone.

The average elevation in each compartment is estimated from the topography or topographic map. For each compartment, its average difference in elevation from that of the station is determined. The attraction corresponding to the elevation difference is then read from the tables. The sum of all these attractions gives the total terrain correction at the station for the density for which the tables are computed. Finally, this sum multiplied by the ratio of the actual density to the table density gives the final correction.

[1] For theory and tables for calculation of terrain corrections, see Hammer, 1939.

The attraction at the station of topography above the elevation of the station has a vertical component which is upward. For compartments below the elevation of the station the effect also is upward because of the absence of the attraction of the material in this space that was assumed present in making the simple Bouguer correction. Therefore, the effect at the station of topography either above or below the elevation of the station is upward (tends to decrease the gravity value), and the terrain correction itself, therefore, always is positive.

Details of the computation of terrain correction tables with numerical results are given in Appendix II, page 144.

DETERMINATION OF SURFACE DENSITIES

Both the Bouguer correction and the terrain correction depend on the density of the surface material within the range of the
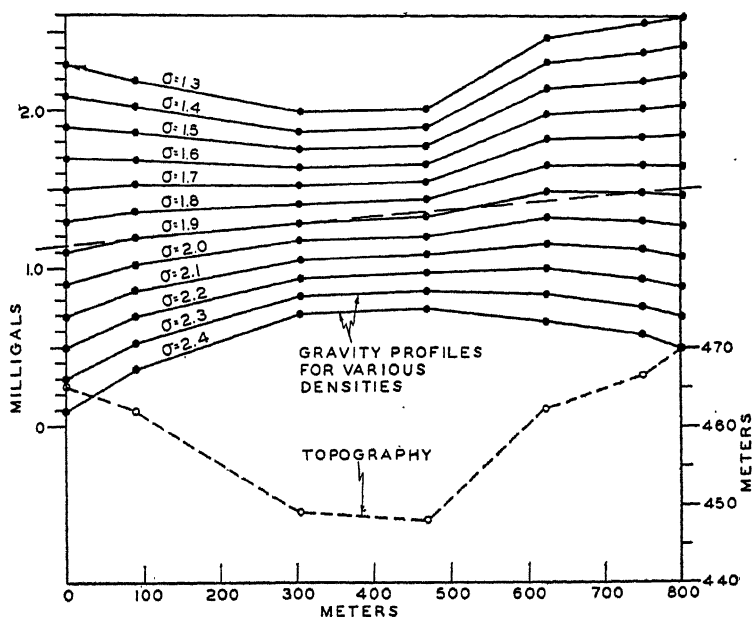
FIG. 27.—Density profile for measurement of surface density with a gravimeter. This profile indicates a density of 1.9.

elevation differences of the survey. Therefore, some sort of estimate or measurement of surface densities must be made.

An estimate can be made from actual density measurements of samples of the surface material. However, it takes a con-

siderable amount of sampling and a large number of measurements to give reliable density values.

Another and commonly fairly satisfactory method is to run a "density profile" with the gravimeter.[1] This consists of taking a series of closely spaced stations over a local topographic irregularity, preferably a hill or valley or both. The gravity values are then reduced for different densities. The criterion for the actual density (Fig. 27) is that which gives the smoothest reduced gravity profile across the topographic irregularity. The method has the advantage that it samples a comparatively large mass of material. It has the disadvantage that very accurate gravity differences are needed, especially if the topographic relief is small. However, this latter disadvantage is compensated to a certain extent because, where the relief is small, a larger error of density is tolerable and, where the relief is large, a more accurate measurement of the density can be made.

In regions where a gravity survey extends across outcrops of rocks of different density, it may be necessary to use variable densities for the reduction of different parts of the survey. In such a case, if the reduction is properly made, it is necessary to make an estimate of the thicknesses of the different beds considered and reduce different elements of the topography with different elevation constants.

TIDAL EFFECTS

The gravitational effects of the sun and moon which produce ocean tides are sufficient to have barely appreciable effects on a gravimeter. The gravitational amplitude of these effects varies with time and latitude, as it depends on the astronomical positions of the sun and moon.[2] The maximum amplitude is about 0.3 mg. At times of maximum amplitude, the change occurs with a period of about 24 hr. At other times, the period is about 12 hr., but the amplitude is smaller (see Figs. 28a and 28b). The maximum rate of change of gravity from tidal effects is only about 0.05 mg. per hour.[3]

---

[1] Nettleton, 1939.

[2] For detailed theory and explanation of tide predictions see Schureman, 1924.

[3] A comparison of observed and theoretical tidal curves is given in Wyckoff, 1936.

Since in most gravimeter operations the instrument is returned to a subbase at intervals of at most a few hours, any tidal effect appears only as a slight modification of the drift curve and therefore does not affect the gravity difference determination. Conse-
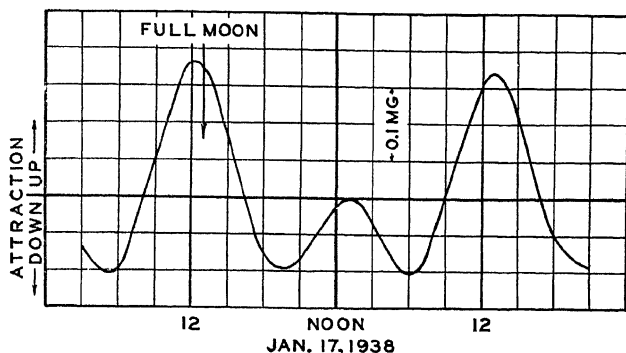
Fig. 28a.—Theoretical tide-producing gravitational attraction at time of full moon. Calculated on tide-predicting machine 2, by courtesy of the U.S. Coast and Geodetic Survey.
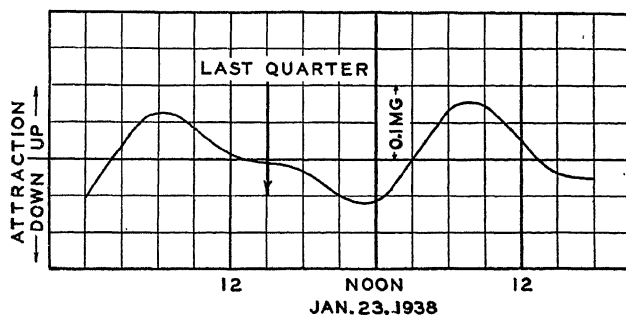
Fig. 28b.—Same as Fig. 28a but calculated at time when moon is in last quarter.

quently, in ordinary gravimeter operations no attention need be given to tidal effects. If an instrument were used for a period of 6 hr. or more without a drift reading, and if it were stable enough so that its drift could be interpolated reliably to 0.1 mg. or better over that period, and if gravity differences were being depended on to better than 0.1 mg., then it would be necessary to consider the tidal effects.

EXAMPLE OF REDUCTION OF GRAVITY VALUES

An actual example of a few gravity stations with all corrections is shown by Figs. 29 and 30. These are experimental gravimeter stations made near the Gulf Research Laboratory.

Figure 29 is from the topographic map of the area and shows the location of a line of stations (designated by letters) which crosses the Allegheny River valley. The outline of the zone chart, for calculating the terrain correction, is shown for station *G* only.
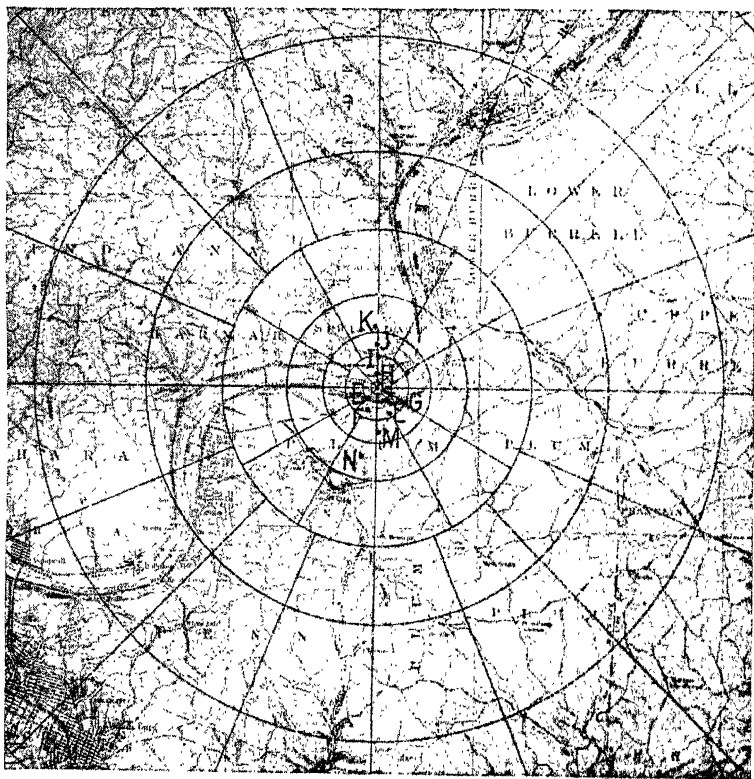
FIG. 29.—Experimental gravimeter station locations near Harmarville (Allegheny County), Pa., with zone chart in place for calculation of terrain correction for station *G* on north bank of Allegheny River.

The data on the stations and the corrections are given by the table on page 61. Station *G* was considered the base, and all gravity values and corrections are referred to that station.

A profile of the stations with the observed gravity and the various corrections and corrected gravity values is shown by Fig. 30. In the table below and the profile, the elevation and Bouguer corrections have been left separate and not combined

Station	Elevation, ft.	Obs. grav. re sta. G, mg.	Lat. corr. re sta. G, mg.	Obs. grav. + lat. cor. mg.	Free-air cor., mg.	Free-air grav., mg.	Bouguer cor., (σ=2.4) mg.	Bouguer grav., mg.	Terrain cor., mg.	Final cor. grav. mg.
K	991	−12.38	−1.49	−13.87	+21.63	+ 7.76	− 7.04	+ .72	+ 07	+ .79
J	1017	−14.97	−1.04	−16.03	+24.08	+ 8.05	− 7.84	+ .21	+ .23	+ 44
I	877	− 5.97	− .74	− 6.71	+10.91	+ 4.20	− 3.55	+ .65	+ .13	+ .78
H	785	− .92	− .30	− 1.22	+ 2.26	+ 1.04	− .73	+ .31	+ .20	+ .51
G	761	0	0	0	0	0	0	0	+ .77	+ .77
E	781	− 2.50	+ .22	− 2.28	+ 1.88	− .40	− 0.61	−1.01	+2.33	+1.32
F	1289	−35.37	+ .44	−34.93	+49.66	+14.73	−16.17	−1.44	+2.78	+1.34
L	1266	−31.98	+ .57	−31.41	+47.50	+16.09	−15.47	+ .62	+1.24	+1.86
M	1240	−30.14	+ .89	−29.25	+45.05	+15.80	−14.67	+1.13	+ .53	+1.66
N	1134	−23.58	+1.48	−22.10	+35.08	+12.98	−11.42	+1.56	+ .24	+1.80

(as is common practice) in order to show the relative magnitudes of the different corrections.

This particular example shows some stations that would be considered poorly located for a geophysical survey. This applies
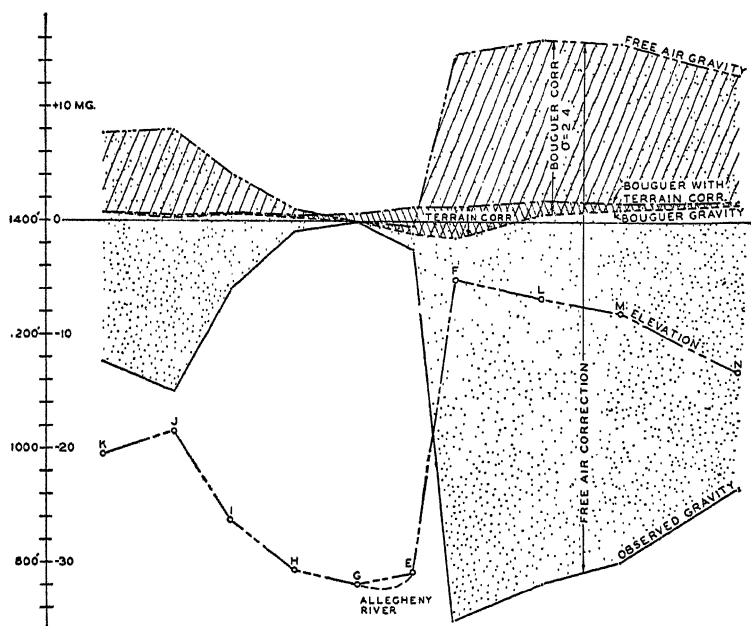
FIG. 30.—Profile of experimental gravity stations, showing elevation, observed gravity, and gravity values after successive reductions for free-air, Bouguer, and terrain effects.

particularly to stations E and F which are at the bottom and top of the high bluff at the river bank and have very large terrain corrections. Terrain corrections of this magnitude are difficult to calculate accurately from the zone chart, and the corrections used were calculated, in part, with the aid of a dot chart (see page 115). However, by selecting a location back from the bluff and with relatively flat topography near the site, such as station H, the terrain correction can be greatly reduced and can be calculated quite accurately with a zone chart. Thus, if some freedom in choice of station locations is allowed, fairly good gravity stations may be made in moderately rough topography.

CHAPTER V

THE EÖTVÖS TORSION BALANCE

The torsion balance is an instrument that measures the distortion, or warping, of the gravitational field rather than the intensity of the field, such as is measured by the gravimeter and pendulum. It was invented by Baron Roland von Eötvös,[1] a Hungarian physicist, about 1880. Eötvös was interested in measuring the space variations of gravity as a measure of the departure of the shape of the earth from a spherical form. The instrument was first used in geological prospecting in 1915 and was first introduced into the United States for oil prospecting in 1922. It has been used for geophysical prospecting much longer and more extensively than the direct gravity measuring instruments. From the standpoint of its basic theory it is considerably more complicated than those instruments.

FIG. 31.—Moving system of Z-beam torsion balance.

The essential elements of a torsion balance are a pair of masses m_1 and m_2 (Fig. 31) suspended by a sensitive torsion fiber τ and supported so that they are displaced both horizontally and vertically from each other. If the gravitational field is not perfectly uniform, there will be a very slight difference in the direction of the gravitational force on the two weights. This slight difference in direction causes slight horizontal force components on the two weights which tend to rotate the suspended system about the suspending fiber. By measuring the rotation produced, it is possible to calculate the amount of distortion of the gravitational field and to infer something as to the nature of

[1] Eötvös, 1896, 1909.

ιe mass irregularities that have produced the gravitational
.sturbance.

· DISTORTION OF THE GRAVITATIONAL FIELD

Let us consider the manner in which an otherwise uniform
ravity field would be distorted by a local mass irregularity.
α Fig. 32 the small arrows represent the gravitational effects

FIG. 32.—Distortion of gravitational field by a disturbing mass.

due to the disturbing mass (represented as a sphere), and the
larger arrows show the resultant of this, together with the much
larger uniform vertical field of the earth. We see that the
normal field will be increased slightly and deflected toward the
disturbing excess mass. Now a level surface is, by definition,
perpendicular to the direction of gravity. If we indicate a level
surface by a line perpendicular to the gravitational vectors, this

the mass irregularities that have produced the gravitational disturbance.

· DISTORTION OF THE GRAVITATIONAL FIELD

Let us consider the manner in which an otherwise uniform gravity field would be distorted by a local mass irregularity. In Fig. 32 the small arrows represent the gravitational effects
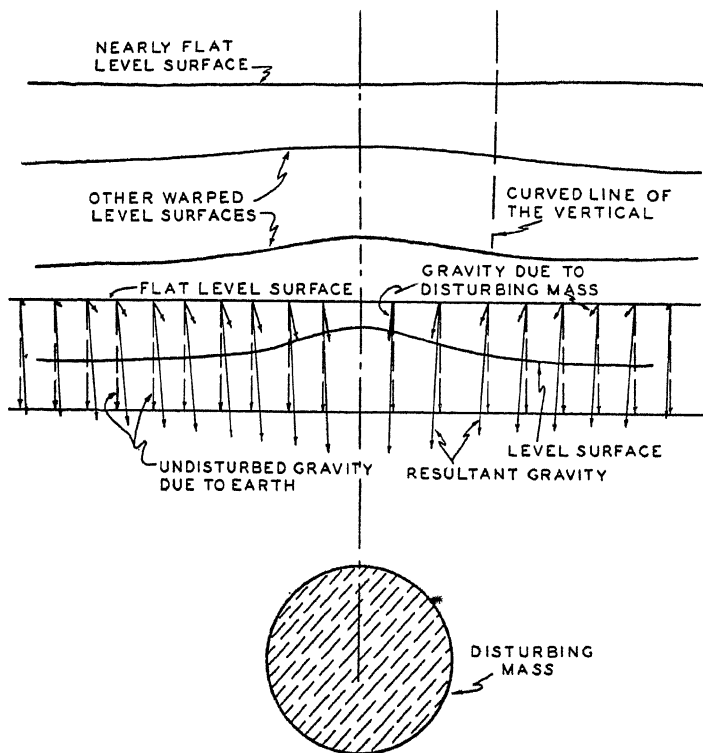
FIG. 32.—Distortion of gravitational field by a disturbing mass.

due to the disturbing mass (represented as a sphere), and the larger arrows show the resultant of this, together with the much larger uniform vertical field of the earth. We see that the normal field will be increased slightly and deflected toward the disturbing excess mass. Now a level surface is, by definition, perpendicular to the direction of gravity. If we indicate a level surface by a line perpendicular to the gravitational vectors, this

line will be curved up in a "hump" over the disturbing mass. If we draw successive level surfaces farther and farther away (upward) from the disturbing mass, this hump in the level surface will gradually disappear until finally the level surface will be horizontal. The line of the vertical is perpendicular to the level surface. Therefore, in going upward away from the disturbing mass the line of the vertical is curved. This curvature of the vertical is what produces the horizontal forces to which the torsion balance responds.

Let us consider the beam system of a torsion balance to be suspended in a region where the vertical is curved (Fig. 33). The gravitational forces acting on the two masses are F_1 and F_2. Because the vertical (direction of gravity) is curved, these two forces are not strictly parallel and hence have horizontal components H_1 and H_2 which exert a torque on the suspension.

The picture outlined above is somewhat oversimplified. To calculate more exactly the
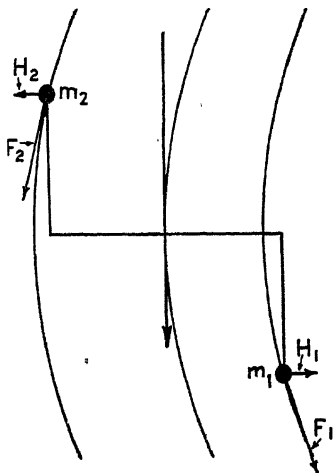
FIG. 33.—Torsion balance beam in a curved field of force.

relation of the torque on the beam to the quantities expressing the space variations of the gravitational field, we must define these quantities.

The Gravitational Potential.—In general, in mathematical theory, a "potential" is a mathematical expression such that its derivative or rate of change in any particular direction is a force of some kind in that direction. The gravitational potential U, referred to in the following, is a function of space such that its partial derivative (or rate of change) in any direction is the gravitational force in that direction.[1] Thus, if we let X, Y, and

---

[1] In connection with electricity, magnetism, etc., where elements of like sign repel, the potential is the negative of the force function and is identical with the potential energy. However, if elements of like sign attract, as in gravitation, the potential is the force function and the negative of the potential energy. See Kellogg, 1929, p. 53.

Z represent components of the gravitational force vectors in the x, y, and z coordinate directions, respectively,

$$X = \frac{\partial U}{\partial x}; \qquad Y = \frac{\partial U}{\partial y}; \qquad Z = \frac{\partial U}{\partial z} \qquad (27)$$

If the z coordinate is taken vertically downward, $\partial U/\partial z = g_z$ is the ordinary gravitational force.

Second Derivative of the Potential.—In connection with the torsion balance quantities we need to consider the second partial derivatives of the potential. Thus, the variation in, for instance, the vertical component g_z of gravity between two points a distance Δx apart is given by $(\partial g_z/\partial x)\Delta x$. But since g_z is already a partial derivative of the potential in the direction z, the variation in g_z over the distance Δx may be expressed as

$$\frac{\partial}{\partial x}\left(\frac{\partial U}{\partial z}\right)\Delta x = \left(\frac{\partial^2 U}{\partial x\, \partial z}\right)\Delta x = U_{zx}\, \Delta x \qquad (28)$$

where U_{zx} is simply an abbreviation for $\partial^2 U/\partial x^2$. Similarly, the variation of the vertical component of gravity between two points at a distance Δy apart would be

$$\frac{\partial}{\partial y}\left(\frac{\partial U}{\partial z}\right)\Delta y = \left(\frac{\partial^2 U}{\partial y\, \partial z}\right)\Delta y = U_{yz}\, \Delta y \qquad (29)$$

Now we may take the space derivative of any component in any direction. Thus, the variation in the horizontal component X might be considered in going in any of the coordinate directions. Let us consider, for instance, that the horizontal force component X is zero at a certain point but changes in space as we go away from that point. Then if we go to another point with coordinates Δx, Δy, and Δz, the value of X at this point will be given by the rate of variation of X along each of the three coordinate directions times the distance we go in those directions. Thus, the value of X at the point with coordinates Δx, Δy, and Δz will be

$$(X)_{\Delta x, \Delta y, \Delta z} = \frac{\partial}{\partial x}\left(\frac{\partial U}{\partial x}\right)\Delta x + \frac{\partial}{\partial y}\left(\frac{\partial U}{\partial x}\right)\Delta y + \frac{\partial}{\partial z}\left(\frac{\partial U}{\partial x}\right)\Delta z$$
$$= U_{xx}\, \Delta x + U_{xy}\, \Delta y + U_{xz}\, \Delta z \qquad (30)$$

Similarly,

$$(Y)_{\Delta x, \Delta y, \Delta z} = U_{yx}\, \Delta x + U_{yy}\, \Delta y + U_{yz}\, \Delta z$$

With these definitions in mind, let us consider the horizontal forces acting on the torsion balance.

THE TORQUE ON THE TORSION BALANCE BEAM

The z-axis (Fig. 34) is taken as the direction of the vertical at the center of gravity of the suspended system. The x- and y-axes will be taken as north and east, respectively. At the center of gravity, there will be no horizontal force components
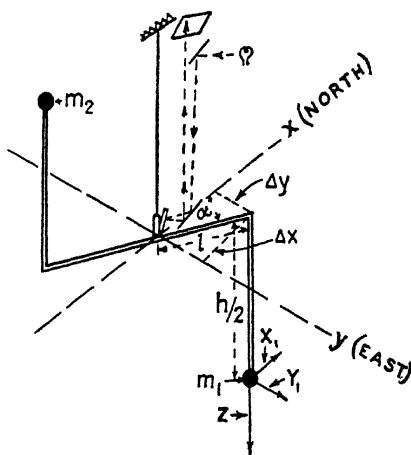
FIG. 34.—Diagram for analysis of torque-producing forces on a torsion balance beam.

because the balance hangs freely on the torsion wire so that

$$X_0 = 0; \qquad Y_0 = 0; \qquad Z_0 = g \qquad (31)$$

At the two masses m_1 and m_2 there will, in general, be horizontal force components, such as X_1 and Y_1, at mass m_1. These horizontal force components exert a torque tending to twist the torsion wire. If we let T_1 = torque from forces on m_1, T_2 = torque from forces on m_2, from the symmetry of the moving system, $T_1 = T_2$ and the total torque $T = 2T_1$.

Now the torque (in a clockwise direction) from the forces on m_1 is

$$T_1 = m_1 Y_1 \Delta x - m_1 X_1 \Delta y \qquad (32)$$

where Δx and Δy are the perpendicular distances at which the force components Y_1 and X_1 act.

If we consider the distances Δx, Δy, Δz as measured from the center of gravity where $X_0 = 0$, $Y_0 = 0$ [Eq. (31)], then, by Eq. (30), Eq. (32) becomes

$$\frac{T_1}{m_1} = \Delta x \left(U_{xy}\Delta x + U_{yy} \Delta y + U_{yz} \Delta z \right) -$$

$$\Delta y(U_{xx} \Delta x + U_{xy} \Delta y + U_{xz} \Delta z)$$
$$= [(\Delta x)^2 - (\Delta y)^2]U_{xy} + \Delta x \, \Delta y(U_{yy} - U_{xx}) + \Delta x \, \Delta z U_{yz} -$$
$$\Delta y \, \Delta z U_{xz} \quad (33)$$

But, from the diagram (Fig. 34) it is evident that

$$\Delta x = l \cos \alpha; \qquad \Delta y = l \sin \alpha; \qquad \Delta z = \frac{h}{2}$$

where l = the half length of the horizontal part of the balance
      arm.

    h = the vertical separation of the two masses.

    α = the angle between the balance arm and the x-axis.
Thus Eq. (33) becomes

$$\frac{T_1}{m_1} = l^2(\cos^2 \alpha - \sin^2 \alpha)U_{xy} + l^2 \cos \alpha \sin \alpha(U_{yy} - U_{xx}) +$$

$$\frac{h}{2} l \cos \alpha U_{yz} - \frac{h}{2} l \sin \alpha U_{xz} \quad (34)$$

If we abbreviate $(U_{yy} - U_{xx}) = U_\Delta$, and since

$$\cos^2 \alpha - \sin^2 \alpha = \cos 2\alpha;$$

$$\cos \alpha \sin \alpha = \sin 2\alpha/2,$$

Eq. (34) may be written as

$$\frac{T_1}{m_1} = l^2 \cos 2\alpha \cdot U_{xy} + \frac{l^2}{2} \sin 2\alpha \cdot U\Delta + \frac{h}{2} l \cos \alpha \cdot U_{yz} -$$

$$\frac{h}{2} l \sin \alpha \cdot U_{xz}$$

The total torque T on the beam is $2T_1$, which, on dropping the subscripts for the two different weights, may be written

$$T = mhl(U_{yz} \cos \alpha - U_{xz} \sin \alpha) +$$
$$ml^2(2U_{xy} \cos 2\alpha + U_\Delta \sin 2\alpha) \quad (35)$$

The angular rotation θ produced by the torque T acting on the torsion wire with a torque constant τ (dyne centimeters per

radian) is

$$\theta = \frac{T}{\tau} \qquad (36)$$

The deflection of the spot of light on a photographic plate at a distance D from the mirror on the balance beam is

$$n - n_0 = 2ND\theta$$
$$= \frac{2NDT}{\tau} \qquad (37)$$

where n_0 is the position the light beam would have if there were no torque acting on the suspended system, n is the deflected position, and N is the number of reflections from the mirror on the moving system (see page 75). Finally, substituting for T from Eq. (35),

$$n - n_0 = \frac{2NDmhl}{\tau} (U_{yz} \cos \alpha - U_{xz} \sin \alpha) +$$
$$\frac{2NDml^2}{\tau} (2U_{xy} \cos 2\alpha + U_\Delta \sin 2\alpha)$$
$$= P(U_{yz} \cos \alpha - U_{xz} \sin \alpha) +$$
$$Q(2U_{xy} \cos 2\alpha + U_\Delta \sin 2\alpha) \qquad (38)$$

where $P = 2NDmhl/\tau$ and $Q = 2NDml^2/\tau$, so that P and Q are fixed constants of the instrument.

DETERMINATION OF THE GRAVITATIONAL QUANTITIES FROM THE BEAM DEFLECTIONS

Equation (38) contains four unknown gravitational quantities (U_{yz}, U_{xz}, U_{xy}, and U_Δ); also n_0 is not reliably constant and must be determined with each setup of the instrument. This makes a total of five unknown quantities. For each value of α there is an independent equation like (38). Thus, if we make measurements at five different α's, we have five independent equations which can be solved for the five unknown quantities.

The actual balance always is double and has two parallel beams with the hanging weights at opposite ends. Thus, for the second beam the angle α always differs by 180 deg. from that of the first beam. For each setting of the balance there are, therefore, two values of α and two equations like Eq. (38).

However, a second n_0 is introduced so that now there are six unknowns. A minimum of three positions of the balance is therefore required to give six values of α for the solution of the six unknown quantities.

In practice the three positions that are used are predetermined and symmetrical. The balance is first oriented to the north, and a reading taken. It is then turned 120 deg., and another reading is taken. It is then turned another 120 deg., and a third reading taken. These three readings are theoretically adequate to determine the six unknowns. In practice it is usual to take at least one and sometimes several more readings which serve as checks.
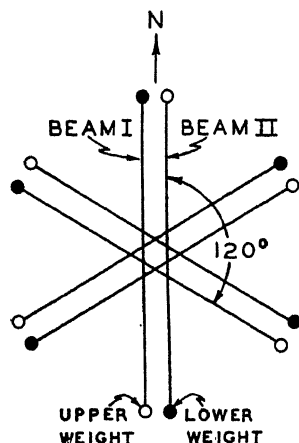
Fig. 35.—Successive positions of double-beam torsion balance in normal three-position operation.

Let the diagram (Fig. 35) represent the two beams in each of the three positions of the balance. From the values of α for each beam in each position we can insert the values for the sine and cosine of α and 2α in Eq. (38), as given in the table below.

The three symmetrical balance positions give six equations that can be solved simultaneously for the four gravitational quantities and the two unknown zero positions. Without carry-

FORMULAS FOR THREE POSITIONS

Position	1	2	3	1	2	3
Angle α, degrees...	0	120	240	180	300	60
Point on plate.....	n_1	n_2	n_3	n_1'	n_2'	n_3'
$\sin \alpha$............	0	0.866	−0.866	0	−0.866	0.866
$\cos \alpha$............	1	−0.500	−0.500	−1	0.500	0.500
$\sin 2\alpha$............	0	−0.866	0.866	0	−0.866	0.866
$\cos 2\alpha$............	1	−0.500	−0.500	1	−0.500	−0.500

ing out the details of the algebra, the results are as follows where the unprimed quantities refer to beam I and the primed quantities to beam II:

$$U_{xz} = \frac{0.577a'}{ab' + a'b} \left(\Delta_2 - \Delta_3 \right) - \left(\Delta_2' - \Delta_3' \right) - \left(\frac{a}{a'} - 1 \right) \left(\Delta_2' - \Delta_3' \right)$$

$$U_{yz} = \frac{a}{ab' + a'b} \left(\Delta_2 + \Delta_3 \right) - \left(\Delta_2' + \Delta_3' \right) - \left(\frac{a}{a'} - 1 \right) \left(\Delta_2' + \Delta_3' \right) \Bigg\}$$ (39)

$$U_\Delta = \frac{0.577b'}{ab' + a'b} \left(\Delta_2 - \Delta_3 \right) + \left(\Delta_2' - \Delta_3' \right) + \left(\frac{b}{b'} - 1 \right) \left(\Delta_2' - \Delta_3' \right)$$

$$2U_{xy} = \frac{b'}{ab' + a'b} \left(\Delta_2 + \Delta_3 \right) + \left(\Delta_2' + \Delta_3' \right) + \left(\frac{b}{b'} - 1 \right) \left(\Delta_2' + \Delta_3' \right)$$

(Note that the right-hand terms vanish if the constants for the beam systems are equal.)

The Δ's are the deflections from the zero position, thus:

$$\Delta_1 = n_1 - n_0; \quad \Delta_2 = n_2 - n_0; \quad \Delta_3 = n_3 - n_0 \Big\}$$
$$\Delta_1' = n_1' - n_0'; \quad \Delta_2' = n_2' - n_0'; \quad \Delta_3' = n_3' - n_0' \Big\}$$ (40)

and since

$$\frac{n_1 + n_2 + n_3}{3} = n_0; \qquad \frac{n_1' + n_2' + n_3'}{3} = n_0'$$

we must have

$$\Delta_1 + \Delta_2 + \Delta_3 = 0; \qquad \Delta_1' + \Delta_2' + \Delta_3' = 0$$ (41)

Also

$$2a = \frac{2NDK}{\tau} = Q; \qquad 2a' = \frac{2ND'K'}{\tau'} = Q'$$

where K = moment of inertia of moving system about the axis of suspension, and

$$b = \frac{2NKlmh}{\tau} = P; \qquad b' = \frac{2ND'l'm'h'}{\tau'} = P'$$ (42)

The constants a, a', b, and b' are physical constants of the instrument. They must be determined for each beam of the balance. Once they are determined, they remain fixed unless there is a major readjustment of the balance, such as replacing a broken suspension wire.

For routine field operation the balance is nearly always used in the three positions, and the torsion balance quantities calculated as shown above. However, other values of α can be used. For instance, with four symmetrical values of α differing by 90 deg., the U_{xz} and U_{yz} terms can be calculated separately from each beam:

$$
\left.
\begin{aligned}
U_{xz} &= -\frac{n_4 - n_2}{2b} = \frac{n_4' - n_2'}{2b'} \\
U_{yz} &= +\frac{n_3 - n_1}{2b} = \frac{n_3' - n_1'}{2b'}
\end{aligned}
\right\}
\tag{43}
$$

where, as before, unprimed characters refer to beam I, primed to beam II.

With five symmetrical positions of α, differing by 72 deg., each of the four torsion balance quantities can be determined from each beam; *i.e.*,

$$
\left.
\begin{aligned}
U_{xz} &= \frac{1}{b}\,0.3804(n_2 - n_5) + 0.2351(n_3 - n_4) \\
U_{yz} &= \frac{1}{b}\,0.3236(n_5 + n_3 - 2n_1) - 0.1236(n_5 + n_2 - 2n_1) \\
U_\Delta &= \frac{1}{a}\,0.2351(n_2 - n_5) - 0.3804(n_3 - n_4) \\
2U_{xy} &= \frac{1}{a}\,0.1236(n_4 + n_3 - 2n_1) - 0.3236(n_5 + n_2 - 2n_1)
\end{aligned}
\right\}
\tag{44}
$$

These equations are for beam I. For beam II the signs of the U_{xz} and U_{yz} (gradient) terms must be reversed.

TORSION BALANCE INSTRUMENTS AND FIELD OPERATIONS

Although its fundamental parts are simple, the practical torsion balance field instrument is a quite precise and moderately complex piece of apparatus. The extreme sensitivity of the torsion fiber requires special protection from temperature irregularities which would produce convection currents in the surrounding air of sufficient magnitude to disturb the instrument. For this reason, the instrument is commonly built with three separate metal cases, one inside the other, thermally insulated from one another, to insure temperature uniformity and absence of air convections in the inner case holding the moving system itself. The sensitivity of the system to slight disturbances may be appreciated from the fact that the torsion period of a balance may be as much as 25 *min.* The instrument itself is nearly always placed in a protecting house, or "hut," during the time required for an observation.

Modern torsion balances are usually self-recording and entirely automatic in their operation. Clockworks are provided which rotate the balance from one position to another, turn on a small electric lamp to record the balance position on a photographic plate, etc. Because of the long period of the suspended system, it is necessary for the instrument to wait for a period of 20 min. to 1 hr. (depending on the type of instrument) after it is disturbed, before the moving system comes to rest and its position can be recorded.

The operations of making a torsion balance observation are as follows:

A base plate is set on three stakes, the hut erected over this plate; the instrument is set on the plate, oriented with a compass (to give a reference direction from which the angle α is measured), and leveled. A photographic plate is inserted in the instrument, and the clocks and stops properly set. The balance system is let down on to the suspending wire. The operator then leaves the instrument alone. At the end of a certain period (20 min. to 1 hr.) a clock makes an electric contact which turns on a small light for about 1 min. A beam of light, reflected from a mirror on the moving system, is focused on the photographic plate and records the position of the beam by the spot of light on the plate. The clock next turns off the light and starts a spring motor which slowly rotates the entire main body of the instrument through a predetermined angle (120 deg. for a three-position observation). The instrument then stands for another period during which the moving system comes to rest again. At the end of this period, the light is turned on again; another spot is recorded on the plate which measures the deflection of the beam in the second position. Then the whole operation is repeated with the balance turning itself another 120 deg. to the third position. If the balance is left alone, it will continue these operations until the clocks run down (12 to 15 positions). Usually (for a three-position observation) the instrument is let run for four or five periods, the extra ones (beyond the minimal three) serving as checks. When he returns to the instrument, the operator usually develops the plate (in the hut or in a special developing box) to see that a proper recording has been made. The instrument is then packed in its carrying case, and the hut and instrument are loaded on a light truck and moved on to the next station.

TYPES OF TORSION BALANCE INSTRUMENTS

A number of different sizes and types of torsion balances have been built by different instrument makers at different times.

FIG. 36.　　　　　　　FIG. 37.　　　　　　　FIG. 38.

FIG. 36.—Exterior view and schematic diagram of moving system of large torsion balance. (*Photograph courtesy American Askania Co.*)
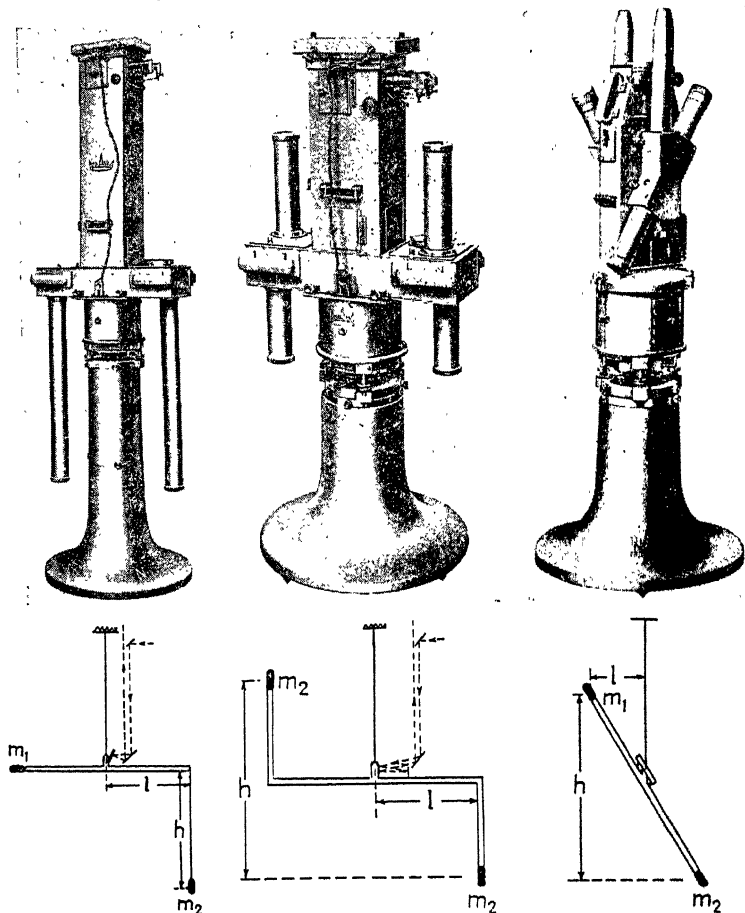
FIG. 37.—Exterior view and schematic diagram of moving system of Z-beam torsion balance. (*Photograph courtesy American Askania Co.*)

FIG. 38.—Exterior view and schematic diagram of moving system of inclined-beam torsion balance. (*Photograph courtesy American Askania Co.*)

By far the greatest number of instruments have been made in Germany and Hungary. No commercial torsion balance has

been made in America. In recent years considerable effort has been devoted to reducing the size of the balance so as to increase the ease of portability and also to reduce the period of the moving system so as to reduce the time required for an observation.

Three somewhat different types of moving system have been used, as indicated by the diagrams (Figs. 36, 37, 38). For one manufacturer's instruments[1] the constants are approximately as given below.

Large torsion balance (see Fig. 36)	Z-beam balance (see Fig. 37)	Inclined-beam balance (see Fig. 38)
$m = 30$ g.	$m = 22$ g.	$m = 40$ g.
$l = 20$ cm.	$l = 20$ cm.	$l = 10$ cm.
$h = 60$ cm.	$h = 45$ cm.	$h = 35$ cm.
$\tau = 0.5$ dyne cm./ radian	$\tau = 0.44$	$\tau = 1.2(0.6)*$
$K = 25{,}000$ g. cm.^{2}	$K = 17{,}600$ g. cm.^{2}	$K = 8{,}000$ g. cm.^{2}
$D = 75$ cm. $= 1{,}500$ ½-mm. units	$D = 46$ cm. $= 920$ ½-mm. units	$D = 75$ cm. $= 1{,}500$ ½-mm. units
$N = 1$	$N = 2$	$N = 2$
$T = 1{,}500$ sec.	$T = 1{,}250$ sec.	$T = 510$ sec. (720)*
$P = 2Dmhl/\tau =$ $0.216 \cdot 10^9$	$P = 2NDmhl/\tau =$ $0.16 \cdot 10^9$	$P = 2NDmhl/\tau =$ $0.07 \cdot 10^9$ $(0.14 \cdot 10^9)*$
$Q = 2DK/\tau =$ $0.15 \cdot 10^9$	$Q = 2NDK/\tau =$ $0.15 \cdot 10^9$	$Q = 2NDK/\tau =$ $0.04 \cdot 10^9$ $(0.08 \cdot 10^9)*$
Time per position = 60 min.	Time per position = 40 min.	Time per position = 20 min. (30 min.)*

* Numbers in parentheses refer to constants with optional torsion wire with smaller value of τ.

In the large balance, the horizontal beam is a light aluminum tube with the weight m_1 (cylindrical in form) attached rigidly to one end. The hanging weight m_2 is suspended on a wire from the other end of the beam. In the Z-beam and inclined-beam balances, both weights are fixed rigidly to the light tubular aluminum beam. Both these balances also use a double reflection of the light path ($N = 2$) so that the angular deflection of the reflected light is four times the angular deflection of the balance beam.

[1] American Askania Co., 1936.

The backbone of a torsion balance is the torsion wire, and the satisfactory performance depends on having a wire which does not drift and which has a small temperature coefficient of elasticity and of angular position. A special platinum-iridium alloy wire is commonly used. Tungsten wires also are used and are quite satisfactory. The wires are specially heat-treated. Approximate dimensions of some torsion balance wires are shown in the following table:

Balance	Wire material	Diameter, millimeter	Length, centimeter	Torque constant	Ultimate tensile strength, g.
Large Askania...	Platinum-iridium	0.045	54	0.5	200
Large Askania...	Tungsten	0.041	54	0 6	300
Z beam.........	Tungsten	0.025	26	0 47	160

The distances on the photographic plate are commonly measured in $\frac{1}{2}$-mm. units, so the distance D (length of light path from balance mirror to photographic plate) is given in these units. The values for P and Q calculated are he deflections of the spot on the plate produced by 1 c.g s. unit of the second derivatives measured. The Eötvös unit, which is used for measuring the torsion balance quantities is 10^{-9} c.g.s. unit. Thus, the value of P (of the large balance, for example) of 0.216×10^9 means that a gradient of 1 Eötvös unit (if directed perpendicular to the plane of the balance) would produce a deflection of 0.216 unit (of $\frac{1}{2}$ mm.), or an actual deflection of 0.108 mm. at the photographic plate. Thus, by reading positions of the spots on the photographic plate to 0.1 mm. such an instrument can measure gradients to about 1 Eötvös unit.[1]

[1] A special instrument, called a "gradiometer," designed to measure gradients but not curvatures, has been used in some British geophysical work. It was designed to give gradient measurements as accurate as those by an ordinary torsion balance but to have a much shorter period and, therefore, to be capable of making a measurement in a much shorter time. For a very complete and mathematically elegant treatment of the general theory of torsion balances, as developed for the design of the gradiometer, see Lancaster-Jones, 1932.

CALCULATION OF GRAVITATIONAL QUANTITIES
FROM THE TORSION BALANCE PLATE

The values of n_1, n_2, n_3, n_1', n_2', n_3' are usually determined by measurements on a photographic plate on which a spot of light or image of a scale from each beam is recorded for each orientation of the instrument. The same plate commonly carries two
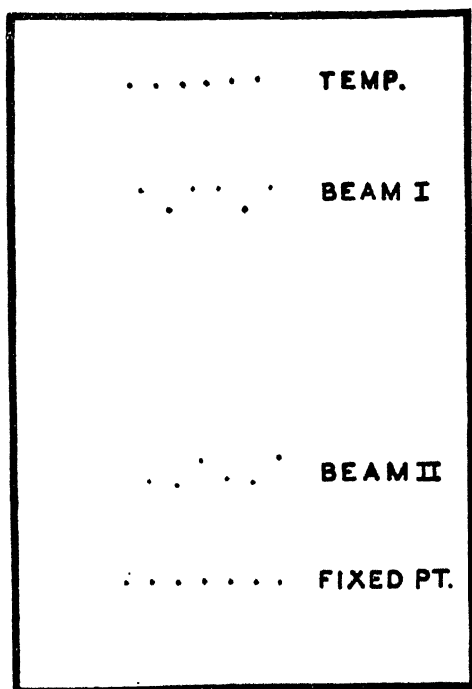
FIG. 39.—Torsion balance plate, normal three-position operation, (full size) made with large Askania torsion balance. Plate shows total of six positions, or two complete revolutions of instrument.

other images for each balance position; one of these is reflected from a mirror carried by a bimetallic thermometer to record the temperature inside the balance, and the other is reflected from a fixed mirror to serve as a reference point from which the deflections are measured.

Figure 39 is reproduced from an actual torsion balance plate made with a large Askania balance. For this particular plate the instrument made a total of six recordings. Figure 40 shows

the same plate under a reading plate ruled with $1\frac{1}{2}$-mm. lines. The distance of each spot from the reference line is read by this ruled plate. Examples of a number of other torsion balance plates are shown by Fig. 41.[1]
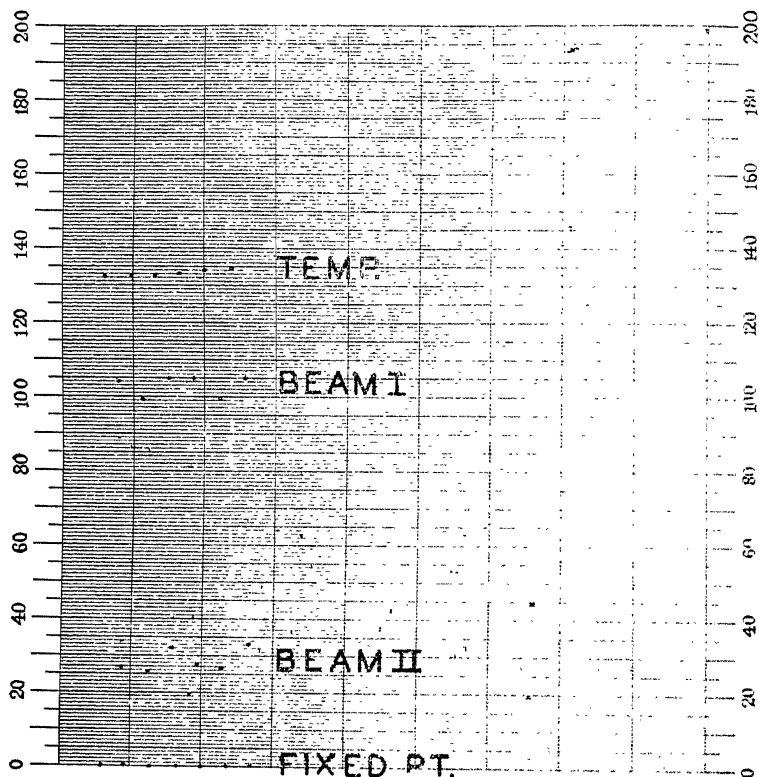
FIG. 40.—Torsion balance plate with reading plate in position for reading deflections.

The measured positions of the spots as read on the ruled plate are entered in a simple computation form, one type of which is shown by Fig. 42. This has been filled out with numerical values as read from the ruled grid in Fig. 40. The figures in the columns n and n' are those read the reading having been made at

[1] On plate 2 of Fig. 41, in the third position from the bottom, it will be noticed that there is an odd dot near the temperature dots. This is caused by beam I sticking to the side of the case. Note the absence of the dot for this position in the record for beam I.

the right-hand edge of the dots.   The numbers in the columns n_0 and n_0' are the average positions (*i.e.*, $n_0 = (n_1 + n_2 + n_3)/3$. It will be noticed that these values are not quite constant; this is the result of a slight temperature effect on the zero point of the instrument, the change in temperature being indicated by the

TORSION BALANCE PLATES
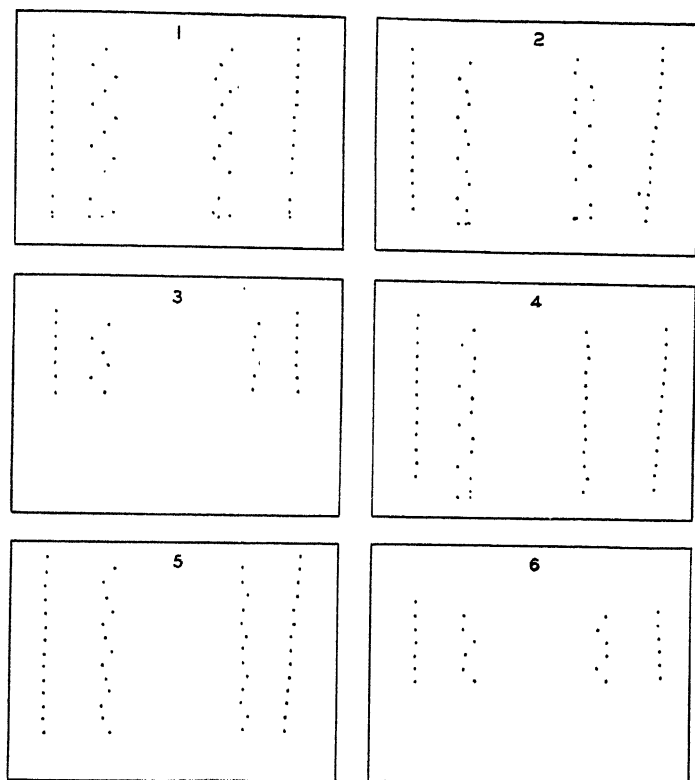
Fig. 41.—Typical torsion balance plates.

slight curvature in the line of temperature dots.   The first and last n_0''s are extrapolated from the general run of the numbers in the four intermediate values where the averages can be determined.   The Δ's ($\Delta_1 = n_1 - n_0$, etc.) are entered in appropriate columns, and the mean Δ's are then entered at the bottom of the table.   As a check, the sum of the mean Δ's should be zero.

The computation of the torsion balance quantities from the Δ's then becomes a simple matter. The sums and differences as indicated are formed and entered above the little tables at the bottom.

STA. NO.
INST. NO.
DATE
LAST POSITION
DISTRICT
COUNTY
STATE
TROOP NO.

FIRST BALANCE

No.	n	n_0	Δ_1	Δ_2	Δ_3
1	106.0	102.1	+1.9		
2	99.0	102.5		-3.5	
3	104.6	102.9			+1.7
1	105.0	103.0	+2.0		
2	99.5	103.2		-3.7	
3	105.2	103.4			+1.8
1					
2					
3					
1					
2					
3					
1					
2					
3					
MEAN Δ			+1.9	-3.6	+1.8

$\Sigma = +1$

SECOND BALANCE

No.	n'	n'_0	Δ'_1	Δ'_2	Δ'_3
1	27.0	28.3	-1.3		
2	26.0	28.5		-2.5	
3	32.5	28.7			+3.8
1	27.7	29.1	-1.4		
2	27.0	29.4		-2.4	
3	33.6	29.7			+3.9
1					
2					
3					
1					
2					
3					
1					
2					
3					
MEAN Δ'			-1.4	-2.5	+3.9

$\Sigma = 0$

$$\Delta_2 - \Delta_3 = -5.4$$
$$\Delta_2 - \Delta'_3 = -6.4$$

DIFF.	x O	=Uxz
+1.0	1.33	+1.3
SUM	x q	=UΔ
-11.8	3.85	-45.4

$$\Delta_2 + \Delta_3 = -1.8$$
$$\Delta'_2 + \Delta'_3 = +1.4$$

DIFF.	x P	=Uyz
-3.2	2.31	-7.4
SUM	x r	=2Uxy
-0.4	6.57	-2.6

	OBS. VALUE	NORMAL VALUE		TERR. CORR.			
Uxz	+1.3	+7.7	-6.4	+1.6	-15.0	2 Uxy	-15.1
Uyz	-7.4			-.69	-2.5	UΔ	-14.2
UΔ	-45.4	+7.0	-52.4	-36.2	-16.2	R	28.9
2Uxy	-2.6			+22.5	-25.1	λ	331°26'

REMARKS:

Fig. 42.—Torsion balance calculation form.

The values o, p, q, and r are simply the coefficients of the bracket terms [Eq. (39), page 71]. If we assume that the two beams are alike and that the values of P and Q are as given in the table of constants for the large torsion balance (page 75), the values

of o, p, q, and r are those entered on the calculation form. Finally the differences

$$(\Delta_2 - \Delta_3) - (\Delta_2' - \Delta_3') \quad \text{and} \quad (\Delta_2 + \Delta_3) - (\Delta_2' + \Delta_3')$$

and the sums

$$(\Delta_2 - \Delta_3) + (\Delta_2' - \Delta_3') \quad \text{and} \quad (\Delta_2 + \Delta_3) + (\Delta_2' + \Delta_3')$$

are entered in the appropriate places and are multiplied by the coefficients o, p, q, or r to give the torsion balance quantities.

The values so obtained (in the example given, $U_{zz} = 1.3$, $U_{yz} = -7.4$, $U_\Delta = -45.4$ and $2U_{xy} = -2.6$) are the observed torsion balance quantities. These are entered in the "Obs. Value" column in the table at the bottom of the sheet. The normal and terrain corrections are then applied to give the corrected gradient and curvature components which are plotted on the map at the point corresponding to the location of the instrument in the field.

A convenient practice is to provide a form on the back of the same sheet for the terrain corrections. Then all the observational and reduction data for each station are given on a single sheet.

THE MEANING OF THE TORSION BALANCE QUANTITIES

We have seen that a torsion balance measures two groups of second derivatives. The first group, U_{zz} and U_{yz}, measures the "gradient"; the second, U_Δ and $2U_{xy}$, measures the "curvature."

The Gradient.—The quantity U_{zz} is the rate of change in the x-direction of the vertical component of gravity or is the component in the x (north) direction of the horizontal gradient of gravity. Similarly, U_{yz} is the y (east) component of the horizontal gradient of gravity. Thus, if we plot U_{zz} in th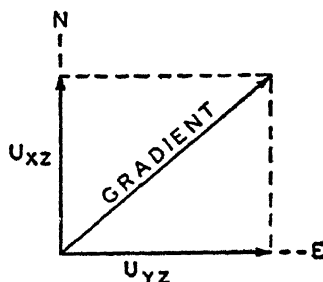e north direction and U_{yz} in the east direction and take the vector sum of these two (Fig. 43), we have a vector the magnitude of which represents the total horizontal gradient of gravity and the direction of which indicates the direction in which the horizontal rate

FIG. 43.—Gradient components.

of change of gravity is a maximum. Thus, a gradient symbol is quite analogous to a strike-and-dip symbol, for the gradient indicates the direction in which gravity changes at its maximum rate in a similar way to that in which the dip arrow indicates the direction in which a stratum is changing in elevation at a maximum rate (in making this analogy, we must remember that the sign convention of the two indications is opposite, for the gravity gradient indicates the direction in which gravity is increasing, whereas a dip symbol indicates the direction in which elevation is decreasing).

Differences in gravity can be computed from the gradient, just as differences in elevation can be computed from dips or slopes. Thus, a difference in gravity between two points is the average gradient between those points multiplied by the distance between them, just as the difference in elevation between two points is the elevation gradient (*i.e.* the tangent of the slope angle) multiplied by the horizontal distance between the two points.

FIG. 44.—Schematic diagram of the Eötvös unit.

The Eötvös Unit.—The unit for measuring gradients and curvatures is the Eötvös unit. It is conveniently defined with reference to the gradient.

One Eötvös unit = 10^{-9} gal per horizontal centimeter. This means that in an area where the gradient is 1 Eötvös unit, the difference in gravity between two points 1 cm. apart is 10^{-9} gal. This may be illustrated by Fig. 44 in which the arrow on the left represents a total value of gravity, assumed exactly 980 gals, and the arrow on the right indicates the increased gravity at a horizontal distance of 1 cm. when the gradient is 1 Eötvös unit.

The Curvature.—The quantities U_{xy} and U_Δ (or $U_{yy} - U_{xx}$) are closely related to the curvature of the equipotential or level surface. When the gravitational field is distorted, the level surfaces are curved. Over small distances (of the order of magnitude of the dimensions of the torsion balance) the level surface may be considered as a second-order surface. There is a theorem of differential geometry which shows that, in general, through any point on a curved surface two planes can be passed, in one of which the radius of curvature is a maximum and in the other of which the radius of curvature is a minimum, and that

these two planes are mutually perpendicular.[1] We shall refer to these as the "principal planes." For the moment let us consider the special case in which the x- and y- axes are taken in the directions of these principal planes. We can then represent the curved level surface and the principal planes as in Fig. 45.

Let the direction of the vertical and the value of gravity at the points a, b, c, d, be g_a, g_b, g_c, g_d, respectively. Also, let ρ_1 and ρ_2
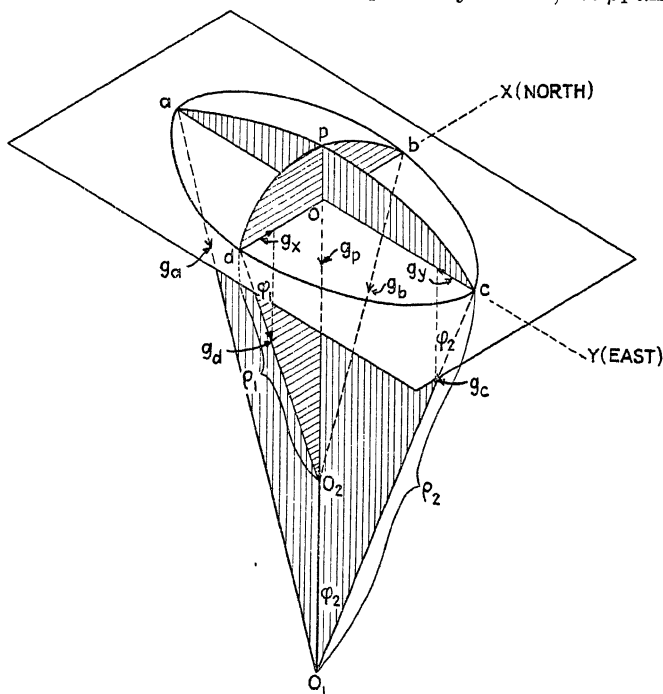
FIG. 45.—Curved equipotential surface and horizontal gravitational forces.

be the radii of curvature in the two principal planes. Now, remembering that the gravity vector is always perpendicular to the level surface, and considering the horizontal dimensions of the figure as small differentials over which the second derivatives of the potential are constant, we have the following relations:

The small horizontal gravity component g_y is the rate of change of the horizontal force in the y-direction $\left[\dfrac{\partial}{\partial y} \left(\dfrac{\partial U}{\partial y} \right) = U_{yy} \right]$ times

[1] For a proof using only the fundamental ideas of the differential calculus, see Slotnick. 1932.

the horizontal distance oc.   Thus

$$g_y = -U_{yy} \cdot oc \tag{45}$$

But this same horizontal force is the projection of the slightly inclined total gravity g_c, so that

$$
\begin{aligned}
g_y &= g_c \sin \varphi_2 \\
&= g_c \frac{oc}{\rho_2} \qquad \left(\text{for } \sin \varphi_2 = \frac{oc}{\rho_2} \right)
\end{aligned}
\tag{46}
$$

Equating (45) and (46),

$$-U_{yy} \cdot oc = g_c \frac{oc}{\rho_2}$$

$$U_{yy} = -\frac{g_c}{\rho_2}$$

Similarly,

$$U_{xx} = -\frac{g_d}{\rho_1}$$

Then for this special case of the principal planes in the x- and y-axes, and since, very nearly, $g_c = g_d = g$,

$$U_{yy} - U_{xx} = g \left(\frac{1}{\rho_1} - \frac{1}{\rho_2} \right) \equiv \Re \tag{47}$$

For this special choice of axes the other curvature component U_{xy} is zero.   The quantity $g \left(\dfrac{1}{\rho_1} - \dfrac{1}{\rho_2} \right)$ is the "differential curvature" (or "horizontal directive tendency," or H.D.T., of some of the English writers).[1]   We see that this quantity is the acceleration of gravity times the difference in the curvatures in the two principal planes.   For a spherical level surface the two radii of curvature are equal, and the differential curvature is zero.

For the more general case in which the coordinate axes do not correspond with the directions of the two principal planes it can be shown that

$$g \left(\frac{1}{\rho_1} - \frac{1}{\rho_2} \right) = [(U_{yy} - U_{xx})^2 + (2U_{xy})^2]^{1/2} = \sqrt{U_\Delta^2 + 4U_{xy}^2} \tag{48}$$

[1] See Edge and Laby, 1931, p. 302.

and that the azimuth angle λ between the x-axis and the principal plane in which the curvature is algebraically minimum is given

$$\tan (2\lambda) = \frac{2U_{xy}}{-U_\Delta}[1]$$ (49)

The symbol conventionally used to represent the differential curvature is a line the length of which is proportional to $\Re$ and the direction of which is the direction of the principal plane in which the curvature is an algebraic minimum. If we plot $-U_\Delta$ in the north direction and $2U_{xy}$ in the east direction (see Fig. 46) and take the vector sum of these two, we shall have the vector $\Re$ making an angle 2λ with the x-axis. We now plot the curvature
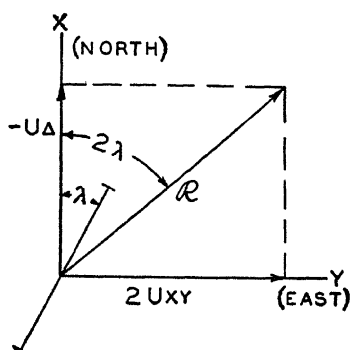
Fig. 46.—Curvature components.   Fig. 47.—Curvature forces on a horizontal beam.
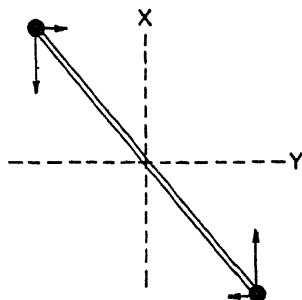
symbol by drawing a line of length $\Re$ at the angle λ with the x-axis and centered at the torsion balance station. This line then has the direction of the plane of minimum curvature (*i.e.*, the long axis of Fig. 45), and the length of this line is a measure of the departure of the level surface from a spherical form.

The curvature quantity has the dimensions of g/ρ, or an acceleration divided by a length. This is the same as the dimensions of the gradient, and it is measured in the same units, so curvatures as well as gradients are expressed in Eötvös units.

In order to get a physical picture of the action of the curvature components on the torsion balance beam, it is convenient to consider a horizontal beam with weights at the two ends suspended by a torsionless fiber. In Fig. 47 let the arrows repre-

[1] See Slotnick, 1932.

sent the horizontal force components of Fig. 45. It is evident that these components will be larger in the x-direction in which the radius of curvature is shorter than in the y-direction where the radius of curvature is greater. Now let us consider the beam as suspended in this field of force. It is evident that the horizontal force components acting on the weights will be greater parallel to the x-axis than parallel to the y-axis. There will thus be a tendency for the beam to orient itself parallel to the plane in which the radius of curvature is a maximum (i.e., the curvature is a minimum). This is the direction in which, by convention, the curvature symbol is drawn. Thus, to estimate for a given mass distribution the direction in which the curvature will lie, we can imagine a horizontal beam with weights on its two ends as suspended by a torsionless fiber at the point at which the curvature is to be considered and imagine the orientation that it would take as a result of the attraction of the surrounding masses on the suspended masses. Thus, if we were to hang such a beam over the axis of an anticline, it is evident that the excess mass along the anticline would attract the suspended masses and the beam would tend to orient itself parallel to the anticlinal axis. If we should hang it over the axis of a synclinal area, the weights would be attracted by the excess masses on the flanks of the syncline, and therefore the beam would orient itself perpendicular to the synclinal axis. For this reason, curvatures parallel to geologic axes are called "anticlinal" (also commonly taken as positive), and curvatures perpendicular to geologic axes are called "synclinal" (commonly taken as negative). On the downthrow side of a fault the beam would tend to orient itself toward the fault plane on account of the attraction of the excess mass at the side and would, therefore, be synclinal. On the upthrow side of the fault it would tend to orient itself parallel to the excess mass along the fault and would, therefore, be anticlinal. Therefore, the curvatures show a reversal from synclinal on the downthrow to anticlinal on the upthrow side of a fault. This characteristic makes the curvatures particularly useful for finding faults.

A simple geometrical method may be used for obtaining qualitative pictures of a differential curvature profile over a mass that is long in the direction perpendicular to the profile. This depends on the ability to draw a profile representing approxi-

mately the equipotential surface. This can usually be done in a
qualitative way by simple considerations, for we know that
gravity increases over a heavy mass and decreases over a light
mass and that the equipotential surface rises and falls when the
gravity increases and decreases. A smooth curve can be drawn
to represent such a rise and fall of the equipotential surface.
Where this curve is concave downward, the curvature is positive;
and where it is concave upward, the curvature is negative. A
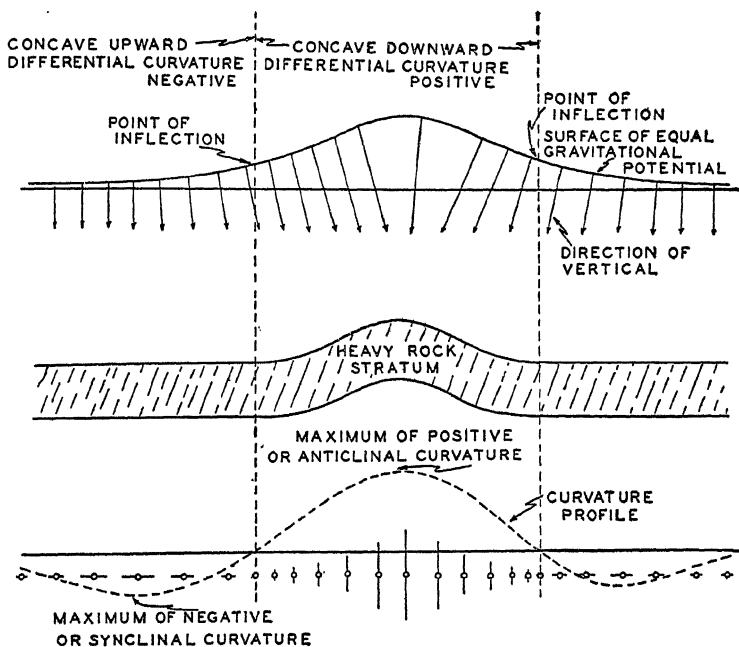
FIG. 48.—Curvatures over an anticline.

point of inflection of this curve corresponds to a differential
curvature reversal. Figure 48 shows the direction of the vertical,
the equipotential surface, and the differential curvature for a
simple anticline. (The variation in the direction of the vertical
and the curvature of the potential surface are greatly exag-
gerated.) The lateral parts of this curve, which are concave
upward, give the negative, or synclinal, differential curvatures
which are observed on the flanks of an anticline; the central part,
which is strongly concave downward, gives a larger positive
differential curvature parallel to the anticlinal axis which is

observed over the central part of an anticline. It must be remembered that these considerations apply only to bodies or structures that are long in the direction perpendicular to the profile; for the curvature in this direction has been taken as zero,
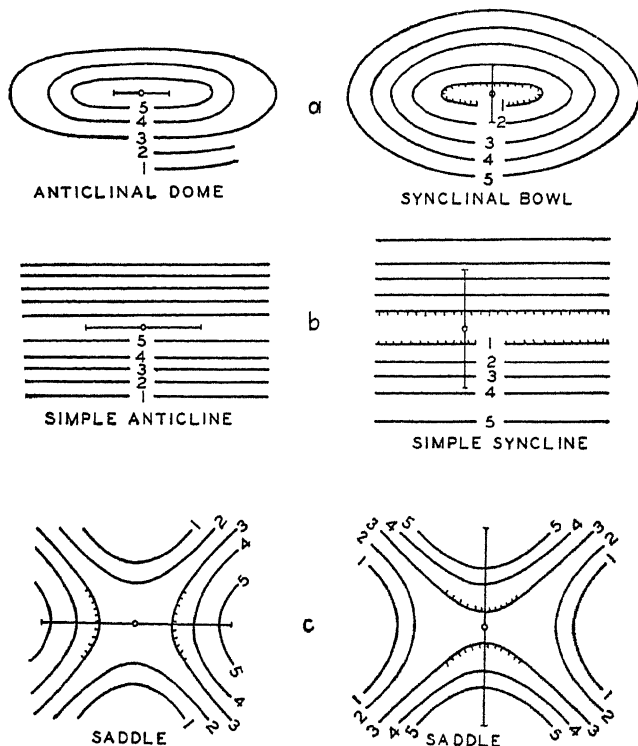
FIG. 49.—Anticlinal, or positive, curvatures. Figures *a*, *b*, and *c* show the successive increase in the magnitude of positive curvatures from an elongated dome, through a long, simple anticline to an anticlinal saddle.

FIG. 50.—Synclinal or negative curvatures. Figures *a*, *b*, and *c* show the successive increase in the magnitude of negative curvatures from an elongated basin, through a simple syncline to a synclinal saddle.

so that the differential curvature is reduced to only the curvature in the direction of the profile.

When considering the curvatures in cases where one component is not zero, it must always be kept in mind that we are considering the *differential* curvature and that the curvature symbol is drawn in the direction of the plane in which the curvature is an *algebraic minimum*. This is illustrated by considering

the curvatures of the different potential surfaces as indicated by contours (Figs. 49 and 50).

In Figs. 49a, 49b, 49c an anticlinal dome is developed into a simple anticline and then into a saddle. This development can

FIG. 51.—Curvature from a heavy cylinder.

FIG. 52.—Curvature from a heavy sphere.

be thought of as brought about by successively decreasing the curvature along the larger (horizontal) axis to zero to give the anticline and further decreasing this curvature to a negative value to give the saddle shape, keeping the curvature along the vertical axis constant. The differential curvature in each case is

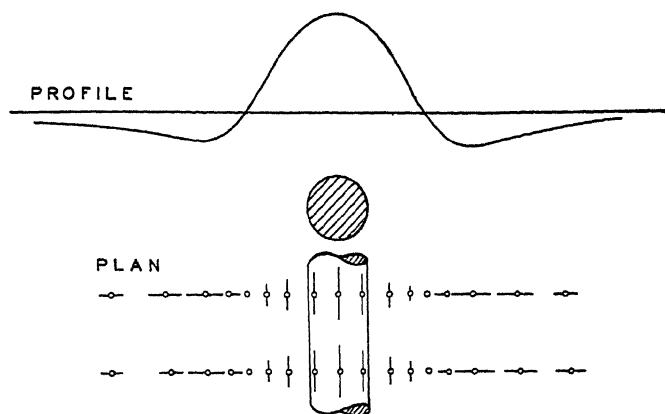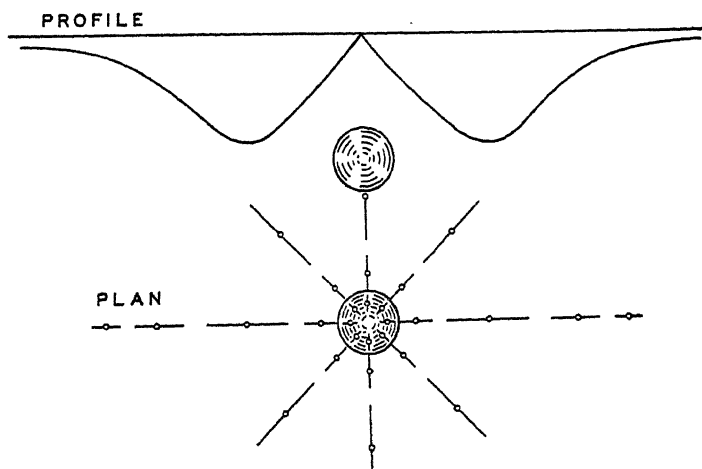represented in direction and approximate magnitude. Since in these changes the differential curvature is obtained by subtracting a successively smaller (algebraically) curvature from a fixed curvature, the resulting differential curvature successively increases in value as shown. Figures 50*a*, 50*b*, 50*c* show a similar succession of shapes, starting from a synclinal bowl which is developed through a simple syncline to a saddle.[1]

Profiles and plans for curvatures for an ideal horizontal cylinder and an ideal sphere are shown by Figs. 51 and 52.

CORRECTIONS TO THE TORSION BALANCE QUANTITIES

Normal Corrections.—We have seen in connection with gravity measurements that corrections must be made for the variation in gravity due to the departure of the earth from a perfectly spherical form and its rotation. Corrections for these same effects must be made to torsion balance quantities. We have calculated [Eqs. (25) and (26), page 52] the value for the horizontal rate of change of gravity at the surface. This, of course, corresponds to a normal gradient of gravity. If we write Eq. (26) in terms of c.g.s. units, it becomes

$$K = 8.122 \cdot 10^{-9} \sin 2\varphi \text{ (c.g.s. units, } i.e., \text{ gals/cm.)}$$
$$= 8.122 \sin 2\varphi \text{ Eötvös units}$$

The gradient correction therefore is

$$U_{xz} = -8.122 \sin 2\varphi \tag{50}$$

The normal level surfaces also are distorted from a spherical form so that the radii of curvature are not equal and a normal curvature correction also must be made. The normal value of the curvature is

$$U_\Delta = 10.36 \cos^2 \varphi \tag{51}$$

These are the proper corrections if the instrument is oriented with the *x*-axis directed toward the astronomic north (*i.e.*, the beams are in a north-south plane for the first position). In this orientation there is no normal correction on the U_{xz}- and U_{xy}-

[1] For diagrams showing various types of equipotential surfaces and the corresponding curvatures, see Jung, 1930, pp. 128 and 130, and Haalck, 1934, p. 73.

components. Frequently, the balance is oriented to lie in the magnetic meridian. If, for this or any other reason, the balance is oriented so that the x-axis makes an angle δ with the astronomic meridian, the correction components become

$$\left.\begin{array}{l} U_{xz} = -8.122 \sin 2\varphi \cos \delta \\ U_{yz} = -8.122 \sin 2\varphi \sin \delta \end{array}\right\} \qquad (50a)$$

$$\left.\begin{array}{l} U_{\Delta} = 10.36 \cos^2 \varphi \cos 2\delta \\ 2U_{xy} = 10.36 \cos^2 \varphi \sin 2\delta \end{array}\right\} \qquad (51a)$$

Terrain Corrections.—The torsion balance is such a sensitive instrument that the gravitational attractions from any mass irregularities near the instrument have appreciable effects, and it is necessary to make corrections for such irregularities. The survey necessary for making these corrections is one of the major items of torsion balance field operations.

A variety of systems of survey and computation have been used for making these corrections.[1] They are all based on dividing the topography up into certain elements and computing the effects of these elements on each of the torsion balance quantities. Usually tables of some sort are used which give the effect at the instrument of each element of topography in terms of the average elevation of each compartment into which the surface is divided by a predetermined array of azimuthal lines and circles. The elevations at each compartment are multiplied by coefficients or by numbers read from tables, and the effects on each of the torsion balance quantities from each compartment are added up. The coefficients for the effects depend on the height of the center of gravity of the balance above the ground, and therefore the instrument must be set up a a standard height. The coefficients for the close distances particularly decrease rapidly as the height of the center of gravity of the balance is raised, so that it is an advantage to have a relatively high center of gravity.

The effects of the topography on the curvature are rather close to proportional to the elevations of the compartments, and therefore the curvature corrections can be given quite closely by coefficients multiplied by the height of the terrain in each compartment. For the gradients the effects are not linear with the height; in fact, the effect on the gradient changes sign when the

[1] Heiland, 1929a; Lancaster-Jones, 1929, pp. 525–528; Heiland, 1933, p. 44.

height of the topography becomes greater than the height of the center of gravity of the balance.   Therefore, if the terrain heights are more than a rather small fraction of the height of the center of gravity of the balance, it is necessary either to use tables giving the effects for each compartment at various elevations or to use coefficients that are multiplied by the squares of the elevations.[1]

The terrain effects decrease with distance much more rapidly for gradients than they do for curvatures.   For instance, at a distance of 100 meters the effect for a given small unit of topography is almost 100 times as large on the curvatures as on the gradients.   For this reason the curvature results in torsion balance surveys are apt to be poor to useless in rolling to gently rugged topography unless the terrain surveys are carried out to large distances and careful corrections made.   In gently rolling topography with elevations of a few hundred feet, appreciable curvature effects may still be present at distances of $1\frac{1}{2}$ mile or more.   In really rough topography it is almost impractical to make accurate corrections for the curvatures.

Because of their rapid decrease with distance the gradient corrections are reduced considerably if the topography in the immediate vicinity of the station is relatively flat.   Therefore a comparatively small change in a station site may reduce the corrections materially.   A gentle slope of the surface has a comparatively large effect on the gradients, a slope of 1 deg., for instance, having an effect of about 14 Eötvös units.   However, if the slope is fairly uniform, its effect can be quite accurately computed, and it is not a very serious detriment to obtaining an accurate final result.   A uniform slope does not affect the curvature.   An appreciation of the terrain effects on the instrument

---

[1] Tables of numerical coefficients for terrain corrections were first given by Eötvös but contained numerical errors that were not recognized for some years.   The theory of terrain corrections with tables of linear coefficients for gradients and curvatures which have been widely quoted and probably widely used were given by Schweydar, 1924. Coefficients for gradient corrections depending on squares of elevations were given by Schweydar, 1927.   Detailed directions for the use of these coefficients, with tables of effects versus heights, are given by Heiland, 1933.

The use of linear coefficients for gradient corrections where the terrain height is greater than the height of the center of gravity of the balance is worse than useless, for the corrections so calculated are opposite in sign from the proper values.

and good judgment in selecting instrument station sites, with a view to minimizing the terrain effects, are important qualifications of a torsion balance field operator.

One of the most commonly used methods of terrain survey is to take levels at distances of 1.5, 3, 5, 10, 20, 30, 40, 50, 70, and 100 meters, in each of eight azimuth directions, at angles of 45 deg. The level readings at these points are assumed to represent the topography in a compartment centered at the point of reading. If the topography is too irregular to be represented by such an array, it is common to use the same distances but divide up the area into more compartments by increasing the number of
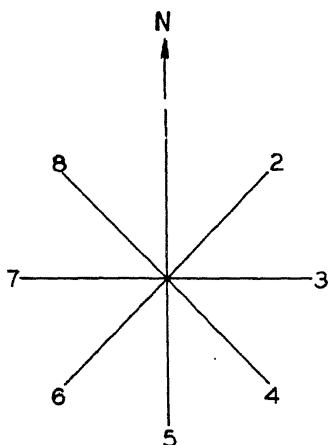
Fig. 53.—Eight-ray terrain survey. Fig. 54.—Sixteen-ray terrain survey.
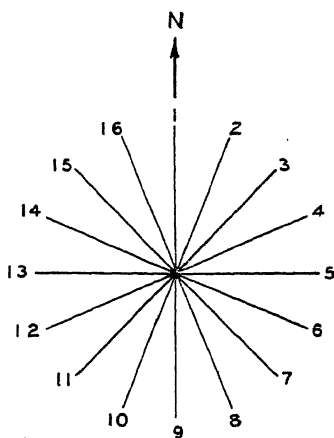
azimuthal divisions or rays to 16 or 32. When the topography becomes more severe, it may be necessary to use special charts which count areas on cross sections along the radial lines or to compute the effects from readings on contour maps by means of another type of special chart.

For eight rays (Fig. 53), at 0, 45, 90 deg., etc., from the x(north)-axis, the effects are added as follows:

Let G_1, G_2, etc., be the sums of the gradient effects for all distances along ray$_1$, ray$_2$, etc., at azimuths 0, 45 deg., etc., from the x-axis   Similarly, let K_1, K_2, etc., be the corresponding sums for the curvature effects. Then the total effect for each torsion balance quantity is

$$\left.\begin{aligned}
U_{xx} &= G_1 - G_5 + 0.707(G_2 - G_4 - G_6 + G_8) \\
U_{yz} &= G_3 - G_7 + 0.707(G_2 + G_4 - G_6 - G_8) \\
U_\Delta &= K_1 - K_3 + K_5 - K_7 \\
2U_{xy} &= K_2 - K_4 + K_6 - K_8
\end{aligned}\right\} \quad (52)$$

For 16 rays (Fig. 54) the corresponding summations are

$$\left.\begin{aligned}
U_{xx} &= G_1 - G_9 + 0.924(G_2 - G_8 - G_{10} + G_{16}) \\
&\quad + 0.707(G_3 - G_7 - G_{11} + G_{15}) \\
&\quad + 0.383(G_4 + G_6 - G_{12} - G_{14}) \\
U_{yz} &= G_5 - G_{13} + 0.924(G_4 + G_6 - G_{12} - G_{14}) \\
&\quad + 0.707(G_3 + G_7 - G_{11} - G_{15}) \\
&\quad + 0.383(G_2 + G_8 - G_{10} - G_{16}) \\
U_\Delta &= K_1 - K_5 + K_9 - K_{13} + 0.707(K_2 - K_4 - K_6 + \\
&\quad\quad K_8 + K_{10} - K_{12} - K_{14} + K_{16}) \\
2U_{xy} &= K_5 - K_9 + K_{13} - K_1 + 0.707(K_6 - K_8 - K_{10} + \\
&\quad\quad K_{12} + K_{14} - K_{16} - K_2 + K_4)
\end{aligned}\right\} (53)$$

Or, in general, for n rays at angles θ_n from the x-axis:

$$\left.\begin{aligned}
U_{xx} &= \Sigma G_n \cos \theta_n \\
U_{yz} &= \Sigma G_n \cos (\theta_n - 90°) \\
U_\Delta &= \Sigma K_n \cos 2\theta_n \\
2U_{xy} &= \Sigma K_n \cos 2(\theta_n - 90°)
\end{aligned}\right\} \quad (54)$$

By whatever means they are determined, the terrain effects of the different compartments are added up separately in different directions to give the final total effect at the instrument. These effects (together with the normal, or geodetic, effects) are then subtracted before plotting the final torsion balance quantities which then represent the irregularities in the gravitational field at the instrument that are caused by irregularities in mass below the surface.

CONSTRUCTION OF TORSION BALANCE MAPS

After plotting the results of a torsion balance survey as gradients and curvatures on a map, it is customary to make a gravity contour map from the gradients. In general, the gravity contours, or lines of equal gravity, are perpendicular to the gradients (just as strike is perpendicular to dip). Where gradients are large, contours are close together; where small, contours are far apart.

Gravity differences are calculated from the product of gradient times distances just as height differences could be calculated from the product of slope times distance. Thus, gravity differences in c.g.s. units (gals) are given by

$$\Delta g = 10^{-9} GS \tag{55}$$

where G is a gradient (or gradient component) in Eötvös units and S is an actual distance (on the ground) in centimeters. If we measure a distance S_m (in centimeters) on a map with a scale ratio $1:K$, and if we measure gravity differences in milligals Eq. (55) becomes

$$(\Delta g)_{mg} = 10^{-6} GKS_m \tag{56}$$

Suppose that we have a series of torsion balance stations along an irregular line (Fig. 55) and wish to calculate gravity differences
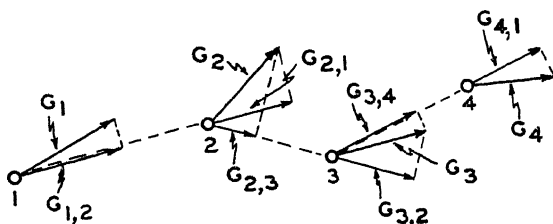
Fig. 55.—Gradient components for calculation of station-to-station gravity differences.

from station to station along this line. At each station the gradient component along the line is simply the projection of the gradient on to the line between stations. Since, in general, the components along the line will be different at different stations, about the best we can do is to assume that the variation is uniform and take the average of the gradients at the two stations as representative of the gradient in the interval between stations. Thus, if we have a line of gradients G_1, G_2, G_3, G_4, etc., at stations 1, 2, 3, 4, etc. (Fig. 55), and let the component of gradient G_1 in the direction of station 2 be $G_{1,2}$, etc., the gravity differences from station to station will be given

$$\left.\begin{aligned} (\Delta g)_{1,2} &= \frac{G_{1,2} + G_{2,1}}{2} S_{1,2} \\ (\Delta g)_{2,3} &= \frac{G_{2,3} + G_{3,2}}{2} S_{2,3} \text{ etc.} \end{aligned}\right\} \tag{57}$$

where $S_{1,2}$ is the distance between stations 1 and 2, etc.

A graphical chart[1] which is convenient and rapid for computing the Δg's as indicated by Eq. (57) is shown by Fig. 56. In opera-

THE GULF RESEARCH LABORATORY.

CHART FOR INTEGRATING GRADIENTS OF GRAVITY.

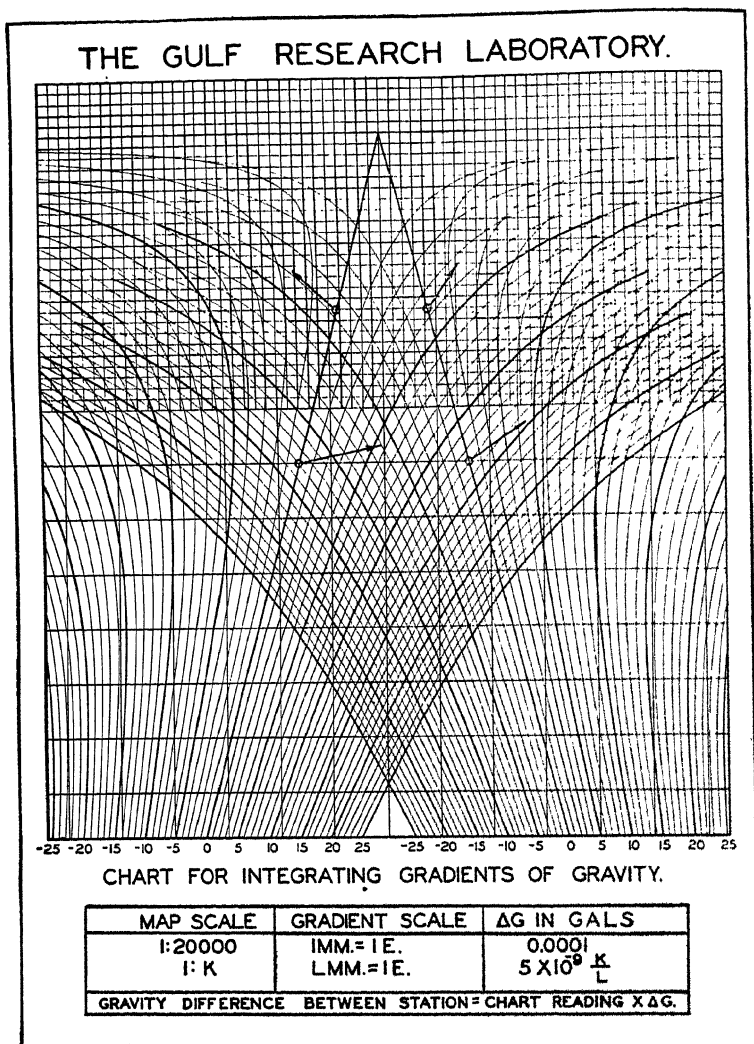| MAP SCALE	GRADIENT SCALE	ΔG IN GALS
1:20000	1MM.= 1 E.	0.0001
1: K	L.MM.= 1 E.	$5 \times 10^9 \frac{K}{L}$
GRAVITY DIFFERENCE	BETWEEN STATION=	CHART READING X ΔG.

Fig. 56.—Chart for integrating gradients. (*After Oserezky.*)

tion, the transparent chart (made by photographing a master chart to the scale desired and printing on photographic film) is

[1] Oserezky, 1930.

simply laid on the map with the two stations between which the gravity is to be computed located on the heavy zero lines in the central part of the chart and on a horizontal line. Then the projections of the gradients on to the horizontal line through the stations are read, and the component of the gravity difference between the two stations is then given by reading the position of the projection of the gradient on to the curved scales. The sums of the components from the two gradients give the gravity difference between the two stations. For instance, for the two upper gradients the gravity difference is $-0.15 + 0.11 = -0.04$ mg.; for the lower gradients the gravity difference is $+0.63 + 0.40 = +1.03$ mg.

ADJUSTMENT AND CONTOURING OF TORSION BALANCE VALUES

It is always necessary to make some sort of adjustment of the gravity differences read from torsion balance stations. The gravity difference between two points should be the same, no matter what path is taken between those points; *i.e.*, the gravity difference around any closed circuit of torsion balance stations should be zero. In practice this is almost never so, and there is, therefore, an "error of closure" which must be taken care of. A variety of methods are used for adjusting out the errors of closure. The problem is identical in principle with the adjustment of errors of closure of level traverses in surveying, and the same methods can be used. Theoretically, the best method is to make a least squares adjustment of the network of closed traverses.[1] This, however, is a laborious process if a large number of traverses is involved, and it is somewhat doubtful that the greater probable accuracy of the adjustment is worth the labor involved. A fairly satisfactory method is to take gravity differences between different points on the map by a number of different paths of connecting stations and take the average value over the different paths as the adjusted gravity difference.[2] If this is done by careful selection of paths, a quite satisfactory adjustment can be made.

[1] See Leland, 1921, pp. 64–71, or Avers, 1935, pp. 53–74, which discuss the adjustment of level nets. The application of such methods to the adjustment of torsion balance nets is given in Barton, 1929*b*, and Roman, 1932, pp. 486–504.

[2] Barton, 1929*b*, pp. 1170–1171.

The final contouring of gravity values from torsion balance gradients requires a considerable degree of practice and judgment, as it is nearly always necessary to make some choice as to individual gradients that are considered as probably representative of the general gravity configuration and those which are probably locally disturbed or have inadequate terrain corrections. Field notes on station sites are helpful in making such selections. In any case the map is started at any arbitrary point by drawing a contour perpendicular to the gradients. Other contours are spaced in according to either the length of the gradients or previously determined adjusted gravity values along the traverses.

A convenient way to sketch in contours approximately is to make a table that gives for a given contour interval and map scale the distance between contour lines in terms of the length of the gradient.

Let $(\Delta g)_c$ represent the gravity difference between gravity contours in gals; L, the length of the gradient arrow in millimeters; E, the number of Eötvös units per millimeter; S, the distance between contours on the map in millimeters; and K, the map scale ratio. Then

$$(\Delta g)_c \cdot 10^{-3} = (L \cdot E \cdot 10^{-9}) \left(\frac{KS}{10} \right) \tag{58}$$

In this equation the expression on the left side represents the gravity difference between contours in milligals. The first bracket term on the right side represents the gradient in c.g.s. units, and the second bracket term on the right represents the distance on the ground in centimeters. We can now solve for the product of the length of the gradient (in millimeters) times the distance on the map between contours (also in millimeters) as

$$L_{mm.} S_{mm.} = \frac{\Delta g \cdot 10^7}{EK} \tag{59}$$

We make a table of this product. For instance, suppose that we have a map at a scale 1 in. = 1 mile on which gradients are plotted at a scale of $\frac{1}{2}$ mm. = 1 Eötvös unit and we wish to draw gravity contours at an interval of 1 mg. For this case $\Delta g = 1$, $E = 2$, $K = 63,360$, and the product comes out $L \times S = 79$. We then make a table as follows:

CHAPTER VI

GRAVITY CALCULATIONS AND INTERPRETATION

THE SOURCE OF GRAVITY VARIATIONS

The preceding chapters have shown the basis of the fieldwork by which gravity or torsion balance values are produced. The fieldwork usually is completed by the preparation of a map showing station locations with the reduced or corrected gravity values (*i.e.*, with latitude, elevation, Bouguer, and terrain corrections made) or the corrected torsion balance gradients and curvatures (*i.e.*, with normal and terrain corrections made). The interpretation of these results in terms of probable geologic conditions below the surface is usually a quite separate undertaking from the conduct of the fieldwork.

The distribution of reduced gravity (or of torsion balance quantities) shown by a map is caused by all departures from the mass distribution which has been assumed in reducing the stations. This means that the gravity pattern of the map is caused by the sum of all departures from the uniform ideal spheroidal shape of the earth, beginning at the grass roots and extending deep into its interior.

In so far as its gravity effects are concerned, the earth may be considered as made up of a series of shells which may be of different density. Therefore, gravity measurements are not sensitive to vertical variations in density so long as the density is constant in horizontal (*i.e.*, level) layers. However, any horizontal variation in density will cause a horizontal variation in gravity (and its derivatives), and it is these horizontal variations which a gravity map indicates.

Any geologic condition that results in a horizontal variation in density will cause a horizontal gravity variation or a gravity "anomaly." Thus, a geologic structure that causes an uplift of beds of different density will cause a gravity anomaly the magnitude of which will depend on the density contrasts involved

and the magnitude and form, or "sharpness," of the geologic disturbance. A structure, no matter how large or how sharp, will not cause a gravity anomaly if the beds involved are all of the same density.

DENSITIES OF ROCKS

It is evident that the density variation below the surface is a primary factor in the consideration of the magnitude and type of gravity anomaly which might be caused by geologic structure and which might be detected by gravity measurements. The following table gives a few figures for average densities of various types of rock.[1]

Unconsolidated sediments...........	1.8 to 2.3, usually increasing with depth on account of compaction of the shales
Sandstones.......................	2.0 to 2.5, varying principally with the porosity
Salt........	2.2
Limestone.......	2.5 to 2.7
Granite..........................	2.6 to 2.8
Basalt (sial).....................	3.0
Dunite (sima)........	3.3
Average density of crustal rocks above sea level......................	2.67

It is only differences in these densities, where rocks of different character are brought into horizontal juxtaposition, that can cause gravity anomalies. From this table it is evident that the density contrasts involved in usual sedimentary sections will rarely be more than about 0.5. As a matter of experience, a fair figure to keep in mind as a density contrast commonly involved in geologic movement is around 0.25.

THE AMBIGUITY OF GRAVITY INTERPRETATION

The interpretation of a gravity (or torsion balance) map in terms of a definite mass distribution below the surface is never

[1] The variation of density with depth is discussed by Barton, 1938, pp. 374–376. Detailed information regarding the densities of sedimentary rocks will be found in Athy, 1930. For a discussion of the density of the deeper layers see Jeffreys, 1937. For tables of densities of various types of rock, see Reich, 1930, pp. 7–17. For comments on densities of various geologic horizons in different areas, see p. 127 below.

unique on the basis of gravity information alone. This results
from the fact that a given gravity distribution can be produced
by a variety of mass distributions. Therefore, any mass dis-
tribution or geologic condition that is given as a solution for the
cause of a given gravity distribution *depends on additional control
other than gravity.* This lack of uniqueness of the solution for the
cause of a given gravity picture cannot be emphasized too
strongly.

The additional control may be given by actual subsurface con-
tacts from drilling which give depths at one or more points to a
density contrast. It may be given by another geophysical
method (*e.g.*, seismograph). If no definite physical data are
available, it is given by general considerations of the geology of
the area under consideration and geologic reasonableness which
may be able to discriminate between different solutions that are
geophysically possible, or at least to say that one solution is more
probable than another.

Because of this ambiguity, it is impossible to calculate a unique
mass distribution as the cause of a given gravity distribution.
Therefore, it is usual to assume mass distributions, based initially
on whatever control is available, calculate the gravity effects
that they produce, and compare the computed with the observed
effect. The mass distribution is modified, within the limits set
by other control, the calculations and comparisons repeated, and
this cut-and-try process continued until a satisfactory fit is
achieved. Here, again, it may be emphasized that the achieve-
ment of a fit between calculated and observed results is not a
proof that the mass distribution that gives the fit is the only
answer to the problem. The degree to which the solution is
unique depends quite as much on the other control as it does on
the gravity data.

GRAVITY EFFECTS OF GEOMETRICAL FORMS

The computations of gravity effects of a few simple geometrical
forms serve as very useful guides to the magnitude and form of
gravity effects that may be expected from mass anomalies, even
though such forms are rarely close to the actual forms that
geologic mass anomalies have in nature. If little or no other
control is available, the comparison of the effects of such simple
forms with those observed may give as close a fit to the observed

data as is justified by other uncertainties of the problem. There-
fore, the equations for the gravity and torsion balance effects of
a few simple mass anomalies are given below.

The Sphere.—The sphere is the simplest geometric form for
which we can compute gravity effects. Not many geologic
structures approach spheres in form (although salt domes fre-
quently do), but such simple calculations are useful to indicate
the approximate magnitudes that roughly spherical density
contrasts would produce.

Gravity Effect.—The gravity effect of a sphere of mass m at
the point P at a distance r from its center (Fig. 57) is simply
$g = \gamma m/r^2$, where γ is the gravitational constant. This, how-
ever, is directed toward the center of the sphere.

We are always interested in the
vertical component g_z which will
be

$$g_z = g \cos \theta$$
$$= g \frac{z}{r}$$
$$= \frac{\gamma m z}{r^3} \qquad (60)$$
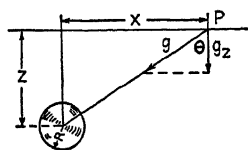
FIG. 57.—Gravity effect of a heavy
sphere.

If R is the radius of the sphere and σ its density (or density con-
trast), its mass anomaly is

$$m = \tfrac{4}{3}\pi R^3 \sigma$$

and

$$g_z = \frac{\gamma 4\pi R^3 \sigma z}{3r^3} = \frac{4\pi\gamma\sigma R^3}{3} \cdot \frac{z}{(z^2 + x^2)^{3/2}} \qquad (61)$$

This gives g in gals when r, R, x, and z are in centimeters. If we
change the units to express g in milligals and express r, R, x,
and z in thousands of feet (kilo-feet) and include the values of
the numerical constants (π and γ), Eq. (61) becomes

$$(g_z)_{\text{mg.}} = 8.53\sigma \left[\frac{R^3 z}{(z^2 + x^2)^{3/2}} \right]_{\text{kilo-ft.}} \qquad (62)$$

It is often convenient to express equations of this type in units
of the depth. This is done by dividing through by z so the
independent variable is the ratio x/z. Then Eq. (62) becomes

$$g_z = 8.53\sigma R^3 \frac{z}{z^3[(x/z)^2 + 1]^{3/2}} = \frac{8.53\sigma R^3}{z^2} f\left(\frac{x}{z}\right) \qquad (63)$$

$$= Kf\left(\frac{x}{z}\right) \qquad (63a)$$

where

$$f\left(\frac{x}{z}\right) = \frac{1}{[(x/z)^2 + 1]^{3/2}} \qquad (64)$$

and

$$K = \frac{8.53\sigma R^3}{z^2} \qquad (65)$$

where R and z are in units of kilo-feet. A curve for Eq. (64) is given by curve 1 of Fig. 58.
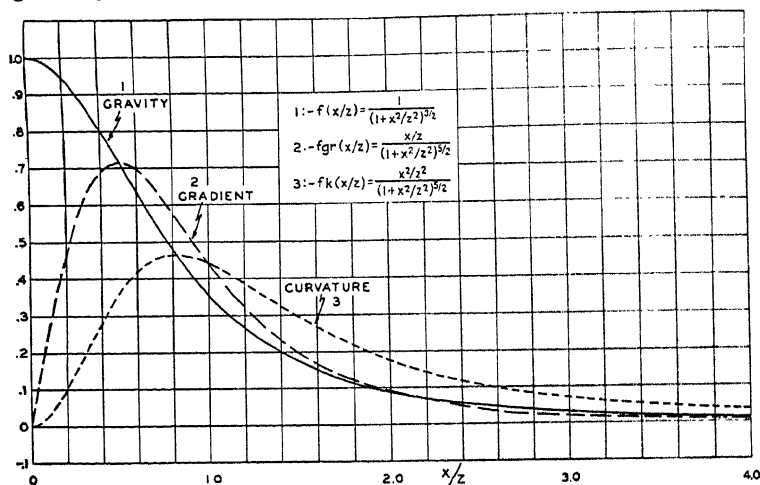
FIG. 58.—Gravity, gradient, and curvature for a sphere.

Suppose that we wish to calculate the gravity profile for a sphere, with a radius R of 3,000 ft., depth to center of 5,000 ft., and density contrast of 0.25. Then the value of K [Eq. (65)] is (remembering that R and z are in kilo-feet units)

$$K = \frac{8.53 \cdot 0.25 \cdot 27}{25} = 2.31$$

Over the center of the sphere (where $x = 0$ and $f(x/z) = 1$) its gravity effect will be 2.31 mg. Gravity effects at other distances then can be written down readily from curve 1 of Fig. 58, as is illustrated for a few points by the following table:

Distance x, feet	x/z	$f(x/z)$	g, mg.
0	0	1	2.31
2,500	½	0.71	1 62
5,000	1	0.35	0.81
10,000	2	0.09	0.21

As another example, if we calculate the gravity effect at the point over the center of a sphere with a depth to the center of 1 mile, a radius of 1,000 ft., and a density contrast $\sigma = 0.25$, we find that such a body would have a total gravity anomaly of 0.085 mg. The total excess mass that this body represents is 33 million tons. The comparatively small effect that this enormous mass produces at the surface shows why gravity measurements must be made to the order of 0.1 mg. or better to be sufficiently accurate for the demands of geophysical exploration.

Torsion Balance Effects.—The gravitational potential at a distance r of a sphere of mass m is simply

$$U = \frac{\gamma m}{r} \tag{66}$$

By taking the partial derivatives corresponding to, say, the torsion balance gradient, we find

$$\frac{\partial^2 U}{\partial x\,\partial z} = U_{xz} = 3\gamma m\,\frac{xz}{r^5} \tag{67}$$

If the sphere is of density (or density contrast) σ and radius R,

$$m = \tfrac{4}{3}\pi R^3 \sigma$$

and

$$U_{xz} = 4\pi\gamma\sigma\,\frac{R^3 xz}{r^5} \tag{68}$$

Similarly, for the other torsion balance quantities

$$U_{yz} = 4\pi\gamma\sigma\,\frac{R^3 yz}{r^5} \tag{69}$$

$$U_{xy} = 4\pi\gamma\sigma\,\frac{R^3 xy}{r^5} \tag{70}$$

$$U_\Delta = U_{yy} - U_{xx} = 4\pi\gamma\sigma R^3 \cdot \frac{y^2 - x^2}{r^5} \tag{71}$$

Gradient.—Suppose that we wish to calculate the gradient profile for a sphere, on a line through the point above the center of the sphere. Let this line be the x-axis; then

$$r = (x^2 + z^2)^{1/2}$$

and we can write

$$U_{xz} = 4\pi\gamma\sigma R^3 \frac{xz}{(x^2 + z^2)^{5/2}}$$

Dividing through by z, this becomes

$$U_{xz} = 4\pi\gamma\sigma \frac{R^3}{z^3} \frac{x/z}{[(x/z)^2 + 1]^{5/2}} \tag{72}$$

and since the gravitational constant $= 200/3 \cdot 10^{-9}$ (page 15), this becomes

$$U_{xz} = 4\pi \cdot \frac{200}{3} \cdot 10^{-9}\sigma \frac{R^3}{z^3} f_{gr}\left(\frac{x}{z}\right)$$

where

$$f_{gr}\left(\frac{x}{z}\right) = \frac{x/z}{[(x/z)^2 + 1]^{5/2}} \tag{73}$$

Since 1 Eötvös unit $= 10^{-9}$ c.g.s. unit, the factor 10^{-9} occurs on both sides and may be dropped, and

$$U_{xz} = 837\sigma \left(\frac{R}{z}\right)^3 f_{gr}\left(\frac{x}{z}\right) \text{ Eötvös units}$$

$$= Kf_{gr}\left(\frac{x}{z}\right)$$

where

$$K = 837\sigma \left(\frac{R}{z}\right)^3 \tag{74}$$

A curve for $f_{gr}(x/z)$ is given by curve 2 of Fig. 58. For the same sphere as used above,

$$U_{xz} = 837 \cdot 0.25 \cdot \left(\frac{3}{5}\right)^3 f_{gr}\left(\frac{x}{z}\right)$$

$$= 36.9 f_{gr}\left(\frac{x}{z}\right)$$

Gradient effects at a few distances then would be

Distance x, ft.	x/z	$f_{gr}(x/z)$	U_{xz}, Eötvös units
0	0	0	0
2,500	½	0.285	10.5
5,000	1	0.178	6.6
10,000	2	0.040	1.5

By differentiating the expression for $f_{gr}(x/z)$ and equating to zero it can be shown that the maximum value for the gradient occurs at a distance $x/z = \frac{1}{2}$. This also is evident from the curve (curve 2 of Fig. 58).

Curvature.—For the curvature, it is convenient to take the equation for U_Δ. For a line through the point above the center of the sphere, $U_{yy} = 0$, and Eq. (71) reduces to

$$U_\Delta = -U_{xx} = -4\pi\gamma\sigma R^3 \frac{x^2}{r^5}$$

$$= 4\pi\gamma\sigma R^3 \frac{x^2}{(x^2 + z^2)^{5/2}} \tag{75}$$

$$= 4\pi\gamma\sigma \frac{R^3}{z^3} \frac{x^2/z^2}{[(x/z)^2 + 1]^{5/2}}$$

$$= 837\, \sigma \left(\frac{R}{z}\right)^3 f_k\left(\frac{x}{z}\right)$$

where

$$f_k\left(\frac{x}{z}\right) = \frac{x^2/z^2}{[(x/z)^2 + 1]^{5/2}} \tag{76}$$

A curve of $f_k(x/z)$ is given by curve 3 of Fig. 58. For the same sphere calculated before,

$$U_\Delta = 837 \cdot 0.25 \cdot \left(\frac{3}{5}\right)^3 f_k\left(\frac{x}{z}\right)$$

$$= 36.9 f_k\left(\frac{x}{z}\right)$$

and the curvature effects at a few distances are

Distance x, ft.	x/z	$f_k(x/z)$	U_Δ, Eötvös units
0	0	0	0
2,500	½	0.143	5.2
5,000	1	0.176	6.5
10,000	2	0.074	2.7

By differentiating the expression for $f_k(x/z)$ and equating it to zero, it can be shown that the maximum value for the curvature occurs at a distance $x/z = 2/\sqrt{6} = 0.818$. This also is qualitatively evident from curve 3 of Fig. 58.

The Horizontal Cylinder.—Another simple geometric form which is often useful in estimating the gravity effects of simple geologic structures is a horizontal line element or horizontal cylinder. This can be taken as roughly equivalent to structures that are very much longer in one dimension than the other.
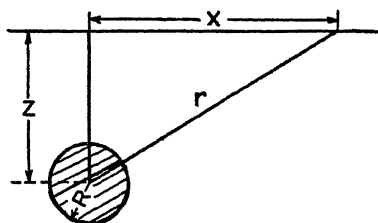
FIG. 59.—Gravity effect of a heavy cylinder.

Gravity Effect.—The vertical component of gravity from a horizontal line element of infinite length can be shown, by integration of the effect for a mass point, to be

$$g_z = \frac{2\gamma m z}{r^2} \tag{77}$$

where m is now the mass per unit length. If we replace the horizontal line element by a cylinder of density σ the mass per unit length (Fig. 59) is

$$m = \pi R^2 \sigma$$

and

$$g_z = 2\pi\gamma\sigma R^2 \frac{z}{r^2} = 2\pi\gamma\sigma R^2 \frac{z}{z^2 + x^2} \tag{78}$$

Again, putting in the numerical constants, changing the length units to kilo-feet, and expressing gravity in milligals, this becomes

$$(g_z)_{\text{mg.}} = 12.77\sigma \left(\frac{R^2 z}{z^2 + x^2} \right)_{\text{kilo-ft.}} \tag{79}$$

Expressing (79) in terms of x/z,

$$g_z = 12.77\sigma R^2 \frac{z}{z^2[(x/z)^2 + 1]} = \frac{12.77\sigma R^2}{z} f'\left(\frac{x}{z}\right)$$

$$= K'f'\left(\frac{x}{z}\right)$$

where

$$f'\left(\frac{x}{z}\right) = \frac{1}{(x/z)^2 + 1} \tag{80}$$

and

$$K' = \frac{12.77\sigma R^2}{z} \qquad (81)$$

A curve for $\dfrac{1}{(x/z)^2 + 1}$ is given by curve 1 of **Fig. 60.**

This curve can be used for calculation in the same way as that for the sphere. Suppose, for instance, that we take a cylinder
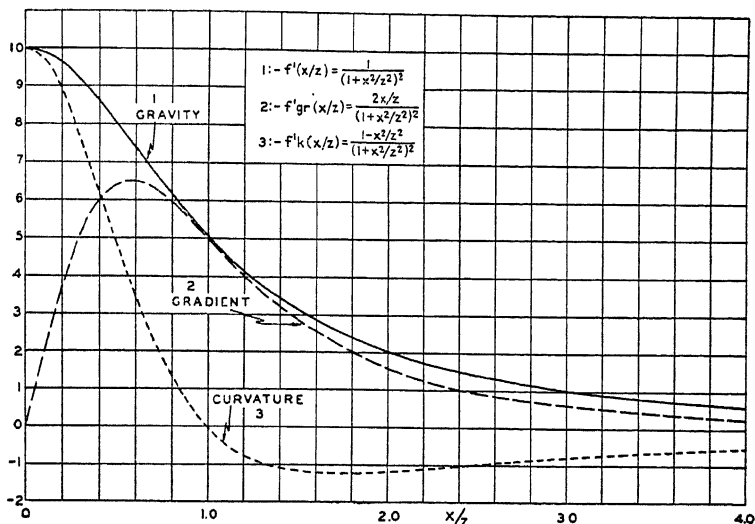
Fig. 60.—Gravity, gradient, and curvature for a horizontal cylinder.

with the same depth, radius, and density as the sphere used above. Then

$$K' = \frac{12.77 \cdot 0.25 \cdot 9}{5} = 5.72$$

Gravity effects at a few distances then would be

Distance x, ft.	x/z	$f'(x/z)$	g, mg.
0	0	1	5.72
2,500	½	0.80	4.58
5,000	1	0.50	2.86
10,000	2	0.20	1.14
15,000	3	0.10	0.57

Torsion Balance Effects.—The torsion balance effects for an infinite horizontal cylinder parallel to the *y*-axis can be shown by integration of the effects for a sphere to be as follows:

$$U_{xz} = \frac{4\gamma mxz}{r^4} \tag{82}$$

$$U_{yz} = 0 \tag{83}$$

$$U_\Delta = \frac{2\gamma m(y^2 - x^2)}{r^4} \tag{84}$$

$$2U_{xy} = 0 \tag{85}$$

m is the mass per unit length, or

$$m = \pi R^2 \sigma$$

Gradient.—For a gradient profile across a cylinder, we take the axis of the cylinder parallel to the *y*-axis (Fig. 59) and $r = (x^2 + z^2)^{1/2}$

$$U_{xz} = 4\pi R^2 \gamma \sigma \frac{xz}{(x^2 + z^2)^2} \tag{86}$$

$$= 2\pi\gamma\sigma \frac{R^2}{z^2} \frac{2x/z}{[(x/z)^2 + 1]^2}$$

$$= 418\sigma \left(\frac{R}{z}\right)^2 f'_{gr}\left(\frac{x}{z}\right)$$

where

$$f'_{gr}\left(\frac{x}{z}\right) = \frac{2x/z}{[(x/z)^2 + 1]^2} \tag{87}$$

A curve for $f'_{gr}(x/z)$ is given by curve 2 of Fig. 60.

Taking the same cylinder as calculated above (*i.e.*, $R = 3,000$ ft., $z = 5,000$ ft., $\sigma = 0.25$) gradient effects at a few distances are

Distance x, ft.	x/z	$f'_{gr}(x/z)$	U_{xz}, Eötvös units
0	0	0	0
2,500	½	0.64	48.0
5,000	1	0.50	37.6
10,000	2	0.16	12.0

By differentiating the expression for $f'_{gr}(x/z)$ and equating to zero, it can be shown that the maximum gradient occurs at a distance

$$\frac{x}{z} = \frac{1}{\sqrt{3}} = 0.578 \tag{88}$$

This also is qualitatively evident from the curve of Fig. 60.

Curvature.—For a curvature profile across a cylinder

$$-U_\Delta = 2\pi\gamma R^2\sigma \frac{z^2 - x^2}{(x^2 + z^2)^2} \tag{89}$$

$$= 2\pi\gamma\sigma \frac{R^2}{z^2} \frac{1 - (x/z)^2}{[(x/z)^2 + 1]^2}$$

$$= 418\sigma \left(\frac{R}{z}\right)^2 f'_k \left(\frac{x}{z}\right)$$

where

$$f'_k \left(\frac{x}{z}\right) = \frac{1 - (x/z)^2}{[(x/z)^2 + 1]^2} \tag{90}$$

A curve for $f'_k(x/z)$ is given by curve 3 of Fig. 60.

Taking the same cylinder as calculated above, the curvature effects for a few points are

Distance x, ft.	x/z	$f'_k(x/z)$	U_Δ, Eötvös units
0	0	1	75.2
2,500	½	0.58	43.6
5,000	1	0	0
10,000	2	−0.12	−9.0

Figure 60 shows that the maximum curvature is over the axis of the cylinder. A reversal occurs at a distance from the axis equal to the depth, and at all greater distances the curvature is negative.

The Semi-infinite Horizontal Plane, or Fault.—A convenient approximation to a common geologic situation is a semi-infinite horizontal slab of material (Fig. 61). This can be used to approximate a fault where a stratum of density contrast σ is abruptly broken off.

The exact expressions for the gravity and torsion balance effects of a fault are somewhat complicated[1] and contain the parameter t (the thickness of the slab) or its equivalent in terms of the angles to the corners. Such expressions cannot be expressed in simple terms of the ratio of depth to thickness as has

[1] Exact formulas for the gravity, gradient, and curvature effects at point O

been done above for the sphere and horizontal cylinder. However, a good approximation to the effect of a slab of finite thickness t and density σ can be made by assuming the material condensed on a thin sheet of mass σt per unit area at depth z (the mean depth of the slab), as indicated by the heavy broken line of Fig. 61. The error of this approximation is less than
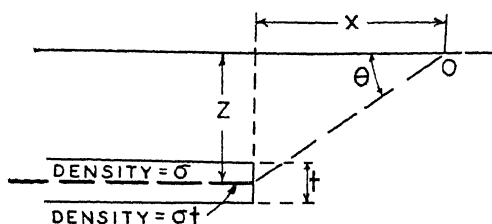
FIG. 61.—Gravity effect of a fault.

2 per cent when t is as great as $\frac{1}{2}z$ but decreases rapidly for smaller values of t (which also commonly correspond with cases in nature).

Gravity, Gradient, and Curvature for a Fault.—With the approximation just indicated, the expressions for gravity, gradient, and curvature, at point O (Fig. 61), can be written in terms of the ratio x/z, where x is the distance from point O to the surface

for the vertical fault shown are
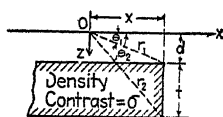
$$G_z = 2\gamma\sigma\left[xln\frac{r_2}{r_1} + \pi t - (t+d)\theta_2 + d\theta_1\right]$$

$$U_{xz} = 2\gamma\sigma ln\frac{r_1}{r_2}$$

$$U_\Delta = 2\gamma\sigma(\theta_2 - \theta_1)$$

Here

$$\theta_1 = \arctan\frac{d}{x}; \qquad \theta_2 = \arctan\frac{t+d}{x}$$

$$r_1 = \sqrt{x^2 + d^2}; \qquad r_2 = \sqrt{x^2 + (t+d)^2}$$

For formulas, tables, and graphs of gravity and torsion balance effects from various types of faults, see Jung, 1930, and Shaw, 1932.

projection of the trace of the fault and z is the depth to the equivalent density sheet. For then

$$\text{Gravity} = g_z = 2\gamma\sigma t \left(\frac{\pi}{2} - \tan^{-1} \frac{x}{z} \right) \tag{91}$$

$$= 2\gamma\sigma t f'' \left(\frac{x}{z} \right)$$

where

$$f'' \left(\frac{x}{z} \right) = \frac{\pi}{2} - \tan^{-1} \frac{x}{z} \tag{92}$$

$$\text{Gradient} = U_{zz} = \frac{2\gamma\sigma t z}{x^2 + z^2} \tag{93}$$

$$= \frac{2\gamma\sigma t}{z} \cdot \frac{1}{(x/z)^2 + 1}$$

$$= \frac{2\gamma\sigma t}{z} f_g'' \left(\frac{x}{z} \right)$$

where

$$f_{gr}'' \left(\frac{x}{z} \right) = \frac{1}{(x/z)^2 + 1} \tag{94}$$

$$\text{Curvature} = U_\Delta = U_{xz} = \frac{2\gamma\sigma t x}{x^2 + z^2} \tag{95}$$

$$= \frac{2\gamma\sigma t}{z} \cdot \frac{x/z}{(x/z)^2 + 1}$$

$$= \frac{2\gamma\sigma t}{z} f_k'' \left(\frac{x}{z} \right)$$

where

$$f_k'' \left(\frac{x}{z} \right) = \frac{x/z}{(x/z)^2 + 1} \tag{96}$$

Curves for gravity, gradient and curvature corresponding to $f''(x/z)$, $f_{gr}''(x/z)$, and $f_k''(x/z)$ for a horizontal fault are given by curves 1, 2, and 3, respectively, of Fig. 62. To calculate curves for any specific case, it is only necessary to evaluate the coefficients (*i.e.*, $2\gamma\sigma t$ for gravity and $2\gamma\sigma(t/z)$ for gradient and curvature) and multiply the values read from the curves by the proper coefficient. For example, for a fault with a depth to center of 2,000 ft., thickness (or throw) of 400 ft., and density contrast 0.3, the coefficients are

$$2\gamma\sigma t = 2 \cdot {}^{20}\!\%_3 \cdot 10^{-9} \cdot 0.3 \cdot 400 \cdot 30.48$$
$$= 488,000 \cdot 10^{-9} \text{ gal}$$
$$= 0.488 \text{ mg.}$$

(The factor 30.48 changes t in feet to centimeters.)

$$2\gamma\sigma\frac{t}{z} = 2 \cdot \frac{200}{3} \cdot 10^{-9} \cdot 0.3 \cdot \frac{400}{2000}$$
$$= 8 \cdot 10^{-9} \text{ c.g.s. unit}$$
$$= 8 \text{ Eötvös units}$$

From the curves, the total gravity effect of the fault is

$$0.488 \cdot \pi = 1.53 \text{ mg.}$$

The maximum gradient [over the fault trace where $f''_{gr}(x/z) = 1$] is 8 Eötvös units. The maximum curvature (at a horizontal distance $x/z = 1$) is ±4 Eötvös units.
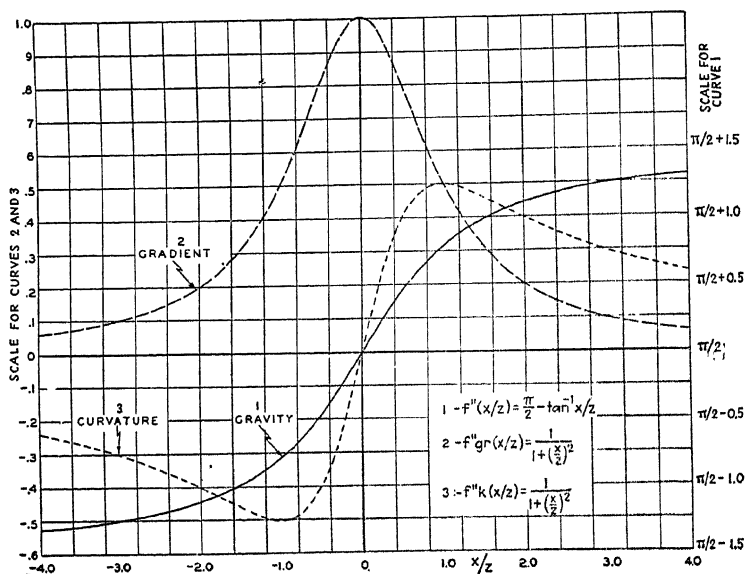

Fɪɢ. 62.—Gravity, gradient, and curvature for a fault.

From Eq. (91) it is evident that the total gravity effect of a slab of material (*i.e.*, the total relief of curve 1 of Fig. 62) is

$$g = 2\pi\gamma\sigma t$$

If g is expressed in milligals, and putting in $\gamma = {}^{200}\!/_3 \cdot 10^{-9}$, this becomes

$$g = 419 \cdot 10^{-6}\sigma t \text{ mg.}$$

From this it is evident that, for unit density contrast, it will require

$$\frac{1}{419 \cdot 10^{-6}} = 2,390 \text{ cm.} = 78 \text{ ft.}$$

of material to produce a gravity effect of 1 mg.

As an easily remembered convenient approximation, the thickness of material of density contrast σ, required to have a gravity effect of 1 mg., is about $80/\sigma$ ft., or $24/\sigma$ meters.

GRAPHICAL AND MECHANICAL COMPUTATION METHODS

The computation of gravity or torsion balance effects for geometric forms becomes quite involved and tedious when they depart from the very simple cross sections such as those for which formulas and curves have been given. Therefore, when more than the simplest forms are involved, graphical or mechanical computation aids are commonly used. In principle, all such aids are means of graphical or mechanical integration of the gravity or torsion balance quantities desired.

Dot Charts.—One of the most useful graphical aids is a transparent "dot chart."[1] Such a chart is made by dividing the chart into units of area so proportioned that they represent elements of mass having equal effects at the origin of the chart. With such a chart it is necessary only to draw an outline or cross section of the mass for which the gravity effect is desired, lay the transparent chart over the outline with the origin at the point at which the effect is to be computed, and count the number of area units within the outline. This number multiplied by a coefficient (which depends on the scale of the cross section for gravity effects but which is independent of the scale for torsion balance effects) gives the effect desired at the origin. By moving the outline to another position on the chart, the effect at another point is computed. By repeating this process, a profile of the computed geophysical effect can be readily determined.

It is useful to represent each area unit on the chart by a single dot and omit the actual boundaries of the units completely. Then for each calculation, it is necessary only to count the number of dots within the mass outline. By using an ordinary hand

[1] For a compilation of mathematical formulas and tables of numerical values for the design of charts for calculation of gravitational potential, gravity, gradient, curvature, and deviation of the vertical, see Breyer, 1938.

tally counter to record the number of dots counted, mathematical work is practically eliminated, and the calculation becomes a very simple process which can be carried out reliably by untrained operators.

An example of a dot chart for computing gravity effects is shown by Fig. 63.

Dot charts are of various types. The easiest to calculate and the most commonly used are designed to operate on a vertical cross section of a mass that is infinitely long in the direction perpendicular to the plane of the chart. Such charts and calculations are commonly called "two-dimensional." If the actual dimension in this direction is several times larger than the dis-
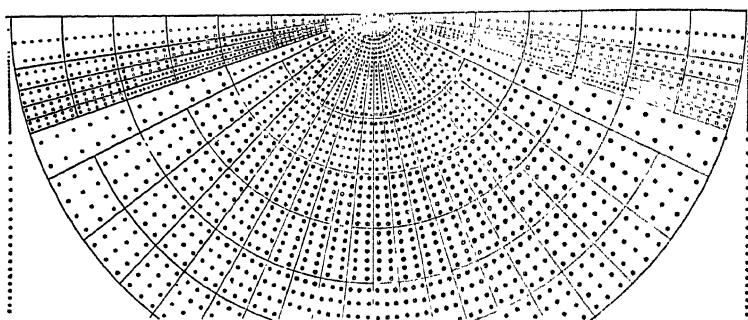
FIG. 63.—Dot chart for calculation of gravity effects of two-dimensional mass forms.

tance from the cross section to the origin of the chart, the error in assuming infinite length is rather small. When the ratio of these dimensions becomes less than 3 or 4, quite large errors result, and corrections to the computed effects must be made to take care of the finite third dimension. In some cases, this is done by making up the charts for certain finite lengths or length ratios in the dimension perpendicular to the chart.[1] Another scheme is to design the chart to read effects for masses within a pie-shaped section between vertical bounding planes at definite angles (say 22½ deg.)[2]. Still another method is to use an auxiliary chart which gives the ratio of the effect of an element of finite length to that for infinite length and multiply the effect read from the two-dimensional chart by this ratio.

[1] Barton, 1929a, pp. 488–489.
[2] Heiland, 1929b.
Haalck, 1929, pp. 111–130.

The "end correction" for reducing gravity effects computed with a two-dimensional chart to those for structures of finite length may be computed readily from the relation

$$\frac{g}{g_\infty} = \frac{1}{\sqrt{1 + (\rho/y)^2}} \equiv F\left(\frac{y}{\rho}\right)$$

Consider that the calculation is being made at the point O (Fig. 64) and that the chart is in the XZ plane and that g is the gravity for an element of finite length y (on one side only of the plane of the chart); g_∞ is the gravity for a semi-infinitely long element ($y = \infty$); ρ is the radial distance (in the plane of the chart) from the point at which the effect is being calculated to the center of the element in question.
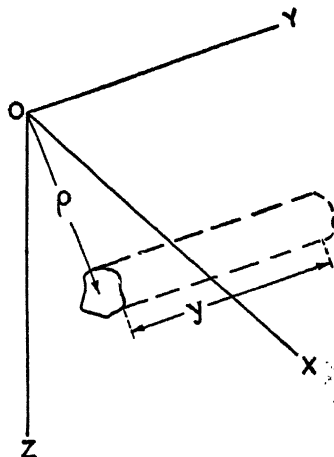
Fig. 64.—"End correction" factor for reducing "two-dimensional" calculations for structures of finite length.

The following table gives values of the correction factor $F(y/\rho)$ for various values of the ratio y/ρ.

y/ρ	$F(y/\rho)$	y/ρ	$F(y/\rho)$	y/ρ	$F(y/\rho)$	y/ρ	$F(y/\rho)$
0.1	0.100	0.7	0.573	1.6	0.848	4.0	0.970
0.2	0.195	0.8	0.620	1.8	0.872	4.5	0.975
0.3	0.286	0.9	0.667	2.0	0.893	5.0	0.981
0.4	0.372	1.0	0.705	2.5	0.927	6	0.986
0.5	0.446	1.2	0 770	3.0	0.948	7	0.990
0.6	0.514	1.4	0 811	3.5	0.960	8	0.993
...	.....	...	.....	...	.....	9	0.994
...	.....	...	.....	...	.....	10	0.995

The correction factors are used in the following fashion. Suppose that the lengths of the structure on the two sides of the plane of the chart are y_1 and y_2 and that the corresponding correction factors are F_1 and F_2. Then the gravity value which is computed from the two-dimensional chart (and which equals $2g_\infty$ in the foregoing notation) must be multiplied by $(F_1 + F_2)/2$ to yield the gravity for the finite structure. If the length of the

structure on one side is the same as the length on the other side, then $y_1 = y_2$, $F_1 = F_2$, and the chart value need be multiplied only by F_1 to yield the gravity for the finite structure.

Another type of calculation chart for gravity or torsion balance effects operates on a horizontal plane. Such a chart gives the effect at the chart origin of a horizontal slab of material with a finite boundary. This can be used for calculation of a mass which is represented by contours and which is considered as made up of a pile of horizontal slabs each having the thickness represented by the contour interval. However, one parameter in the design of such a chart is the ratio of horizontal dimension to depth so that either the contour outline has to be drawn at a
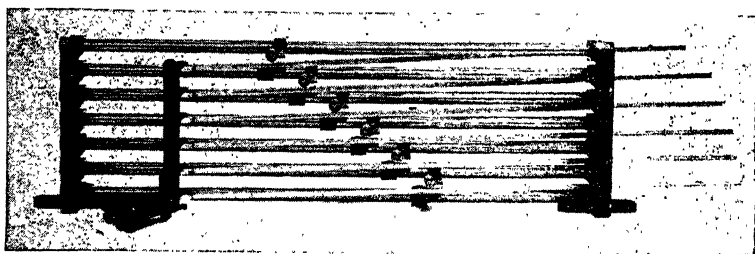
Fig. 65.—Multiple integrator for calculation of gravity effects.

different scale for each depth or the chart has to have a variable scale element to take care of different depths to the slab, the effect of which is being computed. On account of these limitations, the horizontal charts are somewhat more difficult to use than the vertical section charts.

Mechanical Calculators.—For certain cases mechanical calculators can be used. For instance, the expression for the gravity of a two-dimensional body can be represented by a comparatively simple integral taken around the outline of the body in a vertical cross section. A modified planimeter will calculate this integral, and to use such an instrument it is necessary only to run a pointer around the periphery of the cross section and read the planimeter wheel. Multiple integrators operating on this principle have been constructed in which several planimeters are operated simultaneously as a pointer is run around the cross section, thus computing the gravity effect at several points on the surface simultaneously. An instrument of this kind built in

Russia had 10 elements.[1]   Figure 65 shows a calculator having six such elements which has been used quite extensively in the calculation of salt dome mass distribution to fit gravity anomalies.

THE INTERPRETATION OF GRAVITY EFFECTS

The result of a gravity or torsion balance survey is nearly always a gravity contour map.   The interpretation of such a map in terms of geology may be anything from a mere inspection of the map and outlining of trend lines or areas of structural disturbance to very elaborate and detailed calculations to find the size, shape, and position of a mass anomaly that will account for the principal details of the observed effects.   The variation in the degree of useful analysis and in the probable reality of
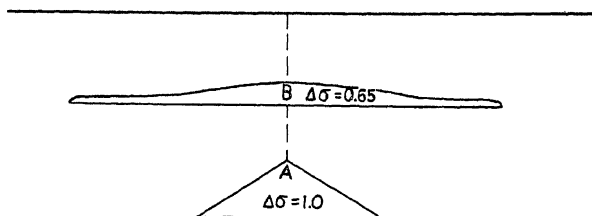
Fig. 66.—Two mass forms which give practically identical gravity effects.

the structural interpretation resulting depends (1) on the closeness and precision of the data; (2) on the degree to which the picture of the possible structure of interest is clouded by disturbing effects which may be shallow or deep; and (3) on the amount of control, either actual or assumed, available to limit the inherent ambiguity in the determination of the mass distribution which can cause a given gravity distribution.   No amount of detailed calculation to find a mass distribution to account for a given gravity distribution is justified unless the premises, *other than the gravity data,* on which such calculations are based are well founded.   This is illustrated by Fig. 66. This shows how a comparatively wide gravity anomaly may be the effect of a wide, shallow density anomaly or of a much narrower and deeper one.   Also, the gravity could be caused by a variety of possibilities intermediate between those shown.

A gravity anomaly is always wider than the mass anomaly that produces it.   Thus a shallow mass anomaly cannot be

[1] Gamburzeff. 1929, p. 90.

wider than the gravity anomaly that it causes, and a deep anomaly cannot be deeper than certain dimensions that can be derived from the gravity effects. Between these limits *the gravity picture itself gives no discrimination,* and any further limitation must come from drilling; from other geophysical data (such as seismic); or, in the absence of other control, from general considerations of geologic reasonableness.

Because of the lack of uniqueness, it is impossible to calculate directly from a gravity effect the mass distribution that causes it. If certain general assumptions are made, such as assuming that the mass anomaly is concentrated in a layer at a certain depth, the mass distribution on such a layer can be calculated as has been shown by Tsuboi[1] and as illustrated by Fig. 67. On
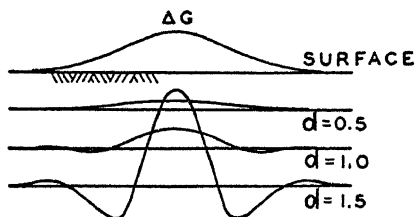
Fig. 67.—Density distributions at different depths which give identical gravity effects. The ordinates of the different curves are proportional to the calculated density distributions concentrated at the different levels below the surface (after Tsuboi and Fuchida, 1937, page 647).

account of these limitations, the usual method of estimating a mass distribution is to compute the effect for an assumed mass, based on whatever auxiliary control is available, compare the computed with the observed effect, modify the mass distribution, and recompute the effect, etc., until a fit of sufficient accuracy has been attained. If only an approximate fit is needed or very little auxiliary control is available, a computation from one of the simple forms, such as sphere, cylinder, or fault, may be all that is justified. Where more auxiliary control and accurate data are available, detailed computation with a dot chart or a mechanical integrator may be well worth while. It should be reiterated that the achievement of a good fit between computed and observed effect is no criterion of the reality of the mass distribution from which the computation was made unless the auxiliary control is

[1] Tsuboi, 1938.

adequate to remove the inherent ambiguity and lend uniqueness to the mass distribution derived.

THE INTERPRETATION OF TORSION BALANCE EFFECTS

Although the foregoing discussion is given primarily with respect to gravity, the same considerations apply also to the interpretation of torsion balance data. At this point it may be well to point out that gradients, curvatures, and gravity are all expressions of the same thing. They all can be derived by differentiation of the gravitational potential. Theoretically, if sufficient data are available, the potential can be derived from a surface integration of gradients or curvatures or gravity. Therefore, if a map of any one kind of gravity data is complete, nothing will be added by having another kind of gravity data over the same area. Usually, however, neither the gradient nor the curvature information is complete, and the two types of information supplement one another.

Interpretation of torsion balance data is often done by inspection or calculation to fit the gradient and curvature profiles. This is quite satisfactory if the geologic features being considered are much longer in one dimension than the other and the profiles are taken perpendicular to the strike. When the masses being considered are three-dimensional, the profiles may be misleading, and the calculations are much more complicated.

Interpretation of torsion balance data also may be made on the basis of a gravity map contoured from the torsion balance gradients. The interpretation of such a map is then exactly the same as it would be for a gravity map derived from direct measurements of gravity by pendulum or gravimeter. In most of the literature on calculations for torsion balance interpretation the methods or charts given are designed for use with gradients (or curvatures) rather than with gravity derived from the gradients.[1] However, the use of gravity has certain advantages, particularly for three-dimensional masses. This follows because the gradient and curvature profiles show only the components along the profile. On a profile taken in another direction these components will have different values, and there is no very simple

[1] See, for example, Jung, 1930, pp. 190–195. For a statement of the advantages of the use of gradients and curvatures rather than gravity, see Klaus, 1938.

way of being sure that the mass distributions that account for the components along one profile are consistent with those which account for the components along another profile.   On the other hand, when the gravity profile is made the basis of the interpretation, the consistency of the interpretation along different profiles can be judged simply from the fact that they must give the same gravity value at the profile intersection.   This often imposes a condition on the assumed structures that is hard to meet in making the calculations but at the same time gives better control on the mass distribution being calculated.

A system of torsion balance interpretation recently proposed by Klaus[1] involves constructing contour maps of each of the four torsion balance quantities.   For any given mass anomaly there is a certain pattern of highs and lows which should be shown by each of the four maps.   If all the maps are consistent in showing the essential elements of the ideal pattern for a given type of mass anomaly, the presence of such an anomaly is much more probable than if it were indicated by, say, a single gradient or curvature profile.   The system is quite independent of regional effects on both gradients and curvatures as long as such effects are reasonably constant over the area of a single anomaly pattern. For the best application of this system, the torsion balance stations should be made not along lines, as is commonly done, but scattered in a regular grid over the area being covered.   Such scattered locations also have the advantage of permitting more freedom in the choice of individual station sites so that, by judicious selection of their location, stations may be made that are relatively free of disturbance from near-by irregularities in terrain.

DEPTH ESTIMATION

For any of the regular geometric forms for which gravity (or gradient or curvature) effects are calculated, there is always a certain definite relation between the width of the effect and the depth of the mass producing it.   The gravity profiles of spheres and cylinders will serve as examples.   Take, for instance, the profile for a cylinder.   The function

$$f' \frac{x}{z} = \frac{1}{(x/z)^2 + 1} \qquad \text{[Eq. (80), page 108]}$$

[1] Klaus, 1938.

has a value of $\frac{1}{2}$ when x/z equals unity, or $Z_c = x_{\frac{1}{2}}$, where Z_c is the depth to the center of gravity of the mass anomaly. This means that, at a horizontal distance from the center equal to the depth, the value of gravity is just half the maximum value. We shall call this distance the "half width" and represent it by $x_{\frac{1}{2}}$. Thus we can estimate the depth to the center of gravity of a mass that corresponds approximately to a cylindrical cross section by measuring the width of the gravity profile at half the maximum height. Also, the horizontal distance from the point where the gravity is one-half the maximum on one side of the center to that where it is one-half the maximum on the other side of the center will be equal to twice the depth.

The profile for a sphere is somewhat sharper. In this case the ratio of x/z for half the maximum gravity is 0.766, and $z_c = 1.305x_{\frac{1}{2}}$.

The following is a table of depths from critical characteristics of gravity and torsion balance curves:

	Sphere[1]	Cylinder[2]	Fault[3]
Gravity...............	$Z_c = 1.305x_{\frac{1}{2}}$	$Z_c = 1.0x_{\frac{1}{2}}$	$Z_c = x_{\frac{1}{2}}$*
Gradient.............	$Z_c = 2.0x_{max}$	$Z_c = 1.733x_{max}$	$Z_c = x_{\frac{1}{2}}$
Curvature...........	$Z_c = 1.225x_{max}$	$Z_c = 1.0x_0$ $= 2.06x_{\frac{1}{2}}$	$Z_c = x_{max}$

Z_c = depth to center of gravity of mass anomaly.
$x_{\frac{1}{2}}$ = half width as defined above.
x_{max} = horizontal distance to maximum or minimum on curve.
x_0 = horizontal distance to zero point on curve.

* $x_{\frac{1}{2}}$ = distance from the fault trace to the point at which the gravity change is one-half the total change from the fault trace to infinite distance.
[1] See curves, Fig. 58, p. 104.
[2] See curves, Fig. 60, p. 109.
[3] See curves, Fig. 62, p. 114.

Calculation of Size and Depth to Top of Mass Anomalies.— From the depth to the center of gravity and the gravity magnitude the radius of the equivalent sphere or cylinder can be computed readily if the density or density contrast is known or assumed. This radius subtracted from the depth to the center will give the depth to the top. Figures for depth, estimated in this way, are only approximate. Also, they give maximum depths to the centers. Wider mass anomalies can give nearly the

same gravity anomalies and be at considerably shallower depths. For this reason, depth estimates based on such simple approximations to observed gravity are maximum values only, and shallower depths are possible.

For instance, for a sphere we have, from Eq. (62), that the gravity over the center (where $x = 0$) is

$$g_{max.} = 8.53\sigma \frac{R^3}{z^2} \tag{97}$$

when $g_{max.}$ is in milligals and R and z are in kilo-feet units. From this

$$R = 0.489 \sqrt[3]{\frac{g_{max.}z^2}{\sigma}} \tag{98}$$

For example, suppose that a gravity anomaly which looks as if it might come from a spherical mass anomaly has a gravity relief of 3 mg. and a "half width" of 5,000 ft. From the table (page 123) the depth to the center is

$$Z_c = 5,000 \cdot 1.305 = 6,525 \text{ ft.} = 6.5 \text{ kilo-ft.}$$

If we postulate that the mass anomaly is a deep salt dome with salt having a density of 2.2 and the surrounding sediments a density of 2.45, the density contrast is 0.25. Then the radius, calculated from Eq. (98), is

$$R = 0.489 \sqrt[3]{\frac{3 \cdot (6.5)^2}{0.25}} = 3.9 \text{ kilo-ft.}$$

The depth to the top of the sphere, of course, is

$$Z_t = Z_c - R$$

which for the present example comes out $6.5 - 3.9 = 2.4$ kilo-ft., or 2,400 ft.

For a cylinder, we find, from Eq. (79), that the gravity over the center (where $x = 0$) is

$$g_{max.} = 12.77\sigma \frac{R^2}{z} \tag{99}$$

where $g_{max.}$ is in milligals and R and z are in kilo-feet. From this

$$R = 0.280 \sqrt{\frac{z g_{max.}}{\sigma}} \tag{100}$$

Suppose that a gravity profile across a long, narrow anomaly, approximated as a horizontal cylinder, has a relief of 3 mg. and a half width of 5,000 ft. From the table (page 123) the depth to the center

$$Z_c = x_{1/2} = 5,000 \text{ ft.} = 5 \text{ kilo-ft.}$$

If we assume a density contrast of 0.25, the radius of a cylindrical mass that could cause the anomaly is

$$R = 0.280 \sqrt{\frac{3 \cdot 5}{0.25}} = 2.2 \text{ kilo-ft.} = 2,200 \text{ ft.}$$

and the depth to the top is

$$Z_t = Z_c - R = 5 - 2.2 = 2.8 \text{ kilo-ft.} = 2,800 \text{ ft.}$$

Isolation of Gravity Anomalies.—The foregoing discussions of means of calculation are all concerned essentially with the determination of a single mass unit to fit a single gravity anomaly. Actually, a gravity map as constructed from field data will rarely show a single anomaly that is not contaminated by the effects of smaller or larger disturbances.

The smaller disturbances arise from local irregularities nearer the surface than those in which we are interested and commonly affect only a single or at most a very few stations. Such effects can be removed by judicious smoothing ·or selection of the measured results.

The larger disturbances arise from density irregularities which may be at much greater depth than those of possible structures in which we are interested and presumably arise frequently from density variations in the basement far beneath the sedimentary section. These effects are commonly called "regional," and their estimation and removal are often desirable. Several different means may be employed for the purpose.

In torsion balance work one method is to average all the gradient and curvature components within the area being considered and subtract this average from all the measured values. This assumes that the regional is uniform over the area being considered. Another method is to average only those components which are outside the probable area of influence of the particular anomaly being considered.

In dealing with gravity maps, either from torsion balance or from direct gravity measurements, a contour map of some kind can be drawn for the regional. This involves a considerable amount of arbitrary judgment and is without any very definite quantitative basis. Regional contours may be constructed by simply drawing smooth contours over the contours as drawn from the observed data, *i.e.*, by smoothing out and cutting across the irregularities considered to be of the type that it is desired to bring out by the regional subtraction. In using profiles it is customary simply to draw a straight line or a smooth curve which is estimated as that of the regional gravity or gradient or curvature. In any case, after the regional is determined, it is subtracted either numerically or graphically from the observed quantities to leave the residual anomalies. When contours of the regional gravity are drawn, they can be subtracted from contours of the original, and a third set of contours made to give the difference or residual gravity. This is analogous to a subtraction of one set of geologic contours from another to give a convergence map.

It is not uncommon for two separate mass anomalies to lie so close together that their gravity effects overlap. In such cases it may be difficult to decide whether the mass causing the disturbance is a single feature or is divided into two or more separate masses. The distance apart of features that can be distinguished or resolved is directly related to their depth. For instance, for spherical masses, a gravity profile will begin to show two distinct features when the separation between the centers of the masses is equal to their depth. For some of the torsion balance quantities the resolution is somewhat closer. However, in general, it may be stated that gravity surveys will find it difficult or impossible to distinguish two disturbing masses as separate features if their centers of gravity are closer together than their depth. This subject has been considered in some detail by Elkins and Hammer,[1] and their paper contains a mathematical treatment of the conditions limiting the resolution of combined effects from bodies of several different forms and gives numerical values for limiting separations that can be resolved. This paper should be consulted by anyone interested in the exact relations

[1] Elkins and Hammer, 1938.

between the limiting separation at which disturbing mass (or magnetic) anomalies can be resolved by their various geophysical effects.

RELATION OF GEOLOGIC SECTION TO PROBABLE GRAVITY ANOMALIES

We have seen how the magnitudes of gravity anomalies depend fundamentally upon the density contrasts within the geologic section. The possible density contrasts therefore are a primary consideration in judging the nature of the results to be expected from the gravity survey in a given area. If there are no density contrasts within the geologic section that it is wished to explore, we cannot expect useful results from gravity surveys. Fortunately, there seem to be few instances where there is not sufficient density contrast to make gravity exploration of some value. A brief review of the geologic section in a few areas and the expected gravity results follows.

Gulf Coast.—The sedimentary section is an unconsolidated series of shales and sands with the density increasing from about 1.8 near the surface to around 2.45 at great depths. The increase in density results primarily from compaction of the shales. The success of gravity exploration for salt domes in this area is due to the fact that salt has a density of about 2.2 which is lighter than the sediments at depths of more than about 2,000 ft., and the cap rock has a density of around 2.7 and is much heavier than the sediments. Therefore, salt domes produce gravity minima if the salt is deep, and the cap rock may produce a local gravity maximum if it is shallow. The gravity picture of a salt dome may be almost any combination of these two effects. The gravity minima for salt domes vary from less than 1 mg. for small or deep domes to over 10 mg. for very large domes; and the gravity maxima due to cap rock vary from a few tenths to as much as 4 or 5 mg.[1]

Oklahoma.—Over most of Oklahoma the upper part of the section is Permian or Pennsylvanian red beds composed of sands and shales. Below this the Pennsylvanian section is of generally similar character with some limestones, but, in the main, these are not massive enough to affect the density materially. Therefore, the density from the surface to the bottom of the Pennsyl-

[1] Barton, 1938, pp. 374–376.

vanian is rather uniform with a value of around 2.2 to 2.4. The deeper Mississippian and older Paleozoic rocks contain considerable thicknesses of lime and dolomite (Mississippi lime, Viola, Arbuckle, etc.). Thus, there is a rather marked density contrast at the unconformity at the base of the Pennsylvanian, and most of the strong gravity anomalies in Oklahoma result from this density contrast. The Oklahoma City structure produces a gravity anomaly of between 1 and 2 mg. due to the strong uplift of the Arbuckle at a depth of around 6,000 ft. The Healdton structure produces a gravity anomaly of several milligals because the heavy Viola and Arbuckle limes are brought rather close to the surface where they have a strong density contrast with the surrounding Permian and Pennsylvanian. On the other hand, some pronounced structures, such as Sholem Alechem, have weak or no gravity effect because the structure involves only the rather homogeneous, thick Pennsylvanian section.[1]

California.—The section in most of the California oil-producing areas is composed of a great thickness of unconsolidated Tertiary sediments, ranging in density from about 1.8 near the surface to probably 2.2 to 2.3 at considerable depth. Thus, structures might be expected to have rather small positive gravity anomalies because of the increase of density with depth. However, part of the San Joaquin Valley is underlain by a section of very light, diatomaceous earth with a density of 1.5 or lower. Therefore, when this section is involved in structural uplift, it causes negative gravity anomalies, some of which are very pronounced. The Lost Hills structure, for instance, has a negative gravity anomaly of about 7 mg.[2]

[1] Barton, 1938, p. 376.
[2] Barton, 1938, pp. 377–378.

CHAPTER VII

ISOSTASY

RELATION OF ISOSTASY TO GRAVITY

A great many gravity measurements have been made over the United States and many other parts of the world in connection with exact studies of the shape and mass distribution of the earth. These measurements have led to the theory of isostasy which postulates a system for the distribution of material in the earth's crust to account for the observed gravity values. The values of interest in this connection are those of absolute gravity which are usually made by measuring the period of a pendulum by comparisons with a very accurate chronometer or, as in some later work, by comparison of fixed and movable pendulums. If the measurements are referred to a starting point at which the absolute value of gravity has been determined, say, by a Kater reversible pendulum, then the absolute value can be calculated for all stations.

ORIGIN OF ISOSTATIC THEORY

The isostatic theory had its origin in gravity measurements made in the high mountains of India, beginning around 1850. The measurements were made over a large range of elevation. Then the measured value of gravity was compared with that calculated from the latitude and elevation of the station and the gravity formula (page 17). It was found that when the ordinary free-air correction for elevation and the Bouguer correction for attraction of material above sea level (including irregularities of topography) were applied, the resulting theoretical value was much too large for stations with high elevations; in fact, in many cases a value much nearer the measured value was obtained when the Bouguer correction was omitted entirely. However, since there can be no doubt that a station made at a high elevation must be subject to the attraction of material between sea level and the height of the station, the discrepancy in the values so corrected must be explained in terms of differences in density

of the earth's crust below sea level.   This led to the suggestion
that the material of the earth's crust is lighter under mountains
and continents than it is under places where the surface elevation
is low as under the oceans and ocean deeps.

This same situation had been indicated earlier by a quite
different type of measurement, *i.e.*, by the deflection of the
plumb, or vertical.   By a combination of astronomic and geodetic
measurements, it is possible to measure quite accurately the
deflection of the vertical, *i.e.*, the angle by which a plumb line
departs from the direction that it would have for a uniform earth.

Fig. 68.—Deflection of the vertical
by a mountain mass.

If such measurements are made
on opposite sides of a mountain
(Fig. 68), the vertical would be
expected to be deflected toward
the mountain by an amount
depending on the density and
form of the mountain mass.   When such measurements were
made, it was found that the expected deflections were much
smaller than those calculated, which suggested that the attraction
of the mountain was neutralized by a deficiency in density under
the mountain.

The terms "isostasy" and "isostatic compensation" are used
to designate a variation in density of the earth's crust which is
systematically related to the surface elevation.   The word
"isostasy" was first used by Dutton.   In recent years, Major
William Bowie, recently retired from the U.S. Coast and Geodetic
Survey, has been an ardent exponent of isostasy and has written
a book[1] which should be consulted by anyone wishing to pursue
the subject.

DIFFERENT THEORIES OF ISOSTASY

Two rival theories of isostasy were set forth at the same time
by Pratt and Airy, and the papers that first announced these
theories followed one another in the same number of the *Phil-
osophical Transactions* of the Royal Society of London in 1855.

Airy Theory.—The Airy theory postulates that at some depth
below the earth's crust there is a change in density of the material
and that the lighter upper rigid part floats on the heavier lower
fluid part.   Under mountain areas this lighter part is assumed
to be thicker so that it projects down farther into the heavier

1 Bowie, 1927.

material below, and the mountains are supported by the buoyancy of the rigid "roots" which project down into this lower material, just as the height of an iceberg above the water is proportional to the depth at which the ice projects down into the water. Thus Airy's is referred to as the "roots of mountains" hypothesis.

Pratt Theory.—The Pratt system of isostasy postulates also that the upper material of the earth's crust is lighter than the lower material but differs from that of Airy in assuming that the boundary at which the change in density occurs is essentially horizontal and at a uniform depth called "the depth of compensation." Under a mountain area the material between the depth of compensation and the surface is assumed to be lighter than that under an area of lower topography. This variation in density is assumed to be so related to the surface elevation that the weight of a unit cross section of material from the surface to the depth of compensation is the same for different elevations. This, of course, then gives a uniform pressure at a uniform depth of compensation.

Discrimination between the Two Theories.—Either the Pratt or the Airy system gives a principle by which the gravity observations can be explained, for in either case a high elevation is underlain by a material of low density, and a low elevation is underlain by a material of high density. It turns out that over a large area, such as a broad elevated plateau, the gravitational effect of the deficiency in mass under the elevation, which is postulated on the theory of isostasy, is approximately the same as the gravitational attraction of the material above sea level which would be calculated as the Bouguer correction. Therefore, the two effects approximately compensate one another, which explains the fact that often the free-air reduction, without making the Bouguer correction, gives smaller anomalies than when the Bouguer effect is included.

On the basis of gravity results alone, there is little to discriminate between the Pratt and Airy systems of isostatic compensation. However, it has been observed that for large units of the earth's surface the average density of exposed igneous rocks varies inversely as the average altitude (Bucher's Law X).[1] Also it has been observed that the velocities of earthquake waves under ocean areas are somewhat higher than under continental areas, which may indicate a systematic difference in material

1 Bucher, 1933, p. 44.

that would be consistent with the Pratt hypothesis. Thus, there is external evidence indicating that the Pratt system probably is more nearly in accord with the actual facts than is the Airy system. The former is much more amenable to mathematical treatment and, for this reason also, has been used much more extensively than the Airy system as a basis of computations made to explain observed gravity values on the basis of isostatic compensation. It is quite probable that the actual density distribution is materially different from either ideal system.

INVESTIGATIONS OF GRAVITY AND ISOSTASY

An investigation of isostasy on the basis of gravity measurements has been the subject of very extensive work by the U.S. Coast and Geodetic Survey over a period of many years.[1] The background of this work consists of a net of a few hundred absolute pendulum gravity stations made at scattered points all over the United States. These measurements were made with a single pendulum apparatus, the rates of the pendulum being determined with a chronometer. In this way, after starting from a fixed reference point (in Washington, D.C.) at which the absolute value of gravity was known, the absolute value of gravity was determined at all the other stations. These measurements were not nearly so precise as those made for geophysical prospecting but are quite adequate for the purposes for which they were made, as errors of a few milligals would not interfere with testing the isostatic theory. Also, many gravity measurements have been made at sea (in a submarine[2]), and these have contributed materially to isostatic studies.

As in testing any scientific theory, one of the most satisfactory ways is to compare a measured value with a value calculated on

---

[1] Hayford and Bowie, 1912.

Bowie, 1917.

Bowie, 1924.

[2] Most of the gravity measurements at sea have been made by Dr. F. A. Vening Meinesz who has traveled many thousands of miles in submarines of the Dutch and American navies for this purpose. A special three-pendulum apparatus is mounted within the submarine. Measurements are made with the ship submerged about 100 ft. to be free of wave motion. Very complete descriptions of the theory and practice of this work are given by Vening Meinesz, 1929, 1930, 1932, 1934.

the basis of the theory. In the case of the gravity measurements this involves calculating the value of gravity at the latitude and elevation of the station and comparing it with the value measured at that point. The difference between the measured value and the theoretical value so calculated is the anomaly. The theory which, on the average, gives the smallest anomalies is presumably the most nearly correct.

THE DIFFERENT GRAVITY "ANOMALIES"

Various anomalies may be calculated depending on the effects that are taken into account. The notation below is partly that used by the U.S. Coast and Geodetic Survey.

"Free-air" Anomaly.—The free-air gravity γ is that calculated with only the free-air elevation effect and is

$$\gamma = \gamma_0 - Kh$$

where γ_0 is the theoretical gravity at sea level and the latitude of the station, as calculated from the gravity formula used. K is the free-air coefficient which takes account of the decrease in gravity because an elevated point at height h is farther from the center of the earth.

The free-air anomaly is the difference between the measured value g and the free-air gravity; *i.e.*, free-air anomaly $= g - \gamma$.

Bouguer Anomaly.—The Bouguer gravity includes the calculation of the attraction of material between sea level and the actual earth's surface. Using Bullard's[1] system, this may be divided into two parts: (1) the attraction Bh, which considers the material as a uniform sheet of infinite horizontal extent (with a correction for the curvature of the earth) and of thickness h and uniform density, and (2) the terrain effect T, which takes account of the attraction of departures of the actual terrain from a level surface through the station. Thus, the total Bouguer effect is $Bh - T$; the Bouguer gravity is

$$\gamma'' = \gamma_0 - Kh + Bh - T$$

and the Bouguer anomaly is $g - \gamma''$.

Isostatic Anomaly.—Finally, if we postulate the condition of isostasy, we must calculate the effects at the station of all the mass deficiencies under high elevations and mass excesses under low elevations. Let the sum of all these isostatic effects be I.

[1] Bullard. 1933.

Then the isostatic gravity is

$$\gamma_i = \gamma_0 - Kh + (Bh - T) - I$$

and the isostatic anomaly is $g - \gamma_i$.

For the work by the U.S. Coast and Geodetic Survey the formula used in calculating the theoretical gravity γ_0 is

$$\gamma_0 = 978.039(1 + 0.005294 \sin^2 \varphi - 0.000007 \sin^2 2\varphi)$$

[See page 18, Eq. (9).][1]

The calculation of the term I is a straightforward but long and tedious process. The earth's crust is divided up into zones and compartments by a series of circles and radial lines, just as mentioned above in connection with terrain corrections. The entire surface of the earth is included in these zones. In each zone the density from the surface to the depth of compensation is assigned a value that depends on the average elevation of the zone and is such that the total weight per unit area of a column from the surface to the depth of compensation is uniform. Thus, a zone in an area where the average surface topography is high will have a lower density down to the depth of compensation than one in which the average surface topography is low. The attractions at the station of the mass excesses or deficiencies in all these zones are calculated. The sums of all these attractions constitute the isostatic effect I. This effect will be negative for a station at high elevation, (because of the density deficiency to compensate for the mass excess of the surface elevation) and positive for an ocean station. The process of calculating the isostatic effects has been highly developed and is carried out with the aid of a system of zone charts which are used over topographic maps of different scales, depending on the distance from the station and the detail into which the zones divide the earth's surface.

THE DEPTH OF COMPENSATION

Various figures have been used for the "depth of compensation." One basis for arriving at a figure for this depth has been to calculate isostatic anomalies for stations with a wide range of elevation using different depths of compensation. The depth that gives the smallest average anomaly is considered the most

[1] Recently, the U.S. Coast and Geodetic Survey has recalculated its gravity anomalies on the basis of the International Formula [Eq. (10), p. 18].

probable actual depth of compensation. Also, a figure for the depth of compensation has been derived from measurements of the deflection of the vertical. On the basis of such calculations this depth is approximately 100 km., or 60 miles. As one of its standard figures the U.S. Coast and Geodetic Survey uses a depth of 113.7 km.

Tests of Isostasy by Selected Gravity Stations.—As an example of the degree to which the isostatic theory actually accounts for gravity anomalies, we may consider selected stations in the United States in mountainous regions. For instance, of 36 stations located in mountainous regions but with the stations below the general level of the surrounding topography, the average isostatic anomaly with a depth of compensation of 113.7 km. is −3 mg.; the same for a depth of compensation for 60 km. is 0 mg.; the Bouguer anomaly is −107 mg.; and the free-air anomaly is −8 mg. Similar figures for an average of 20 stations in mountainous areas, but above the general level of the topography, are: isostatic anomaly depth of compensation 60 km., +16 mg.; Bouguer anomaly, −110 mg.; free-air anomaly, +58 mg.

The following table shows the anomalies for a few stations that bring out the differences between the isostatic anomalies and the reductions made without regard to isostatic compensation.

Station	Location	Eleva-tion, meters	Anomalies, mg.				
			Free-air	Boug-uer	Isostatic		
					Depth of compensation		
					56.9 km.	96 km.	113.7 km.
Mountain peak { 43	Pikes Peak, Colo.	4,293	− 15	−219	+ 5	− 4	− 8
55	Mt. Hamilton, Colo.	1,282	+114	− 9	+14	− 1	− 6
102	Cloudland, Tenn.	1,890	+131	− 55	+22	+ 6	+ 1
Deep valley { 69	Grand Canyon	849	−108	−184	0	− 9	−12
46	Grand Junction, Colo.	1,398	− 29	−184	+24	+23	+22
High plateau { 41	Wallace, Kan.	1,005	− 14	−126	− 8	−12	−14
100	Guymon, Okla.	949	− 20	−121	−16	−18	−19
99	Farwell, Tex.	1,259	− 8	−145	−13	−17	−19
271	Bridgeport, Neb.	1,114	− 14	−139	− 6	− 8	− 9

From this table it will be noted that stations on high peaks (55, 102) have large negative Bouguer anomalies and large posi-

tive free-air anomalies and that the isostatic anomaly is very much smaller than either. Stations on high plateaus have large negative Bouguer anomalies, but the free-air and isostatic anomalies are approximately the same. This results from the condition mentioned above, that the deficiency in attraction, due to the deficiency in density of the material between the surface and the depth of compensation over a wide area (width large in comparison with the depth of compensation), approximately balances the Bouguer attraction of the material between sea level and the elevated surface.

The fact that on the average the isostatic anomalies are very much smaller than the free-air, or Bouguer, anomalies indicates that some sort of compensation must actually exist. The details of the mechanism of isostatic compensation are the subject of considerable argument and difference of opinion. It is undoubtedly true that compensation is not uniform and that small elements of topography are supported by the rigidity of the earth's crust and not by exact compensation. There is little doubt that large elements of topography, and certainly those of the continental extent, are on the average quite completely compensated, as is indicated by the fact that the isostatic gravity anomalies on the average are small. Just how broad the boundaries are between relatively complete compensation and lack of compensation is still open to question.

Isostatic compensation has little interest directly in connection with geophysical prospecting. This results because the gravity anomalies of interest as possible indications of local geologic structure which might influence oil accumulation are practically always of such limited horizontal extent that they almost certainly are not compensated, for they result from irregularities in density much too local to be balanced out by other differences in density extending to a depth comparable with the depth of compensation. However, the principle of isostasy is of much interest in connection with very large-scale geologic features, and it is quite possible that, as time goes on and a more complete body of gravity information is built up and studied, it will lead to interesting suggestions as to the details of the density distributions and geologic processes within the earth's crust which are associated with the great tectonic features that control the regional geology of large areas.

APPENDIX I

TABLES OF NORMAL GRAVITY

The following tables give the value of theoretical gravity on the International Ellipsoid, calculated from the International Gravity Formula,

$$\gamma = 978.0490(1 + 0.0052884 \sin^2 \varphi - 0.0000059 \sin^2 2\varphi)$$

for each 10 min. of latitude.

Since the tables are given to the sixth decimal place and the second differences are almost constant for a range of a few degrees, it is possible to interpolate accurately to single minutes or tenths of minutes, by use of a suitable interpolation formula.[1] If a survey of a general area is to be reduced with respect to a local latitude, tables of latitude effects from that reference latitude may be prepared by subtracting the normal gravity for the refer-

---

[1] An interpolation formula that will give values to single minutes of latitude as accurate as the tabulated values is the following:

$$\gamma_{\varphi+n} = \gamma_\varphi + \frac{n}{10} \Delta\gamma_\varphi + K \, \Delta^2\gamma_\varphi$$

where γ_φ = tabulated value at latitude φ.

   n = intermediate minute.

   $\Delta\gamma_\varphi$ = difference in successive values in the table (*i.e.*, the first difference).

   $\Delta^2\gamma_\varphi$ = second difference in values in the table (*i.e.*, the differences in successive values of the first differences).

   K = value given in the small table below.

n, Minutes	K
1	-0.045
2	-0.08
3	$-0\ 105$
4	$-0\ 12$
5	-0.125
6	-0.12
7	-0.105
8	-0.08
9	-0.045

For example, suppose that we wish to interpolate to single minutes in the range between 30°10′ and 30°20′. From the table,

ence latitude from the values interpolated from the tables over the latitude range of the area being covered.

$\Delta\gamma_\varphi = 0.363853 - 0.350787 = 0.013066,$ and $\Delta^2\gamma_\varphi = 0\ 000043.$

Substituting in the interpolation formula, the values to single minutes are

30°10′	979.350787	30°16′	979.358623
11	.352092	17	.359930
12	.353397	18	.361237
13	.354703	19	.362544
14	.356009	20	.363853
15	.357316		

.

VALUES OF THEORETICAL GRAVITY ON THE INTERNATIONAL ELLIPSOID[1]
$$\gamma = 978.0490(1 + 0.0052884 \sin^2 \varphi - 0.0000059 \sin^2 2\varphi)$$

Geographic latitude φ	Gravity, cm./sec.^{2}	Geographic latitude φ	Gravity, cm./sec.^{2}	Geographic latitude φ	Gravity, cm./sec.^{2}
0° 0′	978.049000	6° 0′	978.105265	12° 0′	978.271635
10	.049044	10	.108422	10	.277770
20	.049174	20	.111665	20	.283983
30	.049392	30	.114993	30	.290277
40	.049697	40	.118405	40	.296649
50	.050089	50	.121903	50	.303100
1 0	978.050568	7 0	978.125484	13 0	973.309630
10	.051134	10	.129150	10	.316238
20	.051789	20	.132901	20	.322926
30	.052528	30	.136737	30	.329690
40	.053356	40	.140656	40	.336531
50	.054270	50	.144659	50	.343453
2 0	978.055272	8 0	978.148747	14 0	978.350450
10	.056360	10	.152918	10	.357524
20	.057535	20	.157173	20	.364675
30	.058797	30	.161511	30	.371903
40	.060146	40	.165934	40	.379207
50	.061582	50	.170439	50	.386587
3 0	978.063104	9 0	978.175027	15 0	978.394043
10	.064714	10	.179699	10	.401574
20	.066408	20	.184452	20	.409182
30	.068192	30	.189289	30	.416863
40	.070060	40	.194208	40	.424620
50	.072016	50	.199209	50	.432452
4 0	978.074057	10 0	978.204293	16 0	978.440358
10	.076185	10	.209458	10	.448337
20	.078398	20	.214706	20	.456392
30	.080699	30	.220034	30	.464519
40	.083086	40	.225443	40	.472720
50	.085559	50	.230935	50	.480993
5 0	978.088116	11 0	978.236507	17 0	978.489339
10	.090761	10	.242161	·10	.497757
20	.093491	20	.247896	20	.506248
30	.096306	30	.253710	30	.514810
40	.099208	40	.259605	40	.523445
50	.102194	50	.265580	50	.532150

[1] W. D. Lambert and F. W. Darling, *Bull. Géodesique*, No. 32, October, November, December, 1931.

VALUES OF THEORETICAL GRAVITY ON THE INTERNATIONAL ELLIPSOID.—
(Continued)

Geographic latitude φ	Gravity, cm./sec.^{2}	Geographic latitude φ	Gravity, cm./sec.^{2}	Geographic latitude φ	Gravity, cm./sec.^{2}
18° 0′	978.540926	24° 0′	978.901505	30° 0′	979.337764
10	.549773	10	.912682	10	.350787
20	.558690	20	.923917	20	.363853
30	.567678	30	.935210	30	.376963
40	.576736	40	.946560	40	.390115
50	.585864	50	.957968	50	.403309
19 0	978.595059	25 0	978.969432	31 0	979.416545
10	.604324	10	.980953	10	.429822
20	.613658	20	978.992530	20	.443140
30	.623059	30	979.004164	30	.456498
40	.632530	40	.015851	40	.469897
50	.642067	50	.027592	50	.483337
20 0	978.651671	26 0	979.039389	32 0	979.496812
10	.661343	10	.051240	10	.510328
20	.671081	20	.063144	20	.523882
30	.680886	30	.075102	30	.537473
40	.690756	40	.087112	40	.551103
50	.700692	50	.099174	50	.564768
21 0	978.710694	27 0	979.111288	33 0	979.578470
10	.720761	10	.123454	10	.592207
20	.730892	20	.135671	20	.605981
30	.741089	30	.147940	30	.619789
40	.751348	40	.160257	40	.633632
50	.761671	50	.172626	50	.647508
22 0	978.772057	28 0	979.185044	34 0	979.661419
10	.782507	10	.197510	10	.675362
20	.793019	20	.210025	20	.689338
30	.803594	30	.222589	30	.703345
40	.814230	40	.235201	40	.717385
50	.824928	50	.247860	50	.731455
23 0	978.835687	29 0	979.260565	35 0	979.745556
10	.846506	10	.273318	10	.759688
20	.857387	20	.286117	20	.773850
30	.868327	30	.298961	30	.788040
40	.879327	40	.311850	40	.802260
50	.890386	50	.324785	50	.816507

Values of Theoretical Gravity on the International Ellipsoid.—
(*Continued*)

Geographic latitude φ	Gravity, cm./sec.^{2}	Geographic latitude φ	Gravity, cm./sec.^{2}	Geographic latitude φ	Gravity, cm./sec.^{2}
36° 0′	979.830784	42° 0′	980.359132	48° 0′	980.899782
10	.845087	10	.374093	10	.914747
20	.859417	20	.389063	20	.929704
30	.873773	30	.404042	30	.944650
40	.888155	40	.419028	40	.959587
50	.902563	50	.434022	50	.974511
37 0	979.916995	43 0	980.449023	49 0	980.989425
10	.931453	10	.464031	10	981.004328
20	.945934	20	.479043	20	.019218
30	.960438	30	.494062	30	.034095
40	.974966	40	.509086	40	.048959
50	979.989517	50	.524114	50	.063809
38 0	980.004089	44 0	980.539146	50 0	981.078646
10	.018682	10	.554182	10	.093466
20	.033297	20	.569220	20	.108271
30	.047931	30	.584262	30	.123062
40	.062587	40	.599304	40	.137835
50	.077261	50	.614349	50	.152591
39 0	980.091955	45 0	980.629394	51 0	981.167331
10	.106667	10	.644439	10	.182053
20	.121397	20	.659486	20	.196755
30	.136146	30	.674530	30	.211438
40	.150911	40	.689574	40	.226103
50	.165692	50	.704616	50	.240748
40 0	980.180490	46 0	980.719656	52 0	981.255373
10	.195303	10	.734694	10	.269977
20	.210131	20	.749726	20	.284560
30	.224975	30	.764758	30	.299120
40	.239832	40	.779783	40	.313658
50	.254702	50	.794805	50	.328175
41 0	980.269585	47 0	980.809821	53 0	981.342667
10	.284481	10	.824832	10	.357135
20	.299389	20	.839836	20	.371579
30	.314308	30	.854834	30	.385999
40	.329240	40	.869825	40	.400393
50	.344181	50	.884807	50	.414761

VALUES OF THEORETICAL GRAVITY ON THE INTERNATIONAL ELLIPSOID.—
(Continued)

Geographic latitude φ	Gravity, cm./sec.^{2}	Geographic latitude φ	Gravity, cm./sec.^{2}	Geographic latitude φ	Gravity, cm./sec.^{2}
54° 0′	981.429104	60° 0′	981.923902	66 °0′	982.362437
10	.443419	10	.936939	10	.373622
20	.457708	20	.949932	20	.384749
30	.471968	30	.962881	30	.395815
40	.486200	40	.975785	40	.406823
50	.500404	50	981.988642	50	.417770
55 0	981.514578	61 0	982.001455	67 0	982.428657
10	.528723	10	.014222	10	.439482
20	.542837	20	.026941	20	.450248
30	.556921	30	.039613	30	.460950
40	.570974	40	.052239	40	.471591
50	.584996	50	.064816	50	.482171
56 0	981.598985	62 0	982.077344	68 0	982.492687
10	.612942	10	.089824	10	.503141
20	.626866	20	.102255	20	.513530
30	.640757	30	.114636	30	.523857
40	.654613	40	.126967	40	.534120
50	.668435	50	.139248	50	.544319
57 0	981.682222	64 0	982.151478	69 0	982.554452
10	.695974	10	.163656	10	.564520
20	.709691	20	.175782	20	.574522
30	.723371	30	.187856	30	.584460
40	.737014	40	.199878	40	.594331
50	.750620	50	.211846	50	.604135
58 0	981.764188	64 0	982.223763	70 0	982.613873
10	.777718	10	.235624	10	.623543
20	.791209	20	.247431	20	.633146
30	.804662	30	.259184	30	.642681
40	.818076	40	.270882	40	.652148
50	.831448	50	.282525	50	.661548
59 0	981.844781	65 0	982.294112	71 0	982.670877
10	.858073	10	.305642	10	.680138
20	.871323	20	.317116	20	.689330
30	.884531	30	.328532	30	.698452
40	.897697	40	.339893	40	.707504
50	.910821	50	.351194	50	.716485

Values of Theoretical Gravity on the International Ellipsoid.—
(*Continued*)

Geographic latitude φ	Gravity, cm./sec.^{2}	Geographic latitude φ	Gravity, cm./sec.^{2}	Geographic latitude φ	Gravity, cm./sec.^{2}
72° 0′	982.725396	78° 0′	982.996761	84° 0′	983.164537
10	.734236	10	983.002866	10	.167636
20	.743005	20	.008889	20	.170648
30	.751702	30	.014832	30	.173574
40	.760328	40	.020694	40	.176415
50	.768881	50	.026477	50	.179169
73 0	982.777361	79 0	983.032177	85 0	983.181836
10	.785769	10	.037795	10	.184417
20	.794104	20	.043333	20	.186912
30	.802367	30	.048788	30	.189319
40	.810554	40	.054161	40	.191640
50	.818669	50	.059452	50	.193873
74 0	982.826710	80 0	983.064661	86 0	983.196021
10	.834676	10	.069787	10	.198080
20	.842566	20	.074830	20	.200052
30	.850383	30	.079791	30	.201938
40	.858124	40	.084668	40	.203736
50	.865790	50	.089463	50	.205446
75 0	982.873379	81 0	983.094173	87 0	983.207070
10	.880893	10	.098801	10	.208606
20	.888331	20	.103344	20	.210054
30	.895691	30	.107805	30	.211415
40	.902975	40	.112181	40	.212689
50	.910182	50	.116472	50	.213874
76 0	982.917312	82 0	983.120679	88 0	983.214972
10	.924365	10	.124801	10	.215982
20	.931341	20	.128840	20	.216906
30	.938238	30	.132793	30	.217740
40	.945056	40	.136661	40	.218487
50	.951796	50	.140444	50	.219146
77 0	982.958458	83 0	983.144142	89 0	983.219718
10	.965040	10	.147755	10	.220201
20	.971543	20	.151283	20	.220597
30	.977967	30	.154725	30	.220904
40	.984311	40	.158081	40	.221124
50	.990576	50	.161352	50	.221256
				90 0	983.221300

APPENDIX II

GRAVITY TERRAIN CORRECTION CHARTS AND TABLES

The design of a system of zones and compartments and the calculation of the tables of corresponding gravity effects are described in detail in the publications of the U.S. Coast and Geodetic Survey.[1] The actual zones and tables described in these publications are designed for wide areas and large ranges of elevation and for the correction of stations to a precision of around 1 mg. To be adequate for correction of stations to 0.1 mg. or better, it is necessary to use a system of zones that is divided into smaller compartments at closer distances and to calculate corresponding tables for closer elevation
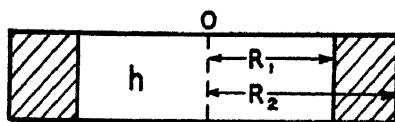
FIG. 69.—Cross section of hollow cylinder corresponding to one ring or "zone" of a terrain correction zone chart.

differences and smaller gravity effects. Special tables designed for terrain corrections for gravimeter surveys have been given by Hammer.[2]

The calculation of terrain effects is based on the formula for the gravitational attraction of a cylinder.

The attraction of a vertical cylinder of radius R, length h, and density σ at a point o at the center of one end is

$$2\pi\gamma\sigma(R - \sqrt{R^2 + h^2} + h) \tag{101}$$

We wish to consider the attraction of a ring of material indicated by the shaded cross section (Fig. 69) with inner radius R_1 and outer radius R_2. From the expression above this is

$$g = 2\pi\gamma\sigma(R_2 - R_1 + \sqrt{R_1^2 + h^2} - \sqrt{R_2^2 + h^2}) \tag{102}$$

The attraction for the entire ring, or "zone," may be divided into as many equal compartments as desired. If n is the number of compartments into which the zone is divided, the attraction for each compartment is simply g/n.

It is convenient to have tables giving for each compartment the limits of the range of elevation corresponding to integral units of gravitational attraction (*i.e.*, the limits are the heights at which the attraction is within ½ unit of a given integral unit of attraction). In calculating such tables it is

[1] Hayford and Bowie, 1912.
Bowie, 1917.
[2] Hammer, 1939.

TABLE I.—TERRAIN CORRECTION TABLES FOR GRAVITY

Zones	Zone B	Zone C	Zone D	Zone E	Zone F	Zone G	Zone H	Zone I	Zone J	Zone K	Zone L	Zone M	T
Compartments	4	6	6	8	8	12	12	12	16	16	16	16	
Inner radius / Outer radius	6.56 / 54.6	54.6 / 175	175 / 558	558 / 1,280	1,280 / 2,936	2,936 / 5,018	5,018 / 8,578	8,578 / 14,662	14,662 / 21,826	21,826 / 32,400	32,400 / 48,365	48,365 / 71,996	
T	± h, ft.	± h, ft.	± h, ft.	± h, ft.	± h, ft.	± h, ft.	± h, ft.	± h, ft.	± h, ft.	± h, ft.	± h, ft.	± h, ft.	T
0	0 to 1.1	0 to 4.3	0 to 7.7	0 to 18	0 to 27	0 to 58	0 to 75	0 to 99	0 to 167	0 to 204	0 to 249	0 to 304	0
0.1	1.1 to 1.9	4.3 to 7.5	7.7 to 13.4	18 to 30	27 to 46	58 to 100	75 to 131	99 to 171	167 to 290	204 to 354	249 to 431	304 to 526	0.1
0.2	1.9 to 2.5	7.5 to 9.7	13.4 to 17.3	30 to 39	46 to 60	100 to 129	131 to 169	171 to 220	290 to 374	354 to 457	431 to 557	526 to 680	0.2
0.3	2.5 to 2.9	9.7 to 11.5	17.3 to 20.5	39 to 47	60 to 71	129 to 153	169 to 200	220 to 261	374 to 443	457 to 540	557 to 659	680 to 804	0.3
0.4	2.9 to 3.4	11.5 to 13.1	20.5 to 23.2	47 to 53	71 to 80	153 to 173	200 to 226	261 to 296	443 to 502	540 to 613	659 to 747	804 to 912	0.4
0.5	3.4 to 3.7	13.1 to 14.5	23.2 to 25.7	53 to 58	80 to 88	173 to 191	226 to 250	296 to 327	502 to 555	613 to 677	747 to 826	912 to 1,008	0.5
1	3.7 to 7	14.5 to 24	25.7 to 43	58 to 97	88 to 146	191 to 317	250 to 414	327 to 540	555 to 918	677 to 1,119	826 to 1,365	1,008 to 1,665	1
2	7 to 9	24 to 32	43 to 56	97 to 126	146 to 189	317 to 410	414 to 535	540 to 698	918 to 1,185	1,119 to 1,445	1,365 to 1,763	1,665 to 2,150	2
3	9 to 12	32 to 39	56 to 66	126 to 148	189 to 224	410 to 486	535 to 633	698 to 827	1,185 to 1,403	1,445 to 1,711	1,763 to 2,086	2,150 to 2,545	3
4	12 to 14	39 to 45	66 to 76	148 to 170	224 to 255	486 to 552	633 to 719	827 to 938	1,403 to 1,592	1,711 to 1,941	2,086 to 2,366	2,545 to 2,886	4
5	14 to 16	45 to 51	76 to 84	170 to 189	255 to 282	552 to 611	719 to 796	938 to 1,038	1,592 to 1,762	1,941 to 2,146	2,366 to 2,617	2,886 to 3,191	5
6	16 to 19	51 to 57	84 to 92	189 to 206	282 to 308	611 to 666	796 to 866	1,038 to 1,129	1,762 to 1,917	2,146 to 2,335	2,617 to 2,846	3,191 to 3,470	6
7	19 to 21	57 to 63	92 to 100	206 to 222	308 to 331	666 to 716	866 to 931	1,129 to 1,213	1,917 to 2,060	2,335 to 2,509	2,846 to 3,058	3,470 to 3,728	7
8	21 to 24	63 to 68	100 to 107	222 to 238	331 to 353	716 to 764	931 to 992	1,213 to 1,292	2,060 to 2,195	2,509 to 2,672	3,058 to 3,257	3,728 to 3,970	8
9	24 to 27	68 to 74	107 to 114	238 to 252	353 to 374	764 to 809	992 to 1,050	1,292 to 1,367	2,195 to 2,322	2,672 to 2,826	3,257 to 3,444	3,970 to 4,198	9
10	27 to 30	74 to 80	114 to 120	252 to 266	374 to 394	809 to 852	1,050 to 1,105	1,367 to 1,438	2,322 to 2,443	2,826 to 2,973	3,444 to 3,622	4,198 to 4,414	10
11	.....	.....	to 127	266 to 280	394 to 413	852 to 894	1,105 to 1,158	1,438 to 1,506	2,443 to 2,558				11
12	.....	.....	to 133	280 to 293	413 to 431	894 to 933	1,158 to 1,209	1,506 to 1,571	2,558 to 2,669				12
13	.....	.....	to 140	293 to 306	431 to 449	933 to 972	1,209 to 1,257	1,571 to 1,634	2,669 to 2,776				13
14	.....	.....	to 146	306 to 318	449 to 466	972 to 1,009	1,257 to 1,305	1,634 to 1,694	2,776 to 2,879				14
15	.....	.....	to 152	318 to 331	466 to 483	1,009 to 1,046	1,305 to 1,350	1,694 to 1,753	2,879 to 2,978				15

Each zone is a circular ring of given radii (in feet) divided into 4, 6, 8, 12, or 16 compartments of arbitrary azimuth. *h* is the range of the mean topographic elevation in feet (without regard to sign) in each compartment with respect to the elevation of the station which has an attraction within ½ unit of the corresponding value of *T*. The tables give the correction *T* for each compartment in units of $\frac{1}{100}$ mg. for density (σ) = 2.0. This correction, when applied to Bouguer anomaly values which have been calculated with the simple Bouguer correction, is always positive.

convenient to transform Eq. (102) into a form such that the height h, of a compartment, corresponding to a given attraction, can be computed directly. Such an equation has been given by Hammer.[1]

Hammer's tables have been carefully designed for calculation of terrain effects for gravimeter stations with a precision of about 0.1 mg. or better. It is believed that the number of compartments used is a practical minimum which will give this precision.
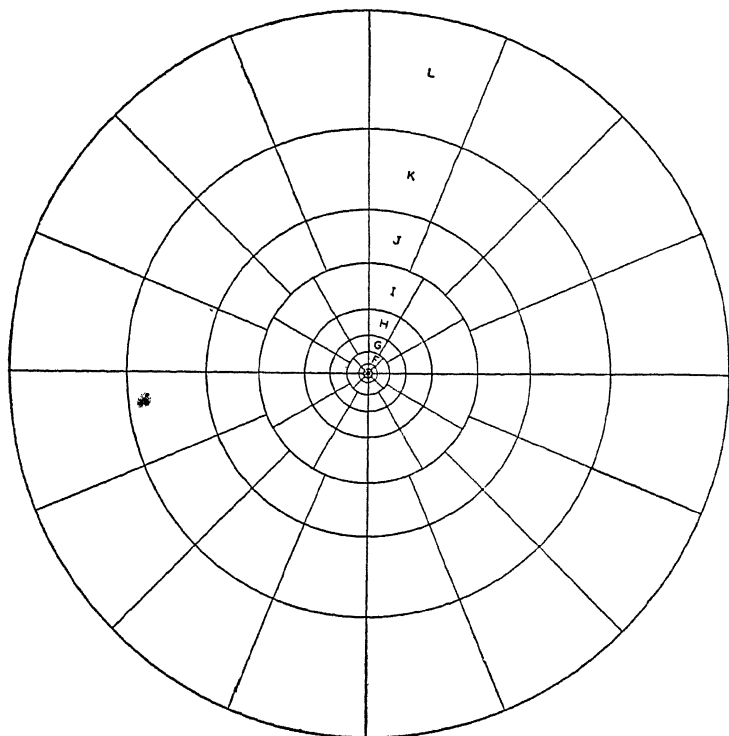
FIG. 70.—Terrain correction zone chart designed for calculation of terrain effects to a precision of 0.1 mg. or less.

The design of suitable tables for terrain correction is principally a matter of choosing a pattern of zones and compartments so proportioned that the various units of topography will be taken into account in proportion to their gravitational effects. Thus, the topography must be divided into small units of area near the station and larger units at greater distances. The heights for the various compartments are calculated and tabulated in increments corresponding with unit increments of gravitational effect.

In using the tables it is convenient to draw a zone chart (Fig. 70) on celluloid at the scale of the topographic maps to be used. The radii and

[1] Hammer, 1939, p. 192.

TABLE II.—TERRAIN CORRECTIONS, STATION *G*, ELEVATION 761 (760 OR 800)

Zone		1	2	3	4	5	6	7	8	9	10	11	12	13	14	15	16	Correction, 0.01 mg. unit
B	Elev.	760	760	760	760													
	Diff.	0	0	0	0													
	Corr.	0	0	0	0													0
C	Elev.	760	760	760	760	760	760											
	Diff.	0	0	0	0	0	0											
	Corr.	0	0	0	0	0	0											0
D	Elev.	780	760	760	720	720	720	750	760									
	Diff.	0	0	0	40	40	40	10	0									
	Corr.	0	0	0	1	1	0	0	0									3.0
E	Elev.	700	760	730	800	800	740	750	760									
	Diff.	0	0	30	40	40	20	10	0									
	Corr.	0	0	0.2	0.3	0.3	0.1	0	0									0.9
F	Elev.	820	740	870	1,150	1,200	1,000	740	800									
	Diff.	60	20	110	390	440	240	20	40									
	Corr.	0.3	0	1	10	13	4	0	0.1									28.4
G	Elev.	980	800	760	1,000	1,200	1,100	1,150	1,100	1,050	750	800	1,000					
	Diff.	220	40	0	240	440	340	290	340	190	10	40	240					
	Corr.	1	0	0	1	3	2	1	2	0.5	0	0	1					11.5
H	Elev.	1,050	750	1,000	1,250	1,200	1,100	1,100	1,100	1,000	780	900	1,100					
	Diff.	290	10	240	490	440	340	340	340	340	20	140	340					
	Corr.	1	0	0.5	2	2	1	1	1	1	0	0.2	1					10.7
I	Elev.	1,000	1,100	1,100	1,100	1,100	1,100	1,100	1,000	900	800	1,000	1,100					
	Diff.	200	300	300	300	300	300	300	300	100	0	200	300					
	Corr.	0.2	0.5	0.5	0.5	0.5	0.5	0.5	0.5	0.1	0	0.2	0.5					4.9
J	Elev.	900	1,000	1,100	1,100	1,000	1,200	1,100	1,100	1,000	1,200	900	900	1,000	1,000	1,000	1,100	
	Diff.	100	200	300	300	200	400	300	300	200	400	100	100	200	200	200	300	
	Corr.	0	0.1	0.2	0.2	0.1	0.3	0.2	0.2	0.1	0.3	0	0	0.1	0.1	0.1	0.2	2.2
K	Elev.	1,200	900	1,000	1,100	1,100	1,200	1,200	1,100	1,100	1,000	900	1,000	1,100	1,000	1,100	1,100	
	Diff.	400	100	200	300	300	400	400	300	300	200	100	200	300	200	300	300	
	Corr.	0.2	0	0	0.1	0.1	0.2	0.2	0.1	0.1	0	0	0	0.1	0	0.1	0.1	1.3
L	Elev.	1,200	1,000	1,100	1,100	1,200	1,200	1,100	1,200	1,100	1,100	1,000	1,000	1,100	1,100	1,200	1,100	
	Diff.	400	200	300	300	400	400	300	400	300	300	200	200	300	300	400	300	
	Corr.	0.1	0	0.1	0.1	0.1	0.1	0.1	0.1	0.1	0.1	0	0	0.1	0.1	0.1	0.1	1.3
																		Total 64.2[1]

[1] Correction for σ = 2.0 is 0.64 mg.; for σ = 2.4, correction is (2.4/2.0)0.64 = 0.77 mg.

number of compartments for each zone are taken from the data given in the column headings of Table I. The chart is then centered at the gravity station which has been located on a topographic map, and the average elevation of the topography in each compartment is estimated from the map. The station elevation is then subtracted from each compartment elevation to give the height difference between the compartment and the station, which is the value of h. Then, for each zone the attraction in units of 0.01 mg. is read from the T column of the table as the value corresponding to the range within which the h value falls.

The process will be clear from Table II which shows the terrain calculation for station G of Figs. 29 and 30 for the zone chart in the position shown on Fig. 29.

Note that for the outer zones (zone I and beyond) heights and differences are estimated only to about 100 ft. Inspection of the tables shows that this precision is adequate; also it is impractical to estimate average elevations more closely in the large compartments.

If topographic maps are not available, it is necessary to do enough surveying to estimate the elevations of the compartments having significant terrain effects. Also, even when good maps are available, it is usually necessary for the surveyor or instrument operator to measure or estimate any corrections within zones B and C, as the maps will not be closely enough contoured to be useful at points so near the station.

With some practice a surveyor or gravity instrument operator may train himself to judge by inspection of the topography in the vicinity of a station whether or not a terrain correction is necessary. Frequently a station site can be selected by comparatively small change from an originally intended position so that the terrain correction will be materially reduced. For instance, a station at the edge of a bluff (assumed vertical) with a height of 200 ft. would have a terrain correction of 1.5 mg. (for a density of 2.4). If the station were moved back 200 ft. from the bluff, the terrain correction would be 0.41 mg.; if 500 ft. back, the correction would be 0.31 mg.; and 1,000 ft. back, the correction would be reduced to 0.24 mg. In general, it desirable to select a station site such that the topography within the first few hundred feet of the station is not too rough. A little study of the tables and practice in the complete calculation of terrain corrections will indicate the amount of topography that can be tolerated without terrain correction consistent with the retention of a given precision in the final reduced gravity values.

BIBLIOGRAPHY

1896

EöTVöS, ROLAND v.: Untersuchungen über Gravitation und Erdmagnetismus, *Annalen der Physik*, vol. 59, pp. 354–400.

1909

EöTVöS, ROLAND v.: Geodätische Arbeiten in Ungarn, besonders über Beobachtungen mit der Drehwage, Verhandlungen der XVI. allgemeinen Konferenz der internationalen Erdmessung in London und Cambridge.

1910

HELMERT, F. R.: "Die Schwerkraft und die Massenverteilung der Erde," in "Encyklopädie der mathematischen Wissenschaften," Band VI, Teil 1, Heft 7, pp. 85–177, B. G. Teubner, Leipzig, 1906–1925.

1912

EöTVöS, ROLAND v.: Über Arbeiten mit der Drehwage ausgeführt im Auftrage der Kön. Ungarischen Regierung in den Jahren 1909–1911, Bericht an die XVII. allgemeine Konferenz der internationalen Erdmessung, Kais. u. Königl. Hofbuchdruckerei Viktor Hornyánszky, Budapest.

HAYFORD, JOHN F., and WILLIAM BOWIE: The Effect of Topography and Isostatic Compensation upon the Intensity of Gravity, *U.S. Coast and Geodetic Survey, Special Pub.* 10.

1917

BOWIE, WILLIAM: Investigations of Gravity and Isostasy, *U.S. Coast and Geodetic Survey, Special Pub.* 40.

1918

ISING, G.: Förslag till en tyngdkraftsnätare, *Skandinav. Geofysikermötet i Goteborg, Förhandlinger,* 1918.

1921

LELAND, ORA MINER: "Practical Least Squares," McGraw-Hill Book Company, Inc., New York.

1923

BOYS, CHARLES VERNON: "The Mean Density of the Earth," in "A Dictionary of Applied Physics," ed. by Richard Glazebrook, Vol. III, pp. 279–285, Macmillan & Company, Ltd., London.

1924

BOWIE, WILLIAM: Isostatic Investigations and Data for Gravity Stations in the United States Established since 1915, *U.S. Coast and Geodetic Survey, Special Pub.* 99.

SCHUREMAN, PAUL: A Manual of the Harmonic Analysis and Prediction of Tides, *U.S. Coast and Geodetic Survey, Special Pub.* 98.

SCHWEYDAR, W.: Die topographische Korrektion bei Schweremessungen mittels einer Torsionwage, *Zeitschr. f. Geophysik*, vol. 1, pp. 81–89.

1927

BERROTH, A.: Referenzpendelmessungen am Salzhorst Oldau-Hambühren (Hann.), *Zeitschr. f. Geophysik*, vol. 3, pp. 1–16.

BOWIE, WILLIAM: "Isostasy," E. P. Dutton & Company, Inc., New York.

POYNTING, J. H., and J. J. THOMSON: "A Textbook of Physics," Vol. I, "Properties of Matter," 11th ed., Charles Griffin & Company, Ltd., London.

SCHWEYDAR, W.: Die topographische Korrektion bei Schweremessungen mittels einer Torsionwage, Zweite Mitteilung, *Zeitschr. f. Geophysik*, vol. 3, pp. 17–23.

1928

HUBBERT, M. K., and FRANK A. MELTON: Gravity Anomalies and Petroleum Exploration by the Gravitational Pendulum, *Bull. Am. Assoc. Petroleum Geologists*, vol. 12, pp. 889–899.

1929

a. BARTON, DONALD C.: Calculations in the Interpretation of Observations with the Eötvös Torsion Balance, "Geophysical Prospecting, 1929," *Trans. Am. Inst. Min. Met. Eng.*, vol. 81, pp. 480–504.

b. BARTON, DONALD C.: Control and Adjustment of Surveys with the Magnetometer and Torsion Balance, *Bull. Am. Assoc. Petroleum Geologists*, vol. 13, pp. 1163–1186.

c. BARTON, DONALD C.: The Eötvös Torsion Balance Method of Mapping Geologic Structure, "Geophysical Prospecting, 1929," *Trans. Am. Inst. Min. Met. Eng.*, vol. 81, pp. 416–479.

GAMBURZEFF, G. A.: Mechanische Integratoren zur Auswertung von Beobachtungen an gestörten Schwere- und Magnetfeldern, *Gerlands Beitr. z. Geophysik*, vol. 24, pp. 83–93.

HAALCK, H.: "Die gravimetrischen Verfahren der angewandten Geophysik," Verlag von Gebrüder Borntraeger, Berlin.

a. HEILAND, C. A.: A Cartographic Correction for the Eötvös Torsion Balance, "Geophysical Prospecting, 1929," *Trans. Am. Inst. Min. Met. Eng.*, vol. 81, pp. 544–560.

b. HEILAND, C. A.: A New Graphical Method for Torsion Balance Topographic Corrections and Interpretations, *Bull. Am. Assoc. Petroleum Geologists*, vol. 13, pp. 39–74.

KELLOGG, O. D.: "Foundations of Potential Theory," Verlag von Julius Springer, Berlin.

LANCASTER-JONES, E.: Computation of Eötvös Gravity Effects, "Geophysical Prospecting, 1929," *Trans. Am. Inst. Min. Met. Eng.*, vol. 81, pp. 505–529.

VENING MEINESZ, F. A.: "Theory and Practice of Pendulum Observations at Sea," Technische Boekhandel en Drukkerij J. Waltman, Jr., Delft.

1930

ATHY, L. F.: Density, Porosity and Compaction of Sedimentary Rocks, *Bull. Am. Assoc. Petroleum Geologists*, vol. 14, pp. 1–24.

HEYL, PAUL R.: A Redetermination of the Constant of Gravitation, *Bur. Standards, Jour. Research*, vol. 5, pp. 1243–1290.

HOLWECK, F., and P. LEJAY: Un instrument transportable pour la mesure rapide de la gravité, *Comptes rendus*, vol. 190, pp. 1387–1388.

HOSMER, GEORGE L.: "Geodesy," 2d ed., John Wiley & Sons, Inc., New York.

JUNG, KARL: "Gravimetrische Methoden der angewandten Geophysik," in "Handbuch der Experimentalphysik," ed. by W. Wien and F. Harms, Band XXV, Teil 3, pp. 47–208, Akademische Verlagsgesellschaft m.b.H., Leipzig.

MEISSER, O.: Ein neuer Vierpendelapparat für relative Schweremessungen, *Zeitschr. f. Geophysik*, vol. 6, pp. 1–12.

OSEREZKY, W.: Ein Diagramm zur Bestimmung der Differenz der Schwerestörung Δg in zwei Beobachtungspunkten, *Zeitschr. f. Geophysik*, vol. 6, pp. 69–71.

REICH, H.: "Geologische Unterlagen der angewandten Geophysik," in "Handbuch der Experimentalphysik," ed. by W. Wien and F. Harms, Band XXV, Teil 3, pp. 1–46, Akademische Verlagsgesellschaft m.b.H., Leipzig.

VENING MEINESZ, F. A. and F. E. WRIGHT: The Gravity Measuring Cruise of the U.S. Submarine S-21, *Pub. U.S. Naval Observatory*, 2d ser., vol. 13, Appendix I, United States Government Printing Office, Washington.

1931

BROUGHTON EDGE, A. B., and T. H. LABY (editors): "The Principles and Practice of Geophysical Prospecting; Being the Report of the Imperial Geophysical Experimental Survey," Cambridge University Press, London.

LAMBERT, WALTER D. and F. W. DARLING: Tables for theoretical gravity according to the new international formula, *Bull. géodesique* No. 32, octobre-novembre-décembre 1931, pp. 327–340.

1932

HARTLEY, KENNETH: A New Instrument for Measuring Very Small Differences in Gravity, *Physics*, vol. 2, pp. 123–130.

LANCASTER-JONES, E.: Principles and Practice of the Gravity Gradiometer, *Jour. Sci. Instruments*, vol. 9, pp. 341–353, 373–380.

ROMAN, IRWIN: Least Squares in Practical Geophysics, "Geophysical Prospecting, 1932," *Trans. Am. Inst. Min. Met. Eng.*, vol. 97, pp. 460–506.

SHAW, H.: Interpretation of Gravitational Anomalies, "Geophysical Prospecting, 1932," *Trans. Am. Inst. Min. Met. Eng.*, vol. 97, pp. 271–366.

SLOTNICK, M. M.: Curvature of Equipotential Surfaces, *Bull. Am. Assoc. Petroleum Geologists*, vol. 16, pp. 1250–1259.

VENING MEINESZ, F. A.: "Gravity Expeditions at Sea; 1923–1930," Vol. I, "The Expeditions, the Computations and the Results," N. V. Technische Boekhandel en Drukkerij J. Waltman Jr., Delft.

1933

BUCHER, WALTER H.: "The Deformation of the Earth's Crust," Princeton University Press, Princeton, N. J.

BULLARD, E. C.: The Observation of Gravity by Means of Invariable Pendulums, *Proc. Royal Soc.*, vol. 141, pp. 233–258.

HEILAND, C. A.: "Directions for the Use of the Askania Torsion Balance," American Askania Corporation.

1934

HAALCK, HANS: "Lehrbuch der angewandten Geophysik," Verlag von Gebrüder Borntraeger, Berlin.

VENING MEINESZ, F. A., J. H. F. UMBGROVE, and PH. H. KUENEN: "Gravity Expeditions at Sea; 1923–1932," Vol. II. "Report of the Gravity Expedition in the Atlantic of 1932 and the Interpretation of the Results," N. V. Technische Boekhandel en Drukkerij J. Waltman Jr., Delft.

1935

AVERS, HENRY G.: Manual of First-order Leveling, *U.S. Coast and Geodetic Survey, Special Pub.* 140.

SCHLEUSENER, A.: Das Thyssengravimeter, *Beitr. angew. Geophysik*, vol. 5, pp. 303–314.

1936

American Askania Corporation, Pamphlet Geo 120E, "Torsion Balances for Use in Geophysical Prospecting."

ECKHARDT, E. A.: Comparative Torsion-balance and Gravimeter Survey, abstract only, *Geophysics*, vol. 1, pp. 292–293.

HOSKINSON, ALBERT J.: Recent Developments in Gravity Instruments, *Trans. Am. Geophys. Union*, 17th annual meeting, pp. 44–45.

LAMBERT, WALTER D.: The Figure of the Earth from Gravity Observations, *Jour. Washington Acad. Sci.*, vol. 26, pp. 491–506.

WYCKOFF, R. D.: Study of Earth-tides by Gravitational Measurements, *Trans. Am. Geophys. Union*, 17th annual meeting, pp. 46–52.

1937

BARSCH, O.: Der Aufbau der geophysikalischen Reichsaufnahme, *Öl und Kohle*, vol. 13, pp. 641–644.

BARTON, DONALD C., and W. T. WHITE: Accuracy of Modern Gravimeter-measurements, *Trans. Am. Geophys. Union*, 18th Ann. Meeting, pp. 106–107.

BRYAN, A. B.: Gravimeter Design and Operation, *Geophysics*, vol. 2, pp. 301–308.

CASSINIS, A., P. DORÉ, and S. VALLARIN: "Fundamental Tables for Reducing Gravity Observed Values," Royal Italian Geodetic Committee, Milan.

CHAMPION, F. C., and N. DAVY: "Properties of Matter," Prentice-Hall, Inc., New York.

HORSFIELD, W., and E. C. BULLARD: Gravity Measurements in Tanganyika Territory Carried out by the Survey Division, Department of Lands and Mines, *Monthly Notices Royal Astronomical Soc., Geophysical Supplement*, vol. 4, pp. 94–113.

a. ISING, GUSTAV: "The Astatised Pendulum as a Static Instrument for Gravity Measurements," IIme Congrès Mondial du Petrole, Vol. I, pp. 665–670, Paris.

b. ISING, GUSTAF: Use of Astatized Pendulums for Gravity Measurements, *Am. Inst. Min. Met. Eng.*, Tech. Pub. 828.

JEFFRIES, HAROLD: On the Materials and Density of the Earth's Crust, *Monthly Notices Royal Astron. Soc., Geophys. Supplement*, vol. 4, pp. 50–61.

MOTT-SMITH, L. M.: Gravitational Surveying with the Gravity-meter, *Geophysics*, vol. 2, pp. 21–32.

TOMASCHEK, R.: Schwerkraftmessungen, *Naturwiss.*, vol. 25, pp. 177–183.

TSUBOI, CHŪJI, and TAKATO FUCHIDA: Relations between Gravity Values and Corresponding Subterranean Mass Distribution, *Bull. Tokyo Univ. Earthquake Research Inst.*, vol. 15, pp. 636–649.

VACQUIER, VICTOR: Ultimate Precision of Barometric Surveying, *Bull. Am. Assoc. Petroleum Geologists*, vol. 21, pp. 1168–1181.

1938

BARTON, D. C.: "Gravitational Methods of Prospecting," in "The Science of Petroleum," ed. by A. E. Dunstan *et al.*, Vol. I, pp. 364–381, Oxford University Press, London.

BREYER, FRIEDRICH: Zusammenstellung der Auszähldiagramme in der Gravimetrie, *Beitr. angew. Geophysik*, vol. 7, pp. 317–336.

ECKHARDT, E. A.: Gravity Difference Bench Marks for Gravimeter Calibration and Control Thereof, (title only) *Geophysics*, vol. 3, p. 160.

ELKINS, THOMAS A., and SIGMUND HAMMER: The Resolution of Combined Effects, with Applications to Gravitational and Magnetic Data, *Geophysics*, vol. 3, p. 315–331.

GRAF, A.: Ein neuer statischer Schweremesser zur Messung und Registrierung lokaler und zeitlicher Schwereänderungen, *Zeitschr. f. Geophysik.*, vol. 14, pp. 152–172.

HAALCK, H.: Der statische (barometrische) Schweremesser für Messungen auf festem Lande und auf See, *Beitr. angew. Geophysik*, vol. 7, pp. 285–316.

HAMMER, SIGMUND: Investigation of the Vertical Gradient of Gravity, *Trans. Am. Geophys. Union*, 19th annual meeting, pp. 72–82.

HEDSTROM, HELMER: A New Gravimeter for Ore Prospecting, *Am. Inst. Min. Met. Eng., Tech. Pub.* 953.

a. HOYT, ARCHER: Gravimeter, U.S. Patent 2,131,737, Oct. 4, 1938.

b. HOYT, ARCHER: Helical Ribbon Spring Measuring Apparatus, U.S. Patent 2,131,739, Oct. 4, 1938.

c. HOYT, ARCHER: Optical System, U.S. Patent 2,131,738, Oct. 4, 1938.

KLAUS, H.: An Introduction to the Second Derivative Contour Method of Interpreting Torsion Balance Data, *Geophysics*, vol. 3, pp. 234–246.

LUBIGER, F.: Fehlerhäufigkeitskurven als Messgenauigkeits-Kriterium und ihre Anwendung auf Thyssen-Gravimeter, *Beitr. angew. Geophysik*, vol. 7, pp. 230–244.

MOTT-SMITH, LEWIS M.: Torsion Gravimeter, U.S. Patent 2,130,648, Sept. 20, 1938.

STEINMANN, KURT: Portability and Speed Feature New Gravimeters, *Oil Weekly*, vol. 91, No. 1, pp. 58–66, Sept. 12, 1938.

a. THYSSEN-BORNEMISZA, STEPHAN v.: Gravitational instrument, U.S. patent 2,108,421, Feb. 15, 1938.

b. THYSSEN-BORNEMISZA, STEPHAN v.: Gravitational instrument, U.S. patent 2,132,865, Oct. 11, 1938.

c. THYSSEN-BORNEMISZA, STEPHAN v.: Vergleiche zwischen direkten und Schleifenmessungen mit dem Thyssen-Gravimeter, *Beitr. angew. Geophysik*, vol. 7, pp. 218–229.

TSUBOI, CHUJI: Gravity Anomalies and the Corresponding Subterranean Mass Distributions, *Proc. Imp. Acad. Tokyo*, vol. 14, pp. 170–175.

WRIGHT, F. E., and J. L. ENGLAND: An Improved Torsion Gravity Meter, *Am. Jour. Sci.*, Fifth series, vol. 35A, pp. 373–383.

1939

BROWN, HART: Model, Mechanism and Field Tests of a New Type Gravimeter, (title only) *Geophysics*, vol. 4, p. 144.

HAMMER, SIGMUND: Terrain Corrections for Gravimeter Stations, *Geophysics*, vol. 4, pp. 184–194.

HEILAND, C. A.: Gravimeters: Their Relation to Seismometers, Astatization and Calibration, *Am. Inst. Min. Met. Eng., Tech. Pub.* 1049.

NETTLETON, L. L.: Determination of Density for Reduction of Gravimeter Observations, *Geophysics*, vol. 4, pp. 176–183.

PART II

MAGNETIC METHOD

CHAPTER VIII

FUNDAMENTAL PRINCIPLES AND UNITS

INTRODUCTION

The background of the magnetic method of geophysical prospecting has much in common with that of the gravitational method. Both are "potential" methods, having their fundamentals in potential theory. Just as the gravitational force in a given direction is the derivative, or rate of change, in that direction of the gravitational potential, so also the magnetic force in a given direction is the derivative in that direction of the magnetic potential.

In the gravitational case we may consider the gravitational effect of a body as the sums of the effects of the mass particles constituting the body. In the magnetic case we may consider the magnetic effects of a body as the sums of the effects of the magnetic particles or poles that give the body its magnetic state. An essential difference is that the magnetic case is inherently more complicated because there are two kinds of magnetic poles of opposite sign. Also, the positions of these poles determine a vector that may be in any direction. Thus, the magnetic state or magnetization of a body is defined by a magnitude and a direction rather than by a single magnitude (mass) as in the case of gravity.

PHYSICAL BACKGROUND AND DEFINITIONS

In considering the magnetic state of a body it is convenient to think of the magnetized state as having its origin in a large number of elementary magnets, or dipoles, within the body. These elementary dipoles each consist of a positive and a negative pole. The dipoles are more or less responsive to the influence of an external magnetic field. In the ordinary, or demagnetized, state the elementary dipoles may be considered as having a random distribution and orientation. The fields of the different particles neutralize each other so that there is no resultant field

157

and no magnetic influence outside the body. If the body is placed in a magnetic field, the elementary magnets tend to align themselves parallel with the field. The stronger the field, the more completely they are aligned. When the alignment begins, the magnetic fields of the elementary magnets begin to cooperate, and the stronger the directing field the more pronounced is the cooperation of these elementary magnets and the stronger the external effect or external field produced by the body. The body has now become magnetized and has a field of its own in the space around it. If the external magnetizing field is removed, the alignment will largely disappear for soft, ferrous, easily magnetized materials, and they lose their magnetic properties. In some hard materials, the alignment of the elementary magnets will persist, and we have a permanent magnet.

The magnetic properties of materials vary over very wide limits. The variation of magnetic properties in ferromagnetic materials may be considered as a variation in the volume density of the elementary magnets, the ease with which they may be disturbed or oriented, and the persistence with which they maintain a given orientation once it has been acquired. The various magnetic properties are accurately described in terms of certain quantities that have definite mathematical meanings. Also, it is convenient to use "lines of force" to describe the magnetic field.

The following paragraphs give brief discussions of the fundamental magnetic quantities. The letter in parentheses in each paragraph heading is the symbol that will be used for that quantity.

A system of magnetic units and definitions may be built up from various points of view. In that which follows, an attempt has been made to explain and define the various essential quantities in a manner that will give them a physical picture and that will lead to an emphasis on the quantities most commonly used in magnetic prospecting.

Force between Magnetic Poles (F).—It is easily shown by experiment that there is a force between magnetic poles, and it was proved by Coulomb that this force varies inversely as the square of the distance between the poles. The force is one of attraction if they are of opposite sign and of repulsion if of like sign. By convention, the "north-seeking" pole corresponding to that at the "north" end of a compass needle is called "positive";

and the "south," or "south-seeking," pole is called "negative."

Magnetic Pole Strength (P).—The force between magnetic poles is proportional to the pole strength. Thus the law of force can be expressed as

$$F = \frac{CP_1P_2}{r^2} \tag{103}$$

where P_1 and P_2 are the strength of the poles, r is the distance between them, and C is an undetermined constant. We now can use this equation to define unit pole strength. If we consider P_1 and P_2 as equal poles, they will be defined as having unit strength when they exert unit force (1 dyne) when they are unit distance (1 cm.) apart. By this definition the constant C becomes unity, and we have simply

$$F = \frac{P_1P_2}{r^2} \tag{104}$$

Magnetic Field Strength (H).—The force between magnetic poles may be considered as the reaction of one pole on the magnetic field of the other. Thus a unit field strength exerts a force of 1 dyne on a unit pole, and such a field has a strength of 1 oersted.[1] A magnetic field can be produced by a magnet or by electrical means. The magnetic field H is a vector quantity with a magnitude and direction defined as that of the force acting on a unit positive pole.

The magnetic field is represented conveniently by "lines of force," and the strength of the field by the density of the lines or number of lines per square centimeter in a section perpendicular to their direction. These lines are maxwells, and the strength of the field in oersteds is the number of maxwells per square centimeter.

Lines of force are directed outward from a positive pole and inward toward a negative pole. The field strength is 1 maxwell per square centimeter at a distance of 1 cm. from a unit pole. Since the total area of a sphere of unit radius around such a unit pole is 4π sq. cm., it is evident that a total of 4π maxwells, or lines of force, are associated with a unit pole.

Magnetic Moment (M).—Magnets of any form may nearly always be considered as made up of pairs of positive and negative

[1] See footnote, p. 160.

poles.   The magnetic moment of such a dipole is a vector quantity with magnitude

$$M = PL \qquad\qquad (105)$$

where P is the pole strength and L the distance between poles and with a direction from the negative to the positive pole. The effect that a magnet produces at a distance large compared with its length is proportional to its magnetic moment.

Intensity of Magnetization or Polarization (I).—The intensity of magnetization at any point within a magnetized body is the magnetic moment per unit volume.   It may be considered as representing the number and degree of orientation of the elementary magnetic dipoles of the body.   The intensity of magnetization is a vector quantity having a direction parallel to the direction of magnetization.   A uniformly magnetized body has the same intensity of magnetization and the same direction throughout.

Susceptibility (k).—When a magnetizable body is placed in a magnetic field, it takes on a certain degree of magnetization which is proportional to the field and also depends on the ease of magnetization.   The measure of the ease of magnetization is the susceptibility.   Thus,

$$I = kH \qquad \text{or} \qquad k = \frac{I}{H} \qquad\qquad (106)$$

The susceptibility may be considered as a measure of the number of elementary magnets per unit volume of the material and of their mobility or the ease with which they are oriented.

Magnetic Induction (B).—The magnetic induction is a measure of the field strength within a magnetized body.   In terms of lines of force it may be considered as the number of lines per square centimeter.   The unit of induction is the "gauss."[1]

---

[1] An international commission has recently proposed that the unit of B be the gauss, and that of H the oersted.   This definition requires that Eq. (107) be written

$$B = \mu_0 H + 4\pi I \qquad\qquad (107a)$$

where μ_0 is permeability of the air, with a numerical value of 1.   Thus, B and H are dimensionally different, and the ratio B/H has the dimension μ. Equation (107a) is dimensionally correct, for B has the same dimensions as I. For further discussion, see Kennelly, 1931.   In much of the literature both B

The total induction B within a magnetized body may be con-sidered as made up of the lines of the original magnetizing field H plus those resulting from the magnetization I caused by that field. Now I means magnetic moment per unit volume. Con-sider a unit cube (Fig. 71) having unit magnetic moment and therefore unit intensity of magnetization, and let the sides be parallel and perpendicular to the direction of magnetization. Let the unit moment be considered as made up of positive poles on one face of the cube with a total strength of unity and negative poles on the opposite face, also with a total strength of unity. Now each unit pole has associated with it 4π lines (of which 2π lines correspond to those shown in the diagram and another 2π are associated with the implied opposite pole of the adjacent elementary cube of material). Thus, unit moment, and there-fore unit intensity of magnetization, has 4π lines. Then the total induction consists of H lines of the original magnetizing field $+4\pi I$ lines from the induced mag-netization, and
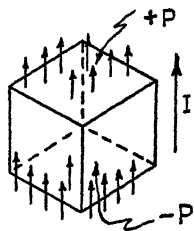
Fig. 71. — Unit cube of magnetic material, polarized parallel to vertical edges.

$$B = H + 4\pi I * \tag{107}$$

but, by Eq. (106),

$$I = kH, \quad \text{so} \quad B = H(1 + 4\pi k) \tag{108}$$

Permeability (μ).—If the magnetizing field H and resulting induction B are parallel (as they usually are), the permeability is defined by the equation

$$\mu = \frac{B}{H} \tag{109}$$

From the definition of B [Eq. (108)] it is evident that

$$\mu = 1 + 4\pi k \tag{110}$$

and H are expressed in terms of gauss. In geophysical literature the field intensity of the earth is frequently referred to in gauss. The correct unit in the system here referred to is oersted.

* The usual derivation and discussion of this equation may be found on pp. 184–185 of Thomson, 1921.

DISTORTION OF MAGNETIC FIELD BY A MAGNETIZABLE BODY

The distortion or modification of the magnetic field by a magnetizable body may be pictured (Fig. 72) as a concentration of lines of induction within the body (increase of magnetic induction) and a rarefaction (decrease of magnetic induction) in the space immediately outside the body. This concentration may be thought of as the resultant of the original field H, plus the field $4\pi I$, due to the magnetized body. Similarly, the spreading out of the magnetic lines in the region just outside the magnetic body may be considered as the resultant of the original field H
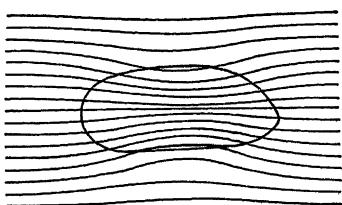
minus the effect of the field due to the polarized body, for the lines of force due to the polarized body have a direction opposite to those of the original field in this region. Considered in this way, we do not have to distinguish between a magnetization induced by an external field and that which may be

Fig. 72.—Distortion of magnetic field by a magnetizable body.

due to permanent magnetization of the material. If a material is magnetized for any reason, it has a field around it that causes a distortion, or an anomaly, in the normal field in its vicinity.

From these considerations it is evident that the intensity of magnetization or the polarization, I, is the most important property of material with which we are concerned in magnetic prospecting. It corresponds in importance to the density in gravitational prospecting. Just as the gravitational effect of a homogeneous body at a distance depends on its size, shape, and density, so the magnetic effect of a homogeneously magnetized body depends on its size, shape, and the intensity and direction of its magnetization.

UNITS USED IN MAGNETIC PROSPECTING

The quantity ordinarily measured in magnetic prospecting is a component of the intensity of the magnetic field at the surface of the earth. Therefore, the most commonly considered unit is that of intensity (which, strictly, should be named "oersted"[1] but is commonly called "gauss"). The ordinary c.g.s.

[1] See footnote, p. 160.

unit is inconveniently large because the quantities of interest are a small fraction of one such unit. Therefore, in magnetic prospecting the common unit is the "gamma" (γ) which is defined as

$$1\gamma = \frac{1}{100,000} \text{ oersted, or } 10^{-5} \text{ oersted}$$

Magnetic anomalies range from a few gamma up to several hundred, or, in exceptional cases, a few thousand gamma. To detect the smallest anomalies of interest in geophysical prospecting, differences in magnetic intensity must be measured to a few gamma.

Contours, or lines of equal magnetic intensity, are commonly called "isogams."[1]

Susceptibilities of rocks are usually measured in terms of 10^{-6} c.g.s. unit. As is shown in detail later, most sedimentary rocks are relatively nonmagnetic, with susceptibilities of less than $100 \cdot 10^{-6}$. Igneous rocks are much more magnetic, ranging in susceptibility from a few hundred to tens of thousands of c.g.s. units $\cdot 10^{-6}$.

Polarization is usually measured and referred to either directly in c.g.s. units or in 10^{-6} c.g.s. unit. Sedimentary rocks are usually very weakly polarized with polarization in the range 0 to $50 \cdot 10^{-6}$ c.g.s. unit (see page 203), whereas igneous rocks are commonly in the range 0.001 to 0.005 c.g.s. unit.

---

[1] The term "isogam" has been used, erroneously and apparently for want of a better name, in referring to gravity contours, especially in older torsion balance literature. To be consistent with the unit of gravitational intensity, gravity contours should be called "isogals."

CHAPTER IX

MAGNETISM OF THE EARTH

THE GEOMAGNETIC FIELD

Magnetic measurements necessarily are made in the magnetic field of the earth. Therefore, some knowledge of the magnetic properties and conditions of the earth as a whole is necessary so that proper account may be taken of the contribution of the earth to the measured magnetic effects.

Study and measurement of the magnetism of the earth have been carried out for centuries. Extensive measurements of the magnetic elements have been made at sea because of their importance in connection with the use of the magnetic compass for navigation, and on land in connection with the use of the compass for surveying. Long-time studies of the magnetic elements have been made at magnetic observatories on land to study slow, or "secular," changes in the geomagnetic field.

These various measurements have shown that the earth's magnetic field at a given place and time may be considered as made up of three parts:

1. A relatively large, slowly changing "secular" part caused by the internal state of the earth and having a form roughly that which would be given by the earth as a simple, not quite uniformly polarized sphere.

2. Minor variations in the field from place to place which are caused by magnetic inhomogeneities of the earth's crust. This is the part that is the chief interest of magnetic prospecting, and we shall call it the "anomaly" part.

3. A relatively small "diurnal" part which changes somewhat erratically with time but is repeated approximately in daily cycles.

The secular and diurnal parts must be evaluated and removed to measure the anomaly part, for a geomagnetic measurement necessarily is affected by the sum of all three parts.

THE INNER FIELD OF THE EARTH

To a first approximation the general form of the magnetic field at the surface of the earth is that of a polarized sphere, with one

magnetic pole near the north geographic pole and one near the south pole.

We have defined (page 158) a positive magnetic pole as that corresponding to the north-seeking pole of a compass. Since the compass tends to point toward an opposite pole, it is evident that the magnetic pole near the north geographic pole is negative; that near the south pole is positive.

The exact internal cause of the earth's magnetic field is one of the great unsolved problems of geophysics. Many suggestions have been made, but all have theoretical difficulties. For instance, it has been suggested that the field is due to a magnetized iron core of the earth, for from the mean density of the earth it is probable that its center is metallic, and there is evidence in support of this idea in earthquake seismology. However, the interior of the earth is almost certainly at a temperature much above that at which iron loses its magnetic properties. Probably the most reasonable hypothesis is that the field is due to electric currents circulating in the metallic core, although the mechanism by which such currents would be maintained is not clear. Some relation between the rotation of the earth and its magnetization seems probable because of the approximate coincidence of the magnetic axis with the axis of rotation.

Long-time magnetic measurements have shown that there are secular variations of the earth's field. These changes result in a slow variation of the field at any given place and also a slow shift in the geographic positions of the magnetic poles. There is some evidence that the changes are roughly cyclic with a period of about five hundred years. By means of magnetic observations made at many stations which are repeated from time to time, the U.S. Coast and Geodetic Survey[1] has prepared maps and tables that show the magnetic elements over the United States, together with their annual rate of change.

The correspondence between the magnetic and geographic poles is only approximate, the magnetic poles being located in 1906 about as follows[2]:

Negative magnetic pole: 70°30′ N lat., 97°40′ W. long.
Positive magnetic pole: 73°39′ S. lat., 146°15′ E. long.

[1] Howe and Knapp, 1938.
[2] Haalck, 1927.

Picturing the earth as a uniformly polarized sphere, we have "lines of induction" somewhat as shown by the right half of Fig. 73. Near the poles the lines are close together, giving a
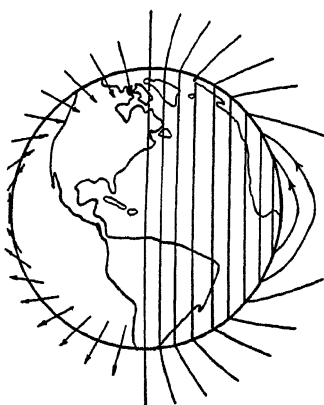
relatively strong field, pointing in near the north geographic pole, out near the south geographic pole. Near the equator the field has about half its intensity at the poles, is parallel to the surface, and points north. The arrows on the left half of the figure indicate the direction of the earth's field relative to the surface and, by their relative length, its approximate magnitude. As we go north or south from the magnetic equator, the angle with the surface, or the magnetic "dip," increases rapidly until it is vertical at the magnetic poles. The increase of dip and increase of strength both contribute to a pronounced increase in the vertical component of the earth's field as we go north or south from the magnetic equator where, of course, its value is zero. In magnetic prospecting for oil a correction is always made for this normal northward increase in the vertical component.

Elements of the Magnetic Field.—The direction and magnitude of the geomagnetic field at any point on the earth's surface are represented by a vector or arrow parallel to the direction of the field, pointing in the direction of force on a positive pole and having a length proportional to the strength of the field at that point.

Fig. 74.—Elements of the magnetic field vector.

We shall refer this vector to a set of mutually perpendicular axes directed astronomically north and east and vertically downward. Let us consider the vector as passing diagonally from the origin to the far corner of a rectangular box (Fig. 74) oriented with its edges parallel to the coordinate

axes. The various magnetic elements then correspond to certain sides and angles of this box (or parallelopiped) as follows:

F = the total intensity or total length of the field vector.

X, Y, V = the north, east, and vertical components of the magnetic field, respectively.

H = the total horizontal component.

d = the angle of declination or the angle between the direction of the horizontal component (the direction taken by a compass needle) and the true astronomic north.

i = the angle of inclination or dip of F below the horizontal plane.

Various combinations of three of these quantities will completely define the direction and magnitude of F. In terrestrial magnetic work and magnetic charts, the quantities H, d, and i are usually used. In magnetic prospecting we shall be concerned primarily with the quantity V and to a lesser extent with d and H.

The following relations between the various quantities are obvious.

$$F = \frac{H}{\cos i} \qquad (111a)$$

$$F^2 = H^2 + V^2 \qquad (111b)$$

$$X = H \cos d \qquad (111c)$$

$$Y = H \sin d \qquad (111d)$$

$$\frac{V}{H} = \tan i \qquad (111e)$$

The ranges of values of the magnetic elements within the United States are roughly[1]

V = 0.4 to 0.6 oersted = 40,000 to 60,000γ

H = 0.14 to 0.28 oersted = 14,000 to 28,000γ

d = 24°E. (in northwest part) to 20°W. (in northeast part)

i = 55 to 75°

THE EXTERNAL FIELD OF THE EARTH

If accurate determinations of the earth's magnetic field are made continuously at a fixed point, it is found that the intensity changes by an appreciable amount over short-time intervals. These changes have a more or less regular daily cycle which is

[1] Howe and Knapp, 1938.

approximately the same at the same solar time at different points but differs materially in detail from place to place and from day to day.

The external field is probably due to electric currents high in the earth's atmosphere. It is well known that the upper atmosphere is ionized (the Kennelly-Heaviside layer which is important in the transmission of radio signals). This ionization is caused by ultraviolet radiation from the sun and also perhaps by electrons shot out from the sun. Any variation in the number of ions or the velocity of their motion also causes a change in the magnetic field at the surface of the earth. The tidal circulation of the upper air, induced by the gravitational attraction of the sun and the moon, furnishes a fairly satisfactory explanation of the daily magnetic variations.[1] The amplitude of the daily change is greater in the summer than in the winter. The range of the daily variation in vertical intensity may be as great as 100γ.[*]

Occasionally the magnetic field may be disturbed suddenly and irregularly by magnetic storms. Apparently they are caused by sudden changes in the ionization of the upper atmosphere for they seem to be associated with sunspots and the aurora. Occasionally magnetic storms are so severe as to interfere seriously with accurate magnetic surveying or even to make it temporarily impossible. Such conditions usually last for only a few hours or at most for one or two days.

THE "ANOMALY" FIELD OF THE EARTH

This consists of that part of the field which is caused by irregularities in the distribution of magnetized material in the outer crust of the earth. If this crust were uniform to a depth of some tens of miles, there would be no anomaly field. The fact that variations in the magnetic field exist which, from their nature and extent, must have their source within the outer crust of the earth tells us that this crust is not magnetically homogeneous. The whole purpose of magnetic prospecting is to measure the anomaly field and to attempt to interpret the magnetic inhomogeneities indicated in terms of geologic structure. This interpretation is the subject of Chap. XII of this section.

[1] Bartels, 1926, pp. 415–419.

[*] For sample daily variation curves, see Figs. 83a, 83b; also Vacquier, 1937; Soske, 1933.

CHAPTER X

GEOMAGNETIC MEASURING INSTRUMENTS

Many different instruments and methods have been used for geomagnetic measurements. These include some quite elaborate and complicated instruments for making absolute determinations of the magnetic elements (usually horizontal intensity, declination, and dip) which furnish the data for various magnetic charts on land and sea. With all the very extensive work of this kind we are not concerned, as it is only of indirect interest in geophysical prospecting.

DIP NEEDLES

Probably the earliest magnetic instrument used for geophysical prospecting was the "dip needle." This consists of a magnetic needle pivoted on a horizontal axis but differs from the ordinary "dip circle" in that the needle carries an adjustable weight.[1] The gravitational force acting on this weight turns the needle to a considerable angle (roughly perpendicular) with the earth's field. This arrangement greatly increases the angular deflection of the instrument which is produced by a given magnetic change. In commercial dip needles, an angular change of 1 deg. is produced by magnetic changes of 160 to 750γ with a median of about 300γ.[*] The dip needle has been used extensively in prospecting for iron ores, igneous intrusions, and other situations where subsurface conditions of economic interest produce comparatively large magnetic anomalies. Its sensitivity is too low for effective use in finding the low relief anomalies which are usually the type that are of interest in oil prospecting.

A modification of the dip needle to increase its sensitivity is the Hotchkiss "super dip."[2] In this instrument the magnetic needle carries a small weighted arm at an angle with the needle

[1] For a detailed description of the construction, properties, and uses of the dip needle, see Stearn, 1929b.

[*] Stearn, op. cit., p. 352.

[2] For a description of this instrument and its application to geological problems, see Stearn, 1932.

which is adjustable. When the instrument is adjusted so that the magnetic needle is perpendicular to the earth's field and the weight arm is horizontal, it becomes unstable and has a theoretically infinite sensitivity and a practical sensitivity limited by mechanical factors, principally the bearings. Its sensitivity can be controlled readily by adjusting the angle between the needle and the weight arm to a position slightly different from that for the unstable condition Its actual maximum sensitivity 's about one scale division for a 3γ change in magnetic intensity.[1] This instrument has been used to some extent in geolog'cal exploration. However, its sensitivity and dependability are not so great as are those of the field balances described below, and the quantity measured (*i.e.*, the variation in total intensity of the earth's field) is not so readily interpreted in terms of geologic structure as are the vertical or horizontal component measurements. Therefore, the application of this instrument to oil prospecting has been very limited and is almost negligible in comparison with that of the magnetic field balances.

MAGNETIC FIELD BALANCES

Nearly all the geophysical prospecting for oil by the magnetic method has been done with the Schmidt type magnetic field balance. This balance consists essentially of a permanent magnet (actually a pair of magnets) pivoted on a horizontal knife-edge. The vertical magnetometer is arranged so that the magnets are horizontal and measures variations in the vertical component of the magnetic field. The horizontal magnetometer is arranged so that the magnets are vertical and measures variations in the horizontal component of the field. The measurements of variations in vertical intensity are somewhat easier to make and usually are simpler to interpret, so that the vertical magnetometer has been used much more extensively than has the horizontal magnetometer. Nearly always in connection with oil prospecting a "magnetic survey" refers to one in which variations in the vertical component only of the earth's magnetic field are measured.

THEORY OF THE VERTICAL MAGNETOMETER

The moving system of a vertical magnetometer consists essentially of a pair of bar magnets, carrying a mirror, balanced on a

[1] Stearn, 1932, p. 179.

horizontal knife-edge perpendicular to the magnetic axis and
with the center of gravity of the moving system displaced hori-
zontally and vertically with respect to the knife-edge so that the
magnetic axis is substantially horizontal.

In the schematic diagram (Fig. 75) let
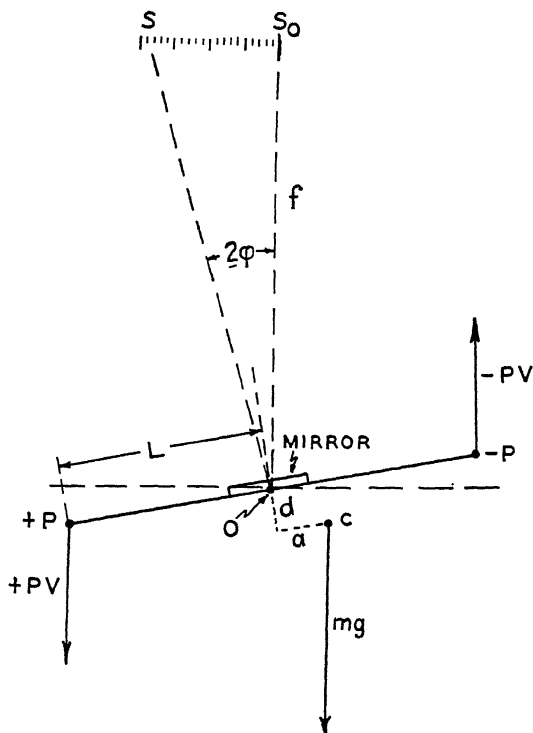
Fɪɢ. 75.—Diagram for theory of vertical magnetometer.

P = pole strength of magnet.
L = half length of magnet.
V = vertical component of magnetic field.
o = point of support or position of knife-edge.
c = position of center of gravity of moving system.
d, a = components of displacement of center of gravity from
the knife-edge perpendicular and parallel to magnetic
axis, respectively.
m = mass of moving system.
g = acceleration of gravity.

φ = angle between magnetic axis and the horizontal.

f = focal length of optical system.

s_0, s = zero position and deflected position of the reflected index on the instrument scale.

The magnetometer is always oriented with its magnetic axis in an east-west direction so that the horizontal component produces no torque on the moving system. Therefore, we need consider only the effects of the vertical component.

The moving system will be acted on by two torques: *i.e.*, (1) the magnetic torque (tending to rotate it counterclockwise in the figure) resulting from the reaction of the vertical component of the earth's field V on the poles of the magnet and (2) a gravitational torque (tending to rotate it clockwise in the figure) resulting from the weight mg acting at the center of gravity c. At the equilibrium position these two torques are equal, and

$$2PVL \cos \varphi = mg(d \sin \varphi + a \cos \varphi) \tag{112}$$

Since $2PL = M$, the moment of the magnet system, and dividing throu̇gh by $\cos \varphi$,

$$MV = mg(d \tan \varphi + a)$$
$$\tan \varphi = \frac{MV - mga}{mgd} \tag{113}$$

The rotation of the moving system causes a deflection on the scale of

$$s - s_0 = f \tan 2\varphi$$

For small angles (φ is always small, *i.e.*, less than 2 deg.)

$$\tan 2\varphi = 2 \tan \varphi$$

so we can measure the deflection angle φ as

$$\tan \varphi = \frac{s - s_0}{2f} \tag{114}$$

Equating the right sides of Eqs. (113) and (114),

$$\frac{s - s_0}{2f} = \frac{MV - mga}{mgd} \tag{115}$$

If we now take the instrument to a new location where the

strength of the vertical component is V', we have

$$\frac{s' - s_0}{2f} = \frac{MV' - mga}{mgd} \qquad (116)$$

Subtracting (116) from (115), the difference in deflection due to the difference in the field strength at the two places is

$$\frac{s - s'}{2f} = \frac{MV - MV'}{mgd}$$

and

$$s - s' = (V - V')\frac{2fM}{mgd} \qquad (117)$$

Therefore, the difference in the magnetic intensity between any two points is simply

$$V - V' = (s - s')\frac{mgd}{2FM} = K(s - s') \qquad (118)$$

where K is the scale constant of the instrument, and

$$K = \frac{mgd}{2fM} \qquad (119)$$

The smaller the factor $mgd/2fM$ is made, the more sensitive the instrument becomes. Thus, the sensitivity can be increased by decreasing the distance d, by decreasing the mass m of the moving system, by increasing the magnetic moment M of the moving magnets, or by increasing the focal length f. Ordinarily m, M, and f are fixed by the design of the instrument. The distance d can be adjusted by turning a screw in or out which raises or lowers the center of gravity of the instrument with respect to the knife-edge. As used in ordinary fieldwork, the scale constant is made about 10 to 20γ per scale division. By careful operation with such an instrument, magnetic measurements can be made to a precision of about $\pm 2\gamma$.

THEORY OF THE HORIZONTAL MAGNETOMETER

The moving system of the horizontal magnetometer is essentially the same as that of the vertical component instrument, except that the magnetic axis is substantially vertical. However, in the horizontal magnetometer the effect of the vertical component cannot be eliminated completely. Therefore, this instru-

ment is somewhat more complicated in theory and operation because of the contribution of this unwanted component. The reference characters in the diagram (Fig. 76) represent the same quantities as do those in Fig. 75.

From the equilibrium between the gravitational and magnetic torques,

$$2PHL \cos \varphi - 2PVL \sin \varphi = mg(a \cos \varphi + d \sin \varphi) \quad (120$$

Dividing by $\cos \varphi$, and since $2PL = M$,

$$MH - MV \tan \varphi = mga + mgd \tan \varphi$$
$$\tan \varphi(mgd + MV) = MH - mga$$

$$\tan \varphi = \frac{MH - mga}{mgd + MV} \qquad (121)$$

Also,

$$\tan \varphi = \frac{s - s_0}{2f}$$

Therefore,

$$\frac{s - s_0}{2f} = \frac{MH - mga}{mgd + MV} \qquad (122)$$

At a point such that the magnetic axis is vertical and the horizontal field is H_0,

$$s = s_0$$
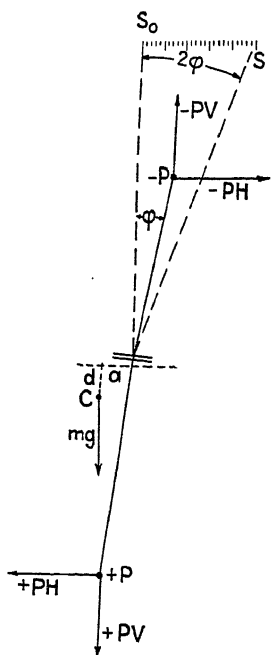
FIG. 76.—Diagram for theory of horizontal magnetometer.

and

$$MH_0 - mga = 0$$
$$a = \frac{MH_0}{mg}$$

Substituting this value of a in (122),

$$\frac{s - s_0}{2f} = \frac{MH - MH_0}{mgd + MV}$$
$$H - H_0 = (s - s_0)\frac{mgd + MV}{2fM} \qquad (123)$$
$$= K'(s - s_0)$$

where K' is the scale constant of the horizontal instrument, given by

$$K' = \frac{mgd}{2fM} + \frac{V}{2f} \qquad (124)$$

The first term of Eq. (124) is exactly the same as the scale constant for the vertical magnetometer [Eq. (119)], but we see that the horizontal magnetometer has an additional term depending on the intensity of the vertical component. This, of course, represents the control or restoring force exerted by the vertical component of the earth's field tending to orient the axis of the magnet system into a vertical position.

It is evident that for high sensitivity (*i.e.*, small values of K') the two terms on the right side of Eq. (124) may have to be of opposite sign. This means that the first term must be negative, which means that the quantity d must be negative. This requires that the center of gravity of the moving system be above the knife-edge. It has been shown by Joyce[1] that for the Askania horizontal magnetometer to have a sensitivity of less than 15γ per scale division, d will be negative if the value of V is greater than 20.000γ.

Since the scale constant depends on the vertical intensity, it is not truly constant, and a correction is necessary if the variation in the vertical intensity is large over the area surveyed.

Thus, let the value of K' at a base station P_1, where $V = V_1$, be

$$K_1' = \frac{mgd}{2fM} + \frac{V_1}{2f}$$

and

$$H_1 - H_0 = K_1'(s_1 - s_0) \tag{125}$$

At another point P_2, where $V = V_2$,

$$K_2' = \frac{mgd}{2fM} + \frac{V_2}{2f}$$

and

$$H_2 - H_0 = K_2'(s_2 - s_0) \tag{126}$$

Now Let $V_2 - V_1 = \Delta V$; then

$$K_2' - K_1' = \frac{\Delta V}{2f}; \qquad K_2' = K_1' + \frac{\Delta V}{2f}$$

and

$$H_2 - H_0 = \left(K_1' + \frac{\Delta V}{2f}\right)(s_2 - s_0) \tag{127}$$

[1] Joyce, 1937, p. 20.

Subtracting (125) from (127),

$$H_2 - H_1 = K_1'(s_2 - s_1) + \frac{\Delta V}{2f}(s_2 - s_0) \qquad (128)$$

which is the working equation for the horizontal magnetometer.

To use this equation, the value of K_1' must be that determined at the base station 1, where the vertical intensity is V_1. Note,
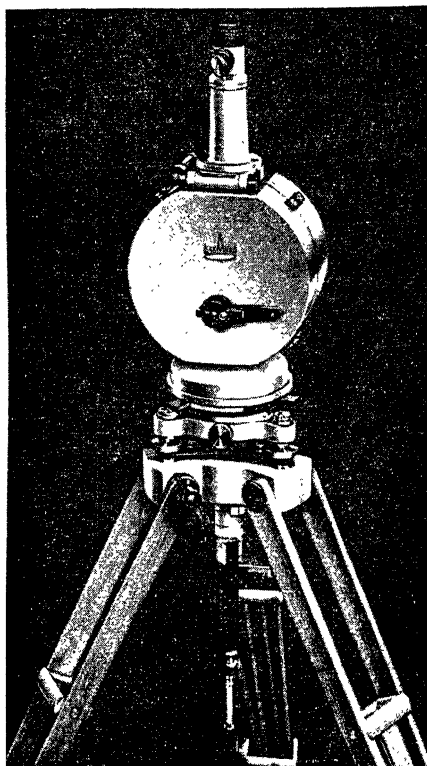
FIG. 77.—Vertical field magnetometer. (*Photograph courtesy American Askania Co.*)

also, that the correction term depends on the deflection at the station being determined (*i.e.*, station 2) and therefore on the scale difference $(s_2 - s_0)$ between that deflection and the position (*i.e.*, where $s = s_0$) at which the magnetic axis is vertical.

It is probable that the horizontal magnetometer is of greatest use in connection with very local features (see page 188 below), where the variation of V would rarely be great enough to cause

very material corrections to the scale constant. This is especially true with the newer type magnetometer with longer focal length (*i.e.*, larger value of f; see page 179 below). However, Joyce[1] calculates a possible example where the correction for
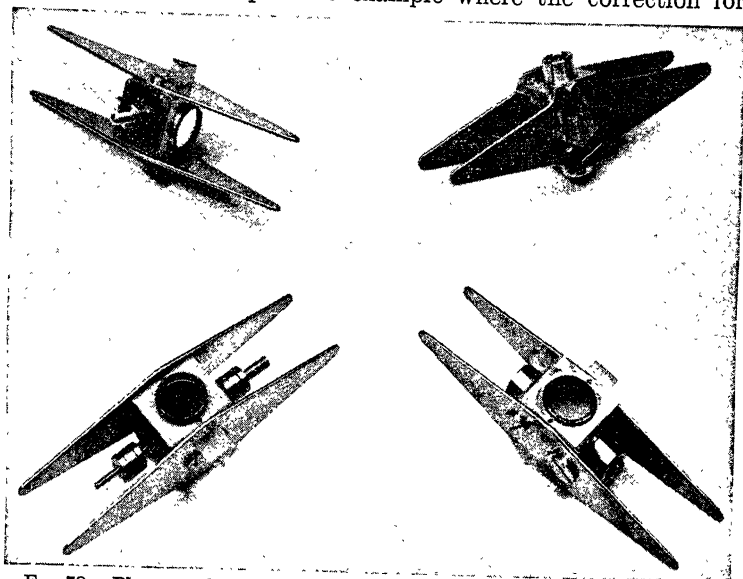
Fig. 78.—Photographs of moving systems for horizontal and vertical magnetometers. Upper left, temperature-compensated system for horizontal magnetometer; lower left, same for vertical magnetometer; upper right, same for horizontal magnetometer. (*Photograph courtesy American Askania Co.*)

change in vertical intensity amounts to 90γ (for the older type instrument).

THE VERTICAL MAGNETOMETER

A large proportion of all the magnetic prospecting in the United States has been done with the field balance designed by A. Schmidt and manufactured by the Askania Werke in Berlin. Therefore, a description of this instrument is given in some detail.

Figure 77 shows a general view of the instrument (new type); Fig. 78 shows the moving system both compensated for temperature effects (left) and the old type uncompensated system (right).

The essential parts of the magnetometer are shown by the schematic diagram (Fig. 79) and are:

[1] Joyce, *op. cit.*, p. 22.

1. A moving system (Fig. 78) consisting of a pair of flat, elliptical cobalt-steel permanent magnets mounted on a central cubical block or shell which carries a horizontal quartz knife-edge which, in turn, rests on quartz cylindrical surfaces so that the entire moving system rotates freely on a horizontal axis. The central member also supports adjustable weights by which the horizontal and vertical position of the center of gravity with respect to the knife-edge can be varied. These adjustments provide control of the gravitational torque which balances the torque due to the reaction of the
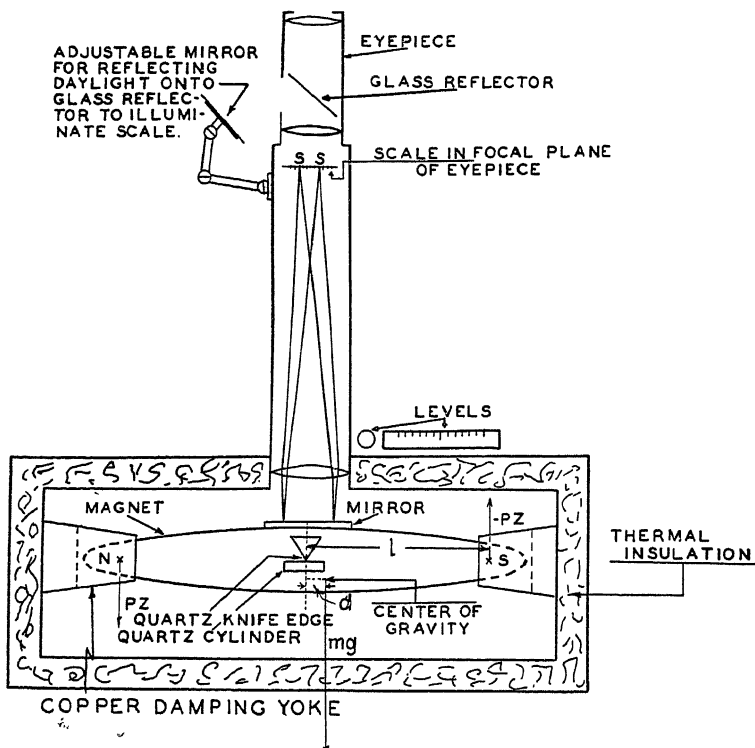
FIG. 79.—Schematic cross section of vertical magnetometer.

magnets with the normal vertical component of the geomagnetic field. In the temperature-compensated moving system (Fig. 78, left) the weights are carried on arms of invar and aluminum and can be so adjusted that changes in magnetic and gravitational torque, arising from changes in temperature, are effectively compensated. The moving system also carries a small mirror.

2. A telescope and scale which measure the angular rotation of the moving system resulting from small changes in the magnetic intensity. In earlier instruments the optical system is so arranged that the image of a scale in the focal plane of the eye piece, reflected from the mirror on the

moving system, is focused also in the focal plane of the eye piece. The new type instrument uses the reflection of a single fiducial line which moves over a fixed scale.

3. A damping system consisting of heavy copper yokes within which the ends of the magnets move. The eddy currents produced in the copper by the moving magnet quickly bring the moving system to rest.

4. An arresting and clamping mechanism by which the moving system is lifted and securely clamped so that the knife-edge is lifted off its supports except during the actual reading of the instrument.

5. An outer aluminum case with a thermally insulating cover and provided with thermometers and a window for reading the temperature inside the case.

6. A tripod with leveling screws and a rotating head for leveling and orienting the instrument. The instrument support also carries a vertical tube and scale by which a permanent magnet may be held in an adjustable position below the instrument. This magnet can be used for calibrating the instrument or for adjusting the zero position of the moving system.

7. An auxiliary compass for orienting the instrument with respect to the magnetic meridian.

THE HORIZONTAL MAGNETOMETER

The horizontal magnetometer contains the same parts enumerated above for the vertical magnetometer, with the essential difference that the moving system is vertical instead of horizontal. In the older type Askania instrument, the outer case is a vertical cylinder.

The New Type Magnetometer.—In the latest type magnetometer made by Askania the outer case is a short horizontal cylinder (Fig. 77) and is so arranged that either a horizontal or a vertical moving system may be used. Thus, by a simple modification the same instrument may be used for measuring either the vertical or the horizontal component. This instrument also has a modified optical system by which the effective focal length of the telescope is increased (on the principle of the Galilean telescope) and which gives about two and one-half times the number of scale divisions for the same angular movement of the moving system. Also, the reflected image of the scale is replaced by a single reflected index which moves over a fixed scale.

For further details, the reader is referred either to the maker's catalogue[1] or to published descriptions of the instrument and its manipulation, such as that by Joyce.[2]   •

[1] Askania, 1936.
[2] Joyce, 1937.

SENSITIVITY OF THE MAGNETOMETER

For practical fieldwork, the vertical field balance can be adjusted to a sensitivity of about 10γ per scale division or a little better. Such an instrument can be read to 1 or 2 gamma. However, to be reliable to this precision, the instrument must be handled with a great deal of care, for very minute changes in the moving system may affect the delicate balance between magnetic and gravitational forces upon which successful use of the instrument depends. Probably the most frequent causes of error are from minute cracking or chipping of the knife-edge, caused by carelessness in releasing the moving system and setting the knife-edge down on the bearing cylinders or from mechanical changes in the moving system caused by severe jars to the instrument in transit or handling.

The sensitivity of the magnetic field balance may be appreciated by comparing it with a chemical balance. The magnetic moment of the moving system is around 1,000 c.g.s. units. For such a system, the torque produced by a change of, say, 5γ is about 0.05 dyne-cm. The half length of the magnet system is about 5 cm., so measuring a change of 5γ is equivalent to measuring a mass change of 0.01 milligram at the end of the magnet. Such a change is small enough to tax the limiting sensitivity of a very good chemical balance permanently set up in a laboratory.

TEMPERATURE EFFECTS

The moving system of the magnetometer is affected by temperature in two ways, *i.e.*, (1) the moment of the magnets decreases with increasing temperature, and (2) the horizontal position of the center of gravity of the entire moving system, with respect to the knife-edge, changes with changes in temperature. Both these effects tend to disturb the balance between gravitational and magnetic torque and hence cause a shift in the scale reading with temperature. With an uncompensated moving system (Fig. 78, right), the temperature effect is around 10 to 20γ per degree centigrade for a vertical field of around $50,000\gamma$. Correction for this effect is not very satisfactory, because the moving system is quite well insulated from its surroundings, and its actual temperature depends not only on the reading of the

thermometer in the case but also on the rate of change of temperature. The uncertainties of temperature effects and their correction are the greatest source of error in magnetic measurements with an uncompensated moving system.

Most magnetic prospecting is now done with an improved moving system (Fig. 78, left) in which the temperature effects are largely compensated. In this system the weights for adjusting the horizontal position of the center of gravity are carried on comparatively long arms, one of invar and one of aluminum.[1] The parts are so proportioned and adjusted that the temperature effects tending to cause a shift in the scale reading are compensated. The adjustment of the compensating weights depends on the magnitude of the normal vertical component of the earth's field, and therefore the system must be readjusted if the instrument is moved to a new area where this component is quite different. Theoretically, the temperature compensation can be made complete. Actually there is usually a small residual effect of the order of 1γ per degree centigrade or less.

Determination of the Temperature Coefficient.—The determination of the temperature correction requires that the instrument temperature be changed in some way while the magnetic field is constant or known. A box of insulating material may be placed around the instrument and heated electrically or by an oil lamp. It is necessary that the temperature be held constant for some time (at least ½ hr.) at each value where a determination is to be made, because the moving system is well insulated and takes considerable time to come into equilibrium with the case in which the temperature is read by the thermometers. Effects due to air convection currents are present also as long as the temperature is changing, so that reliable readings cannot be made until the entire instrument has reached the same temperature. The temperature coefficient is nearly linear, so that determinations of the scale reading at two or three widely different temperatures are usually sufficient. If the temperature changes require considerable time, it is desirable to have another instrument at constant temperature in order to determine changes in the earth's field which may occur during the time the temperature change is taking place.

[1] For a more detailed description see, for instance, Joyce, 1937, pp. 40–44.

CALIBRATION OF THE MAGNETOMETER

Before making readings it is necessary to calibrate the instrument so that scale readings can be converted to standard units (gamma). To do this, the deflection produced by a known field is determined. The known field can be produced conveniently either by a magnet or by an electric current.

Auxiliary Magnet.—The magnetometer tripod is provided with a tube for holding a small magnet vertically below the instrument. For a vertical magnetometer, a vertical magnet is used, for which the magnetic field strength at a point on its axis at a distance large compared with its length is

$$H = \frac{2M}{d^3} \tag{129}$$

where M = moment of the magnet.

d = distance to the center of the magnet.

For a horizontal magnetometer, a horizontal magnet is used for which the corresponding expression for the field strength is

$$H = \frac{M}{d^3} \tag{130}$$

The magnetometer is provided with several auxiliary magnets of known moment which can be used for calibration by noting the deflection when the magnet is brought to a certain distance below the instrument or is simply reversed (changed end for end) at a fixed position.

Helmholtz Coil.—A more precise and generally more satisfactory calibration can be obtained by determining the deflection produced by a known field set up by an electric current in a pair of Helmholtz coils[1] with their axis vertical for a vertical magnetometer and horizontal for a horizontal magnetometer. The

[1] A "Helmholtz coil" consists of a pair of similar coaxial coils with their distance apart equal to their radius. Near the center of such a system the magnetic field produced by a current in the coils is

$$H = \frac{64\pi n i}{\sqrt{5}\, r}$$

This gives H in gamma where n is the number of turns in one coil, i is the current in milliamperes, and r is the coil radius in centimeters.

magnetic field in the space between such coils can be calculated accurately from the dimensions and electric current.

The coils are so mounted that they can be set over the instrument in such a way that the moving system comes in the center

Fig. 80.—Magnetometer in the field, with Helmholtz coils in position for determination of scale constant (for vertical component). Instrument box contains battery, measuring and control apparatus for passing a known current through the coils. (*Photograph courtesy American Askania Co.*)

of the space between them (Fig. 80). An auxiliary box contains a battery, rheostat, milliammeter, and reversing switch. The deflection resulting from the reversal of a known current is read. The field produced is known from the constant supplied by the maker. Since the coils are mechanically simple and rugged, this method of calibration is quite reliable and much more so than the use of an auxiliary magnet. Also the Helmholtz coil is very flexible, as fields of different magnitudes can be produced readily,

and the constant checked over different ranges of instrument deflection.

FIELD OPERATION OF THE VERTICAL MAGNETOMETER

It is not intended to attempt to describe all the details of field operation and manipulation of the instrument. However, the

Fig. 81.—Vertical magnetometer in the field; leveling instrument.

essential field operations for making a magnetometer observation may be outlined briefly as follows:

1. The tripod is set firmly. The tripod head is leveled approximately by a "bull's-eye" level.

2. The auxiliary compass is set on the tripod head, the head oriented until the zero of the compass scale is magnetic north, and the reading of the scale on the tripod head noted. (This is for the purpose of later orienting the instrument with its magnetic axis perpendicular to the magnetic meridian.)

3. The compass is removed, and the instrument is set upon the tripod and carefully leveled (Fig. 81).

4. The instrument is oriented until its magnetic axis is perpendicular to the meridian, the moving system released (let down on the knife-edge), and a reading taken.

5. The instrument is rotated through 180 deg., and the reading repeated.

6. The thermometers inside the case are read for making temperature corrections.

7. The moving system is clamped; the instrument is returned to its case; the operator returns to his car or other means of transportation and proceeds to the next station.

.In routine field operation the aforementioned operations are carried out very quickly. A skilled operator will set up an instrument and complete his reading in 2 to 5 min. By far the larger part of the time is spent in travel from station to station.

Certain simple precautions must be observed in making the field observations and selecting station locations. Stations should not be set near magnetic material of any kind which might give local disturbances, such as a railroad or a concrete highway with steel reinforcing. The operator, of course, must be free of any magnetic material about his person. The car, if one is used for transportation, must be removed at the time of observation to a distance from the instrument such that its magnetic disturbances are negligible (usually around 200 ft. away).

MANNER OF CONDUCTING A MAGNETIC SURVEY

The exact manner of conducting a survey will depend upon the purpose of the survey, the type of country, the ease of transportation, and the type of anomalies to be expected. If anomalies of low magnetic relief are to be of interest, more care will be necessary than where large features or the "grain of the country" are to be determined. The scheme of fieldwork also is influenced by the manner of making corrections for diurnal change (see page 190). In moderately detailed work in the middle western or western states, for instance, it is a common practice to take readings at each section corner (stations one mile apart each way). For such a survey, and if the precision is not better than about 10 gamma, the repeat reading method of making the diurnal correction may be satisfactory. A base station is selected to which all the readings are referred. Some care should be exercised to see that bases are free from local magnetic disturbances, such as electric lines or machinery or magnetic material which may be moved. The first reading is taken at the base station. After several field readings are taken, a check is made at the base. The order of taking stations is made so that

returns to the base are effected with a minimum of extra travel. This type of operation is very similar to gravimeter operation, with the magnetometer base station readings for determining the diurnal variation corresponding to the gravimeter base station observations for determining the instrument drift.

If a fixed instrument is used for the daily variation, the frequent checks at the base are not necessary, and morning and evening checks are sufficient. Also, it is obvious that one fixed instrument may be used for as many field instruments as may be in operation in its general vicinity.

When stations are too far from the first base, a new base is established, and the difference in magnetic intensity between it and the original base is determined. The new base may be any station of the previous survey for which the difference in magnetic intensity relative to the original base is established with sufficient accuracy, and a station that is to be used as a base should be carefully checked. Base stations may be set out as the survey expands. Alternatively, base stations may be established in advance by a special net of readings, choosing locations that are easily accessible over good roads. Such a net can be checked for closure, and residual errors adjusted before using the bases as references for other stations. For instance, when repeat readings are used for diurnal variation control, a base might be established for each township, and a series of stations over about one township (about 36 stations) may be referred to this base. In general, much greater distances between base stations will be used when the diurnal change is determined by a fixed instrument than when it is determined by repeat observations.

In less open or less populated country, it may be necessary to confine the measurements to roads or streams along which travel is relatively simple and make the survey as a series of traverses of comparatively closely spaced stations, perhaps carrying at the same time a position survey for mapping the station locations. The repeat station method of making corrections for diurnal variation is not well adapted to such work, as too much extra time for travel is required. The fixed instrument is then very much preferable. If a camp is maintained, the reference instrument can be read at the camp. Since the instrument is left set up throughout the day, all that is required of the operator is to read the scale every 10 or 15 min. The same operator then

can perform other duties, such as reducing the field observations of the previous day and making maps. If a continuous recording instrument is used, no attention is required during the day.

COMPARISON OF QUANTITIES MEASURED BY VERTICAL AND HORIZONTAL MAGNETOMETERS

It has been pointed out above that the vertical magnetometer measures variations in the vertical component of the earth's field and the horizontal magnetometer measures variations in the horizontal component. Let us examine the implications of this statement in some detail.

Referring to the elementary components of the earth's field (Fig. 74, page 166), it is evident that the definition of the three components V, X, and Y depends on the definition of a system of coordinates which, as commonly used, are (1) the vertical, (2) astronomic north, and (3) astronomic east.

When we set up a vertical magnetometer, level it, and orient it with its magnetic axis in an east-west direction, we eliminate completely any effect of the two horizontal components X and Y. Therefore, a vertical magnetometer as ordinarily used measures differences in the vertical component only.

The case is quite different with the horizontal magnetometer. It is oriented so that its axis of rotation is perpendicular to the magnetic meridian. Thus, it measures differences in the total horizontal component H, where

$$H^2 = X^2 + Y^2$$

and does not measure either of the individual components X and Y. To illustrate, let us consider a few possible cases of magnetic differences between two points as measured by the horizontal magnetometer. In Figs. 82 the vector H_1 represents the total horizontal intensity at one point; H_2 represents the total horizontal intensity at a second point with the vector origins superposed. Then the vector ΔH is the true difference in horizontal intensity between the two points. However, since the magnetometer measures only the component in the magnetic meridian, it measures a quantity indicated in the diagrams by $\Delta' H$, which may be quite different from the true change ΔH. Only when the anomaly is parallel with the meridian and causes no change in declination (Fig. 82b) will the measured anomaly be the same as

the true anomaly. If the anomaly is perpendicular to the meridian (Fig. 82c) and causes a change in declination only and no change in total horizontal intensity, it will not be measured by the horizontal magnetometer.

To be comparable with the vertical magnetometer, it would be necessary to make an accurate determination of the declination for each horizontal magnetometer observation. With such a measurement it is possible to determine separately the two components of the variation of the horizontal intensity and to
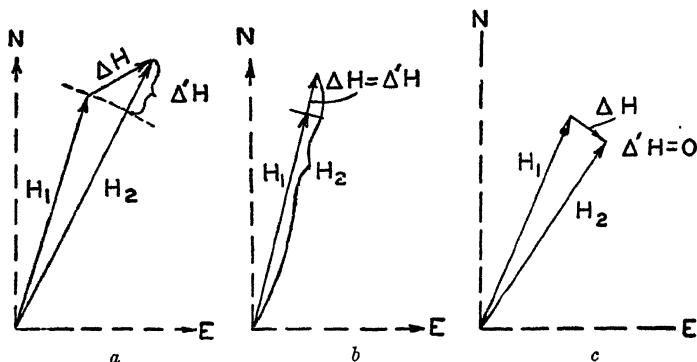
Fig. 82.—Diagrams to illustrate the variation of the effect of a given small increment of the horizontal component ΔH on the total horizontal component.

plot the variation as a vector[1] which would correspond in a general way with a torsion balance gradient.

To estimate the required precision of the declination determination, let us suppose that the normal horizontal component is $20,000\gamma$. A local variation of, say, 5γ directed perpendicular to the meridian would make a change in declination of $5/20,000$ radian, or about 1 minute of angle. Thus, to determine each of the components of the variation in the horizontal intensity with the same precision as is obtained for the vertical intensity with the vertical magnetometer, a horizontal intensity magnetic survey would need to be supplemented by a transit survey or by astronomic observations for the accurate determinations of a reference azimuth or of true north to a precision of 1 minute or better. Also, a special compass would be required, as the ordinary compass cannot be read to this precision.[2]

[1] For examples of vector representations, see Ambron, 1928, pp. 98–101.
[2] Heiland, 1929b, p. 162.

It is evident from the foregoing that the nature of a horizontal magnetic anomaly as measured by the horizontal magnetometer without declination determinations will depend on the relation to the magnetic meridian of the magnetic body causing the anomaly. For instance, the horizontal anomaly of a long dike could be measured quite well if the dike lay perpendicular to the magnetic meridian, so that the anomaly components were parallel to the meridian, but small anomalies could not be measured at all if the dike lay parallel to the meridian.

If we assume that polarization is due to induction by the earth's field, the horizontal anomaly components should usually be parallel to the normal field. If the anomaly were of a generally circular form, it is evident that a profile of horizontal intensity variations could be made to the best advantage if the traverse were made parallel to the magnetic meridian.

REDUCTION OF MAGNETOMETER OBSERVATIONS

CORRECTIONS TO MAGNETOMETER OBSERVATIONS

The reading of a magnetometer is affected by the sum of all contributions to the magnetic field at the time and place of observation. The object of the survey is to map the magnetic expression of the anomaly part of the total magnetic field (page 164). Thus it is necessary to remove all those parts of the total observed effect on the instrument which are extraneous to the picture desired. Careful evaluation and removal of such extraneous contributions are absolutely essential to the attainment of a satisfactory picture of magnetic anomalies of small relief. The magnetic expressions of geologic structures that may be economically important in the search for oil are often very weak. Therefore, careful attention to the various corrections to magnetometer readings is much more important in the application of the magnetometer to oil prospecting than to the exploration for iron ores or igneous intrusions or contacts where the magnetic anomalies are much stronger and usually much more local and definite. It is a relatively simple procedure for a magnetometer operator to set up his instrument and make a reading to a precision of 2 or 3γ. It is quite a different matter to be sure that when the final map is made the magnetic values thereon will truly represent to the same precision the local variations in the magnetic intensity that are of interest.

THE DIURNAL CORRECTIONS

It has been pointed out (Chap. IX) that the magnitude of the diurnal variations of the earth's magnetic field is from 10 to 100γ or more. Therefore, corrections must be made for their removal if the results of a magnetic survey are to be accurate to better than these magnitudes. Since the anomalies of interest in oil prospecting are commonly of lower relief than the magnitude of the daily variation, magnetic surveys for such prospecting

always include the measurement and removal of the diurnal variation.

It has been shown by Vacquier[1] and Soske[2] that the details of the daily variation change from day to day and from hour to hour and that simultaneous measurements at different places may give materially different daily variation curves. The curves of these papers give a fairly definite criterion for the care and frequency of daily variation observations required for precise correction of magnetic observations.

The three general methods used for making diurnal corrections are described briefly below.

By Observatory Measurements.—Certain magnetic observatories make continuous records of the magnetic elements. Data on the daily variation thus recorded or copies of the magnetograms themselves can be obtained and used to measure the daily variation that has occurred during a day's work on a magnetic survey. At the present time there are two such observations in the United States, located at Cheltenham, Md., and Tucson, Ariz. However, there are two serious objections to this method: (1) the data for correction are not available until many days after the fieldwork, and (2) the assumption is necessarily made that the magnetic variation at the observatory is the same as at the place of measurement. The papers mentioned above show that this is far from true, and such an assumption may lead to such large errors as to vitiate the correction almost completely.

By Repeat Observations.—If the field magnetometer is returned at intervals during the day to the same point (or to points between which the magnetic intensity differences have been determined previously), the readings at the same station would check if the magnetic intensity were constant. The variation in these readings, therefore, is a measure of the magnetic variation during the day. If readings are made at intervals of not over two or three hours, a fair measure of the daily variation may be obtained in this way. However, an inspection of the sample daily variation curves (Fig. 83) will show that readings

---

[1] Vacquier, 1937, gives detailed simultaneous comparisons of daily variation curves at places in the United States, separated by distances up to 1,500 miles.

[2] Soske, 1933, gives simultaneous variation curves over a geographic range of about 100 miles in southern California.

at an interval as great as 2 hr. could miss details of the daily variation of as great as 10γ (*e.g.*, curve for Oklahoma City, 6-18-35, between hours 10 and 12; curve for Lamar, Colo.,

a
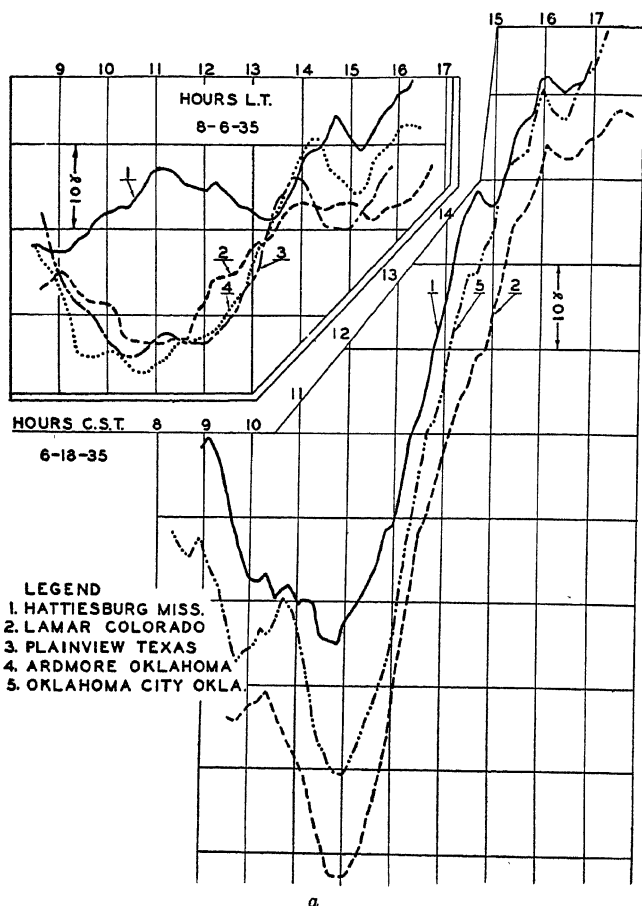
Figs. 83*a* and 83*b*.—Samples of simultaneous daily variation curves at different localities. All curves made from continuous observation of a fixed base station instrument. (*After Vacquier,* 1937.)

6-15-35, between hours 13 and 15). Therefore, this method is not adequate for magnetic work in which a precision of a few gamma is attempted.

By Continuous Reading or Recording.—In this method an auxiliary base instrument is used which may be either an ordinary

field magnetometer read at frequent intervals (preferably not over 10 to 15 min.) or a recording instrument.[1] By either method a continuous curve is obtained of the daily variation at the base location. This curve may be used for correcting as many field

HOURS C.S.T.
6-11-35

6-15-35

LEGEND
1. HATTIESBURG MISS.
2. LAMAR COLORADO
3. PLAINVIEW TEXAS
4. ARDMORE OKLA.
5. OKLAHOMA CITY OKLA

b
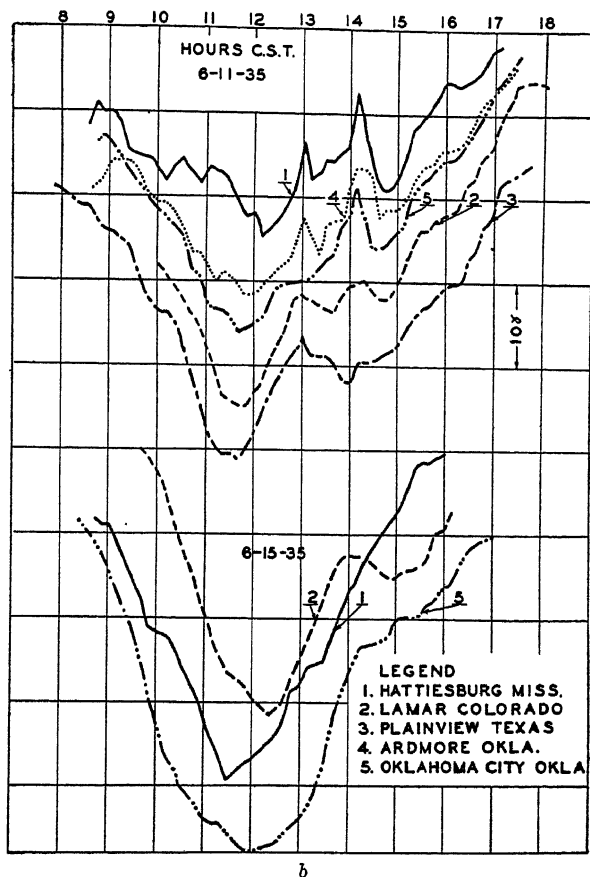
Fig. 83*b*.—(*Continued*).

instruments as are operating in the general vicinity of the base instrument. Just how far afield it is safe to depend on the curve at a given point is not definitely known. Vacquier[2] shows the statistically probable variation in magnetic intensity as a function

[1] For description of recording magnetometers for vertical and horizontal components, see, for example, Askania, 1936.

[2] Vacquier, 1937, Fig. 7.

of distance between stations to be less than 3γ for station separations up to 500 miles and only 4γ for station separations up to 1,500 miles. However, on individual days or for short periods the variations may be much greater. For example, in Fig. 83a compare the curves for Hattiesburg, Miss., on 8-6-35, with curves for other points at the same time. Soske's curves cover much smaller distance intervals (20 to 100 miles); but even over these small distances the diurnal curves differ by 10 to 15γ in some instances.[1] From the rather incomplete data available up to the present, it is probable that a given diurnal curve can be used quite safely for corrections to a few gamma for distances of 50 miles, and usually for much greater distances, from the point at which it is determined.

By whatever means it is obtained, the daily variation curve for a given day is taken as a measure of the simultaneous fluctuation of the magnetic intensity over the area covered by the survey for that day. The measurements are referred to a certain zero time at a given reference, or base station. The time of each field measurement is recorded, and the measured differences in intensity are then corrected by adding or subtracting the amount by which, at the time of the field reading, the daily variation curve is below or above its value at the zero time. Thus, in effect, the magnetic differences are reduced to what they would have been if read simultaneously.

TEMPERATURE CORRECTIONS

Thermometers are provided in the instrument by which its temperature may be determined at each reading. The temperature effect is a simple shift of the balance position of the instrument and thus contributes an effect proportional to the departure from the standard temperature (commonly 20°C. but can be taken as any other temperature, such as that of the base station at the beginning of the day's work) and independent of the

[1] Soske, *op. cit.*, Fig. 1, p. 113, particularly Huenime (July 6, 1932) between hours 12 and 15, distance 80 miles, variation about 15γ; Upper Ojai, between hours 10 and 14, distance 80 miles, variation about 10γ. These variations are not in accord with Soske's statement that "there is no indication that the daily variation for any day was different at the two recording stations by an amount sufficient to impair the use of any one record for a corresponding day anywhere in the entire region" if corrections are to be accurate to, say, 5γ or less.

instrument reading. The temperature effect is calculated from this departure multiplied by the temperature coefficient and is added to or subtracted from the station reading to give the value that would have been read if the instrument had been at the standard temperature.

Probably the greatest source of error in making temperature corrections arises from the differences between the actual temperature of the moving system and that of the thermometers inside the case. The slower any changes in temperature are the more closely will the thermometers indicate the true temperature of the moving system. This is the principal reason for surrounding the instrument case with a layer of thermally insulating material.

The temperature-compensated moving system has greatly reduced the temperature effects. However, for precise work they should not be ignored, as temperature corrections may amount to several gamma.

NORMAL CORRECTIONS

The normal correction is made to remove the normal variation of magnetic intensity over the earth's surface. It corresponds in a general way to the latitude correction of gravity values. However, no accurate mathematical expression is available by which normal magnetic effects may be calculated, and they must be determined empirically from magnetic charts.

The magnetic charts of the United States, such as those published by the U.S. Coast and Geodetic Survey,[1] are very useful for determining normal effects. This publication contains maps of the United States with values for declination (map 1) and dip (map 2), both contoured to 1 deg.; and horizontal intensity (map 3) and vertical intensity (map 4), both contoured to 0.01 c.g.s. or 1,000γ. These charts are based on magnetic observations at all county seats reduced to the same epoch (1935) by correcting for secular changes.

The corrections may be made by drawing contours of normal variations at a convenient interval, such as 10γ, over the area of the survey. The direction and distance between contours are estimated from the magnetic chart. For instance, in central Oklahoma, the distance between the 1,000γ vertical intensity

[1] Howe and Knapp, 1938.

Row number	Station	B	1	2	3	4	5	6	7	8	9	10	B
1	Time	9:58	10:20	11:01	11:19	11:49	12:09	12:29	1:10	1:41	2:09	3:00	3:59
2	Temp.	18.2	20.1	21.1	22.0	22.5	23.0	23.3	23.9	24.1	24.0	23.8	23.1
3	E.	10.6	9.6	9.5	8.6	7.5	6.4	6.1	8.0	8.0	9.1	9.8	10.6
4	W.	11.2	10.4	10.3	9.5	8.6	7.1	6.9	8.4	8.7	9.6	10.5	11.6
5	Avg.	10.9	10.0	9.9	9.05	8.05	6.75	6.50	8.2	8.35	9.35	10.15	11.1
6	K·A	160.0	147.0	146.0	133.0	118.0	99.0	96.0	120.0	123.0	137.0	149.0	163.0
7	α·T	− 7.0	− 9.0	− 10.0	− 11.0	− 11.0	− 12.0	− 12.0	− 13.0	− 13.0	− 13.0	− 12.0	− 12.0
8	D.V.	13.0	15.0	28.0	30.0	30.0	26.0	22.0	18.0	20.0	20.0	17.0	11.0
9	Reg.	−371.0	−335.0	−342.0	−330.0	−361.0	−382.0	−390.0	−359.0	−368.0	−341.0	−347.0	−371.0
10	B.C.	962	......	......	......	......	......	......	......	......	......	......	962
11	Z	757	780	784	784	738	693	678	728	734	765	769	753

NOTE: Base value, 755γ; instrument constant, 14.7γ per scale division; temperature coefficient, 0.9γ per degree centigrade.

The entries in the various rows may be explained as follows:

Row 1, Time: This is the time of reading the field instrument that is necessary for making the diurnal correction.

Row 2, Temp.: This is the temperature reading of the instrument thermometer at the time of reading.

Row 3, E. ⎫
Row 4, W. ⎬: These are the instrument readings, the E. reading being made with the instrument oriented so that the north pole of the magnet is toward the magnetic east, the W. reading with it toward the magnetic west.

Row 5, Avg.: This is the average of the E. and W. readings.

Row 6, K · A: This is the average reading multiplied by the instrument scale constant (14.7) to give the value in gamma corresponding with the reading.

Row 7, α · T: This is the temperature correction. The base temperature is taken as 10°C. Therefore, the value is the temperature coefficient (−0.9) times the difference between the actual instrument temperature (row 2) and the base temperature.

Row 8, D.V.: This is the daily variation correction. It is the departure of the daily variation curve at the time of reading (row 1) from the reference time which in this case was 8:10 A.M. (see curve 3 of Fig. 83b).

Row 9, Reg.: This is the regional, or normal, correction which is determined from the station position and the map of smooth regional contours.

Row 10, B.C.: This is the base correction. It is added in to make a convenient way of calculating station values referred to the primary base rather than the local base station B. Its value is such that the average of the base station readings (at beginning and end of the day) together with their appropriate corrections, plus this correction, gives the base station value. In this case, the base station value is 755γ, which had been determined previously by special base tie observations. Thus, for the first base station observation, the value of the reading plus corrections is

$$160 - 7 + 13 - 371 = -205;$$

for the second base observation, $163 - 12 + 11 - 371 = -209$; average $= -207$. Therefore, the base constant is

$$755 - (-207) = 962.$$

Row 11, Z: This is the reduced value of the station with all corrections, referred to the primary base. The numerical value is the sum of the values in rows 6, 7, 8, 9, and 10.

contours is about 75 miles, and their direction is about N.73°W., S.73°E. For this area, therefore, the normal correction is 1,000/75 = 13.3γ per mile, and 10γ correction contours would be 0.75 mile apart with a direction parallel to that of the 1,000γ contours on the map. From such contours, the normal effect can be read off for any station from its position on the map, and the corresponding correction applied.

Alternatively, the north-south and east-west components of the normal rate of change of intensity may be estimated from the magnetic chart, and the corrections figured from the coordinates of the station. For the example above, the north-south component is 12.8γ per mile increase northward; the east-west component is 3.9γ per mile increase eastward. If a station is, say, 9 miles north and 13 miles east of the base, its normal correction would be $9 \cdot 12.8 + 13 \cdot 3.9 = 165.9\gamma$.

If a survey covers only a relatively small area, the second method may be satisfactory. It is not satisfactory if the surveyed area is large or is connected in with other surveys, because the factors for the north-south and east-west components of the normal variation are not constant. For large or connected surveys the normal corrections should be determined from smooth normal contours, based on a generalized magnetic map of a still larger area.

EXAMPLE OF MAGNETIC MEASUREMENTS WITH CORRECTIONS

The table (page 196) gives detailed numerical examples of the reduction of a series of magnetometer observations. The diurnal variation was determined by a continuously read base station instrument, and, in fact, the curve used is curve 3 of Fig. 83*b* (Plainview, Tex., 6-11-35).

MAGNETIC CALCULATIONS AND INTERPRETATION
THE SOURCE OF MAGNETIC VARIATIONS

The results of a magnetic survey are usually presented as a map showing station locations with the reduced or corrected magnetic values. Presumably these values are free from magnetic contributions of diurnal and normal variation and from temperature effects on the instrument. The fieldwork may be considered as complete with the preparation of such a map.

The assumption of a smooth variation of magnetic intensity over the earth's surface is the basis for the normal corrections. This assumption is consistent with a laterally homogeneous magnetic condition of the earth to a depth of at least some tens of miles. Any departures from this condition remain as irregularities, or anomalies, on the magnetic map. Therefore, the reduced magnetic map is essentially a picture of all departures from a horizontally homogeneous magnetization in the earth's crust. The problem of the interpreter of magnetic results is the explanation of the observed magnetic anomalies in terms of a possible distribution of magnetic material which, in turn, must be explained in terms of reasonable geologic conditions in such a way that inferences may be drawn as to subsurface geology that will be pertinent to the detection of local geologic structure.

The source of magnetic anomalies is magnetized material in the rocks. The details of and quantitative values for magnetization of rocks are still in a rather unsatisfactory state because of the lack of experimental determination of magnetic properties of rocks in low magnetic fields.

The magnetic property of rocks which is of fundamental importance in connection with magnetic prospecting is their polarization I. It is probable that in many, especially the more magnetic rocks, there are two contributions to the total polarization, so that we should write

$$I = kH + I_p \tag{131}$$

where kH may be called the "susceptibility polarization" and represents that part of the polarization which is induced by the present earth's field of strength H acting on material with susceptibility k, and I_p is the remnant or permanent polarization which the rock may retain from a previous state of magnetization and which may or may not be in the same direction as H. Equation (131) therefore is strictly a vector equation.

It is evident from the foregoing that the susceptibility k is of primary importance in magnetic prospecting, as it is a major factor in determining the probable polarization of rocks. Geophysical and other literature contains numerous tables of measured susceptibility values of rocks and minerals.[1] However, it has been pointed out by Slichter[2] that the susceptibility values for rocks and minerals vary over very wide ranges depending on the magnetic field strength in which they are measured. Nearly all the published values are measured in field strengths much greater than that of the earth, and therefore it is very doubtful that any reliance can be placed on these figures as a measure of the probable polarization of rocks that may be expected from induction by the earth's field. In general, the susceptibility measured in a relatively strong field will be lower than when measured in a field as low as that of the earth.

Magnetite (Fe_3O_4) is by far the most common and most magnetic of the magnetic minerals. It is probable that the magnetic properties of most rocks are directly dependent on the amount of magnetite that they contain.

Slichter's careful study of the properties of magnetite indicates that its effective susceptibility in a field of the strength of that of the earth's, when in powdered and highly disseminated form, as it would be expected to occur as a constituent of rocks is around 0.3* (or $300,000 \cdot 10^{-6}$) c.g.s. unit. For closely packed pulverized magnetite, k is about 0.8; and for solid magnetite it is around 1.5 to 10. Probably the most useful figure for our consideration is that for powdered magnetite disseminated until it is only a small fraction of the total rock volume. On this

---

[1] Reich, 1930, pp. 28–31.
Haalck, 1934, pp. 116–117.
Stearn, 1929a, p. 327.
[2] Slichter, 1929.
* Slichter, *op. cit.*, Fig. 6, p. 247.

basis we might expect to estimate the susceptibility of a rock as

$$k = k_m P = 300,000 \cdot 10^{-6} P \qquad (132)$$

where P is the percentage (by volume) of disseminated magnetite and k_m is the susceptibility of magnetite in powdered, disseminated form for which Slichter's figure may be used. For instance, Slichter[1] gives measured susceptibilities of two samples of gabbro, with magnetite percentages of 0.15 and 0.24 as 0.00043 and 0.00068, respectively. The susceptibilities calculated by Eq. (132) are 0.00045 and 0.00072, respectively, which are in rather surprisingly good agreement with those measured.

MAGNETIC PROPERTIES OF ROCKS

Polarization of Igneous Rocks.—On the basis of Eq. (132) we can take the values of average percentage of magnetite in various rocks as given, for instance, by Stearn[2] and calculate the following

Rock	Average magnetite, per cent	Calculated $k \cdot 10^{-6}$	Polarization for $H = 0.6$
Quartz porphyries.............	0.82	2,460	0.0015
Rhyolites....................	1.00	3,000	0 0018
Granites.....................	0.90	2,700	0.0016
Trachyte—syenites...........	2.04	6,120	0.0037
Eruptive nephelites...........	1.51	4,530	0.0027
Abyssal nephelites............	2.71	8,130	0 0049
Pyroxenites..................	3.51	10,530	0.0063
Gabbros.....................	2.40	7,200	0.0043
Manzonite—latites...........	3.58	10,740	0.0065
Leucite rocks................	3.27	9,810	0.0059
Dacite-quartz diorites.........	3.48	10,440	0.0063
Andesites....................	4.50	13,500	0.0081
Diorites.....................	3.45	10,350	0.0062
Peridotites..................	4.60	13,800	0.0083
Analcite rocks................	5.54	16,620	0.0100
Basalts......................	4.76	14,280	0.0086
Diabases.....................	4.35	13,050	0.0078
Basaltic rocks................	4.80	14,400	0.0086
Fermic syenites...............	5.24	15,720	0.0094

[1] Slichter, p. 242.

[2] Stearn, *op. cit.*, p. 331.

table of average susceptibilities and of polarizations in the earth's field with an assumed strength of 60,000γ.

In general, the susceptibilities calculated above are of the same order of magnitude but somewhat higher than those given as the result of susceptibility measurements on igneous rocks. From the general run of values in the table it is to be expected that the susceptibility polarization of igneous rocks in the earth's field will lie in the range from 0.001 to 0.01 with a roughly most probable value for the most common igneous rocks (granite, porphyry, etc.) around 0.002.

The magnitude of the permanent polarization which forms the second term of Eq. (131) is not definitely known, as there are few measurements of permanent polarization. Some measurements by Koenigsberger[1] indicate that the permanent polarization is from 20 to 80 per cent of the magnitude of the induced polarization for most samples measured and that its direction is quite variable and not, in general, parallel with the present earth's field. Some rocks, especially lavas and quartz-porphyries, have a permanent polarization that is from several to many times greater than the induced polarization. It has been shown by experiment (Koenigsberger) that such rocks become polarized while cooling from the Curie point (and have retained a high degree of polarization acquired under special and probably critical conditions).

Present magnetic anomalies are caused by the present state of polarization of the rocks, however it may have been acquired. Because of our uncertain knowledge of the contributions of permanent polarization and the indications that it is smaller than the induced polarization, especially for the older rocks,[2] about all we can do is estimate the polarization as that calculated from the susceptibility and the present strength of the earth's field. On the basis of the foregoing figures, a general figure for probable polarization of an average igneous rock is around 0.002 c.g.s. unit. Its direction is probably that of the present earth's field. However, it must be remembered that in any particular case the values for polarization may differ enormously from this figure, which is particularly true in some of the applications of magnetic work to mining problems in which iron-bearing ore

[1] Koenigsberger, 1930.
[2] Koenigsberger, 1933.

bodies are of interest. As an extreme example, the famous Kursk ore body in Russia has a susceptibility estimated as 2.7[*] and a magnetic anomaly of 200,000γ!

In large-scale magnetic prospecting for oil it is seldom that even very large and broad anomalies, such, for instance, as the frequently mentioned Crosby anomaly in West Texas, has a relief of more than 1,000γ.[†] The greatest possible magnetic relief would be produced by a sharp contact of two large masses of rock with different polarizations (Fig. 84). The relief so produced would be

$$\Delta V = 2\pi(I_1 - I_2) \quad (133)$$

Therefore, if we say that the regional magnetic anomalies seldom have a relief greater than 1,000γ, we can calculate that a common upper limit for $I_1 - I_2$ is given by

FIG. 84.—Maximum vertical magnetic anomaly, resulting from a vertical contact between rocks with polarization I_1 and I_2.

$$I_1 - I_2 = \frac{0.01}{2\pi} = 0.0016 \quad (134)$$

Because the probable range of polarizations is quite large, we should expect the individual values of I_1 and I_2 to be of the same order of magnitude as their difference. Therefore, the foregoing consideration also indicates an order of magnitude for polarizations and polarization contrasts of igneous rocks in the neighborhood of 0.002.

Polarization of Sedimentary Rocks.—In general, the polarization values for sedimentary rocks are very much lower than those for igneous rocks. Measurements of susceptibilities of sediments are no more satisfactory than those for igneous rocks, as nearly all have been made in fields many times greater than that of the earth. The published values are mostly in the range from 1 to 100 · 10^{-6}.[‡] On the other hand, Stearn estimates the average

[*] Slichter, 1929, p. 251.

[†] Also see, for instance, the magnetic map of southwest Alabama, Eby and Nicar, 1936.

[‡] See, for instance, Reich, 1930, pp. 28–31; and Haalck, 1934, pp. 116–117.

magnetite content of sediments as 0.07 per cent[1] which, by Eq. (132), indicates a corresponding average susceptibility of about $200 \cdot 10^{-6}$. Barrett[2] claims that susceptibilities of sediments can cause measurable magnetic anomalies; but his susceptibility curves are in arbitrary units. Collingwood[3] gives an average value of $49.6 \cdot 10^{-6}$ from measurements on 376 samples of sedimentary rocks, measured in a field of 18 gauss. This paper also gives magnetite content for some samples, from which values of k calculated by Eq. (132) are of the same order of magnitude as those measured.
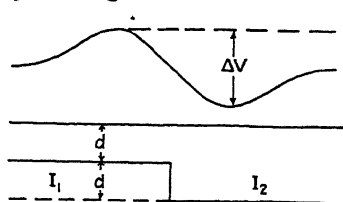
FIG. 85.—Magnetic anomaly for a fault with displacement equal to depth.

If we apply Fig. 84 and Eq. (133) and calculate the minimum detectable polarization contrast for, say, a 10γ magnetic effect, it comes out 0.000016, and the corresponding susceptibility contrast (for $H = 0.6$) would be about $25 \cdot 10^{-6}$. However, only under very ideal geologic conditions (such as a fault with a displacement large compared with its depth) would such a condition be realized. More specifically, if we consider a fault with a displacement equal to the minimum depth of the magnetic contrast (Fig. 85), the required polarization contrast to give $\Delta V = 10\gamma$ would be 0.00007, and the corresponding susceptibility contrast (for $H = 0.6$) would be $120 \cdot 10^{-6}$. From these considerations it is probable that in the type of structure more commonly of interest in oil prospecting, a susceptibility contrast of the order of $100 \cdot 10^{-6}$ or more would be required before it would produce a measurable magnetic anomaly. From such data as are available, it seems unlikely that susceptibilities as high as $100 \cdot 10^{-6}$ are at all common in sediments, although there are some definite exceptions.[4] Therefore, in most cases of

---

[1] Stearn, *loc. cit.*, p. 330.

[2] Barrett, 1937.

[3] Collingwood, 1930a.

[4] Some claims are made (*e.g.*, Barrett, *loc. cit.*) that magnetic anomalies result directly from structure of magnetized sedimentary rocks. Calculations indicate that such effects should be extremely small in magnetic relief, and there is doubt that the examples given are not partly caused by contributions from underlying igneous rocks. Also, in some examples of magnetic effects of structure known from drilling, the measured anomalies

magnetic prospecting for oil, the measurements may be considered as being made on a plane (*i.e.*, the surface of the ground) which is supported on a nonmagnetic medium (*i.e.*, the sediments) and that the effects measured are caused by undulations of the magnetic surface (*i.e.*, the surface of the igneous rocks) and polarization contrasts below that surface.

THE AMBIGUITY OF MAGNETIC INTERPRETATION

The magnetic method is similar to the gravity method (see page 119) in that its interpretation is not unique. A given magnetic anomaly may be explained by a variety of causes. We may be able to find a certain distribution and polarization of magnetic material from which magnetic effects may be calculated that will explain completely a given magnetic picture. The achievement of a fit between calculated and observed effects is no guarantee that the form so arrived at is correct, for an equally good fit might be obtained from a quite different distribution and polarization of material. Therefore, just as in the gravitational case, any magnetic distribution or geologic condition given as the cause of a given distribution of magnetic intensity at the surface *depends on additional control other than magnetics.* This control may be direct, as when a well actually gives a contact on a boundary at which there is a magnetic contrast, or it may be postulated on the basis of geological or other considerations.

Practically, the magnetic method has one advantage over the gravitational because the probable source of magnetic anomalies is more limited. Since, as has been pointed out, the source of magnetic effects usually is at or below the basement surface, possible contributions from within the depth range of the sedi-

---

are quite probably influenced by magnetic effects from buried well casing. There is some evidence for slight negative magnetic anomalies from salt domes which result from the practically zero or slightly negative polarization of the salt contrasted with slightly magnetic sediments. For a specific example, a long salt column with a diameter equal to twice its depth below the surface and having zero polarization contrasted with an assumed polarization of the surrounding sediments of $50 \cdot 10^{-6}$ would have a magnetic effect over its center of -9γ. On the other hand, Lynton, 1931, has shown that certain sediments in California have strong magnetic effects because they contain the magnetic mineral vivianite ($Fe_3P_2O_8.8H_2O$).

ments usually can be ignored. For this reason, magnetic surveys are principally useful for oil prospecting by giving indications of the depth and form of the basement surface. Since many geologic deformations or structures that form traps for oil accumulation are underlain by basement uplifts, the detection of such uplifts is useful. Also, even a rough estimate of basement depths may be very valuable for giving an indication of the available thickness of sedimentary section in which oil accumulations may occur.

In some areas uncertainty is added to magnetic interpretation by surface disturbances. Small, local concentrations of magnetic material, which would cause no measurable anomaly if buried a few hundred feet, may cause local magnetic disturbances which interfere with accurate magnetic work. Such effects are usually noticeable as a general roughness of the magnetic map, for they give differences between near-by stations that are too large or too irregular to be ascribed reasonably to the basement surface. Naturally surface disturbances are more noticeable when stations are close together and may not be evident at all in a survey of widely spaced stations. They are particularly troublesome in glaciated areas. About the only treatment is to make an excess number of stations and use a system of averaging with the hope that the average values will be reasonably typical of the desired magnetic effects from deep below the surface.

THE RELATION BETWEEN MAGNETIC AND GRAVITATIONAL EFFECTS

In connection with the calculation of magnetic effects from bodies of regular form, it is of interest to note the general relation between magnetic and gravitational effects from bodies of similar geometric form and position.

Just as the gravitational force in a given direction is the derivative of the gravitational potential in that direction (page 65), the magnetic force in a given direction is the derivative of the magnetic potential in that direction. Poisson has shown that there is a simple relation between the gravitational and magnetic potentials for an important special case.

Let U be the gravitational potential due to the mass of a body with uniform density σ. If this same body is polarized uniformly in a direction i with an intensity of magnetization I, and if W is

the magnetic potential, then, according to Poisson,

$$W = -\frac{I}{\gamma\sigma}\frac{\partial U}{\partial i} \tag{135}$$

The magnetic force in any direction is the negative of the derivative in that direction of the magnetic potential. Thus the magnetic force in any direction S is

$$-\frac{\partial W}{\partial S} = \frac{I}{\gamma\sigma}\frac{\partial}{\partial S}\left(\frac{\partial U}{\partial i}\right) \tag{136}$$

For the special case[1] where the polarization is vertical (downward in northern latitudes) and we wish the vertical component V of the magnetic field,

$$V = -\frac{\partial W}{\partial z}$$

where z is measured vertically downward. Then, from Eq. (135),

$$V = +\frac{I}{\gamma\sigma}\frac{\partial^2 U}{\partial z^2} \tag{137}$$

In many areas where magnetic measurements are made, the vertical component is the principal part of the magnetic field. Therefore, a very simple and rough but often useful approximation is to consider the vertical magnetic effects of bodies vertically polarized. In this special case the effects can be derived quite simply from the gravitational effects by means of Eq. (137).
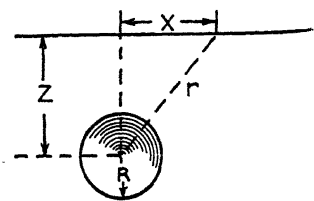
FIG. 86.—Diagram for vertical magnetic effect of a vertically polarized sphere.

The Sphere.—The gravitational potential of a sphere (Fig. 86) is

$$U = \frac{\gamma m}{r} \tag{138}$$

and

$$\frac{\partial^2 U}{\partial z^2} = \gamma m \frac{2z^2 - x^2}{r^5} \tag{139}$$

[1] For a more general treatment see, for instance, Haalck, 1930, p. 325.

If the same sphere is uniformly polarized in the vertical direction, the vertical magnetic intensity is, by Eq. (137),

$$V = \frac{I}{\gamma \sigma} \cdot \gamma m \cdot \frac{2z^2 - x^2}{r^5} \tag{140}$$

$$= \frac{I}{\gamma \sigma} \cdot \gamma \cdot \frac{4}{3} \pi R^3 \sigma \cdot \frac{2z^2 - x^2}{r^5}$$

$$= \frac{4}{3} \pi R^3 I \cdot \frac{2z^2 - x^2}{(x^2 + z^2)^{5/2}}$$

$$= \frac{4\pi R^3 I}{3z^3} \cdot \frac{2 - (x/z)^2}{[1 + (x/z)^2]^{5/2}} \tag{141}$$

$$= K \cdot f\left(\frac{x}{z}\right)$$

where

$$f\left(\frac{x}{z}\right) = \frac{2 - (x/z)^2}{[1 + (x/z)^2]^{5/2}} \tag{142}$$

and

$$K = \frac{4\pi R^3 I}{3z^3} \tag{143}$$

A plot of $f(x/z)$ is given by Fig. 87.

$$f(x/z) = \frac{2 - (x/z)^2}{(1 + x^2/z^2)^{5/2}}$$

MAGNETIC EFFECT OF VERTICAL POLARIZED SPHERE

X/Z →
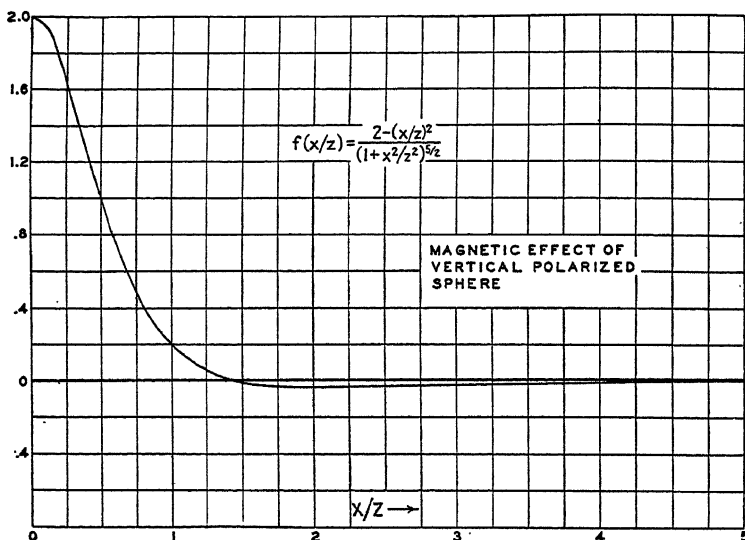
Fig. 87.—Type curve for vertical magnetic effect of a vertically polarized sphere.

Suppose, for instance, that we wish to plot a profile of vertical magnetic intensity for a sphere of radius R of 3,000 ft. depth to

center z of 5,000 ft., which is polarized vertically with an intensity of 0.002 c.g.s. unit.   Then,

$$K = \frac{4\pi \cdot 0.002}{3}\left(\frac{3}{5}\right)^3 = 0.00181$$

Over the center of the sphere [where $x = 0$, $f(x/z) = 2$] its vertical magnetic effect will be 0.00362 oersted $= 362\gamma$.   Vertical magnetic effects at other distances can be written down readily from the curve of Fig. 87, as is illustrated by the following table:

Distance, feet	x/z	$f(x/z)$	V
0	0	2	362γ
2,500	½	1	181
5,000	1	0.177	32
10,000	2	−0.036	−6.5

The Horizontal Cylinder.—The gravitational potential of a horizontal cylinder (Fig. 88) is

$$U = 2\gamma m \log\frac{1}{r} \qquad (144)$$

where m is now the mass per unit length, and

$$\frac{\partial^2 U}{\partial z^2} = 2\gamma m\frac{z^2 - x^2}{(z^2 + x^2)^2} \quad (145)$$

Fig. 88.—Diagram for vertical magnetic effect of a vertically polarized horizontal cylinder.

If this same cylinder is polarized in the vertical direction, the vertical magnetic intensity is [by Eq. (137)]

$$V = \frac{I}{\gamma\sigma}\cdot 2\gamma\pi R^2\sigma\cdot\frac{z^2 - x^2}{(z^2 + x^2)^2}$$

$$= \frac{2\pi R^2 I}{z^2}\cdot\frac{1 - (x/z)^2}{[1 + (x/z)^2]^2} \qquad (146)$$

$$= K'f'\left(\frac{x}{z}\right) \qquad (147)$$

where

$$f'\left(\frac{x}{z}\right) = \frac{1 - (x/z)^2}{[1 + (x/z)^2]^2} \qquad (148)$$

and

$$K' = \frac{2\pi R^2 I}{z^2} \qquad (149)$$

A plot of $f'(x/z)$ is given by Fig. 89.

Suppose that we wish to plot a profile of vertical magnetic intensity for a cylinder of radius R of 3,000 ft., depth to center z of 5,000 ft., which is polarized vertically with an intensity of 0.002 c.g.s. unit. Then

$$K' = 2\pi \cdot 0.002 \cdot (\tfrac{3}{5})^2 = 0.00452$$

Over the center of the cylinder [where $x = 0$, $f'(x/z) = 1$] its vertical magnetic effect $= 0.00452$ oersted $= 452\gamma$. Vertical magnetic effects at other distances can be written down readily

$$f'(x/z) = \frac{1 - (x/z)^2}{[1 + (x/z)^2]^2}$$

MAGNETIC EFFECT OF VERTICAL POLARIZED HORIZONTAL CYLINDER

$X/Z \longrightarrow$
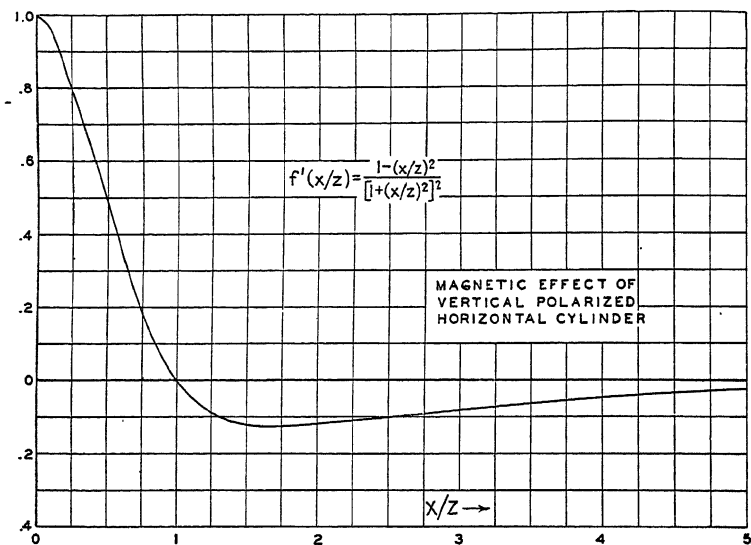
Fig. 89.—Type curve for vertical magnetic effect of a vertically polarized cylinder.

from the curve for $f'(x/z)$ (Fig. 89), as is illustrated by the following table:

Distance, ft.	x/z	$f'(x/z)$	V
0	0	1	452γ
2,500	$\frac{1}{2}$	0.481	218
5,000	1	0	0
10,000	2	-0.120	-54

RELATION BETWEEN VERTICAL MAGNETIC AND CURVATURE EFFECTS OF "TWO-DIMENSIONAL" BODIES

For two-dimensional bodies (*i.e.*, bodies for which the cross section does not vary) there is a simple relation between the vertical magnetic intensity and the torsion balance curvature.

If we consider a two-dimensional body as infinite along the y-axis, then

$$\frac{\partial^2 U}{\partial x\, \partial y} = 0; \qquad \frac{\partial^2 U}{\partial y^2} = 0$$

and the curvature quantity $\Re$ (page 84) reduces to

$$\Re = \frac{\partial^2 U}{\partial x^2} \tag{150}$$

and since, by Laplace's general equation,

$$\frac{\partial^2 U}{\partial x^2} + \frac{\partial^2 U}{\partial y^2} + \frac{\partial^2 U}{\partial z^2} = 0$$

for the two-dimensional case, $\dfrac{\partial^2 U}{\partial y^2} = 0$, and

$$\frac{\partial^2 U}{\partial x^2} = -\frac{\partial^2 U}{\partial z^2}; \qquad \Re = \frac{\partial^2 U}{\partial z^2}$$

and we have, by Eq. (137), if the same body is polarized vertically,

$$V = \frac{I}{\gamma\sigma} \frac{\partial^2 U}{\partial z^2}$$
$$= \frac{I}{\gamma\sigma} \Re \tag{151}$$

Thus, the vertical magnetic effect of a vertically polarized two-dimensional body is of the same form as its curvature effect, and by using the proper constant one may be converted to the other. For example, we have calculated [page 111, Eq. (89)] that, for a horizontal cylinder,

$$-U_\Delta(= \Re) = 2\gamma\pi R^2\sigma\, \frac{z^2 - x^2}{(z^2 + x^2)^2} \tag{152}$$

Substituting the value of $\Re$ from (152) in (151),

$$V = 2\pi I\, \frac{R^2}{z^2}\, \frac{z^2 - x^2}{(z^2 + x^2)^2} \tag{153}$$

which is the same as Eq. (146) derived more directly.   Therefore, $f'(x/z)$ as plotted in Fig. 89 is the same as $f'_K(x/z)$ (curve 3 of Fig. 60) which is the curvature curve for a horizontal cylinder.

The Fault.—We can use the relation between magnetic effect and curvature to compute, for example, the vertical magnetic effect for a vertically magnetized semi-infinite horizontal plane or fault.   With certain approximations we have seen [page 113, Eq. (95)] that the curvature for this case is

$$\frac{\partial^2 U}{\partial x^2} = \frac{2\gamma\sigma tx}{x^2 + z^2} = R$$

Substituting this in Eq. (151),

$$V = \frac{2Itx}{x^2 + z^2}$$

$$= \frac{2It}{z} \frac{x/z}{(x/z)^2 + 1} \tag{154}$$

$$= \frac{2It}{z} f''_K\left(\frac{x}{z}\right) \tag{155}$$

where $f''_K(x/z)$ is the same function that is plotted as curve 3 of Fig. 62.

In a similar way the curvature profile for any two-dimensional body may be used to give the vertical magnetic profile for the same body uniformly polarized vertically.

GENERAL NATURE OF THEORETICAL MAGNETIC ANOMALIES

The special cases of vertical magnetic intensities produced by vertically polarized bodies which have been considered are of value in giving the approximate nature of vertical fields.   However, the direction of polarization may be far from vertical, especially in low latitudes.   A general and only qualitative but often useful approximation to the kind of magnetic effect that a body of given form and polarization will produce may be obtained by considering the volume magnetization of a body as replaced by magnetic poles on its surface.

By Gauss's theorem, for effects at points outside a magnetized body, the volume magnetization within the body can be replaced by a surface distribution of magnetization.   This means that for effects at external points the magnetic moment within the body can be replaced by a certain distribution of magnetic poles on its

surface. The total amount of positive and of negative magnetization on the surface must be equal. Thus, for each positive pole on one side of the body there must be an equal negative pole on the other side (for simple bodies simply magnetized). Thus, the volume magnetization may be considered as replaced by pairs of positive and negative poles on opposite sides of the body.

In ordinary magnetic prospecting with the vertical magnetometer we are concerned only with the vertical component of the magnetic field. Therefore, the discussion that follows is, for simplicity, restricted to the vertical component only and mainly, also, to vertical magnetization.

Single Magnetic Pole.—The vertical component of the magnetic field due to a single isolated pole P, at a point p (Fig. 90), is simply
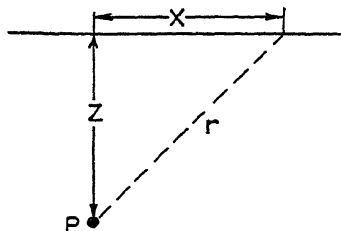
FIG. 90.—Diagram for vertical magnetic effect of an isolated magnetic pole.

$$V = \frac{Pz}{r^3} = \frac{Pz}{(x^2 + z^2)^{3/2}} \tag{156}$$

Now, the integral of this field over all points on the surface is

$$\int_0^{2\pi} \int_0^\infty \frac{Pzr\ dr\ d\theta}{(r^2 + z^2)^{3/2}} = 2\pi Pz \left[\frac{-1}{(r^2 + z^2)^{1/2}} \right]_0^\infty = 2\pi P \tag{157}$$

This shows that the total magnetic flux over the horizontal plane depends only on the pole strength P and not at all on its depth. Thus, for an elemental magnet with equal and opposite poles $+P$ and $-P$ its total magnetic flux over the horizontal plane is zero. Since the volume polarization of any magnetized body can be replaced by a surface polarization in pairs of equal positive and negative poles, it follows that the magnetic intensity due to any disturbing body, integrated over an infinite horizontal plane, is zero. From this we infer that every positive anomaly caused by a single magnetized body should be accompanied by a negative anomaly, and vice versa.

The concept of the volume magnetization of a body being equivalent to a surface distribution of magnetic poles may be used to work out in a qualitative way the nature of the magnetic

curves that a body of a given form will produce.   This is illustrated for a few simple cases below.

Vertically Magnetized Sphere.—The volume magnetization of a sphere, polarized vertically, may be considered as replaced by a surface distribution of negative poles over the upper half and positive poles over the lower half (Fig. 91a).   In a rough, qualita-
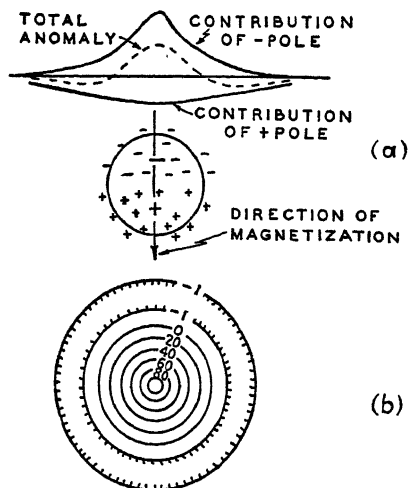
Fig. 91a.—Qualitative picture of vertical magnetic effect of a vertically polarized sphere, showing contribution of positive poles over upper half of surface, negative poles over lower half of surface, and total effect.

Fig. 91b.—Contours of vertical magnetic intensity from a vertically polarized sphere.
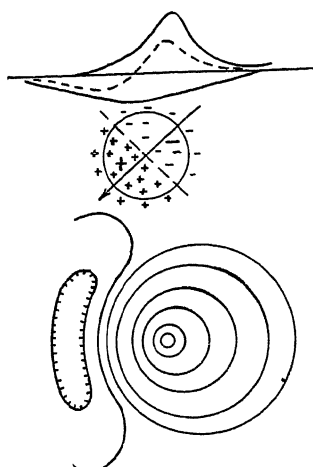
Fig. 92a.—Qualitative picture of vertical magnetic effect of a sphere polarized at angle of 45 deg. with the vertical.

Fig. 92b.—Contours of vertical magnetic effect for a sphere polarized at angle of 45 deg. with the vertical.

tive way the upper half can be represented by a single large negative pole [represented by the large minus (−) sign], and the lower half by a single large positive pole.   The magnetic contribution of the nearer, negative pole will be somewhat as represented by the upper curve.   That of the more remote positive pole will be somewhat as indicated by the lower curve.   The total anomaly is the algebraic sum of the two, as indicated by the dotted curve.   The accurate profile for this case is given by $f(x/z)$, [Eq. (142)], and the curve (Fig. 87).   This curve shows that there will be a central positive high zone surrounded by a broad negative zone, and a contour map of the anomaly is shown by Fig. 91b.   The product of the area times the average strength

of the anomaly will be the same for the positive and negative parts. From the formula for $f(x/z)$ this contour map will have the following characteristics: zero contour at a distance

$$x = \pm\sqrt{2}\,z$$

bottom of negative zone at a distance $x = +2z$; maximum depth of negative zone $= 1.79$ per cent of the maximum height of positive zone.

Magnetized Sphere with Magnetization Inclined.—This case (Fig. 92a) is quite similar to that just considered except that now the positive and negative curves do not have their maximum effects in the same vertical line. The negative zone is somewhat stronger and is no longer symmetrical but is steeper on the side toward which the magnetization vector dips.[1] The contours (Fig. 92b) show a sharp high, partially surrounded by a low on one side. From such considerations, we should expect that if the magnetization of rocks is caused by the earth's field, strong positive anomalies would, in the Northern Hemisphere, have weak negative anomalies on their north sides. Actually such cases are rarely observed clearly, probably because the dip is usually too near to the vertical and because the negative zone is relatively so weak that it is confused by other unrelated magnetic disturbances.

Vertical Cylinder, Magnetized Vertically.—For this case (Fig. 93) the equivalent pole distribution is a sheet of negative poles over the upper end and a sheet of positive poles over the lower end, each sheet having an intensity of I per unit area,

[1] Haalck, 1934, p. 134, gives the following formulas for the vertical and horizontal components, respectively, of the magnetic anomaly of a sphere polarized in a field having vertical and horizontal components Z_0 and H_0:

$$V = -C\frac{Z_0}{r^5}\left[x^2 - 2z^2 + 3xz\frac{H_0}{Z_0}\right]$$

$$\dot{H} = -C\frac{H_0}{r^5}\left[z^2 - 2x^2 + 3xz\frac{Z_0}{H_0}\right]$$

where $C = \dfrac{\frac{4}{3}\pi k R^3}{1 + \frac{4}{3}\pi k}$

$k =$ difference between susceptibility of the sphere and that of the surrounding material,

and R, r, x, and z are as given in Fig. 86.

where I is the magnetic moment per unit volume of the material (see page 160). From such a sheet of poles it can be shown that the magnetic intensity at a point is proportional to the solid angle subtended at that point by the sheet. For this case the positive and negative sheets are circular disks. It is evident that at a point over the axis, the solid angle of the upper circle will be larger and, therefore, that it will produce a positive anomaly. At points beyond a certain distance outside the edge of the disk, the solid angle of the lower disk will be greater and will give rise to a negative anomaly. The change in the solid angles of the two disks on a profile across the cylinders will result in a magnetic curve somewhat as shown by the profile. It is evident that the magnitude of the anomaly will depend very much on the
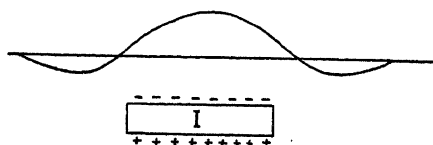
Fig. 93.—Vertical magnetic effect of a short vertical cylinder with vertical polarization.

thickness of the cylinder. If it is thin, the solid angles of the upper and lower surfaces are nearly equal and will nearly cancel each other, and the net effect will be small. If the cylinder is thick, the solid angle of the lower end will be small, and its contribution will be smaller, leaving a stronger positive anomaly. Finally, in the limit when the cylinder is infinitely long, the effect of the lower end becomes vanishingly small (although spread over a very wide area so that the product of effect times area is the same), and we have remaining only the positive contribution of the solid angle of the upper end of the cylinder with a pole strength of I per unit area.

Semi-infinite Horizontal Sheet (Fault).—Consider a magnetized sheet covering a half plane, with a sharp boundary (Fig. 94). This corresponds to a fault in a magnetic layer. Consider the magnetization vertical. Again the volume magnetization I (magnetic moment per unit volume) will be replaced by a uniform surface distribution of poles (of strength I per unit area). At points far removed from the edge of the slab, the solid angle subtended by the upper and lower sheets of poles will be nearly the same, and the total effect is very near zero. As we approach

the edge from the left (Fig. 90), the solid angle of the upper negative sheet is greater, and there is a positive anomaly which increases to a maximum a little back from the edge. Over the edge, the solid angles of both sheets are both 2π, and the net effect is zero. On the side away from the slab, the solid angle of the positive sheet is slightly greater so there will be a negative effect on that side, which will be antisymmetric with the positive effect on the other side. Thus, the curve for the net magnetic effect will be somewhat as shown in the profile. This corresponds to the curve $f_k''(x/z)$ as shown by Eqs. (154) and (155) (page 212), which is plotted as curve 3 of Fig. 62.
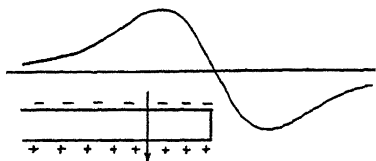
Fig. 94.—Vertical magnetic effect of a fault with vertical polarization.

Formulas and curves for magnetic effects of a variety of regular bodies may be found in the geophysical literature.[1] Also, as pointed out above (page 211), curves for torsion balance curvature of two-dimensional bodies may be used as the magnetic effect of the same bodies when vertically polarized. For instance, a wide range of such curvature curves for dikelike slabs at various angles and depth are given by Shaw.[2]

CALCULATION OF MAGNETIC EFFECTS FOR IRREGULAR FORMS

The examples and descriptions given on previous pages will serve to show the general form and order of magnitude of the magnetic anomalies which may be expected from magnetic bodies that can be approximated by geometric forms. For bodies of more complex form, it is usually necessary to resort to graphical or mechanical calculation methods. For cases of two-dimensional bodies, polarized vertically, the charts or methods designed for calculation of torsion balance curvatures can be used directly. For three-dimensional bodies, or bodies polarized at an angle

[1] Haalck, 1927. The formulas and curves on pp. 55–62 of this book are incorrect.

Haalck, 1930, pp. 333–336.

Haalck, 1934, pp. 134–149.

Joyce, 1937, pp. 115–118.

[2] Shaw, 1932a, 1932b, especially the series of diagrams, pp. 278, 279, 302–311, 339, 355–359.

with the vertical, the calculations are considerably more involved. Limited examples of charts for such calculations are given in the literature.[1]

MAGNETIC EFFECT OF BURIED WELL CASING

The question of the disturbance of the magnetic field to be expected from magnetic material in wells is often pertinent to magnetic prospecting. Thus, it may be considered desirable to make a magnetic survey over a known structure to see what kind
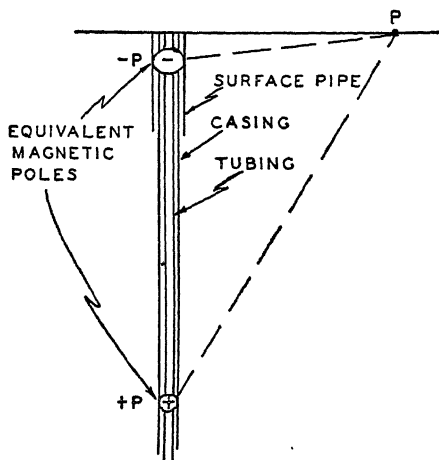
FIG. 95.—Magnetic effect of well casing.

of magnetic picture it would make in order to use such a picture as a guide in the interpretation of other magnetic pictures which might indicate otherwise unknown structure. However, the presence of iron casing and tubing in the wells on the known structure may seriously distort the picture and render it useless as a guide to the interpretation of pictures in undrilled areas. Therefore, we shall consider in some detail the disturbance to the magnetic field that may be expected from magnetic material in wells.

A string of pipe may be considered as roughly equivalent to a long vertical magnet (Fig. 95), the magnetization probably being principally that induced by the earth's field. This magnetization can be replaced by a negative pole near the upper end of the

[1] Haalck, 1930, pp. 336–342.
Heiland, 1929c, pp. 73–74.

pipe and a positive one near the lower end. The total effect of the pipe may be considered as the sum of the effects of two single poles.

For a simple, long magnet, with intensity of magnetization I and cross-sectional area A, the pole strength P will be

$$P = 4\pi I A \tag{158}$$

If the polarization is induced by the vertical component V of the earth's field, in material of susceptibility k, it will be

$$I = kV$$

and

$$P = 4\pi k V A \tag{159}$$

The magnetization of pipe in wells corresponds to a value of k of 300 to 600.[1] From the value of P, calculated by formula (159), the values of positive and negative magnetic effects at any point on the surface, such as p (Fig. 95), can be calculated by Eq. (156).

Since one pole will be very close to the surface, and the other relatively remote, it is evident that the magnetic effects will consist of a very sharp local high[2] and a very broad low. From some measurements and theoretical considerations it turns out that the upper pole is within a few feet of the upper end of the casing.[3] This means that the positive anomaly from the upper pole is all concentrated within a very short horizontal distance of the end of the pipe. On the other hand, the very small negative effect from the much more distant positive pole near the

[1] This value is somewhat higher than might be expected from the initial permeability of steel. However, it seems that the material in wells becomes magnetized more strongly than would be expected, probably in part, at least, on account of mechanical jarring from drilling and pumping equipment. The figure given is estimated from actual measured magnetic effects of buried pipe as given by Barrett, 1931, and Van Weelden, 1933*a*.

[2] This refers to northern latitudes, if the magnetization is induced by the vertical component of the earth's field. South of the magnetic equator, the vertical component is reversed in direction and the upper pole should be negative, the lower one positive.

[3] See, for instance, Van Weelden, *loc. cit.* Also, Barrett, *loc. cit.* From the magnetic curve which can be plotted from Barrett's Table I, the depth to the equivalent upper pole can be calculated readily by Eq. (160). It is evident from such a calculation that the equivalent pole is only about 2 ft. below the end of the pipe.

lower end of the pipe will have a breadth that will depend upon the length of pipe but will, in general, be large compared to the spacing between wells. Therefore, the total magnetic effect of an oil field should be a series of individual extremely sharp highs at each wellhead, together with a broad negative effect which will depend on the total number of wells and on their depth. Thus, if we were making a magnetic profile toward a drilled field, we should expect a negative anomaly on approaching the field. The distance out at which the negative anomaly should begin to be felt would be greater the deeper the drilling. A detailed calculation of this effect for the Healdton field is given by Van Weelden.[1] For this field the actual magnetic survey shows a maximum negative anomaly of approximately 200γ. The magnitude and form of the measured anomaly are quite consistent with those expected from the calculation of the sums of the magnetic effects of the wells in the field.

APPLICATIONS OF MAGNETIC PROSPECTING

The various formulas and calculation methods for estimating the general form and magnitude of the magnetic anomaly that may be expected from a given distribution and polarization of magnetic rocks have been outlined. Such estimates, in turn, can serve as a general guide to the selection of magnetic anomalies that may be the expressions of reasonable geologic structure and excluding those which must have other causes. To a limited extent such calculations may indicate whether or not a given geologic problem has a reasonable chance of being solved by magnetic methods.

It has been shown (page 205) that the expected polarizations of igneous rocks are so much greater than those of the sediments that magnetic anomalies are primarily determined by the depth and attitude of the basement rocks. For most oil prospecting, the contribution of the sedimentary rocks to the magnetic picture is almost negligible.[2]

The oil geologist's interest in determining the configuration of the basement rocks lies in the fact that in many cases sedimentary structures are underlain by basement uplift. If a basement

[1] Van Weelden, *op. cit.*, pp. 88–90.
[2] See calculations and footnote, p. 204.

uplift occurred after the deposition of overlying sediments, the latter would, of course, also be involved in the uplift. On the other hand, if the basement features were present prior to the deposition of the sediments, the overlying sediments would be laid down horizontally over the basement feature. However, even in this case some structure may result from differential compaction of the sediments, as has been pointed out, for
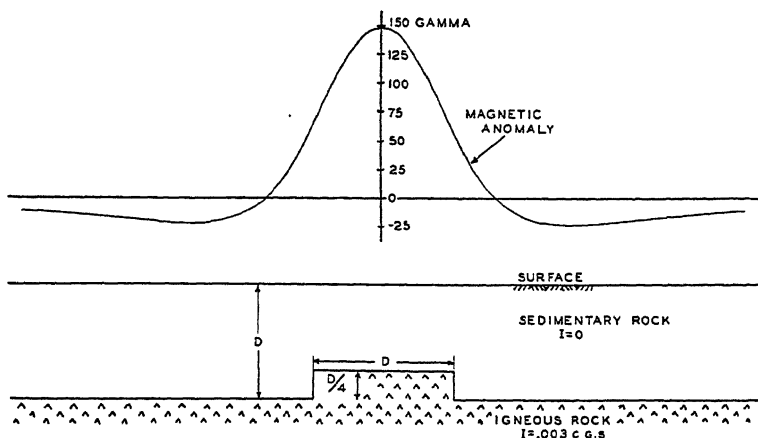
Fig. 96.—Calculated profile of vertical magnetic anomaly from a long ridge with vertical sides, representing an uplift of one-fourth the depth and width equal to depth and with a reasonable average value of polarization.

instance, by Athy.[1] From such considerations it is evident that if magnetic measurements can indicate areas of basement uplift or structure, they may serve as useful guides to the location of interesting sedimentary structure.

When calculations are made of the order of magnitude of the magnetic anomalies that may result from basement structure, it is found immediately that they are small compared with the magnitude of many features that are shown on magnetic maps. For instance, the calculated curve (Fig. 96) is for a structure long in the direction perpendicular to the profile and shows a maximum anomaly of 150γ (for a polarization of 0.003 c.g.s. unit, which is comparatively high) for a feature that has a structural relief of one-quarter of its depth. This means that if, for instance, the basement is 1 mile deep, a long structure which is 1 mile wide

[1] Athy, 1930.

and has a structural relief of $\frac{1}{4}$ mile would have a magnetic effect of only around 150γ. The most elementary considerations of this kind indicate that the magnetic features with relief of hundreds and even thousands of gamma which are commonly observed on magnetic maps must arise not from actual relief of the basement but from differences in the magnetic state within different parts of the basement rock. For this reason, it is evident that in order to bring out the local features of the order of magnitude that might be the result of reasonable basement structure, it is necessary to remove from the picture these much larger effects. Therefore, just as in the gravitational case, it may be desirable to make some sort of regional subtraction from a magnetic picture in order to isolate those anomalies which are most probably of interest.[1]

It is evident from the various formulas and qualitative rules given that the magnitude of a magnetic anomaly depends very much on the distance between the positive and negative poles at the surfaces of the magnetic material causing the anomaly. Therefore, it is apparent that magnetic anomalies of large relief over large areas must arise from differences in magnetization of the basement rocks extending to considerable depths.[2]

An example calculated to illustrate the relative contributions to a magnetic anomaly from possible basement magnetization changes and from basement structure is shown by Fig. 97. This has been calculated for a cylindrical magnetization change extending to great depths on which are superposed the calculated effects of several flat, cylindrical disks which are intended to simulate structure in the basement surface. It is evident that the appearance of the picture given by the "structures" will depend on their position relative to the larger "regional" picture. If this regional is properly estimated and removed, however, the local features will show up in their proper form and relief.

[1] For examples showing the removal of regional effects, see Lynton, 1931, p. 1362; Dick, 1936, pp. 7 and 8; Malamphy, 1936, p. 35.

[2] For notes on the results of drilling on large magnetic anomalies and comments on their causes, see Eby and Nicar, 1936. For a note on large magnetic highs which do not indicate basement structure, see Heiland, 1929a, p. 37. For comments on linear magnetic highs and their interpretation in terms of iron-bearing igneous rocks rather than structure, see MacCarthy, 1936, pp. 399–400.

DEPTH ESTIMATION

It is often useful to know the depth of the basement, as such knowledge will tell the thickness of the sedimentary section in which oil accumulation might occur. The sharpness of magnetic anomalies depends, of course, on their depth. If anomalies come from a shallow basement, they will, in general, be comparatively sharp; if from a deep basement, they will be broader.
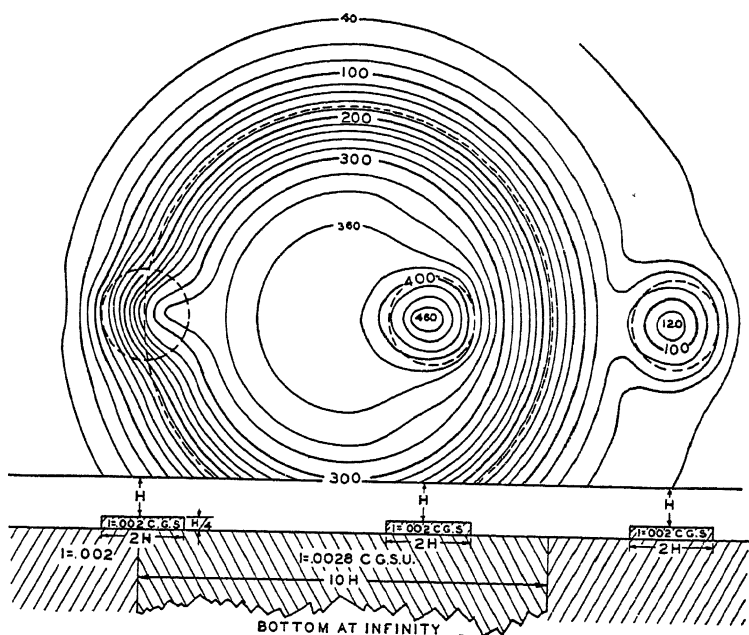
Fig. 97.—Contours of calculated magnetic effects, to show variation of appearance of the effect of a given basement feature depending on its relation to boundaries of regional polarization contrasts.

Some definite rules[1] have been given in the literature for the estimation of the depths to magnetized material of certain forms from the widths of their magnetic effects. These may be illustrated by deriving depth rules from the theoretical magnetic

[1] See, for instance, Eve, 1932, especially the discussion and table of depth rules (by C. A. Heiland), p. 213. Some magnetic depth rules are very old, having been published as early as 1723. For a brief historical review, see the above-mentioned discussion, p. 208 (contributed by Lundberg and Sundberg).

effects in a manner quite parallel to that used to estimate depths of gravity anomalies. The following table of depth rules has been derived from the equations indicated.

Magnetic form	Equation	Depth to center	Equation
Single pole..................	(156), p. 213	$z_c = 1.305x_{1/2}$	(160)
Sphere.....................	(142), p. 208	$z_c = 2.0x_{1/2}$	(161)
Cylinder...................	(148), p. 209	$z_c = 2.05x_{1/2}$	(162)
Fault......................	(154), p. 212	$z_c = x_{max.}$	(163)

$x_{1/2}$ = "half width," or horizontal distance, from the center of the anomaly to the point where its amplitude is half its maximum amplitude.

$x_{max.}$ = horizontal distance from center of fault picture to maximum (or minimum) of the curve (see curve 3 of Fig. 62).

USEFULNESS OF MAGNETIC SURVEYS

The possible usefulness of a magnetic survey in a given area depends on the geologic history of the area that determines the relation of any basement structure to that of the overlying sediments. It depends also on the nature of the basement material and the resulting magnitude of regional magnetic variation and on the depth to the basement.

In the Gulf Coast, for instance, magnetic surveys have been of comparatively little use because the basement is very deep and there seems to be no relation between salt dome uplifts and basement irregularities, indicated by magnetic surveys. Some magnetic anomalies are claimed for salt domes resulting from magnetization contrasts in the sediments but are very small in magnitude and have led to the discovery of no new domes.

Extensive surveys have been made in West Texas, and some drilling has been done on magnetic anomalies but without very definite success.[1] Apparently the large anomalies there are caused principally by magnetization differences within the basement rocks and not by structure.[1]

Magnetic surveys in Kansas have given anomalies that are said to be associated with the granite ridge.[2] In general, magnetic prospecting would be expected to be more useful in this general area where the basement is comparatively shallow.

[1] Heiland, 1929a, p. 37.

[2] Jenny, 1938, p. 339.

A commonly given example of the usefulness of magnetic surveys in indicating oil-bearing structure is in the Texas Panhandle where the buried Amarillo Mountains are the cause of very pronounced magnetic anomalies.

In many cases the regional magnetic anomalies are associated quite closely with regional geologic structure. Probably the most striking example of this kind in the literature is shown by surveys in southern Oklahoma where the Wichita and Arbuckle Mountains and the intervening Anadarko-Ardmore basin are quite clearly and simply related to regional magnetic highs and lows.[1]

Some of the fault zone structures of Texas are very clearly indicated by magnetic anomalies where the structure is caused by serpentine plugs. The serpentine is quite magnetic and in some cases gives strong anomalies.[2]

[1] Van Weelden, 1933*b*.
[2] Collingwood, 1930*a*.

BIBLIOGRAPHY

1921

THOMSON, J. J.: "Elements of the Mathematical Theory of Electricity and Magnetism," 5th ed., Cambridge University Press, London.

1926

BARTELS, J.: "Erdmagnetismus, Erdstrom und Polarlicht," in "Lehrbuch der Geophysik," ed. by B. Gutenberg, pp. 378–433, Verlag von Gebrüder Borntraeger, Berlin.

1927

HAALCK, HANS: "Die magnetischen Verfahren der angewandten Geophysik," Verlag von Gebrüder Borntraeger, Berlin.

1928

AMBRONN, RICHARD: "Elements of Geophysics," trans. by Margaret C Cobb, McGraw-Hill Book Company, Inc., New York.

1929

a. HEILAND, C. A.: Geophysical Methods of Prospecting: Principles and Recent Successes, *Quarterly of the Colorado School of Mines*, vol. XXIV, No. 1, March, 1929.

b. HEILAND, C. A.: Theory of Adolf Schmidt's Horizontal Field Balance, "Geophysical Prospecting, 1929," *Trans. Am. Inst. Min. Met. Eng.*, vol. 81, pp. 261–314.

c. HEILAND, C. A.: A New Graphical Method for Torsion Balance-Topographic Corrections and Interpretations, *Bull. Am. Assoc. Petroleum Geologists*, vol. 13, pp. 39–74.

SLICHTER, L. B.: Certain Aspects of Magnetic Surveying, "Geophysical Prospecting, 1929," *Trans. Am. Inst. Min. Met. Eng.*, vol. 81, pp. 238–260.

a. STEARN, NOEL H.: A Background for the Application of Geomagnetics to Exploration, "Geophysical Prospecting, 1929," *Trans. Am. Inst. Min. Met. Eng.*, vol. 81, pp. 315–344.

b. STEARN, NOEL H.: The Dip Needle as a Geological Instrument, "Geophysical Prospecting, 1929," *Trans. Am. Inst. Min. Met. Eng.*, vol. 81, pp. 345–363.

1930

ATHY, L. F.: Density, Porosity and Compaction of Sedimentary Rocks, *Bull. Am. Assoc. Petroleum Geologists*, vol. 14, No. 1, pp. 1–24, January, 1930.

a. COLLINGWOOD, D. M.: Magnetics and Geology of Yoast Field, Bastrop County, Texas, *Bull. Am. Assoc. Petroleum Geologists,* vol. 14, No. 9, pp. 1191–1197, September, 1930.

b. CÔLLINGWOOD, D. M.: Magnetic Susceptibility and Magnetite Content of Sands and Shales, *Bull. Am. Assoc. Petroleum Geologists,* vol. 14, No. 9, pp. 1187–1190, September, 1930.

HAALCK, H.: "Die magnetischen Methoden der angewandten Geophysik," in "Handbuch der Experimentalphysik," ed. by W. Wien and F. Harms, Band XXV, Teil 3, pp. 303–398, Akademische Verlagsgesellschaft m.b.H., Leipzig.

KÖNIGSBERGER, J. G.: Über die magnetische Eigenschaft von Gesteinen, *Terr. Mag. Atmos. Elec.,* vol. 35, pp. 145–148.

REICH, H.: "Geologische Unterlagen der angewandten Geophysik," in "Handbuch der Experimentalphysik," ed. by W. Wien and F. Harms, Band XXV, Teil 3, pp. 1–46, Akademische Verlagsgesellschaft m.b.H., Leipzig.

1931

BARRETT, WILLIAM M.: Magnetic Disturbance Caused by Buried Casing, *Bull. Am. A soc. Petroleum Geologists,* vol. 15, No. 11, pp. 1371–1399, November, 1931.

KENNELLY, A. E.: *Trans. Am. Inst. Electrical Eng.,* vol. 50, p. 737.

LYNTON, EDWARD D.: Some Results of Magnetometer Surveys in California, *Bull. Am. Assoc. Petroleum Geologists,* vol. 15, No. 11, pp. 1351–1370, November, 1930.

1932

EVE, A. S.: A Magnetic Method of Estimating the Height of Some Buried Magnetic Bodies, "Geophysical Prospecting, 1932," *Trans. Am. Inst. Min. Met. Eng.,* vol. 97, pp. 200–215.

JENNY, W. P.: Magnetic Vector Study of Regional and Local Geologic Structure in Principal Oil States, *Bull. Am. Assoc. Petroleum Geologists,* vol. 16, No. 12, pp. 1177–1203, December, 1932.

a. SHAW, H.: Interpretation of Gravitational Anomalies, I, "Geophysical Prospecting, 1932," *Trans. Am. Inst. Min. Met. Eng.,* vol. 97, pp. 271–335.

b. SHAW, H.: Interpretation of Gravitational Anomalies, II, "Geophysical Prospecting, 1932," *Trans. Am. Inst. Min. Met. Eng.,* vol. 97, pp. 336–366.

STEARN, NOEL H.: Practical Geomagnetic Exploration with the Hotchkiss Superdip, "Geophysical Prospecting, 1932," *Trans. Am. Inst. Min. Met. Eng.,* vol. 97, pp. 169–199.

1933

KÖNIGSBERGER, J. G.: "Residual Magnetism and the Measurement of Geologic Time," *International Geological Congress, Report of* 16*th Session, United States of America,* 1933, vol. 1, pp. 225–231, Washington, D. C., 1936.

Soske, Joshua L.: Differences in Diurnal Variation of Vertical Magnetic Intensity in Southern California, *Terr. Mag. Atmos. Elec.*, vol. 38, No. 1, pp. 109–115, March, 1933.

Van Weelden, A.: Magnetic Anomalies in Oilfields, *Proc. World Petroleum Cong., London*, 1933, Vol. I, pp. 86–90, London, 1934.

Van Weelden, A.: The Regional Tectonical Features of the Wichita-Arbuckle Mountain Region in the Light of Geophysical Observations, *Proc. World Petroleum Cong., London*, 1933, Vol. I, pp. 174–176, London, 1934.

1934

Haalck, Hans: "Lehrbuch der angewandten Geophysik," Verlag von Gebrüder Borntraeger, Berlin.

1936

American Askania Corporation: Pamph'et Geo 118 Ea, "Magnetic Field Balances designed by Ad. Schmidt," Houston, Texas.

Dick, James A.: Progress in Magnetometer Exploration Leads to Resurvey of Many Areas, *California Oil World*, Oct. 29, 1936, pp. 7–8.

Eby, J. Brian, and E. G. Nicar: Magnetic Investigations in Southwest Alabama, *Bull. Geol. Survey of Alabama* 43, University, Alabama, June, 1936.

MacCarthy, Gerald R.: Magnetic Anomalies and Geologic Structure, *Jour. Geology*, vol. 44, pp. 396–406.

Malamphy, Mark C.: Magnetic Prospecting in Santa Catharina, Brazil, *Geophysics*, vol. 1, No. 1, pp. 23–47, January.

1937

Barrett, William M.: "Mapping Geologic Structure with the Magnetometric Methods," William M. Barrett, Inc.

Joyce, J. Wallace: "Manual on Geophysical Prospecting with the Magnetometer," printed by the American Askania Corp., Houston, Tex., under a cooperative agreement with the U. S. Bureau of Mines.

Vacquier, Victor: Short-time Magnetic Fluctuations of Local Character, *Terr. Mag. Atmos. Elec.*, vol. 42, No. 1, pp. 17–28, March, 1937.

1938

Howe, H. Herbert, and David G. Knapp: United States Magnetic Tables and Magnetic Charts for 1935, *U.S. Coast and Geodetic Survey Serial* 602.

Jenny, W. P.: "Magnetic Methods," in "The Science of Petroleum," ed. by A. E. Dunstan, Vol. I, pp. 328–345, Oxford University Press, London.

Königsberger, J. G.: Natural Residual Magnetism of Eruptive Rocks, *Terr. Mag. Atmos. Elec.*, vol. 43, pp. 119–130, 299–320.

PART III
SEISMIC METHODS

CHAPTER XIII

FUNDAMENTAL PRINCIPLES

RELATION TO EARTHQUAKE SEISMOLOGY

The fundamental principles of the seismic method of ge physical exploration for oil are the same as those of the mu older science of seismology which has developed over many yea of study of natural earthquakes. Instruments for detecti and recording the tremors of the earth caused by natural forc have been used since around the middle of the last centur Careful study of the times of travel of the different types waves or phases, as recorded on these records, has led to t development of fairly definite theories of the constitution of t earth and of the propagation of elastic waves through it. fact, our most definite ideas of the nature and physical properti of the earth at great depths have been obtained from the analy of the travel times of earthquake shocks which have been trar mitted through the interior of the earth. As worked out frc such studies, the earth is now believed to consist of a qui definite series of concentric shells of material with differe elastic properties.[1]

Although the general theoretical background of seismic pro pecting has much in common with earthquake seismology, t nature of the seismic waves is somewhat different in the two cas This difference is principally in the period or frequency. Eart quake waves have periods ranging from a few seconds to as lo as 60 sec., but the waves used in seismic prospecting are of ve much shorter wave length with periods of the order of 0.01 to (sec. The fundamental principles of the instruments used ; generally the same, but the details of construction are grea different on account of the difference in the frequency to wh they are designed to respond. Also, of course, the instrume

[1] For an interesting diagram showing the shells and discontinuities wit the interior of the earth as derived from the study of seismic waves, Macelwane, 1936, p. 227.

used in seismic prospecting have to be designed with careful consideration of their portability and their use under exposed conditions in the field.

HISTORY OF SEISMIC PROSPECTING[1]

The first study of the effects of artificial disturbances at the surface of the earth was that of a few large accidental explosions which were recorded by earthquake seismographs. These records gave some idea of the velocity of propagation for comparatively near-surface elastic waves. Also some studies were made of the sound effects produced by such explosions which gave information on the transmission through the atmosphere of intense sound waves over long distances.

Apparently the earliest proposal for the application of artificial elastic waves to the study of comparatively near-surface characteristics of the materials of the earth's crust was made by the English seismologist Mallet as early as 1848. Measurements of velocity of transmission of artificial earth waves were published by Abbott in America in 1878. In 1888 Schmidt proposed the study of time-distance records of artificial disturbances to determine the variation of the speed of seismic waves with depth. In this country Fessenden[2] in 1913 conducted experiments and later obtained patents on a method of exploration that involved the principle of the seismic method.

During the first World War methods and apparatus for the location of big guns were developed in countries on both sides of the conflict, and soon after its close the same principles began to be actively applied to the study of geology. The Germans had attempted to use seismic detectors to locate the positions of big guns by recording the earth disturbance resulting from the recoil of the gun. In this country a considerable amount of experimentation was done, particularly at the Bureau of Standards, in the development of equipment and methods for the location of big guns by sound ranging. It is interesting that several men

---

[1] A detailed history of seismic prospecting is given by Mintrop, 1930. This publication (by Mintrop's Seismos Co.) contains much interesting historical material and patents, although it is prepared to support Mintrop's claims of originality in the practical application of refraction seismic prospecting.

[2] Fessenden. 1917.

(McCollum, Karcher, and Eckhardt) who were among the firs
to undertake active seismic prospecting development were a
engaged in this sound ranging work at the U.S. Bureau of Stanc
ards during the war.

Practical seismic exploration for the determination of geologi
structure started in a small way in Europe in about 1919, an
Mintrop's early patents[1] have been held as fundamental to th
prospecting art.   Early experiments were made by Eckhardt fc
the Marland Oil Company in Oklahoma as early as 1921; bt
the area chosen for this early work was complicated, and th
results did not appear satisfactory.   The real beginning of th
application of seismic prospecting for oil in the United State
was early in 1923 in the Gulf Coast.   About the same time som
work was done in Mexico and along the Balcones fault zone c
Texas.   The intensive application of refraction seismic prospect
ing followed the discovery in 1924 of several salt domes by th
German "Seismos" Company working for the Gulf Productio
Company.   Following that time and with the development c
"fan shooting" beginning in about 1926, a great many shallo'
salt domes were found by the refraction seismic method.

The "refraction" method, which was used for all this earl
seismograph work, uses shot-detector distances several time
greater than the depth explored.   It depends on the refractio
back to the surface of waves that have penetrated to some dis
tance below the surface.   The waves used are always the firs
to reach the detectors and travel by minimum time paths.   Th
"reflection" method depends on the recognition of waves tha
are reflected more or less vertically to detectors at relativel
short distances from the shot point and that arrive considerabl
later than the first disturbances of the detector.

In about 1930 the refraction seismic method began to fin
natural limitations in the Gulf Coast, as most of the shallo
domes were located and the deep ones did not show clearly k
this method, even though very large dynamite charges and lor
shot-detector distances were used.   At about the same time tl
beginnings of the successful application of reflection methods we:
made in Oklahoma where conditions were much more suitab
for their use than in the Gulf Coast.   This reflection wo1

[1] Mintrop, German Patent 371,963, Dec. 7, 1919; also reproduced (
English) in Mintrop, 1930, p. 37.

spread back into the Gulf Coast about two years later.   Since that time the reflection method has almost completely replaced the refraction method and has been applied in all parts of the world where extensive geologic exploration for oil has been conducted.

ELASTICITY

Seismic exploration depends fundamentally on the propagation of waves in elastic media.   To consider the processes involved it is necessary first to define the quantities that describe the elastic properties of matter on which the propagation of such waves depends.

We shall consider the elastic properties of rocks as if they were homogeneous and isotropic, for the theory of elasticity becomes much more complicated without these assumptions.   Although the rocks do not fit these specifications very closely, useful results can be achieved by considering them applicable to a first approximation.   In the practice of seismic exploration the discontinuities in the measured effects serve to indicate any departures from uniform conditions which, in turn, are interpreted in terms of the depth, nature, or attitude of geologic units below the surface.

THE ELASTIC CONSTANTS

The elastic properties of matter are described by certain elastic constants.   As ordinarily used and as applied to seismic prospecting, these constants are idealized for "perfectly elastic" bodies and for deformations within the "elastic limit."   In general, this involves the assumption that the displacements are small and that the body returns exactly to its original form or condition after the displacing force is removed.

Stress and strain are frequently used in discussion of elastic deformation and often loosely.   However, they have perfectly definite and very simple meanings.   "Stress" is the force (per unit area) associated with an elastic displacement.   "Strain" is the deformation (per unit length or per unit volume).   If a body is perfectly elastic, it behaves according to Hooke's law, and strain is proportional to stress.

Most of the elastic constants are measured or defined in terms of ratios of stress to strain produced.   The different constants are defined in terms of different kinds of force or stress (tension, compression, pressure, shear, etc.) and the resulting different

kinds of deformations produced. For homogeneous isotropic materials there are certain simple relations between the various elastic constants, as they all depend on the same fundamental properties of the material. The variety of constants used arises from certain mathematical conveniences in elastic theory, resulting when certain constants are used, and in the variety of ways in which the constants may be defined in terms of the experiments by which they are measured.

The commonly used elastic constants, for homogeneous isotropic media, and the relations between them are as follows:

Young's modulus (E) is a measure of the stress-strain ratio in simple tension or compression. The stress is the force per unit cross-sectional area (*i.e.*, F/A); the strain is the resulting elongation (for tension) or shortening (for compression) per unit length (*i.e.*, $\Delta L/L$). Therefore,

$$E = \frac{F/A}{\Delta L/L} = \frac{FL}{A\,\Delta L} \tag{164}$$

and has the dimensions of force per unit area ($ML^{-1}T^{-2}$) and is measured in dynes per square centimeter in the c.g.s. system (or in pounds per square inch in the English system). Its numerical value can be thought of as the force that would be required to stretch a unit cross section of material to double its length if it were still within its elastic limit. (Of course, there are few, if any, substances that actually can be stretched to twice their length and still be within their elastic limit.)

Bulk modulus (k) is a measure of the stress-strain ratio under simple hydrostatic pressure. The stress is the pressure (*i.e.*, force per unit area $= F/A$). The strain is the resulting fractional change in volume (*i.e.*, change in volume per unit volume $= \Delta V/V$). Therefore,

$$k = \frac{F/A}{\Delta V/V} = \frac{FV}{A\,\Delta V} \tag{165}$$

and also has the dimensions of force per unit area.

Rigidity, or shear modulus (n) is a measure of the stress-strain ratio for simple shear. A shearing force is tangential to the surface displaced (Fig. 98), and a shearing stress is such a force per unit area. The shearing strain is the resulting displacement without change of volume (as a pile of cards might be sheared by

sliding each one successively a slight distance over the next) and is measured by the displacement (ΔL) in the line of force per unit length L perpendicular to the line of force (Fig. 98).   Therefore,

$$n = \frac{F/A}{\Delta L/L} = \frac{FL}{A\,\Delta L} \qquad (166)$$

and also has the dimension of force per unit area.
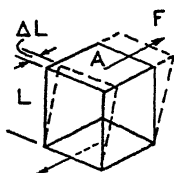
FIG. 98.—Shear stress and strain.

Poisson's ratio (σ) is not a measure of a stress-strain relation but is a measure of a geometric change of shape.   Suppose that a cylindrically shaped test piece (Fig. 99) of original length L is compressed elastically to a length $L - \Delta L$.   Its original diameter D will be increased to $D + \Delta D$.   (The changes are of the same magnitude but opposite in sign if the distorting force is a tension rather than a compression.)   Poisson's ratio is the ratio of the fractional change in length to the fractional change in diameter, or

$$= -\frac{\Delta D/D}{\Delta L/L} \qquad (167)$$

From its relation to other moduli [Eq. (169)], σ cannot have a value greater than $\frac{1}{2}$.   From general physical considerations, negative values of σ would not be expected, and such values have not been observed.   Therefore, practically, the value of σ is limited to the range 0 to $\frac{1}{2}$.   Its actual value is usually in the neighborhood of $\frac{1}{4}$.[1]

FIG. 99.—Change of shape in elastic compression to illustrate Poisson's ratio.

Lame's constants (λ and μ) are a pair of elastic constants which are mathematically convenient in the theory of elasticity.   The first of these is defined as

$$\lambda = \frac{\sigma E}{(1+\sigma)(1-2\sigma)} \qquad (168)$$

[1] From a molecular standpoint, the theoretical value of σ is $\frac{1}{4}$ (originally derived by Cauchy) if the forces acting between individual particles are central (*i.e.*, the forces are in the line between particles and depend only on the distance between them).

and has the same dimension as E. The second constant μ is identical with the shear modulus n defined above.

To define the elastic properties of a homogeneous, isotropic medium, two of the elastic moduli are required. The pairs used are (1) Bulk modulus k and shear modulus n; (2) Young's modulus E and Poisson's ratio σ; (3) Lame's constants λ and μ.

Relations among the Elastic Constants.—The interrelations among the various elastic constants are:[1]

$$k = \lambda + \frac{2}{3}\mu = \frac{E}{3(1-2\sigma)} \tag{169}$$

$$n = \mu = \frac{E}{2(1+\sigma)} \tag{170}$$

$$E = \frac{\mu(3\lambda + 2\mu)}{(\lambda + \mu)} = \frac{9kn}{3k+n} \tag{171}$$

$$\sigma = \frac{\lambda}{2(\lambda + \mu)} = \frac{3k-2n}{6k+2n} = \frac{E}{2\mu} - 1 \tag{172}$$

$$\lambda = k - \frac{2}{3}n = \frac{\sigma E}{(1+\sigma)(1-2\sigma)} \tag{173}$$

$$\mu = n = \frac{E}{2(1+\sigma)} \tag{174}$$

ELASTIC WAVES AND WAVE PROPAGATION

The theory of elasticity shows that a homogeneous, isotropic elastic medium can transmit two types of waves which have different speeds of propagation, depending on the elastic constants. These are:

Longitudinal (compressional), or primary, waves (P) for which the motions of the particles of the medium are parallel to the direction of propagation (like those of sound waves in air). The speed of propagation of longitudinal waves is

$$V_L = \sqrt{\frac{k + \frac{4}{3}n}{\rho}} = \sqrt{\frac{\lambda + 2\mu}{\rho}} = \sqrt{\frac{E}{\rho}\left(1 + \frac{2\sigma^2}{1 - \sigma - 2\sigma^2}\right)} \tag{175}$$

where ρ is the density of the wave-transmitting medium.

Transverse (shear), or secondary, waves (S) for which the motions of particles of the medium are perpendicular to the direc-

[1] Broughton Edge and Laby, 1931, p. 330.
Leet, 1938, p. 106.

tion of propagation (like waves on a vibrating string). The speed of propagation of transverse waves is

$$V_T = \sqrt{\frac{n}{\rho}} = \sqrt{\frac{E}{\rho} \frac{1}{2(1 + \sigma)}} \tag{176}$$

These longitudinal and transverse waves are termed "body waves" because they are transmitted through the body of the material. At a free boundary of the medium there may be surface waves of two types, both of which are characterized by a logarithmic decrease of amplitude with depth so that the wave energy is confined to a zone near the surface. These two types of waves are:

Rayleigh waves (R), which are waves at the free surface of a semi-infinite elastic solid. The motion is a sort of combination of longitudinal and transverse vibration giving rise to an elliptical motion of the particles. (The major axis of the ellipse is perpendicular to the surface and to the direction of propagation; the minor axis is parallel to the direction of propagation.) For the special case of $\sigma = \frac{1}{4}$, the velocity of Rayleigh waves is

$$V_R = 0.9194 \sqrt{\frac{\mu}{\rho}} \text{ *}$$

Love waves (L) are transverse waves propagated in a surface layer having elastic properties differing from those of an underlying semi-infinite elastic solid. The velocity of propagation of Love waves depends on the wave length and varies between that of transverse waves in the surface layer (which is approached as the wave length approaches zero) and that of transverse waves in the lower medium (which is approached as the wave length approaches infinity).

Velocity Ratios.—The ratio of velocities of longitudinal and transverse waves from Eqs. (175) and (176) is

$$\frac{V_L}{V_T} = \sqrt{\frac{k}{n} + \frac{4}{3}} = \sqrt{\frac{\lambda}{\mu} + 2} = \sqrt{\frac{1 - \sigma}{\frac{1}{2} - \sigma}} \tag{177}$$

Equation (177) shows that the velocity of longitudinal waves is always greater than that of transverse waves by an amount depending on the value of the elastic constants. The relation

* Macelwane, 1936, p. 120.

of the constant σ to the velocity ratio is, perhaps, the simplest to appreciate. For the special case of $\sigma = 0.25$ (which is commonly true approximately),

$$\frac{V_L}{V_T} = \sqrt{3} = 1.73$$

For other values of Poisson's ratio, the velocity ratios are

σ	0	0.1	0.2	0.3	0.4	0.5
V_L/V_T	1.41	1.50	1.63	1.87	2.45	∞

For the special case of $\sigma = \frac{1}{4}$, the ratios of the velocities of the three types of waves are

$$V_L : V_T : V_R = 1 : 1/\sqrt{3} : 0.9194/\sqrt{3} = 1 : 0.5773 : 0.5308.$$

Reflection and Refraction of Waves.—The basic principles controlling the propagation, reflection, and refraction of elastic waves are similar to those controlling light waves. For this reason certain terms reviewed here are more commonly associated with optical theory.

Reflection occurs whenever a wave encounters a discontinuity where there is a change in the physical properties of the wave-transmitting medium. The amount of wave energy reflected and its phase relative to the incident wave depend upon the contrast of the physical properties of the media on the two sides of the contact.

Refraction, or a change in direction of propagation, occurs whenever a wave crosses a boundary between wave-transmitting media of different physical properties (except when the wave path is normal to the boundary).

The geometry of the paths or "rays" along which elastic waves are propagated is governed by certain simple rules which have been developed in the study of the propagation of light and which need be reviewed only briefly here.[1]

Huygens' principle states that each point on an advancing wave front in an isotropic, homogeneous medium may be considered a new source of spherical waves. The wave front at any later time is the surface tangent to these new spherical waves.

[1] For geometrical constructions of wave fronts and rays, see Leet, 1938, pp. 108–117; Thornburgh, 1930.

Fermat's principle states that the ray (which is perpendicular to the wave front) reaching a given point from a given source has reached that point by a "minimum time" path between the source and the point. If the intervening medium contains parts having different rates of propagation, the path will, in general, not be straight but will be that which has the minimum over-all propagation time between the two points.

Snell's law is a consequence of Fermat's principle, although it was first found experimentally. This law states that a wave traversing the boundary between two media of velocity V_1 and V_2 (Fig. 100) is refracted in such a way that
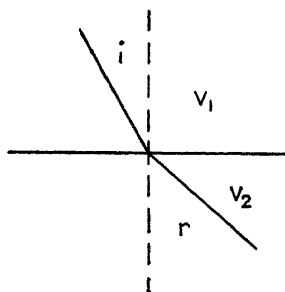
FIG. 100.—Angles of incidence and refraction.

$$\frac{\sin i}{\sin r} = \frac{V_1}{V_2} \qquad (178)$$

where i and r are the angles between the normal to the boundary and the rays in the media with velocities V_1 and V_2, respectively.

In a more general form, Snell's law can be stated as

$$\frac{\sin i}{V} = \text{const.} \qquad (179)$$

for any one ray path.

For a ray in a lower speed medium, striking a discontinuity at the contact with a higher speed medium, there is a certain critical angle of incidence which we shall designate as i_c, for which the angle of refraction r is 90 deg. and the refracted wave is then parallel to the surface of discontinuity. Since, for this case, $\sin r = 1$, it is evident from Snell's law that

$$\sin i_c = \frac{V_1}{V_2} \qquad (180)$$

For any angle of incidence greater than i_c, there can be no refracted ray in the second medium and therefore no penetration into that medium, and all the energy incident at such an angle is reflected. Thus, for incident angles greater than the critical angle we have *total reflection*.

Refraction and Reflection at Elastic Discontinuities.—In general, when a wave strikes a discontinuity where there is an abrupt change of elastic properties, four new waves will be set up. For instance, Fig. 101 shows an incident longitudinal wave P and the resulting reflected longitudinal wave PP_1, reflected transverse wave PS_1, refracted longitudinal wave PP_2, and refracted transverse wave PS_2. [The arrows parallel to the rays (——↔——) indicate longitudinal waves; those perpendicular to the rays (——↥——) indicate transverse waves.] A similar set of four
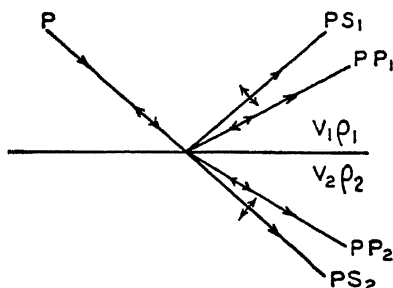
FIG. 101.—Refracted and reflected transverse and longitudinal waves.

waves (but at different angles) would be set up if the incident wave were transverse.

The division of energy between the different waves depends on the velocities and the densities of the two media (*i.e.*, $V_1\rho_1$ and $V_2\rho_2$) and on the angle between the incident wave and the surface of discontinuity. In general (for simple reflection) the proportion of reflected energy will be greater for greater differences in the elastic properties on the two sides of the discontinuity.[1]

In seismic prospecting we are nearly always concerned with the fastest waves and, therefore, with incident longitudinal waves P, reflected longitudinal waves PP_1, and refracted longitudinal waves PP_2. At the present stage of development of seismic prospecting, little, if any, use has been made of the transverse waves.

[1] For numerical values and curves of the amplitudes of reflected waves for various angles of incidence and for different velocity and density ratios, see Muskat, 1938. For extensive tables of reflection and transmission coefficients and their application to seismic prospecting, see Muskat and Meres, 1940*b* and 1940*a*.

ELASTIC CONSTANTS AND WAVE SPEEDS IN ROCKS

The property of rocks of prime importance in seismic prospecting is the speed of propagation of elastic waves and particularly of longitudinal waves. The variations of travel times of such waves, which are the primary quantity measured in seismic prospecting, are the expressions of wave speed changes or contrasts within the rocks. Thus, differences in wave speed are as fundamental to seismic prospecting as differences in density and magnetic polarization are to the gravitational and magnetic methods, respectively.

If rocks were simple, ideal elastic media, it would be possible to calculate the wave speeds from measurements of the elastic constants [see Eq. (175)]. However, it is usually found that measurements of wave speeds for large rock masses in place (by seismic field observations[1]) give speeds appreciably different from those computed from measured elastic constants of the same or similar rocks, and consistent speeds are not generally calculated from different possible combinations of measured elastic constants.[2] For seismic prospecting, the wave speeds are nearly always determined in the field, as will be discussed in some detail later (page 284).

It is evident from Eqs. (175) and (176) that the wave speed is proportional to the square root of the elasticity (*i.e.*, Young's modulus E) and inversely proportional to the square root of the density. From this it might be expected that heavy rocks would have low wave speeds. Usually, however, the reverse is true. It appears that the elasticity of rocks (E, k, or n) varies over a much wider range than the density, and the variations in wave speed are controlled much more by variations in elasticity than by those in density. Hard, well-cemented rocks have much higher speeds than loose, unconsolidated rocks.

Very commonly the wave speed increases with depth. This is particularly true when there are great thicknesses of rocks of rather similar lithology, such as the very thick deposits of sands

[1] Weatherby *et al.*, 1934.
Ewing *et al.*, 1934.
Leet and Ewing, 1932.
[2] Leet, 1938, p. 97.

and shales of the Gulf Coast and California. Apparently, the compaction and cementation under the influence of pressure and geologic time cause an increased amount of hardening of the deeper rocks which results in an increase of the elasticity and consequent increase of the wave speed. Even when strata of very different lithology are present, there is nearly always a general increase of wave speed with depth, although individual strata may have speeds lower than both overlying and underlying beds. It will be seen from Chap. XIV that this is indeed a fortunate circumstance of nature, for the increase of speed with depth causes refraction back to the surface of waves that have penetrated far into the geologic section and thereby makes refraction prospecting useful. If mother nature had been less considerate and wave speeds decreased with depth, there would be no refraction prospecting, but reflecting prospecting would still be possible in principle.

The determination of the actual wave speeds of the geologic section is usually one of the first projects that must be undertaken in beginning seismic prospecting in a new area. For accurate work, particularly precise reflection prospecting, more or less continuous determination of wave speeds and their variation within the area of a survey is necessary. Therefore, there is little utility in listing the speed of propagation or the elastic constants of a large number of rocks. The following short table is given only to show the order of magnitude of the wave speeds for a few general rock types and the wide range of speeds that may be encountered.[1]

Rock Type	Wave Speed for Longitudinal Waves, Feet per Second
Alluvium	1,000 to 2,000
Clay, sandy clay, etc	6,000 to 8,000
Shale	6,000 to 13,000
Sandstone	8,000 to 13,000
Limy sandstone	12,000 to 14,000
Rock salt	15,000 to 17,000

The following are approximate speeds of a few particular geologic units which have been determined in the course of seismic exploration.

[1] Selected and averaged from Reich, 1930, pp. 18 and 19.

	Feet per Second
Arbuckle limestone, Oklahoma............	21,000
Hunton limestone, Oklahoma............	17,000
Viola limestone, Oklahoma...............	18,000 to 19,000
Hogshooter limestone, Oklahoma.........	16,000 to 16,500
Selma chalk, Mississippi.................	14,000
Granite:	
Eastern Venezuela.....................	19,500
Oklahoma............................	17,000
New England.........................	16,500
Gulf Coast sediments:	
Near surface........................	5,500
2,000 ft. deep........................	6,500
4,000 ft. deep........................	7,500
6,000 ft. deep........................	8,500
8,000 ft. deep........................	9,500
Rock salt (in Texas Gulf Coast domes)...	15,100

CHAPTER XIV

THEORY OF REFRACTION SHOOTING

FIRST ARRIVALS

In the refraction method of seismic prospecting the quantity observed is the time between the initiation of the seismic wave by an explosion and the first disturbance indicated by a seismic detector at a measured distance from the shot point. Since first arrivals only are usually considered, the wave causing the disturbance is that which has traveled the minimum time path between shot point and detector. By observing first arrivals for a variety of shot detector distances, a time-distance curve can be constructed. First arrivals, of course, are evidences of the fastest traveling waves, and therefore refraction shooting is concerned only with longitudinal waves. The time-distance relations can be analyzed in terms of the variation with distance of minimum time paths. From these variations deductions can be made of the nature and depth of the elastic discontinuities required to account for the observed time-distance curves, and finally the elastic discontinuities may be interpreted in terms of the nature, depth, and attitude of geologic units below the surface.

As in gravitational and magnetic methods, the expected geophysical effects from assumed subsurface conditions can be calculated quite readily and will give the basis by which probable subsurface conditions can be inferred from observed effects. It is rarely, if ever, possible to solve the inverse problem directly and calculate a unique distribution of elastic properties from observed time-distance relations alone. Therefore, we shall first calculate the time-distance curves for several simple configurations of ideal elastic materials.

MINIMUM TIME REFRACTION PATHS

Let us consider that a circular wave, initiated by an explosion at point a (Fig. 102), spreads out uniformly in a homogeneous,

isotropic medium with velocity V_0 (for longitudinal waves). Let this medium be in contact with an underlying second medium with a higher velocity V_1. Waves striking this contact will, in general, be partially reflected back into the upper medium and partially refracted into the lower medium. In general, the refractions take place according to Snell's law [Eq. (178), page 240]; *i.e.*,

$$\frac{\sin i}{\sin r} = \frac{V_0}{V_1}$$

We are particularly interested in the ray at the critical angle i_c, for which the angle of refraction is 90 deg., so that $\sin r = 1$. This critical angle is defined [Eq. (180), page 240] by

$$\sin i_c = \frac{V_0}{V_1}$$

The wave refracted at the critical angle may be considered as a disturbance traveling along the surface of the velocity discon-
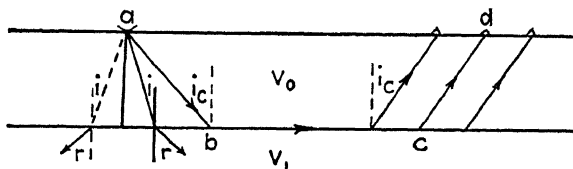
FIG. 102.—Refraction wave paths for a single horizontal velocity contrast.

tinuity, with the velocity of the lower medium. This disturbance, in turn, can be considered as setting up wavelets according to Huygens' principle (see page 239) at the lower boundary of the upper medium. From the velocity relations between the two media, the wave front of these disturbances initiated by these Huygens' wavelets advances in the upper medium along rays also at the critical angle i_c. Thus, wave energy may be considered as going down to the surface of discontinuity along a path ab, at the critical angle i_c, being refracted along that surface and finally being refracted back to the surface of the ground along paths such as cd, again at the same critical angle i_c. Also, it can be shown that this path $abcd$ is a minimum time path.

The process by which appreciable energy could be transmitted in this way is not evident from the simple geometric consideration of the refraction paths. This problem has been considered in

detail by Muskat,[1] and he shows, by an analysis based on wave theory, that a continuous reflection at the surface of the second layer is equivalent to the refraction path just outlined. It follows therefrom that the usual time-distance analysis, based on refraction paths such as those shown in Fig. 102, is quantitatively correct. Muskat's analysis has been extended by Wolf,[2] who calculated energy relations for waves along the various possible paths and found results quite consistent with prospecting experi-
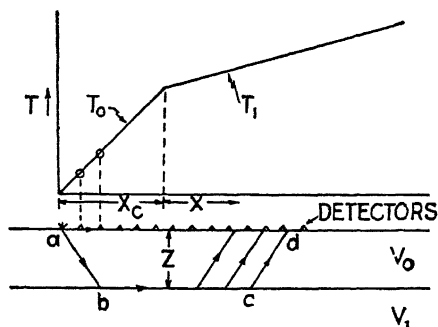
Fig. 103.—Minimum time path and time-distance curve for two layers.

ence.[3] If we accept these demonstrations mentioned as having established refraction paths such as those of Fig. 102 as the minimum time paths, and also that such paths can carry appreciable energy, we can use this geometrical configuration as the basis for the derivation of minimum time-distance curves for various configurations of elastic media.

SINGLE HORIZONTAL DISCONTINUITY

Consider now the special case of a single horizontal discontinuity at depth Z (Fig. 103) at which the velocity increases abruptly from V_0 above to V_1 below. Let there be a series of detectors along the ground surface from the shot point to a distant point. The first waves to reach a detector near the shot point travel horizontally in the upper medium at a velocity V_0 and arrive at a detector at a distance x at times

$$T_0 = \frac{x}{V_0} \tag{181}$$

[1] Muskat, 1933.

[2] Wolf, 1936.

[3] See also a summary of Muskat's and Wolf's work in Leet, 1938, pp. 125–127.

so that the time-distance curve starts out as a straight line through the origin with a slope $1/V_0$.

At a certain distance x_c, a wave that has been refracted along the discontinuity will reach the surface at the same time as one that has traveled the direct horizontal path, with velocity V_0. This occurs when the time gained by traveling the distance bc at the higher speed V_1 makes up for the time lost in going the slant distances ab and cd at the slower speed V_0. At all distances greater than this critical distance x, the wave refracted along the surface of V_1 reaches the earth's surface first and therefore constitutes the first arrival.

Let T_1 be the time required for a wave to traverse this refracted path. This time is

$$T_1 = \frac{ab}{V_0} + \frac{bc}{V_1} + \frac{cd}{V_0} \tag{182}$$

But, from the geometry of the figure,

$$ab = cd = \frac{Z}{\cos i}; \qquad bc = x - 2Z \tan i$$

Also, from Snell's law, the critical angle i_c is given by

$$\sin i_c = \frac{V_0}{V_1}$$

Substituting these quantities in Eq. (182),

$$\begin{aligned}
T_1 &= \frac{2Z}{V_0 \cos i} + \frac{x}{V_1} - \frac{2Z \tan i}{V_1} \\
&= \frac{x}{V_1} + \frac{2Z}{V_0 \cos i} - \frac{2Z \sin i}{V_1 \cos i} \\
&= \frac{x}{V_1} + \frac{2Z}{V_0 \cos i} - \frac{2Z \sin^2 i}{V_0 \cos i} \\
&= \frac{x}{V_1} + \frac{2Z}{V_0 \cos i} (1 - \sin^2 i) \\
&= \frac{x}{V_1} + \frac{2Z \cos i}{V_0} \tag{183}
\end{aligned}$$

From Eq. (183) it is evident the slope of the time-distance curve beyond the critical distance is $1/V_1$. Thus the presence of the subsurface discontinuity will be indicated by the discontinuity of the time-distance curve between the two segments (Fig. 103),

the first having a slope given by $1/V_0$; the second, a slope given by $1/V_1$.

Depth Calculation.—The time-distance curve permits the depth to the discontinuity to be calculated. Since the quantities measurable from the time-distance curve are t, x, V_0, and V_1, it is convenient to write the equation in terms of these quantities.

If we make a simple trigonometric diagram (Fig. 104) from the relation

$$\sin i_c = \frac{V_0}{V_1} \qquad (184)$$
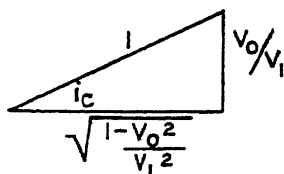
Fig. 104.—Velocity functions of the critical angle.

it is evident that the other trigonometric functions of i_c are

$$\cos i_c = \sqrt{1 - \frac{V_0^2}{V_1^2}} = \frac{1}{V_1}\sqrt{V_1^2 - V_0^2} \qquad (185)$$

$$\tan i_c = \frac{V_0/V_1}{1/V_1\sqrt{V_1^2 - V_0^2}} = \frac{V_0}{\sqrt{V_1^2 - V_0^2}} \qquad (186)$$

If we substitute $\cos i_c$ from Eq. (185) in Eq. (183),

$$T_1 = \frac{x}{V_1} + \frac{2Z\sqrt{V_1^2 - V_0^2}}{V_1 V_0} \qquad (187)$$

We can now calculate the depth Z in various ways, which are all equivalent, but under certain circumstances one or another may be more convenient.

From the Critical Distance.—At the critical distance x_c, $T_0 = T_1$, and therefore

$$\frac{x_c}{V_0} = \frac{x_c}{V_1} + \frac{2Z\sqrt{V_1^2 - V_0^2}}{V_1 V_0}$$

Solving for Z,

$$Z = \frac{x_c}{2}\left(\frac{1}{V_0} - \frac{1}{V_1}\right)\frac{V_1 V_0}{\sqrt{V_1^2 - V_0^2}}$$

$$= \frac{x_c}{2}\frac{V_1 - V_0}{\sqrt{V_1^2 - V_0^2}}$$

$$= \frac{x_c}{2}\sqrt{\frac{V_1 - V_0}{V_1 + V_0}} \qquad (188)$$

From the Intercept Time.—If we project the slope of the T_1 part of the time-distance curve back to zero distance (Fig. 105), the intercept time t_i, given by setting $x = 0$ in Eq. (187), is

$$t_i = \frac{2Z\sqrt{V_1^2 - V_0^2}}{V_1 V_0} \qquad (189)$$

from which

$$Z = \frac{t_i}{2}\frac{V_1 V_0}{\sqrt{V_1^2 - V_0^2}} \qquad (190)$$

Or, from Eq. (183),

$$Z = \frac{t_i}{2}\frac{V_0}{\cos i} \qquad (190a)$$

From a Point on the T_1 Part of the Curve.—If we simply solve Eq. (187) for Z, we have

$$Z = \frac{V_1 V_0}{2\sqrt{V_1^2 - V_0^2}}\left(T_1 - \frac{x}{V_1}\right) \qquad (191)$$
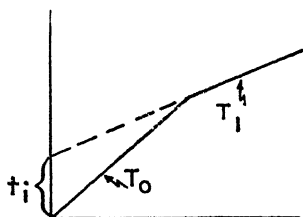
Fig. 105.—Intercept time for two layers.

THE DELAY TIME

We shall now consider the simple two-layer case from a slightly different viewpoint, because of its utility in deriving time-distance relations for other situations.

The "delay time"[1] for any segment of the ray trajectory is defined as the additional time for the wave to travel that segment over the time which would be required to travel the horizontal component of that segment at highest velocity reached by the trajectory. For example, referring to Fig. 106, the delay time associated with the segment ab of the wave path is the extra time required to travel the distance l at velocity V_0 over the time required to travel the distance S at velocity V_1. We shall call this time D_{01}. (The first subscript identifies the layer in which
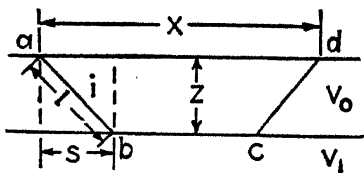
Fig. 106.—Notation for two-layer refraction path.

[1] Gardner, 1939b.

the delay occurs; the second, the layer with respect to which the delay is considered.)   Then

$$D_{01} = \frac{l}{V_0} - \frac{S}{V_1}$$

$$= \frac{Z}{V_0 \cos i} - \frac{Z \tan i}{V_1}$$

$$= \frac{Z}{V_0 \cos i} - \frac{Z \sin i}{V_1 \cos i}$$

$$= \frac{Z}{V_0 \cos i} - \frac{Z \sin^2 i}{V_0 \cos i}$$

$$= \frac{Z}{V_0 \cos i} (1 - \sin^2 i)$$

$$D_{01} = \frac{Z \cos i}{V_0} \tag{192}$$

or, writing $\cos i$ in terms of the velocities [Eq. (185)],

$$D_{01} = \frac{Z\sqrt{V_1^2 - V_0^2}}{V_0 V_1} \tag{193}$$

From this viewpoint we can write the time for a refracted wave path such as *abcd* (Fig. 106) as the time required to travel the distance x at speed V_1 plus the delay times for the two slant segments.   Thus,

$$T_1 = \frac{x}{V_1} + 2D_{01}$$

$$= \frac{x}{V_1} + \frac{2Z \cos i}{V_0} \tag{194}$$

which is the same as Eq. (183) derived directly from the times required for the different segments.

MULTIPLE LAYERS

Consider a geologic situation in which the strata consist of several horizontal layers of thicknesses Z_0, Z_1, Z_2, etc., of successively increasing velocities V_0, V_1, V_2, etc. (Fig. 107).   The paths of rays penetrating to various beds will be segments of straight lines, refracted at the discontinuities according to Snell's law.   We shall designate the angles as i_{mn}, the lengths of the various straight line segments as l_{mn}, and the delay times associated with these segments as D_{mn}, where, in each case, the first subscript refers to the layer in which the segment concerned

occurs and the second subscript refers to the highest speed pene-
trated by the wave path of which that segment is a part.

By Snell's law:

$$\sin i_{01} = \frac{V_0}{V_1}$$

$$\frac{\sin i_{02}}{\sin i_{12}} = \frac{V_0}{V_1}; \quad \text{but} \quad \sin i_{12} = \frac{V_1}{V_2}. \quad \therefore \sin i_{02} = \frac{V_0}{V_2}$$

$$\frac{\sin i_{03}}{\sin i_{13}} = \frac{V_0}{V_1}; \quad \frac{\sin i_{13}}{\sin i_{23}} = \frac{V_1}{V_2}; \quad \sin i_{23} = \frac{V_2}{V_3}$$

$$\therefore \sin i_{03} = \frac{V_0}{V_3}$$

and, in general,

$$\sin i_{mn} = \frac{V_m}{V_n} \tag{195}$$

which shows that the angle of the path in any bed is determined
by the wave speed in that bed and the speed in the fastest bed
penetrated and is independent of the speeds in intermediate beds.
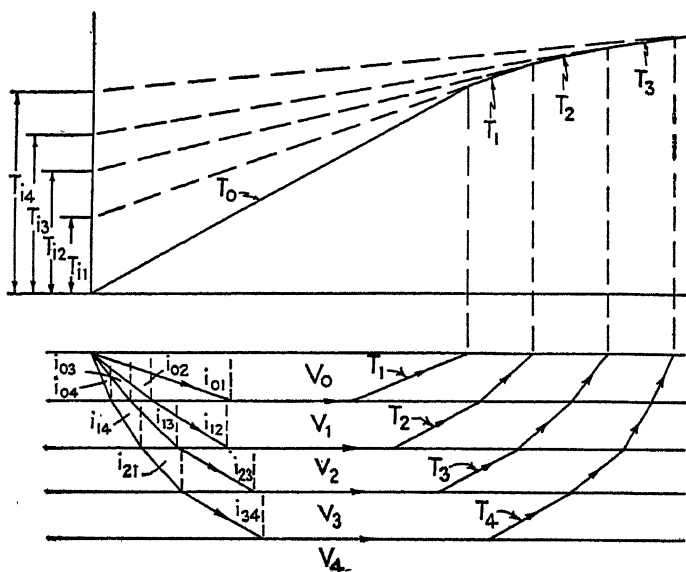
FIG. 107.—Refraction paths for multiple horizontal layers of successively
higher wave speeds and corresponding time-distance curves and intercept
times (schematic only).

We can write out the times for the various wave paths, in terms
of the delay times, as

$$T_0 = \frac{x}{V_0}$$

$$T_1 = \frac{x}{V_1} + 2D_{01}$$

$$T_2 = \frac{x}{V_2} + 2D_{02} + 2D_{12}$$

$$T_3 = \frac{x}{V_3} + 2D_{03} + 2D_{13} + 2D_{23}$$

$$\cdot \quad \cdot \quad \cdot \quad \cdot \quad \cdot$$

$$T_n = \frac{x}{V_n} + 2D_{0n} + 2D_{1n} + 2D_{2n} + \cdots + 2D_{(n-1)n}$$

$$(196)$$

The various delay times are [by Eq. (192)]

$$D_{01} = \frac{Z_0 \cos i_{01}}{V_0}, \text{ etc.}$$

or

$$D_{mn} = \frac{Z_m \cos i_{mn}}{V_m} \qquad . \qquad (197)$$

or they can be written directly in terms of the velocities [by Eq. (193)] as

$$D_{01} = \frac{Z_0\sqrt{V_1^2 - V_0^2}}{V_0 V_1}$$

$$D_{mn} = \frac{Z_m\sqrt{V_n^2 - V_m^2}}{V_m V_n} \qquad (198)$$

Thus, the general expression for the time of a ray penetrating to a layer n [*i.e.*, Eq. (196)] can be written on substituting delay times from Eq. (197) as

$$T_n = \frac{x}{V_n} + \frac{2Z_0 \cos i_{0n}}{V_0} + \frac{2Z_1 \cos i_{1n}}{V_1} + \frac{2Z_2 \cos i_{2n}}{V_2} +$$
$$\cdots + \frac{2Z_{n-1} \cos i_{n-1,n}}{V_{n-1}} \quad (199)$$

or, by substituting delay times in terms of velocities from Eq. (198), as

$$T_n = \frac{x}{V_n} + \frac{2Z_0\sqrt{V_n^2 - V_0^2}}{V_0 V_n} + \frac{2Z_1\sqrt{V_n^2 - V_1^2}}{V_1 V_n} + \frac{2Z_2\sqrt{V_n^2 - V_2^2}}{V_2 V_n} +$$
$$\cdots + \frac{2Z_{n-1}\sqrt{V_n^2 - V_{n-1}^2}}{V_{n-1} V_n} \quad (200)$$

Equation (199) or (200) represents one of a series of linear relations between t and x, each equation of the series representing the relationship for a particular segment of the time-distance curve associated with a given bed. If these segments of the time-distance curve are projected back to the zero-distance axis, they give the intercept times T_{i1}, T_{i2}, etc., as indicated (Fig. 107). These times given by putting $x = 0$ in Eqs. (196), are simply the sums of the delay times.

The thicknesses of the layers can be calculated by formulas similar to those for the simple two-layer case [Eqs. (188), (190), (191)]. Thus, the T_1 part of the time-distance curve can be solved for Z_0. This value is then substituted in the expression for the T_2 part of the curve, and it is solved for Z_1, etc. For example, using intercept times, Eq. (190),

$$Z_0 = \frac{T_{i1}}{2} \frac{V_1 V_0}{\sqrt{V_1^2 - V_0^2}} \tag{201}$$

Then, since

$$T_{i2} = 2D_{02} + 2D_{12}$$
$$= \frac{2Z_0\sqrt{V_2^2 - V_0^2}}{V_0 V_2} + \frac{2Z_1\sqrt{V_2^2 - V_1^2}}{V_1 V_2}$$

we can solve for Z_1 in terms of the previously determined value of Z_0 as

$$Z_1 = \left(T_{i2} - \frac{2Z_0\sqrt{V_2^2 - V_0^2}}{V_0 V_2} \right) \frac{V_1 V_2}{2\sqrt{V_2^2 - V_1^2}} \tag{202}$$

In general,

$$T_{in} = \frac{2Z_0\sqrt{V_n^2 - V_0^2}}{V_0 V_n} + \frac{2Z_1\sqrt{V_n^2 - V_1^2}}{V_1 V_n} + \cdots + \frac{2Z_{n-1}\sqrt{V_n^2 - V_{n-1}^2}}{V_{n-1} V_n} \tag{203}$$

which can be solved for the thickness of the last penetrated bed (Z_{n-1}) in terms of the thicknesses and speeds of the overlying beds, as

$$Z_{n-1} = \frac{V_{n-1} V_n}{2\sqrt{V_n^2 - V_{n-1}^2}} \left(T_{in} - \frac{2Z_0\sqrt{V_n^2 - V_0^2}}{V_0 V_n} - \frac{2Z_1\sqrt{V_n^2 - V_1^2}}{V_1 V_n} - \cdots - \frac{2Z_{n-2}\sqrt{V_n^2 - V_{n-2}^2}}{V_{n-2} V_n} \right) \tag{204}$$

Similar expressions can be written as extensions of the other depth formulas for the simple two-layer case.

These equations are deceivingly simple and, for actual use, calculation of depth by these methods must be strongly qualified. The equations are applicable only if each deeper bed is of higher speed than the one above. Also, the speeds and thicknesses must be such that there is a segment of the time-distance curve associated with each bed. Otherwise, a bed may be masked by shorter time paths coming from beds above and below; its presence may not be indicated by the first arrival time-distance curve at all; and therefore it will not be properly taken into account in the depth calculation. Also, the step-by-step calculation is not very accurate, as small errors in each step tend to multiply and accumulate in computing later steps to calculate depths to successively lower beds. For all these reasons, the calculation of depths by these methods is not very practicable except in areas of very regular and simple geologic situations where the sequence of speeds and thicknesses fulfills the rather special conditions required.

Mapping a "Marker" Bed.—A simple method of estimating variable depths to a high-speed marker bed under a series of substantially horizontal lower speed overlying beds has been described by Gardner.[1] It is based on the use of the delay time (or intercept time) but does not depend on the determination of velocities from the time-distance curve. Rather, a characteristic velocity distribution down to the bed followed and the velocity of the marker bed itself are determined by preliminary accessory measurements and may be used for calculating depths from observed time-distance relations throughout an area where similar geologic and velocity conditions prevail.

From Eq. (199) it is evident that for $x = 0$, t_n becomes the intercept time which is equal to the sum of the delay times (including two parts, *i.e.*, the "down" part at the shot end and the "up" part at the detector end of the wave trajectory). For a given area, over which geologic conditions are substantially constant, it is often possible to draw a standard curve giving the delay time in terms of the depth. This curve may be expressed as

[1] Gardner, 1939*a*.

$$D_z = \frac{Z_0 \cos i_{0n}}{V_0} + \frac{Z_1 \cos i_{1n}}{V_1} + \frac{Z_2 \cos i_{2n}}{V_2} + \cdot\cdot\cdot +$$
$$\frac{Z_{n-1} \cos i_{n-1,n}}{V_{n-1}} \quad (205)$$

which gives the delay time D_z associated with a depth Z which is the sums of the thickness Z_0, Z_1, Z_2 . . . Z_{n-1} of layers with corresponding velocities V_0, V_1, V_2 . . . V_{n-1} overlying a higher speed marker bed with velocity V_n. The curve of D_z versus Z can be plotted from the analysis of a continuous time-distance curve, and that curve may be used as long as the general geologic conditions remain substantially similar. Then, the intercept time t_i is the sum of the delay times $(D_z)_1$ and $(D_z)_2$ associated with the depths Z_1 and Z_2 to the marker bed at the shot and detector end, respectively, of the "spread." If the depth at one starting point is known or estimated, the depth at the detector[1] can be determined simply from the delay-time curve. In this way, depths can be carried on step by step from any one starting point as long as the geologic conditions remain substantially uniform. (See also the somewhat more detailed description of a similar process for the calculation of depth under beds with continuously varying speeds, page 265.)

CONTINUOUS VARIATION OF VELOCITY WITH DEPTH

In some areas there are so many changes in velocity that the time-distance curve is not a series of sudden discontinuities but is characterized by a gradual increase in the indicated velocity. Then it is a reasonable inference that the wave speeds in the rocks increase more or less gradually with depth. For instance, in the Gulf Coast and in parts of California, there are many thousands of feet of sediments that are practically all sands and shales of rather similar origin and mode of deposition. In a general way, the deeper parts of these deposits have higher seismic wave speeds, probably due in part to compaction under the weight of the overlying deposits and in part to increasing cementation or hardening with greater geologic age. In such cases, the wave speed gradually increases with depth. This causes a continuous

---

[1] The depths are actually displaced horizontally from the shot point and detector positions by the "offset distance" which, however, also is determinable from the thicknesses and velocities so that a curve of offset distance versus intercept time can be plotted for a given area.

refraction of the wave path into a curved path (which is concave upward when the velocity increases with depth). These relations are, qualitatively, those which would be anticipated from Fig. 107 if the layers were considered to become thinner and thinner until the series of sudden discontinuities became a gradual change in wave speed.

It has been shown that, theoretically, the velocity distribution can be derived from the time-distance function (under certain mathematical restrictions).[1] However, this may lead to rather
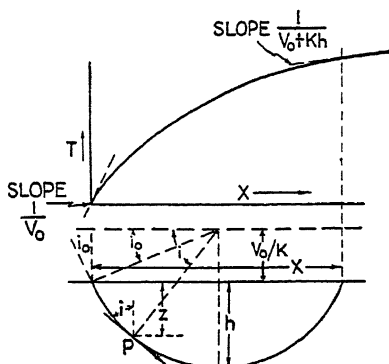
Fig. 108.—Continuous refraction wave paths and time-distance curve for linear increase of velocity with depth.

formidable mathematical difficulties. On the other hand, it is relatively simple to determine the time-distance curve from a given velocity distribution (*i.e.*, the variation of velocity with depth). The velocity distributions that have been analyzed in this way and that have had practical application in seismic prospecting are those in which the velocity is assumed to increase linearly with the depth and to increase exponentially with the depth.[2]

Uniform Increase of Velocity with Depth—In Fig. 108 let the speed at the surface of the ground be V_0, and let the speed increase with depth at the rate K,[3] so that the speed at any

[1] For a general statement of this problem and an outline of the method of solution, see, for instance, Muskat 1937.

[2] Slotnick, 1936, gives a general treatment and also works out the cases for linear and for exponential increase of velocity with depth.

[3] K may be expressed in feet per second per foot of depth or in meters per second per meter of depth (which would have the same numerical value, as K has the dimensions of 1/sec.).

depth z is

$$V = V_0 + Kz \qquad (206)$$

Let P be a point at depth z on a wave trajectory for which h is the maximum depth of penetration (*i.e.*, the depth at which the wave path becomes horizontal). Also, let i be the angle of the trajectory at the point P. Let the maximum speed at the bottom of the trajectory be V_m. Then, from Snell's law,

$$\sin i = \frac{V}{V_m} = \frac{V_0 + Kz}{V_m} = \frac{(V_0/K) + z}{V_m/K} \qquad (207)$$

From the geometry of the figure it is evident that this relation is satisfied if the wave path is a circle of radius

$$\rho = \frac{V_m}{K} \qquad (208)$$

and with its center on the line

$$z = -\frac{V_0}{K} \qquad (209)$$

and conversely. Thus, all the wave paths are segments of circles centered at a height V_0/K above the surface.

If the total horizontal length of the path (*i.e.*, the shot-detector distance) is x, it is evident that the radius of the path also may be written as

$$\rho = \sqrt{\left(\frac{x}{2}\right)^2 + \left(\frac{V_0}{K}\right)^2} \qquad (210)$$

The maximum depth of penetration is

$$h = \rho - \frac{V_0}{K} = \sqrt{\left(\frac{x}{2}\right)^2 + \left(\frac{V_0}{K}\right)^2} - \frac{V_0}{K} \qquad (211)$$

The speed at the bottom of the path is

$$\begin{aligned}
V_m &= V_0 + Kh \\
&= V_0 + K\left[\sqrt{\left(\frac{x}{2}\right)^2 + \left(\frac{V_0}{K}\right)^2} - \frac{V_0}{K}\right] \\
&= \sqrt{\frac{K^2 x^2}{4} + V_0^2} \qquad (212)
\end{aligned}$$

The time required for a wave to travel the circular path is

$$T = 2 \int_0^h \frac{dz}{V \cos i} = 2 \int_0^h \frac{dz}{(V_0 + Kz)\sqrt{1 - \left[\frac{(V_0 + Kz)^2}{V_m^2}\right]}}$$

$$= \frac{2}{K} \cosh^{-1} \frac{V_m}{V_0}* \quad (213)$$

But, from Eq. (212),

$$V_m = V_0 \sqrt{\left(\frac{Kx}{2V_0}\right)^2 + 1}$$

$$\frac{V_m}{V_0} = \sqrt{\left(\frac{Kx}{2V_0}\right)^2 + 1}$$

So that

$$T = \frac{2}{K} \cosh^{-1} \sqrt{\left(\frac{Kx}{2V_0}\right)^2 + 1}$$

$$= \frac{2}{K} \sinh^{-1} \frac{Kx}{2V_0} † \quad (214)$$

The time required for the wave to travel a segment of the circular path from the shot point to any other point on the path with coordinates x and z (with origin at the shot point) is

$$T = \frac{1}{K} \cosh^{-1} \left[\frac{K^2(x^2 + z^2)}{2V_0(V_0 + Kz)} + 1 \right]‡ \quad (215)$$

Since all the wave paths are circles, there can be constructed an orthogonal system of equal time circles (Fig. 109) centered at a variable depth λ, on a vertical line below the shot point and with a radius r, both of which are determined by the time and the constants of the material. These circles give the wave front

---

* The integration to give Eq. (213) comes from the integral formula

$$\int \frac{dy}{y\sqrt{1 - (y^2/a^2)}} = - \cosh^{-1} \left|\frac{a}{y}\right|$$

where $y^2 < a^2$.

†The functions sinh, cosh, sinh⁻¹, cosh⁻¹ are the hyperbolic sines and cosines and inverse hyperbolic sines and cosines, respectively. Numerical values of these functions are given in tables similar to the more familiar tables of the circular functions sine and cosine.

‡ For a derivation of Eqs. (215), (216), and (217), see Appendix, p. 355.
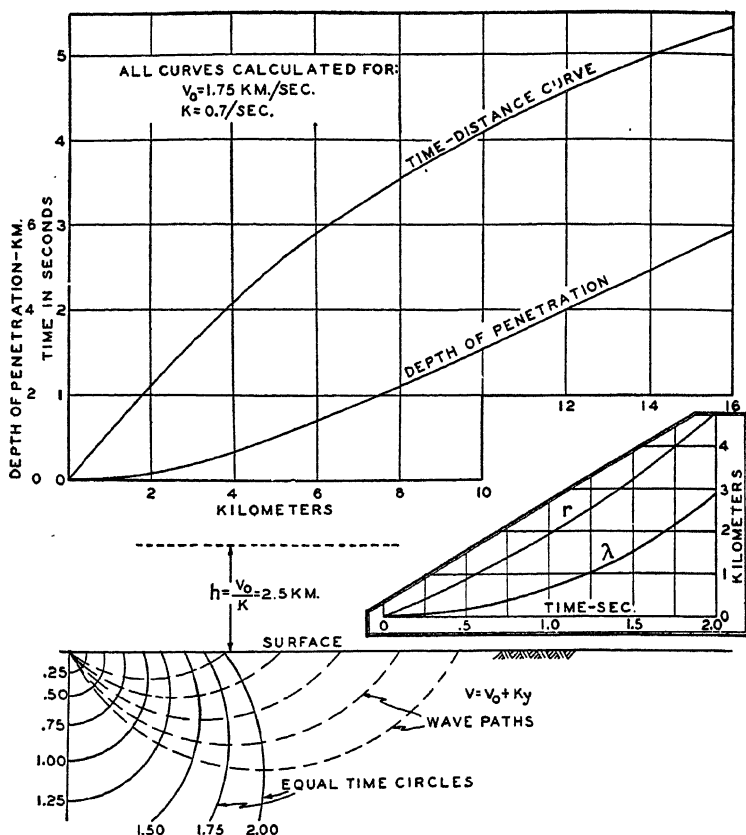
Fig. 109.—Wave paths and equal time circles for continuous refraction in medium with linear increase of velocity with depth. Upper curves show corresponding time-distance curve and depth of penetration. Insert shows curves for the determination of centers and radii of equal time circles [Eqs. (216) and (217)].

at the time for which they are calculated. The parameters λ and r of these equal time circles are

$$\lambda = \left(\frac{V_0}{K}\right)(\cosh KT - 1)* \tag{216}$$

$$r = \left(\frac{V_0}{K}\right)(\sinh KT)* \tag{217}$$

If we substitute a value, say, of $T = 1$ in Eqs. (216) and (217), we have the depth below the shot point λ, and the radius r of a circle which gives the locus of points on a wave front at a time

* For a derivation of Eqs. (215), (216,) and (217), see Appendix p. 355

1 sec. after the shot. By calculating a chart with a series of equal time circles, calculated for a regularly increasing series of times, it is a simple matter to read off the times required for a wave to travel any part or segment of its circular path.

As an example of the application of curved path theory, the following constants are approximately those which give a fairly close approximation to observed time-distance curves in the Gulf Coast.

$$V_0 = 5,500 \text{ ft./sec.}$$
$$K = 0.5 \text{ sec.}^{-1}$$

For these figures,

$$h = \frac{V_0}{K} = 11,000 \text{ ft.}$$

The penetration h and velocity at the bottom of the wave trajectory for various shot-detector distances calculated from these constants by Eqs. (211) and (212) are given in the following table:

x, ft.	h, ft.	$V_{max.}$, ft./sec.	Penetration (h/x), per cent
5,000	240	5,620	5
10,000	1,080	5,940	11
15,000	2,300	6,650	15
20,000	3,870	7,440	19
30,000	7,600	9,300	25
40,000	11,830	11,420	30
50,000	16,300	13,650	33

Experience with long-line refraction shooting in the Gulf Coast indicates that the penetration expected from these calculations may not be realized and that there is relatively little gain in penetration after shot-detector distances of around 7 or 8 miles are used. This probably is caused by a decrease in the rate of increase of velocity with depth (*i.e.*, K is not truly constant but decreases in value at great depth). In fact, some refraction time-distance curves indicate a nearly constant velocity or a relatively high-speed bed beneath which refractions are not obtained at depths greater than 8,000 to 10,000 ft.

High-speed Layer Underlying Variable-speed Section.—A condition sometimes approximated by actual geologic situations is that of a continuous increase of velocity to a discontinuity,

below which the speed is relatively high.   This condition may
exist where a continuous series of sands and shales is deposited
on a granite floor or over a
massive limestone.   In such
cases, the problem arises of cal-
culating the depth to the dis-
continuity from the refraction
time-distance curve.

The situation is indicated by
Fig. 110, which shows an upper
section in which the velocity
increases with depth at the uni-
form rate K, which is underlaid
at a depth Z by material with
velocity V_h.   To a distance x_0

Fig. 110.—Notation for calculation
of delay time for continuous refrac-
tion with linear increase of velocity
with depth.

(Fig. 113) the time-distance relation is the usual curve for linear
increase of speed with depth.   Beyond this distance, first arrivals
are waves refracted along the surface of the high-speed bed with
its velocity V_h.

The minimum time condition requires that the angle of inci-
dence i_h (Fig. 110) must be the critical angle.   The velocity in
the upper medium at the discontinuity is $V_0 + KZ$ where Z is
the depth of the discontinuity, and therefore

$$\sin i_h = \frac{V_0 + KZ}{V_h} \tag{218}$$

Also, since $\sin i / V$ is constant for the entire trajectory,

$$\sin i = \frac{V_0 + Kz}{V_h} \tag{219}$$

where i is the angle of the trajectory at any depth z (Fig. 110).
The time required for the wave to travel the curved path OP is

$$
\begin{aligned}
T &= \int_0^Z \frac{dz}{V \cos i} = \int_0^Z \frac{dz}{(V_0 + Kz)(1 - \sin^2 i)^{1/2}} \\
&= \int_0^Z \frac{dz}{(V_0 + Kz)\{1 - [(V_0 + Kz)^2/V_h^2]\}^{1/2}} \\
&= \frac{1}{K}\left[\cosh^{-1}\frac{V_h}{V_0} - \cosh^{-1}\frac{V_h}{V_0 + KZ}\right]^* \tag{220}
\end{aligned}
$$

* The integration to give Eq. (220) follows from the same integral formula
given in footnote *, p. 259.

Now, the delay time associated with the path OP is the excess time required to travel this path over that required to travel the corresponding horizontal distance S (Fig. 110) at the speed V_h.   Therefore, this delay time is

$$D_z = T - \frac{S}{V_h} \tag{221}$$

From Fig. 110,

$$x = R \cos i_0$$
$$x - S = R \cos i_h$$
$$Z_0 = R \sin i_0$$

Then

$$S = x - R \cos i_h$$
$$= R(\cos i_0 - \cos i_h)$$
$$= \frac{Z_0}{\sin i_0} (\cos i_0 - \cos i_h)$$

Substituting $\sin i_0$, $\cos i_0$, $\cos i_h$ in terms of velocities, and since $Z_0 = V_0/K$,

$$S = \frac{1}{K} \{ \sqrt{V_h^2 - V_0^2} - \sqrt{V_h^2 - (V_0 + KZ)^2} \} \tag{222}$$

Substituting from Eqs. (220) and (222) in (221), the delay time is given by

$$D_z = \frac{1}{K} \left[\cosh^{-1} \frac{V_h}{V_0} - \cosh^{-1} \frac{V_h}{V_0 + KZ} - \sqrt{1 - \left(\frac{V_0}{V_h}\right)^2} + \sqrt{1 - \left(\frac{V_0 + KZ}{V_h}\right)^2} \right] \tag{223}$$

From this equation and with a table of hyperbolic functions, values of the delay time may be computed, and a curve plotted giving D_z as a function of Z for given values of the three constants V_0, V_h, and K.

This calculation can be facilitated by using an auxiliary function χ, defined as

$$\chi(r) = \cosh^{-1} \left(\frac{1}{r}\right) - \sqrt{1 - r^2} \tag{224}$$

In terms of this function, Eq. (223) may be written

$$D_z = \frac{1}{K} \left[\chi\left(\frac{V_0}{V_h}\right) - \chi\left(\frac{V_0 + KZ}{V_h}\right) \right] \tag{225}$$

A general curve of the function χ is shown by Fig. 111. The values for any special delay time curves for given values of K, V_0, and V_h can be read off from the general curve so that the calculation with the hyperbolic function needs to be made only in constructing the curve for the χ function.

A curve calculated in this way for $V_0 = 5,500$ ft. per sec., $K = 0.5$ sec.$^{-1}$, and $V_h = 15,000$ ft. per second is given in
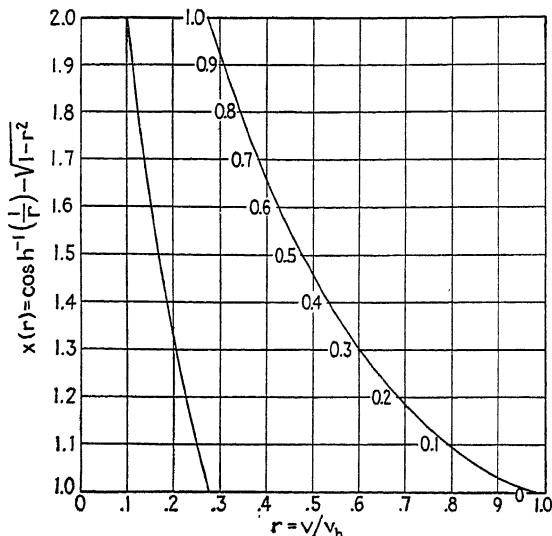
Fig. 111.—Auxiliary function χ for calculation of delay time for continuous refraction with linear increase of velocity with depth.

Fig. 112. (These values of V_0 and K are the same as used for calculating the table, page 261.)

The foregoing derivation assumes that the surface of the high-speed bed is horizontal, and errors will be introduced if substantial dips are present. However, for practical purposes, the approximation is quite satisfactory if departures from the horizontal are less than about 10 deg.[1] The intercept time[2] t_i (Fig.

[1] Gardner, 1939b, p. 5.
[2] It should be noted that the velocity used in projecting the arrival time back to zero time to determine the intercept time must be the true velocity of the high-speed bed which has been determined by shooting "up dip" and "down dip" (see p. 269) and not the apparent velocity indicated by the time-distance curve. Otherwise, any slope of the high-speed bed will give an erroneous apparent velocity and therefore a false intercept time.

113) is the sum of the delay times D_1 and D_2 associated with the depths Z_1 and Z_2 to the high-speed bed near[1] the shot and detector ends, respectively, of the "spread."
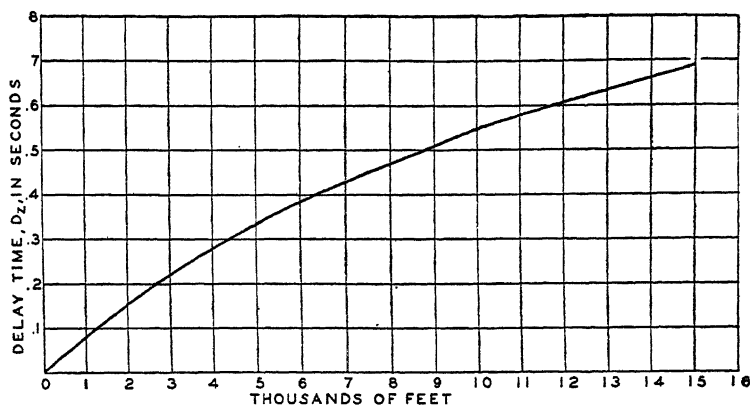
FIG. 112.—Example of delay-time curve for $V_0 = 5,500$ ft./sec. $V_h = 15,000$ ft./sec., $K = 0.5$ sec.$^{-1}$.

This time can be calculated readily (rather than being determined graphically from a plot such as Fig. 113) for

$$t_i = T - \frac{x}{V_h} \qquad (226)$$

where T is the total time to a point at distance x, and V_h is the true velocity of the marker bed. If the depth to the marker bed near one end is known (say, from a well), that near the other can be computed readily from a curve such as Fig. 112. Suppose that in an area where the geologic situation gives the constants used for calculating this curve, the intercept time t_i, for example, is 0.685 sec. and that the depth to the high-speed bed at the offset
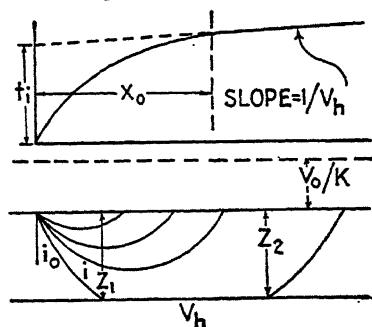
FIG. 113.—Wave paths and time-distance curve for a high-speed layer underlying a section with wave speed increasing linearly with depth.

[1] The position at which the depth is calculated is not under the shotpoint or detector position but is "offset" by the distance S (Fig. 110). The amount of this offset distance can be determined by plotting, from Eq. (222), a curve for S as a function of Z for the values of the constants K, V_0, and V_h which are being used for the area.

distance from the shot point is known to be 5,500 ft. From the curve, the delay time D_1 for a depth of 5,500 ft. is 0.358 sec. The delay time associated with the unknown depth Z_2 must be $0.685 - 0.358 = 0.327$ sec. From the same curve, the depth Z_2 is then read off as 4,850 ft.

SURFACES NOT HORIZONTAL

All the situations considered above have assumed the wave source (shot point) and the seismic detector to be on a plane surface and the velocity discontinuities to be along planes
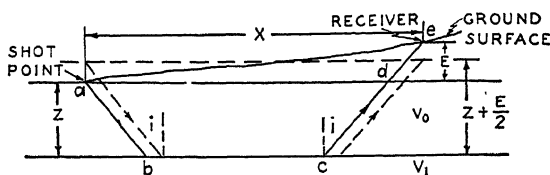
Fig. 114.—Shot and receiver at different elevations.

parallel with that surface. This condition, however, is not ordinarily met in practice. Therefore, it is usually necessary to make allowance in the travel times to take care of differences in elevations of the shot point and detector or of any slope of the refracting beds.

Shot Point and Detector at Different Elevations.—Let the receiver be at a height E (Fig. 114) above the shot point. The time for a wave traveling the path *abcde* is the same as for one traveling the path *abcd* plus the additional time for the path *de*. This path *de* contributes a delay time

$$D_{01} = \frac{E \cos i}{V_0}$$

and the total time will be that for the simple two-layer case [Eq. (183) or (194)] plus this added time or will be

$$T_1 = \frac{x}{V_1} + \frac{2Z \cos i}{V_0} + \frac{E \cos i}{V_0}$$
$$= \frac{x}{V_1} + (2Z + E) \frac{\cos i}{V_0} \qquad (227)$$

Thus the time is the same as if shot point and detector were at the average elevation of the two, for which the equivalent path with this same time would be that shown by the dotted lines of

Fig. 114. The depth from this mean elevation to the high-speed bed will be $Z + (E/2)$. Thus, the depth can be determined just as in the case where shot point and detector are level except that the depth must be figured from the mean elevation of the two ends of the path considered.

Sloping Beds. *Shooting Down Dip.*—Consider next the case in which the velocity discontinuity is assumed to be dipping at an angle θ with the horizontal. Consider first the case in which the slope is downward from the shot point toward the detector. This case is like that just considered for shot point and recorder at different elevations except that x is now measured along the
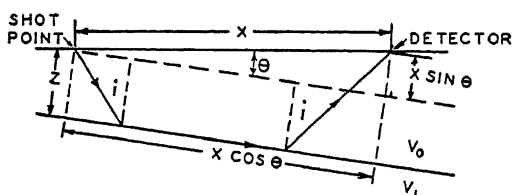
FIG. 115.—Inclined bed. Shooting down dip.

surface of the ground and the distance parallel to the sloping surface is $x \cos \theta$. Also, Z is measured perpendicular to the sloping bed (Fig. 115). The distance corresponding to the difference in elevation becomes $x \sin \theta$. With these substitutions, Eq. (227) becomes

$$T_1 = \frac{x \cos \theta}{V_1} + \frac{(2Z + x \sin \theta) \cos i}{V_0} \tag{228}$$

Substituting $1/V_1 = \sin i/V_0$,

$$
\begin{aligned}
T_1 &= \frac{2Z \cos i}{V_0} + \frac{x \cos \theta \sin i}{V_0} + \frac{x \sin \theta \cos i}{V_0} \\
&= \frac{2Z \cos i}{V_0} + \frac{x}{V_0} (\cos \theta \sin i + \sin \theta \cos i) \\
&= \frac{2Z \cos i}{V_0} + \frac{x}{V_0} \sin (i + \theta) \tag{229}
\end{aligned}
$$

The slope of the T_1 segment of the time-distance curve is now

$$S_- = \frac{\sin (i + \theta)}{V_0} = \frac{\sin (i + \theta)}{V_1 \sin i} \tag{230}$$

Thus, the apparent velocity indicated by the slope of this curve is $V_1[\sin i/\sin (i + \theta)]$ and is lower than the true velocity V_1 of the high-speed bed by the factor $\sin i/\sin (i + \theta)$.

Shooting Up Dip.—For shooting up dip, it is evident from Fig. 116 that the expression for the time becomes
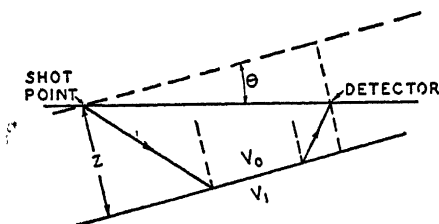
Fig. 116.—Inclined bed. Shooting up dip.

$$T_1 = \frac{x \cos \theta}{V_1} + \frac{(2Z - x \sin \theta) \cos i}{V_0} \tag{231}$$

$$= \frac{2Z \cos i}{V_0} + \frac{x}{V_0} (\cos \theta \sin i - \sin \theta \cos i)$$

$$= \frac{2Z \cos i}{V_0} + \frac{x}{V_0} \sin (i - \theta) \tag{232}$$

The slope of the T_1 segment of the curve is now

Fig. 117.—Time-distance curves for sloping beds.

$$S_+ = \frac{\sin (i - \theta)}{V_0} = \frac{\sin (i - \theta)}{V_1 \sin i} \tag{233}$$

and the apparent velocity indicated by the slope of the curve is $V_1[\sin i/\sin (i - \theta)]$ and is greater than the true velocity V_1 of the high-speed bed by the ratio $\sin i/\sin (i - \theta)$.

Determination of Dip.—From the foregoing, it is evident that from a single seismic profile and the corresponding time-distance curve we cannot separate the effects of dip and of velocity. However, if profiles are shot in opposite directions (Fig. 117), it is possible to separate the dip from the velocity, for from Eqs. (230) and (233), respectively,

$$i + \theta = \sin^{-1} V_0 S_-$$
$$i - \theta = \sin^{-1} V_0 S_+$$

Then, by adding and subtracting these two equations,

$$i = \frac{\sin^{-1} V_0 S_- + \sin^{-1} V_0 S_+}{2} \tag{234}$$

$$\theta = \frac{\sin^{-1} V_0 S_- - \sin^{-1} V_0 S_+}{2} \tag{235}$$

The variation of the apparent velocity or slope with the true velocities and dip may be shown as follows [from Eqs. (230) and (233)]:

$$\sin i \cos \theta + \cos i \sin \theta = V_0 S_-$$
$$\sin i \cos \theta - \cos i \sin \theta = V_0 S_+$$

Adding,

$$2 \sin i \cos \theta = V_0(S_- + S_+)$$
$$\frac{\sin i}{V_0} = \frac{S_- + S_+}{2 \cos \theta}$$

But, since $V_0/\sin i = V_1$, we have

$$V_1 = \frac{2 \cos \theta}{S_- + S_+} = \frac{2}{S_- + S_+} \tag{236}$$

approximately for small θ. From this, it is evident that to a first approximation the true velocity V_1 can be determined as the reciprocal of the average slope of the time-distance curves from shooting up dip and down dip. The error made in this approximation is proportional to the cosine of the dip angle θ, and for angles less than 10 deg. the error is less than 1.5 per cent.

The relations between the slope of the time-distance curve and the angle of dip for various velocity ratios are shown by the curves of Fig. 118. The derivation of these curves is as follows: From Eq. (230)

$$S_- = \frac{\sin (i + \theta)}{V_0} = \frac{\sin i \cos \theta + \cos i \sin \theta}{V_0}$$

Putting $\sin i$ and $\cos i$ in terms of velocities [Eqs. (184) and (185)],

$$S_- = \frac{1}{V_0}\left(\frac{V_0}{V_1} \cos \theta + \sqrt{\frac{V_1^2 - V_0^2}{V_1^2}} \sin \theta\right)$$
$$= \frac{1}{V_0}\left(\frac{V_0}{V_1} \cos \theta + \sqrt{1 - \frac{V_0^2}{V_1^2}} \sin \theta\right)$$

Now, let $V_0/V_1 = r =$ ratio of velocities in upper and lower media. Then

$$S_- = \frac{1}{rV_1} (r \cos \theta + \sqrt{1 - r^2} \sin \theta)$$

$$V_1 S_- = \cos \theta + \frac{\sqrt{1 - r^2}}{r} \sin \theta$$

and, since $V_1 = 1/S$, where S is the slope corresponding to the true velocity in the lower medium,

$$\frac{S_-}{S} = \cos \theta + \frac{\sqrt{1 - r^2}}{r} \sin \theta \qquad (237)$$

Similarly,

$$\frac{S_+}{S} = \cos \theta - \frac{\sqrt{1 - r^2}}{r} \sin \theta \qquad (238)$$

Equations (237) and (238) are plotted in Fig. 118. These curves, then, show the ratio of the slope of the time-distance
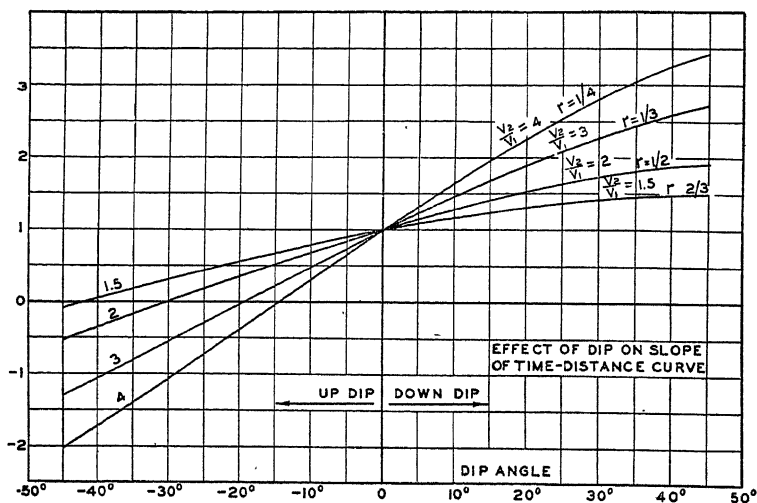
Fig. 118.—Variation of apparent velocity with dip for a single velocity contrast with different ratios of the two velocities. Ordinates are ratio of slope of time-distance curve to that for a flat bed. Up-dip values are $\frac{S_+}{S}$; down-dip are $\frac{S_-}{S}$.

curve for various dip angles to the slope that would be obtained for flat beds. The different curves are calculated for various ratios of the two velocities V_0 and V_1. The negative values of

S_+/S on the up-dip side of the curve correspond to negative slopes of the time-distance curves, which means that first arrivals at more distant points come in earlier than those at nearer points.

Determination of Depth.—Depths can be calculated for the sloping beds by formulas similar to those used for horizontal beds [Eqs. (188), (190), (191)].

From the Critical Distance.—At the critical distance (or break in the slope of the time-distance curve) for the down-dip case:

$$\frac{x_0}{V_0} = \frac{2Z \cos i}{V_0} + \frac{x_0}{V_0} \sin (i + \theta)$$

$$2Z = \left\{\frac{x_0}{V_0} [1 - \sin (i + \theta)]\right\} \frac{V_0}{\cos i} = \frac{x_0}{\cos i} [1 - \sin (i + \theta)] \quad (239)$$

This Z is the distance from shot point perpendicular to the surface of the velocity contrast. The vertical distance h (between shot point and the velocity discontinuity) is $h = Z/\cos \theta$, so that

$$h = \frac{x_0[1 - \sin (i + \theta)]^*}{2 \cos \theta \cos i} \quad (240)$$

For shooting up dip, a similar analysis gives

$$h = x_0 \frac{[1 - \sin (i - \theta)]}{2 \cos \theta \cos i} \quad (240a)$$

From the Intercept Time.—The intercept time t_i, for $x = 0$, is, for either down-dip or up-dip shooting,

$$t_i = \frac{2Z \cos i}{V_0}$$

From which, as for horizontal beds,

$$2Z = \frac{t_i V_0}{\cos i}$$

and

$$h = \frac{t_i V_0}{2 \cos \theta \cos i} \quad (241)$$

From a Point on the T_1 Part of the Curve.—For shooting down dip [from Eq. (229)],

$$T_1 = \frac{2Z \cos i}{V_0} + \frac{x}{V_0} \sin (i + \theta)$$

* Barton, 1929, p. 585.

Solving for Z,

$$2Z = \left[T_1 - \frac{x \sin (i + \theta)}{V_0} \right] \frac{V_0}{\cos i}$$

$$Z = \frac{T_1 V_0}{2 \cos i} - \frac{x \sin (i + \theta)}{2 \cos i}$$

$$h = \frac{Z}{\cos \theta} = \frac{T_1 V_0}{2 \cos i \cos \theta} - \frac{x \sin (i + \theta)}{2 \cos i \cos \theta} \qquad (242)$$

Similarly, for shooting up dip,

$$h = \frac{T_1 V_0}{2 \cos i \cos \theta} - \frac{x \sin (i - \theta)}{2 \cos i \cos \theta} \qquad (243)$$

Faulted Beds.—Consider the case of the high-speed bed broken off by a fault. First, consider the bed broken down indefinitely (Fig. 119). The first part of the time-distance curve (to the distance x_n) will be the same as for the ordinary two-layer case. Beyond x_n, rays will reach the surface by the dotted paths indicated, and it is evident that at large distances they will again have time differences corresponding to the velocity V_0.

Fig. 119.—Fault with large displacement and corresponding time-distance curve.

Therefore, beyond x_n, the slope of the curve will gradually increase to a value $1/V_0$. The time to a point on this part of the curve is

$$T_1' = \frac{Z \cos i}{V_0} + \frac{S}{V_1} + \frac{\sqrt{(x - S)^2 + Z^2}}{V_0} \qquad (244)$$

If the point x_n at which the change of slope occurs can be determined, the distance S to the trace of the fault can be calculated, for

$$S = x_n - Z \tan i \qquad (245)$$

If the high-speed bed is faulted down by a definite amount Z_2 (Fig. 120), the wave paths and time-distance curve will be as shown. It is evident that the first part will be as in Fig. 119; but at greater distance waves that have traveled paths like *abcde* will be the first arrivals, and there will be a second break

in the time-distance curve. For the case where Z_2 is small compared with the horizontal elements of the diagram, we may consider that the time for the path bc is approximately the same as
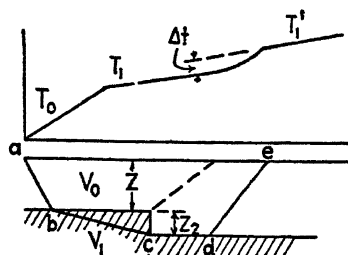
FIG. 120.—Fault with finite displacement and corresponding time-distance curve for shot point on upthrow side of fault.
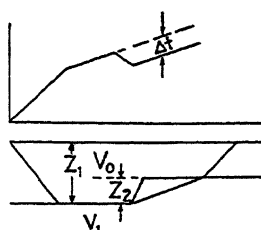
FIG. 121.—Fault with finite displacement and corresponding time-distance curve for shot point on downthrow side of fault.

if this were the horizontal distance. With this approximation,

$$T_1' = \frac{Z_1 \cos i}{V_0} + \frac{(Z_1 + Z_2) \cos i}{V_0} + \frac{x}{V_1} \qquad (246)$$

The stepup in the time-distance curve caused by the displacement Z_2 can be expressed as

$$\Delta t = T_1' - T_1$$

and, since

$$T_1 = \frac{2Z_1 \cos i}{V_0} + \frac{x}{V_1}$$

$$\Delta t = \frac{Z_2 \cos i}{V_0}$$

and the displacement is

$$Z_2 = \frac{\Delta t V_0}{\cos i} = \Delta t \frac{V_0 V_1}{\sqrt{V_1^2 - V_0^2}} \qquad (247)$$

If the shot point is on the downthrow side, and the detector on the upthrow side, the time-distance curve will have a downward break (Fig. 121), and the time will be given by

$$T_1' = \frac{Z_1 \cos i}{V_0} + \frac{(Z_1 - Z_2) \cos i}{V_0} + \frac{x}{V_1} \qquad (248)$$

The displacement (Z_2) can be calculated from the stepdown in time Δt by Eq. (247) as before.

METHODS OF OPERATION

A variety of arrangements of shot points and detectors are used for refraction shooting, depending on the objective of the survey and the general subsurface conditions in the area covered. The different shooting patterns have been developed in attempts to get the most rapid and economical coverage of an area consistent with obtaining the required subsurface information.

Profile Shooting.—As the name implies, this system uses profiles of detectors, usually in a line through the shot point. A profile may consist of a shot point and a series of detector
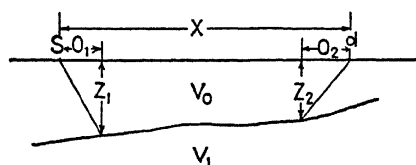
Fig. 122.—Profile shooting.

positions over a wide range of distances to give a more or less complete time-distance curve. Also, it may consist of a series of shots at various distances from a given spread of detector positions. However, for routine work, it is not necessary to shoot complete profiles, as only a small segment of a time-distance curve is sufficient to determine the depth to a high-speed marker bed as long as the speed of the marker and the speed distribution in the overlying beds are substantially constant. The shot may be fired to a comparatively small group of detectors placed at a distance from the shot point that is approximately the optimum for the speeds and the range of depth in a given area. As the work proceeds, the entire arrangement of shot-point and detector spread is moved forward step by step along the profile under which depths are being mapped. An occasional complete time-distance curve, shot with reversed control to permit speed determination, may be used to determine and check the velocity values.

For a simple two-layer case, the time of a first arrival refracted from the lower high-speed bed depends on the sum of the depths to the discontinuity below the shot point and the detector.

Thus, the time for a first arrival at d, from shot point S, which has penetrated V_1 (Fig. 122) is

$$T_1 = \frac{x}{V_1} + D_1 + D_2$$

where D_1 and D_2 are the delay times associated with the depths Z_1 and Z_2, respectively. Therefore with the assumption of $\cos \theta = 1$ (where θ is the angle of dip of the interface between V_0 and V_1),

$$T_1 = \frac{x}{V_1} + (Z_1 + Z_2) \frac{\cos i}{V_0} \qquad (249)$$

Thus, for each point on the T_1 part of the time-distance curve, we can calculate $Z_1 + Z_2$. The values for Z_1 and Z_2 are not directly under the shot and detector positions but are at the "offset" distances O_1 and O_2, respectively (Fig. 122), given by

$$O_1 = Z_1 \tan i; \qquad O_2 = Z_2 \tan i \qquad (250)$$

If a survey is started from a point where Z is known (say, from a continuous profile shot in both directions or from a well), then depths can be carried by shooting only small segments of the complete time-distance curve, as long as the velocities are constant.

Arc Shooting.—Arc shooting is a modification of profile shooting which is designed to reduce the two variables Z_1 and Z_2 [Eq. (249)] to one by keeping one of them constant.[1] The detectors d_n are set out approximately on the arc of a circle (Fig. 123), and the corresponding shot points are set on the arc of a smaller circle[2] the radius of which is approximately the offset distance [Eq. (250) or (222)]. By this arrangement, the depth Z_1 of Fig. 123 is common to all the detector positions. If the shot-detector distances are all equal, the times of first arrivals for waves that have penetrated V_1 would be the same if the beds

---

[1] The arc method apparently was invented by J. H. Jones of the Anglo Persian Oil Company and was applied in southwest Persia. For a description and theory of the method, see Jones, 1933.

[2] This modification of arc shooting suggested by Gardner, 1939a, 1939b, was designed to increase the accuracy of Jones's original method which used a single shot location for the entire arc. Gardner's modification is somewhat more expensive in the field, but the use of a single shot point will lead to errors if there are significant variations in depth around the inner circle.

were horizontal. Then, the differences in these times will be a measure of the differences in depth to the refracting surface. (Actually, it is not necessary that the shot-detector distances be uniform, as corrections for moderate variations of these distances can be made readily.) The depth differences calculated apply to points O_1, O_n, etc., which are inside the detector circle by the offset distance, as indicated by the dashed circle. If the velocities are known and the central depth (Z_1) has been determined, the depths under the various points O_n can be calculated from the delay times [intercept times of Eq. (226)]. An approximate picture of the general configuration of the refracting surface can be obtained by simply mapping the first arrival times (corrected for irregularities of shot-detector distances) at detectors d_n and drawing equal time contours or "isochron" lines. If several arcs are set out intersecting one

FIG. 123.—Arc shooting. Gardner modification of Jones's method.
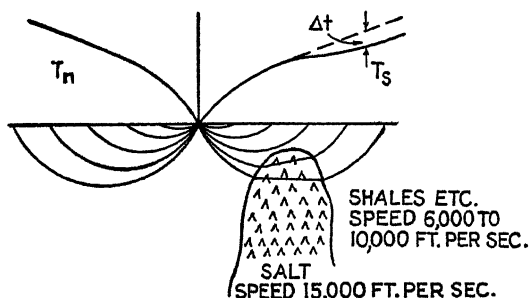
FIG. 124.—Refraction shooting for salt domes. Wave paths and time-distance curves on left for a normal profile; on right for a profile including a salt dome.

another or if their centers are connected by a continuous profile, it is possible to map the depth of the refracting surface quite definitely.[1]

[1] Gardner, 1939a.

The arc shooting method is particularly useful as a reconnaissance method of exploration in open country, as it gives quite definite information on depths to a velocity discontinuity and covers a wide area with a comparatively limited amount of
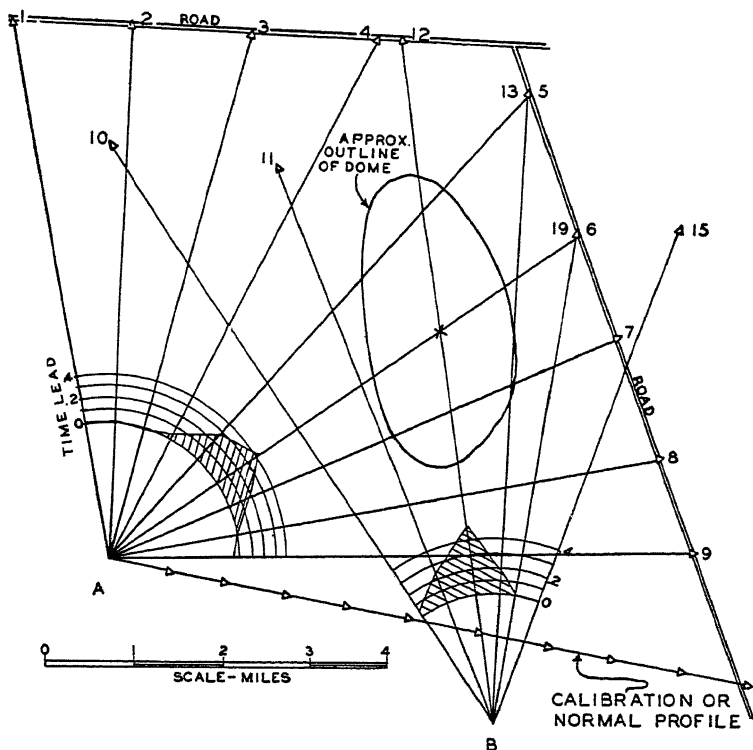
Fig. 125.—Fan shooting map, showing locations of two shot points (*A* and *B*) and corresponding detector locations. Circles about shot points show scale for indicating time "leads." Shaded areas show magnitudes of time leads corresponding to a dome in the approximate position indicated.

shooting. It may have difficulty if surface conditions are irregular or where work has to be confined to roads, for then it may not be feasible to lay out the regular array of detector spreads required.

Fan Shooting.—Fan shooting is a type of operation that was developed in shooting for salt domes in the Texas and Louisiana Gulf Coast. The objective of this work was only to locate and roughly define relatively shallow salt domes.

A salt dome consists of a mass of rock salt intruded into the surrounding sediments. The wave speed in the salt is much greater than that in the sediments. Thus, a dome forms a more or less cylindrical mass of material with a speed considerably higher than that of the surrounding material.

Consider a time-distance curve for a profile passing through a dome and one passing through the normal sequence of sediments
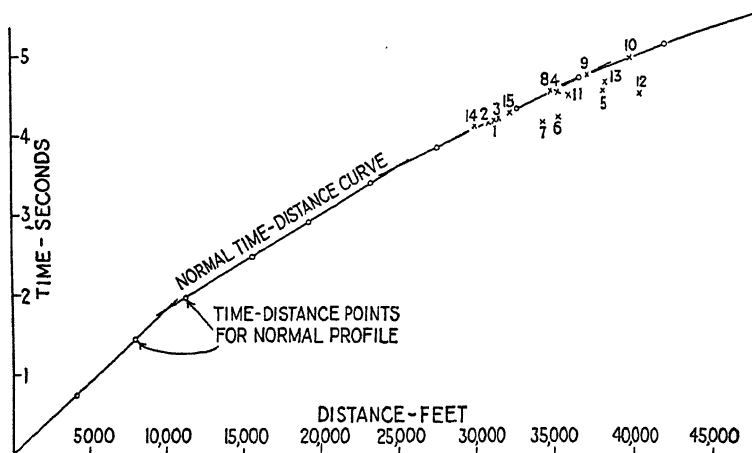
Fig. 126.—Time-distance relations for fan shooting. The line shows a "normal" curve of time versus distance for the normal sedimentary section in the area being investigated. Points below the line indicate "fast" first arrivals of waves that have penetrated a dome. Numbers correspond with numbered detector positions of Fig. 125.

(Fig. 124). The normal time-distance curve T_n is a smooth curve. The curve T_s, for the profile including a dome, is lower for wave paths that have included the dome, for such waves arrive at less than normal time owing to the higher wave speed for that part of the path in the salt. This shortening of time (Δt of Fig. 124) is called the "time lead." In an area where salt domes are expected, any wave reaching a detector at less than the normal time for the shot-detector distance is a possible dome indication, and thus a single shot and detector position might be indicative of a dome. Therefore, the practice in searching for domes is to lay out a "fan" of detectors from a single shot point (Fig. 125). The times of arrival at these detectors are plotted against detector distances and compared with a "normal" curve. The normal time-distance curve, determined from a continuous

profile laid out to be in a normal area (not including any domes), serves as a "calibration curve" for all areas having the same wave speed characteristics. The time leads, read as the differences from the normal curve, of which Fig. 126 is an actual example, are plotted from a zero circle of arbitrary radius about the shot point with a suitable time scale to indicate for each line of the fan the amount by which the first arrival time departs from normal (Fig. 125). If definite time leads are found, the presence of a dome is indicated, but its exact position is not determined, as there is no way to tell the distance along the fan line from the shot point at which the dome lies. Therefore, to locate it more definitely, a "cross fan" is shot and similarly mapped. The intersection of the fan lines having the greatest leads gives the approximate position of the center of the dome. The spread of fans showing leads indicates the approximate horizontal dimensions of the dome.

Literally thousands of such fans were shot in the Gulf Coast of Texas and Louisiana between about 1926[1] and 1930. In the earlier work fan lines were up to 5 or 6 miles long with shots of up to a few hundred pounds of dynamite in shallow holes drilled with hand augers. In the later work, in the search for deeper domes, fan spreads were increased to a maximum of about 10 miles with shots of up to 2,000 lb. of dynamite in holes drilled to around 200 ft. deep. The deeper holes had the advantage of using the dynamite more effectively and also did not blow out craters in the ground and make serious surface disturbances which often led to substantial damage claims.

---

[1] The first prospecting in the Gulf Coast was done by profiles. It was a year or more before the advantages of fan shooting were appreciated and its technique developed. For a description of early field operations, see Barton, 1929.

CHAPTER XV

REFLECTION SHOOTING

THE REFLECTION SEISMOGRAPH METHOD

The underlying principle of the reflection method of geophysical prospecting is as simple as that of calculating the distance of, say, a wall by the time required for an echo to be reflected back from the wall and the speed of propagation of sound waves. The vastly greater technical difficulty in the application of this simple principle to underground investigations arises from the complex nature of the wave-transmitting medium and the difficulty of recognizing a true reflection among the complex motions of the ground surface following the explosion that initiates the elastic wave system.

The active development of the reflection method began in the Gulf Coast when the limitations of refraction shooting for deep domes began to become apparent. The refraction method and especially the fan shooting technique is inherently better adapted to detection of relatively steeply dipping velocity contrasts and is not suitable for the detection of deep domes or structures over deeper domes where the dips of the velocity contrasts are quite small.

Apparently the first serious attempts at reflection prospecting were made in about 1929 in the Gulf Coast.[1] This early work in the Gulf Coast was not very successful. More or less simultaneously, reflection prospecting was tried in Oklahoma where geologic conditions are more favorable. The method was more successful there and became quite well established by about 1931. Then reflection work was tried again in the Gulf Coast, advantage being taken of the experience and improvements of technique gained from the work in Oklahoma, and became fairly successful.

The favorable geologic conditions in Oklahoma and the definite and useful results led to a very rapid application of the reflection method. The number of parties working in that state alone

[1] Rosaire and Adler, 1934.

has been as high as nearly 50. Later improvements in instruments and field technique have made the method applicable to a wide variety of geologic conditions so that reflection seismograph work is now being done with more or less regular success in practically all the actual and recognized prospective oil-producing areas of the world.

At the present time the reflection seismograph is by far the most widely used of all of the geophysical methods for the prospecting for oil. It is estimated that of some 275 to 300 geophysical field units active in the United States (1938), approximately 75 per cent are reflection seismograph parties. Since the average cost of operation of a reflection party is greater than that of the other methods, the percentage of expenditures for this method is even higher and is estimated to be between 85 and 90 per cent of the total outlay for geophysical field work by the oil industry.

What is the reason for this great preference for the reflection method in spite of its much greater cost over that of gravitational and magnetic methods? The answer is that when the method works well, it gives an actual subsurface map of some geological horizon which may be quite near or even actually at that from which oil may be expected. Next to the actual detection of oil itself, the mapping of the oil-producing horizon is about as much as any oil geologist can reasonably expect.

FIELD METHODS

The essential difference between the reflection and refraction methods is in the disposition of the detectors with respect to the shot point. In refraction work the detectors are at distances from the shot point that are several times the depth of the beds being mapped, so that shot-detector distances are commonly several miles, and only minimum time, or "first arrival," events are used. In the reflection method shot-detector distances are a fraction of the depth of the beds being mapped, and later events on the records are used. A series of detectors is usually set in a line passing through the shot point, and the total spread from the shot point to the farthest detector is usually less than ½ mile and is commonly of the order of 1,000 ft. The various detectors are connected through amplifiers (which are usually selective in the frequency that they amplify or transmit) to oscillographs and

a recorder. In this way, records of the ground movement at the various detectors are made side by side on the same photographic tape.

Consider the various wave paths that would be recorded for a continuous series of detectors disposed as in Fig. 127. The first waves to reach the detectors will be those traveling essentially horizontally with the velocity V_0 that will give a first arrival curve with a slope $1/V_0$. Other waves, however, will travel
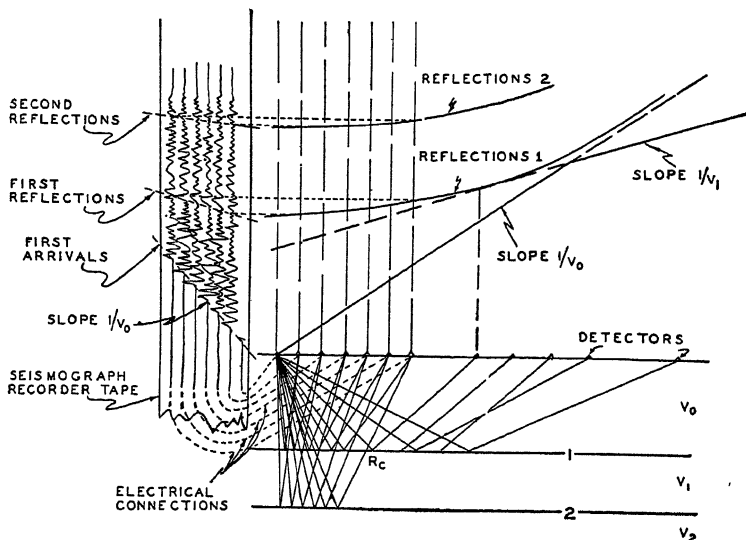
Fig. 127.—Reflection paths to detectors within the critical distance and refraction paths to detectors at greater distance and the corresponding time-distance relations. The schematic reflection record at the left indicates the first arrivals and reflection events as recorded in reflection prospecting.

more or less vertically downward, and some of the elastic wave energy will be reflected at the surface (1) where there is a discontinuity between the velocities V_0 and V_1. The time of arrival of these reflected waves back at the detectors is indicated by the curve "reflections 1." Beyond the reflection point R_c, corresponding to the angle of total reflection, the reflections become refractions, so that at detector positions corresponding to reflections from this point the reflection curve is tangent to the time-distance curve for the second velocity, as indicated by the dotted projection of the line with the slope $1/V_1$. For very great distances the reflection time will approach that for beds traveling horizontally in the medium V_0, and therefore the reflection curve

will approach asymptotically the dotted projection of the line with the slope $1/V_0$.

The corresponding records and different wave arrivals on the seismograph recorder tape are indicated by the hypothetical reflection record at the left of the diagram. The slope of the first arrivals across the tape corresponds to the velocity V_0. The reflections will arrive at the tape at much more nearly the same time than do the first arrivals; but the reflection time-distance curve is not perfectly flat, for there are differences in the lengths of wave paths to the different detectors, because of the different "angularity" by which the paths depart from the vertical. Therefore, the waves reaching more distant detectors travel successively longer paths so that these reflection arrivals cross the tape at a slight angle. If there are reflections from a deeper velocity contrast, such as layer 2, they will arrive later on the record as indicated by the curve "reflections 2." For these reflections the differences in the lengths of the wave paths to the different detectors are smaller than for the shallower reflection, so that these reflections will reach the detectors at more nearly the same time and the reflection arrivals cross the tape at a smaller angle.

The purpose of having several detectors in a line is to be able to recognize the reflections. On any single trace there are so many waves and irregularities that it is not possible to tell which are true reflections and which are disturbances of another kind However, when the various traces on the record show a series of disturbances of similar character at nearly the same time and the times are consistent with the slopes across the record that are characteristic of true reflections, they serve to identify the disturbance as a real reflection and not as some other irregularity. The principal difficulty in the interpretation of reflection shooting results is to be able to recognize reflections on records that may be very badly disturbed and have a great many other irregularities on them.

DEPTH COMPUTATIONS FOR REFLECTION SHOOTING

The reflection record always carries a series of timing lines or marks (usually lines entirely across the record at intervals of 0.01 or 0.005 sec.). Also, the instant of explosion is always shown by a "shot-moment" break of some kind. Therefore,

when a reflection is marked, it is a straightforward matter to read from the record the time from the instant of explosion to the event marked.   Times are usually read to 0.001 sec.

Once the reflections have been identified and marked on a reflection record and the proper corrections to the observed times
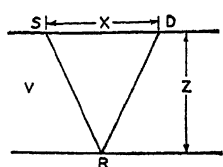
Fig. 128.—Simple reflection path.

(*i.e.*, weathering corrections, etc., as described in Chap. XVI) have been made, the calculation of the depth of the reflecting horizon is quite simple.   For the simple case of a level surface, level reflecting horizon, and uniform velocity (Fig. 128), the travel time for a wave from shot point S to reflection point R and back to detector D is

$$t = 2\frac{SR}{V}$$

$$= \frac{2}{V}\sqrt{\left(\frac{x}{2}\right)^2 + Z^2} \tag{251}$$

$$V^2 t^2 = x^2 + 4Z^2 \tag{252}$$

$$Z = \frac{1}{2}\sqrt{V^2 t^2 - x^2} \tag{253}$$

Usually the depth Z is read off from a chart[1] plotted from Eq. (253) with a given value for V and with different lines on the chart, corresponding to the usual distances to the different detectors, as set out in the field.   Frequently, such charts include a variation of the average velocity with depth, which means that different values for V are used in calculating different parts of the chart.

VELOCITY DETERMINATIONS

The calculation of reflection depths depends fundamentally on a previous determination of the average vertical velocity to the depth of the reflecting horizon.   The different methods used for obtaining this velocity are as follows:

From a Reflection Time-distance Curve.—From Eq. (252) above we may write

$$t^2 = \frac{x^2}{V^2} + \frac{4Z^2}{V^2} \tag{254}$$

[1] Pirson, 1937.

From this equation, it is evident that if we plot t^2 versus x^2 (Fig. 129), we should have a straight line with a slope $1/V^2$ and an intercept $4Z^2/V^2$. Thus, the slope of such a curve should give the velocity. This method, however, is not very accurate, particularly if the detector spread is short or the depth is large, because the slope depends on such very small time differences which are difficult to read accurately from the record. Also, any slope of the reflecting horizon will affect the apparent velocity,

and therefore the "spread" of detectors should be shot from both ends so that any slope can be detected by a difference in the apparent velocity and allowed for (by simple averaging if the difference is small) in computing the velocity. Serious errors will be introduced if the reflecting surface is appreciably curved, and these will not be indicated by reversed shooting.
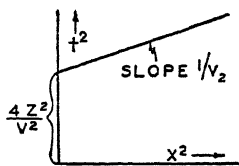
FIG. 129.—t^2 vs. x^2 curve for determining velocity from reflection times.

Shooting at a Well.—Under favorable circumstances the velocity may be determined by correlating reflections with definite geologic horizons as known from a well. A reflection spread is shot preferably with the well near the center of the spread. From the measured travel times of the reflections and the depth to the corresponding reflecting beds, as shown by the drilling, the average velocity can be computed. The success of the method depends upon the ability to correlate definitely reflections on the record with geologic markers at known depths. This may be possible when the section contains very definite lithological discontinuities and has been used fairly successfully in Oklahoma. When several such discontinuities are present, the correlation of them with reflections may be made more certain because the reflections should have time intervals spaced approximately according to the depth spacing of the beds. Where definite heavy limestones are present in a thick shale section and clear reflections result, this method may give quite satisfactory velocity information.

Shooting in a Well.—The best method of determining vertical velocity is to measure it directly by recording the times from shots fired at the surface to a detector at different depths in a well (or in some cases from shots fired in a well to detectors at the surface). This determines directly the quantity desired, *i.e.*,

the vertical travel time and, therefore, the average velocity to a given depth. Special detectors for lowering into wells have been developed and used extensively for such velocity determinations. There are certain cooperative projects among different oil companies and prospecting companies whereby arrangements are made for velocity shooting in dry holes before they are abandoned or in other wells, the resulting information being distributed to the various cooperating companies. In this way a rather extensive body of information on vertical velocities has been secured.

Example of Well Shooting. An example of the field procedure, data, and results of an actual well-shooting survey will illustrate the details of the process. The example chosen is from an area where the geologic section includes materials of very different lithologic character, which have marked effects on the seismic wave speed.

The arrangement of well, shot hole, detector, etc., is shown schematically in Fig. 130, the dimensions being those of the actual survey. The times measured are those for a wave traveling the minimum time path from shot to detector. In the calculations, it is assumed that this path is a straight line. The observed data and calculations of average and interval velocities is shown in the table on page 287.

FIG. 130.—Determination of velocity by shooting in a well.

Depth of detector below shot	Observed time, sec.	Vertical time, sec.	Average vertical velocity, ft./sec.	Vertical detector interval, ft.	Vertical time interval, sec.	Interval velocity, ft./sec.
345	0.068	0.039	8,850			
				532	0.039	13,600
877	0.090	0.078	11,240			
				445	0.031	14,400
1,322	0.117	0.109	12,130			
				515	0.034	15,200
1,837	0.148	0.143	12,850			
				495	0.036	13,800
2,332	0.183	0.179	13,030			
				530	0.035	15,100
2,862	0.217	0.214	13,370			
				488	0.028	17,400
3,350	0.245	0.242	13,840			
				522	0.027	19,300
3,872	0.271	0.269	14,390			
				380	0.019	20,000
4,252	0.290	0.288	14,760			
				363	0.021	17,300
4,615	0.311	0.309	14,940			
				135	0.009	15,000
4,750	0.320	0.318	14,940			
				502	0.040	12,600
5,252	0.360	0.358	14,670			
				423	0.031	13,600
5,675	0.391	0.389	14,590			
				410	0.033	12,400
6,085	0.423	0.422	14,420			
				520	0.028	18,600
6,605	0.451	0.450	14,680			
				630	0.036	17,500
7,235	0.487	0.486	14,890			
				710	0.033	21,500
7,945	0.520	0.519	15,310			

In making the calculation, it is assumed that the wave path is a straight line from shot to detector. The observed time (column 2) multiplied by the cosine of the angle between the wave path and the vertical gives the vertical time (column 3) which is the time that would have been required if the shot had been at the well (assuming, of course, a homogeneous, isotropic medium between each pair of successive detector positions). Then the average vertical velocity is the vertical depth of the detector below the shot point, divided by this time. The interval velocity (column 7), giving the average velocity for the material between detector positions, is given simply from the vertical detector interval (column 5) and the vertical time interval (column 6).

Curves for vertical time, average velocity, and interval velocity from this table are plotted in Fig. 131, together with the lithologic character of the rocks penetrated by the well. This shows that the sections with high interval velocities correspond
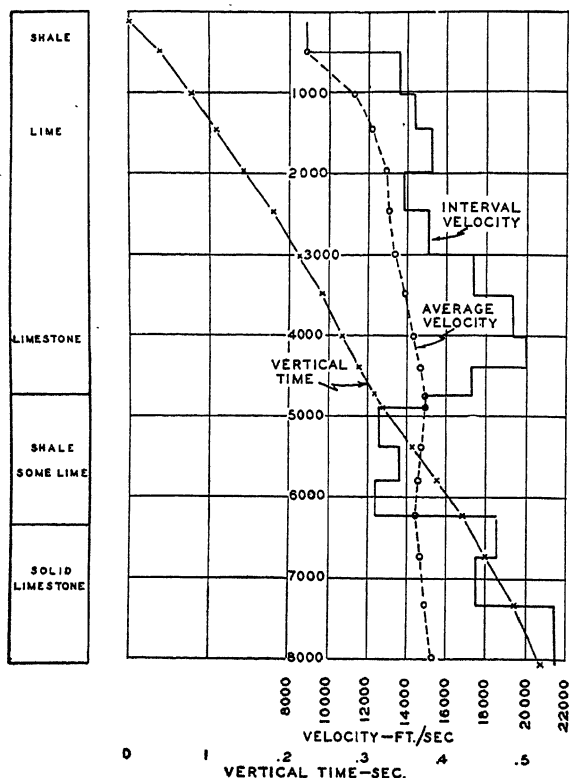
Fig. 131.—Example of results from well shooting. Depths are plotted vertically, and corresponding corrected arrival times, average (or "over-all") velocity, and interval velocity are plotted horizontally. Note changes in interval velocity corresponding to changes in character of the rock penetrated, as indicated by the generalized well log at the left.

with heavy limestones, whereas the intervening shale sections (from 4,750 to 6,350 ft.) have a much lower velocity.

The well-shooting results are used to calculate depths from observed reflection times at other points in the same general area where the geologic section presumably is approximately the same as that penetrated by the well. The observed reflection times may be reduced to actual depth, either by the average velocity curve or by the vertical time curve.

CALCULATION OF DIP

The expressions given for calculating depths have assumed that the reflecting bed is essentially horizontal. If the dip of the bed is only a few degrees, depths still can be calculated by these expressions, as the error introduced depends on the cosine of the dip angle and is less than 0.5 per cent for angles of less than about $5\frac{1}{2}$ deg. However, if the dips are more than 5 to 10 deg., the simple depth calculation becomes inaccurate, and other methods
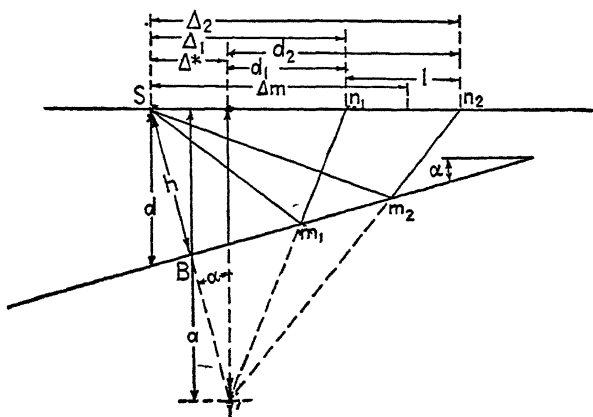
Fig. 132.—Notation for calculation of dip.

which take account of the dip must be used for accurate results.

It was pointed out above (page 283) that there are appreciable time differences between the arrivals of reflections at different detectors, even when the reflecting bed is horizontal. These time differences also will be affected by any dip of the reflecting surface. A simple method of computing the dip angle from these time differences (mostly after Gutenberg[1]) may be derived as follows:

In Fig. 132 consider that two detectors n_1 and n_2 receive reflections from a bed dipping at an angle α and at a perpendicular distance h below the shot point. Let the point I be the image of the shot point in the reflecting bed, so that the distance $SI = 2h$. Let the average velocity from the surface to the reflecting bed be V. The total length of any reflection path from shot point to detector will be the same as the distance from the image point I, to the same detector, so the travel times will be

[1] Gutenberg, 1936, pp. 132–135.

the same as they would be if the shot were at the image point. Let the vertical depth of the image point be a. Also, let

Δ_1 and Δ_2 = distances from shot point to detectors n_1 and n_2, respectively.

Δ_m = mean distance from shot to detectors

$\quad = \dfrac{\Delta_1 + \Delta_2}{2}$

Δ^* = horizontal distance from shot to vertical projection of image point.

d_1 and d_2 = horizontal distance from detectors to vertical projection of image point

l = distance between detectors

Then, from the geometry of Fig. 132, the times t_1 and t_2 from shot to detectors n_1 and n_2 are

$$\left. \begin{array}{ll} t_1 = \dfrac{\sqrt{a^2 + d_1^2}}{V}; & t_2 = \dfrac{\sqrt{a^2 + d_2^2}}{V} \\ V^2 t_1^2 = a^2 + d_1^2; & V^2 t_2^2 = a^2 + d_2^2 \end{array} \right\} \qquad (255)$$

Subtracting,

$$V^2(t_2^2 - t_1^2) = d_2^2 - d_1^2$$

Factoring,

$$V^2(t_2 + t_1)(t_2 - t_1) = (d_2 + d_1)(d_2 - d_1) \qquad (256)$$

But, from the figure,

$$d_2 + d_1 = \Delta_2 + \Delta_1 - 2\Delta^*$$
$$= 2\Delta_m - 2\Delta^*$$
$$d_2 - d_1 = l$$

Also, let

$$t_m = \tfrac{1}{2}(t_2 + t_1)$$

where t_m is the mean reflection travel time to the two detectors,

$$t_d = t_2 - t_1$$

where t_d is the "step-out" time between the two detectors. Substituting these relations in Eq. (256),

$$2V^2 t_m t_d = 2l(\Delta_m - \Delta^*)$$

Solving for Δ^*,

$$\Delta^* = \Delta_m - \frac{V^2 t_m t_d}{l}$$

But, from the geometry of the figure,

$$\Delta^* = 2h \sin \alpha$$

So that

$$\left.\begin{array}{l} 2h \sin \alpha = \Delta_m - \dfrac{V^2 t_m t_d}{l} \\[3mm] \sin \alpha = \dfrac{1}{2h}\left(\Delta_m - \dfrac{V^2 t_m t_d}{l}\right) \end{array}\right\} \tag{257}$$

Now, let the time for the reflection perpendicular to the reflecting bed (*i.e.*, for zero detector distance) be t_0. Then

$$t_0 = \frac{2h}{V}; \qquad 2h = V t_0$$

and Eq. (257) can be written

$$\begin{aligned} \sin \alpha &= \frac{1}{V t_0}\left(\Delta_m - \frac{V^2 t_m t_d}{l}\right) \\[3mm] &= \frac{\Delta_m}{V t_0} - \frac{V t_m t_d}{t_0 l} \end{aligned} \tag{258}$$

In this expression, t_d is positive if the nearer detector has the shorter travel time, so that a positive value of α means shooting up dip (as in Fig. 132), and a negative value of α means shooting down dip. The perpendicular depth to the reflecting bed is given by

$$h = \frac{V t_0}{2} \tag{259}$$

and the vertical depth below the shot point is

$$d = \frac{V t_0}{2 \cos \alpha} \tag{260}$$

Frequently a "split setup" is used in which the shot point is midway between symmetrical detector spreads on each side. Then if the times used are those to a pair of detectors at equal distances on each side of the shot point,

$$\Delta_m = 0; \qquad t_m = t_0 \text{ (approximately)}$$

and Eq. (258) reduces to

$$\sin \alpha = -\frac{V t_d}{l} \tag{261}$$

The dip calculated as just described gives the component in the direction of the detector spread.   To determine the true direction and total magnitude of the dip of the reflecting bed, it is necessary to have reflections from another detector spread in another (usually perpendicular) direction (see page 293).

Example of Dip Calculation.—In practice the calculation of dips does not work out so well as might be expected.   This is because the time differences are quite small if the detector spreads are, as is usual practice, a rather small fraction of the depth to the reflecting bed.   This is illustrated below by an example of dip angles computed from different combinations of the observed data.

The following table gives the times (after surface corrections) observed for two reflections on the same records in an area of rather steeply dipping beds.

Distance of detector from shot point	Time, sec. (1st refl.)	Time, sec. (2d refl.)
1,320 ft. W.	0.798	1.646
960 ft. W.	0.776	1.630
660 ft. W.	0.760	1.619
360 ft. W.	0.746	1.608
0 (shot point)	(0.732)	(1.598)
360 ft. E.	0.718	1.588
660 ft. E.	0.708	1.578
960 ft. E.	0.698	1.592
1,320 ft. E.	0.688	1.563

By plotting the times versus distance (Fig. 133), the times t_0 for zero shot-detector distances were interpolated as 0.732 and 1.598 sec., respectively, for the two reflections.   For the area involved, $V = 10,000$ ft./sec.   The corresponding depths perpendicular to the reflecting plane [Eq. (259) of page 291] are 3,660 and 7,990 ft., respectively.   The dips calculated from Eq. (258) are

First reflection, using distances 360 ft. W. and 1,320 ft. W. $= -27°$
First reflection, using distances 360 ft. E. and 1,320 ft. E. $= +24\frac{1}{2}°$
Second reflection, using distances 360 ft. W. and 1,320 ft. W. $= -20\frac{1}{2}°$
Second reflection, using distances 360 ft. E. and 1,320 ft. E. $= +18°$

Using the split setup formula [Eq. (261)] the dips calculated are

First reflection using distances   360 ft. on each side = 23°
First reflection using distances 1,320 ft. on each side = 25°
Second reflection using distances   360 ft. on each side = 16°
Second reflection using distances 1,320 ft. on each side = 18°

The dips calculated from the detector spreads on the two sides of the shot point are not entirely consistent and also are
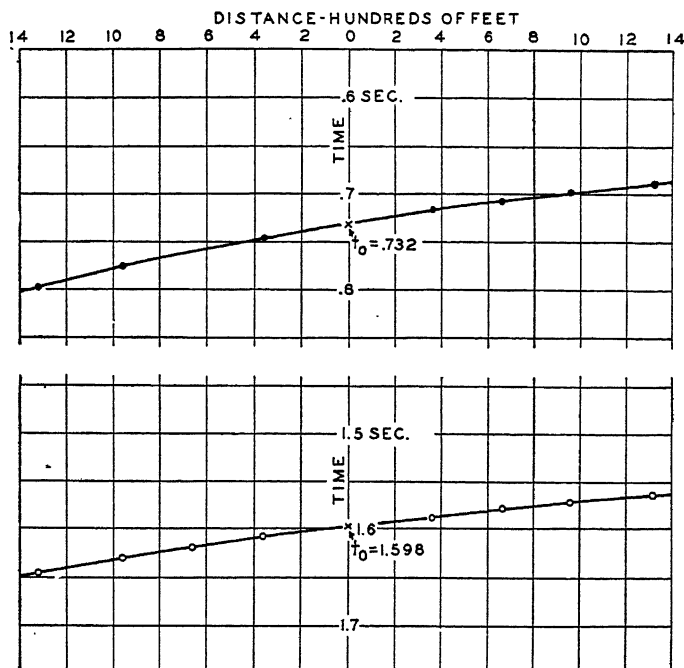
FIG. 133.—Sample of actual reflection times for reflections from dipping beds (after all surface corrections).

somewhat different from those calculated from the times for the split setup. Part of the discrepancy probably is due to an actual change of dip of the reflecting beds, as both reflections indicate steeper dips on the west side of the shot point.

Three-dimensional Dip Calculation.—The method of dip calculation given is derived and applied in a plane containing the shot-detector spread. This will give the true dip only when the spread is perpendicular to the strike of the reflecting plane. In general this will not be true; the wave paths of Fig. 132 will not

be in a vertical plane; and the dip indicated is only a component of the true dip of the reflecting plane. However, if dips are determined from two shot-detector spreads at right angles to each other, the true dip can be calculated readily.

In Fig. 134 let two shot-detector spreads at right angles be along the x- and y-axes, on the surface of the ground. The Z-axis is vertical. The reflecting plane cuts the three axes at points A, B, and C. The line OP is the normal to the reflecting plane passing through the origin.
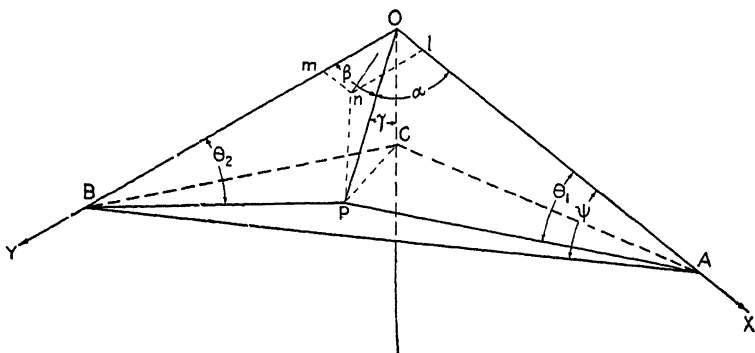
FIG. 134.—Three-dimensional dip calculation.

The incident and reflected rays for a shot-detector spread along the x-axis are in the plane OPA which is normal to the reflecting surface. The dip angle determined in this plane is θ_1. Similarly, for the perpendicular shot-detector spread along the y-axis, the rays are in the plane OPB, and the dip angle is θ_2.

Let α, β, and γ be the usual direction angles between OP and the axes. It is evident that γ is the angle of dip desired. Then, since angles OPA and OPB are right angles,

$$\sin \theta_1 = \cos \alpha; \qquad \sin \theta_2 = \cos \beta$$

and since, in general,

$$\left.\begin{array}{l} \cos^2 \alpha + \cos^2 \beta + \cos^2 \gamma = 1 \\ \sin^2 \gamma = 1 - \cos^2 \gamma = \cos^2 \alpha + \cos^2 \beta \\ \sin^2 \gamma = \sin^2 \theta_1 + \sin^2 \theta_2 \end{array}\right\} \qquad (262)$$

This gives the magnitude of the dip but not its strike. To find the strike direction, let on be the vertical projection of the line

OP in the earth's surface, and let φ be the angle between *on* and the *x*-axis. Thus, φ is the direction of maximum slope.

$$ol = OP \cos \alpha$$
$$om = OP \cos \beta$$

and

$$\tan \varphi = \frac{om}{ol} = \frac{\cos \beta}{\cos \alpha}$$
$$= \frac{\sin \theta_2}{\sin \theta_1} \qquad (263)$$

The strike ψ is perpendicular to the direction of maximum slope, and therefore

$$\tan \psi = - \frac{\sin \theta_1}{\sin \theta_2} \qquad (264)$$

In mapping the dips, it is convenient to draw a vector, such as V, having a length proportional to the dip (*i.e.*, proportional to $\tan \gamma$), azimuth φ, giving the dip direction, and with its origin at the point *n*, vertically above the point of reflection for shot-detector spreads about the origin *o*. The offset distance *on* is

$$on = OP \cos \gamma$$

where *OP* is the perpendicular reflection distance corresponding to the depth *h* of Fig. 132 and Eq. (259).

From a map of dip vectors, with their lengths proportional to the dip angle, it is possible to calculate depth differences and depth contours in just the same way that gravity contours can be calculated from gravity gradients (see page 98).

For routine operations it may be desirable to compute the dips directly from the geometry of the shot-detector "spreads" on the surface of the ground and the "step-out" times [t_d of Eqs. (258) and (261)]. The theory of such calculations has been given by Rock,[1] and special charts to facilitate such computations have been described by Lawlor.[2]

[1] Rock, 1938.
[2] Lawlor, 1938.

CHAPTER XVI

THE REDUCTION OF SEISMIC OBSERVATIONS

The seismic methods of geophysical prospecting are similar to the gravitational and magnetic methods in that the quantities as measured in the field require certain corrections before the formulas for depth, dip, etc., as derived in the two previous chapters can be applied. The observed quantities are the times from the instant of the wave-generating explosion until the arrival of certain resulting waves at detectors at known distances from the shot. The expressions for depths to or attitudes of the refracting or reflecting beds assume a certain regularity and homogeneity of the media through which the waves are transmitted. Any departures from these assumptions that affect the travel times of the waves will give false contributions to the calculated depths or dips unless proper corrections are made. The purpose of this chapter is to outline the corrections that are required and the means used in the field for obtaining the accessory data so that the corrected times will fulfill, as nearly as feasible, the conditions assumed in the previous chapters.

THE "WEATHERED" LAYER

It was found early in the development of seismic prospecting that there is nearly always a "weathered," or surface, layer which has a distinctly lower seismic wave speed than the material immediately underlying it. For instance, its wave speed may be around 2,000 to 2,500 ft. per second, whereas the first under layer. may have a speed of 5,000 to 8,000 ft. per second. This weathered layer usually varies considerably in thickness. Therefore, the time required for seismic waves to travel through this layer is variable, and corrections must be made for these times before accurate calculations of subsurface conditions can be made.

The surface layer is probably not a weathered layer in the sense of being a zone modified by surface or atmospheric conditions. It is often from 50 to as much as 200 ft. thick, which is probably

too deep for such an explanation. It may be associated in some areas at least with ground water. The existence of this layer has become known only through seismic prospecting. From the behavior of seismic waves, it is known that the change in velocity at the base of the surface zone is usually quite distinct and sharp, and it is not a gradual change from a slower speed at the surface to a greater speed at depth.

The spacing of detectors as used in seismic prospecting is not suitable for a measure of the velocity of the surface layer, as the detectors are too far from the shot point. Lester[1] has reported experiments with very close detector spacing (beginning 5 ft. from the shot) which indicated a layer $7\frac{1}{2}$ ft. thick with a speed from 550 to 1,600 ft. per second, underlain by a speed of 5,500 ft. per second. The speed change occurred approximately at the depth of the underground water table. The observed variation and the very low speeds seem to be consistent with Lester's calculation of wave speeds for an earth-air mixture and therefore indicate that the weathered layer is really an "aerated" layer. This one experiment seems to be the only published attempt to measure in detail the properties of the surface zone. Further work is needed to give a clear explanation of the properties and cause of the low-speed surface zone.

WEATHERING CORRECTIONS FOR REFRACTION SHOOTING

In refraction shooting, the "spread" of detectors is at some distance from the shot point. Therefore, it may be necessary to make special local "weathering shots" at each end of the detector spread. Then it is possible to calculate the thickness of the surface layer at each detector, for this determination is essentially a two-layer refraction seismograph problem.[2] The analysis is essentially the same as was outlined above for profile shooting (page 274). In order to determine the variable thickness of the surface zone, we must have enough data to determine the separate unknown depths at the individual detector positions.

Theory of Weathering Shooting.—Consider a line of detectors of which any one is indicated by n (Fig. 135) at each of which waves are recorded from two shot points m and o at opposite

[1] Lester, 1932.
[2] Pirson, 1937.

ends of the line. Let W_m, W_n, W_o indicate the thicknesses of the weathered layer under (approximately)[1] the corresponding points. Let the velocity in the surface layer be V_0; that in the underlying high-speed bed, V_1. Then, the delay time associated with a path through the weathered layer, where the thickness is W_n, is

$$D_n = \frac{W_n \cos i}{V_0}$$

and the total delay time of a wave from shot point m, refracted through the high-speed bed V_1 and recorded at detector n, is

Fig. 135.—Weathering wave paths and time-distance relations.

$D_m + D_n$ which is equal to the intercept time t_{mn} (see Fig. 135). Thus,

$$
\begin{aligned}
t_{mn} &= D_m + D_n \\
&= (W_m + W_n)\frac{\cos i}{V_0}
\end{aligned}
\qquad (265a)
$$

where the first subscript m indicates the shot point, and the second n indicates the detector.

Similarly, the intercept time for a shot to the same detector but from the opposite end o of the spread is

$$
\begin{aligned}
t_{on} &= D_o + D_n \\
&= (W_o + W_n)\frac{\cos i}{V_0}
\end{aligned}
\qquad (265b)
$$

[1] The thicknesses, W are actually under points displaced by the offset distance from the corresponding detector positions, but the possible differences due to this are usually ignored and are so ignored here to simplify the theory and calculations.

Finally, the intercept time for a shot from one end of the spread to the other, recorded by a detector at o, from a shot at m (or by a detector at m from a shot at o) is

$$t_{om} = t_{mo} = D_m + D_o$$
$$= (W_m + W_o) \frac{\cos i}{V_0} \qquad (265c)$$

We now have three unknowns, *i.e.*, W_n, W_m, and W_o, to be solved for from the three Eqs. (265a), (265b), (265c). Subtracting (265c) from (265b),

$$(W_n - W_m) \frac{\cos i}{V_0} = t_{on} - t_{om}$$

Adding this to (265a)

$$2W_n \frac{\cos i}{V_0} = t_{on} - t_{om} + t_{mn}$$

and

$$W_n = (t_{mn} + t_{on} - t_{om}) \frac{V_0}{2 \cos i}. \qquad (266)$$

The other two unknown thicknesses, W_o and W_m, can be solved for similarly. Finally, we can write symmetrical expressions for the three unknown thicknesses as follows (the two sets are quite equivalent, and either may be used. Some may prefer one form of symmetry to the other):

$$\left.\begin{aligned}
W_m &= (t_{mn} + t_{om} - t_{on}) \frac{V_0}{2 \cos i} = (t_{mn} + t_{om} - t_{on}) \frac{V_0}{2 \cos i} \\
W_n &= (t_{mn} - t_{om} + t_{on}) \frac{V_0}{2 \cos i} = (t_{on} + t_{mn} - t_{om}) \frac{V_0}{2 \cos i} \\
W_o &= (-t_{mn} + t_{om} + t_{on}) \frac{V_0}{2 \cos i} = (t_{om} + t_{on} - t_{mn}) \frac{V_0}{2 \cos i}
\end{aligned}\right\} \quad (267)$$

Analysis of Weathering Shot Data.—The calculations of thicknesses of the surface zone at the various detectors are made on special "weathering" records which show first arrivals from the special "weathering shots" that are fired at points m and o at each end of the detector spread (Fig. 136, page 300). From the resulting first arrivals an average velocity is determined from the average of the slopes in the two directions. Lines ·with the slope corresponding to this average velocity are then drawn

passing through the two extreme time-distance points, *i.e.*, through the points giving the time of travel from the shot at one end of the spread to the detector that is at the shot position at the other end of the spread. Since these each represent the time of travel between identical positions but in opposite directions, the two times should be the same. Since the two lines are drawn with the same slopes, the intercepts of these lines at the zero shot distance (t_{mo} and t_{om}, Fig. 136) should be the same. Now consider the arrival times at any other detector, such as n.
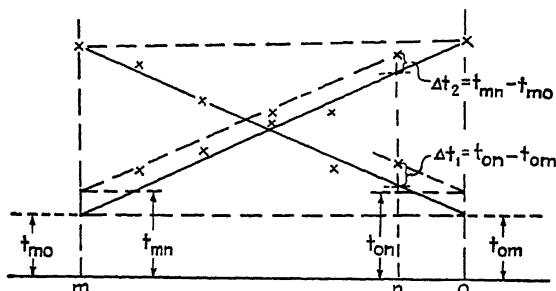
Fig. 136.—First arrival times from shot points at opposite ends of the detector "spread," showing times and time differences used to calculate weathering.

In general, this time will not be exactly on the sloping average velocity line, and let the distance it departs from this line be Δt_1 for the line shown from right to left and Δt_2 for the line shown from left to right. From Eq. (267) we have

$$W_n = (t_{on} + t_{mn} - t_{om}) \frac{V_0}{2 \cos i} \qquad (268)$$

But from the diagram (Fig. 136) it is evident that

$$t_{on} - t_{om} = \Delta t_1$$

and

$$t_{mn} = \Delta t_2 + t_{mo}$$

Substituting these in Eq. (268), it is evident that the depth of the weathering W_n at any point n is given by

$$\left. \begin{aligned} W_n &= (t_{mo} + \Delta t_1 + \Delta t_2) \frac{V_0}{2 \cos i} \\ &= (t_{om} + \Delta t_1 + \Delta t_2) \frac{V_0}{2 \cos i} \end{aligned} \right\} \qquad (269)$$

for $t_{om} = t_{mo}$, or, in terms of the velocities,

$$W_n = (t_{om} + \Delta t_1 + \Delta t_2) \frac{V_0 V_1}{2\sqrt{V_1^2 - V_0^2}} \qquad (269a)$$

The velocity V_1 is determined from the average slope of the two lines as shown in Fig. 136. An alternative way of plotting this figure is to plot both sets of first arrival times as if shot from one shot point by using suitable symbols to indicate the times that belong to the separate shot points (Fig. 137). This
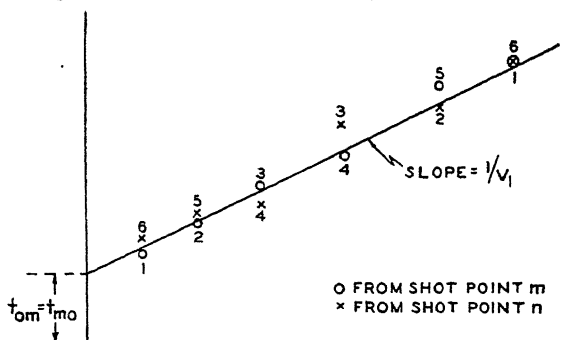
Fig. 137.—First arrival times plotted against shot-detector distance using arrival times from shots at opposite ends of the detector spread to determine the average time-distance slope.

amounts to turning one of the diagrams end to end and superposing it on the other. The average straight line through the points so plotted then gives the average velocity of the first underlying bed.

The velocity V_0 is usually determined by a separate experiment. This may be done by placing detectors very close to a shot point at the surface so that the first arrivals are waves that have traveled through this material. The detectors then have to be placed within a distance from the shot point comparable to the thickness of the weathered layer. Another method is to determine the time from shots at various depths in a hole through the weathered layer to a detector at the top of the hole. This then measures directly the vertical wave speed in the surface zone.

Corrections to Observed Travel Times.—The purpose of weathering and other corrections is to reduce the observed travel times to what they would be if the irregularities of the surface of the ground and of the thickness of the lower speed surface layer were not present. The total time correction will be called

the "surface correction." There are several different ways of considering the surface correction which are equivalent in their final result. The preference among them is largely a matter of personal choice and sometimes of computational convenience. For instance, the surface correction may be made (1) by calculating what the times would be if the material in the surface zone had the same velocity as that underlying it, (2) by calculating what the times would be if the shot and detector were
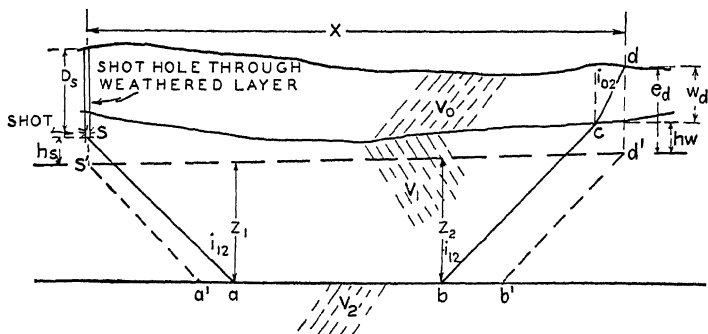
FIG. 138.—Refraction paths through weathered layer showing actual wave path and equivalent ideal wave path after weathering correction.

both at the bottom of the surface zone, and (3) by calculating what the times would be if the shot and detector were both at an arbitrary reference plane or datum level. The following analysis is based on the third method.

Consider a situation as indicated by Fig. 138 where the dotted line represents the datum level. This is a horizontal plane to which all depths and other calculations are to be referred. The object of the surface correction is to determine a time such that when this time is added to or subtracted from the observed travel times, the resulting corrected time will be that which would have been taken if the shot and detector had both been at the datum level.

The usual field practice is to place the shot in a hole drilled through the weathered zone. Referring to the diagram (Fig. 138), the actual path for a wave refracted in a bed with velocity V_2 is $sabcd$. The delay times for the segments sa, bc, and cd of the wave path are

$$(Z_1 + h_s) \frac{\cos i_{12}}{V_1}; \qquad (Z_2 + h_w) \frac{\cos i_{12}}{V_1}; \qquad w_d \frac{\cos i_{02}}{V_0},$$

respectively. Therefore, the actual travel time for the wave path *sabcd* is

$$T_s = \frac{x}{V_2} + (Z_1 + h_s)\frac{\cos i_{12}}{V_1} + (Z_2 + h_w)\frac{\cos i_{12}}{V_1} + \frac{W_d \cos i_{02}}{V_0}$$
(270)

The hypothetical path, from the datum level, for which the reduced time is desired is *s'a'b'd'*. The time for this path is

$$T_d = \frac{x}{V_2} + \frac{(Z_1 + Z_2)\cos i_{12}}{V_1}$$
(271)

The difference between these two is the total surface correction T_w, or

$$T_w = T_s - T_d = (h_s + h_w)\frac{\cos i_{12}}{V_1} + W_d\frac{\cos i_{02}}{V_0}$$
(272)

From Fig. 138, h_s and h_w are the heights above the datum level of the shot and the bottom of the weathering at the detector, respectively, and W_d is the thickness of the weathering at the detector.

If all elevations are referred to the datum plane (by subtracting the elevation of the datum plane from actual surface elevations) and such elevations are described by letters e, so that

e_s = elevation above datum of the surface at the shot point.
D_s = depth of the shot.
e_d = elevation above datum of the detector.
W_d = thickness of the weathering at the detector.

then

$$h_s = e_s - D_s$$
$$h_w = e_d - W_d$$

Substituting these values in Eq. (272),

$$T_w = (e_s - D_s + e_d)\frac{\cos i_{12}}{V_1} + W_d\left(\frac{\cos i_{02}}{V_0} - \frac{\cos i_{12}}{V_1}\right)$$
(273)

The thickness of the surface layer W_d corresponds to one of the thicknesses W_n of Eq. (269). With this substitution, Eq. (273)

can be expressed as

$$T_w = (e_s - D_s + e_d) \frac{\cos i_{12}}{V_1}$$

$$+ (t_{om} + \Delta t_1 + \Delta t_2) \frac{V_0}{2 \cos i_{01}} \left(\frac{\cos i_{02}}{V_0} - \frac{\cos i_{12}}{V_1} \right)$$

$$= (e_s - D_s + e_d) K_{12} + (t_{om} + \Delta t_1 + \Delta t_2) \frac{K_{02} - K_{12}}{2K_{01}} \quad (274)$$

where the coefficients K_{12}, K_{02}, K_{01} are determined by the veloci-
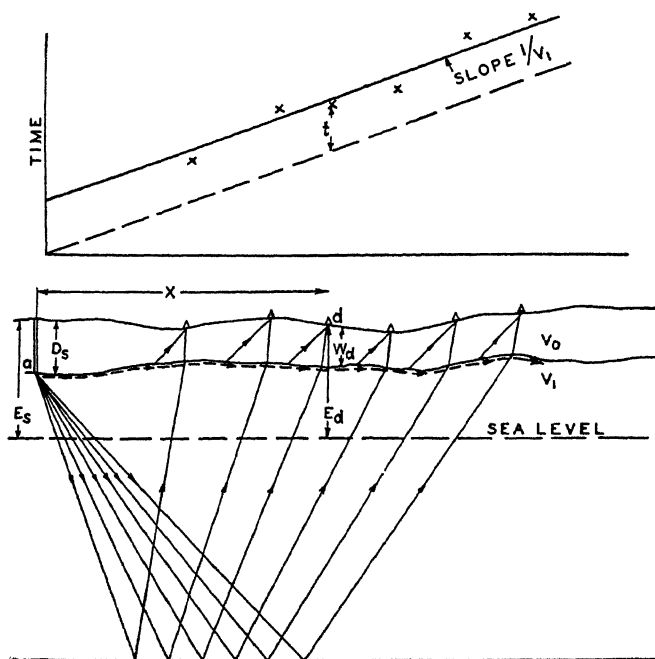
FIG. 139.—Reflection paths, refraction paths in surface zone, and first arrival times used for weathering calculations.

ties of the surface layer V_0, first underlayer V_1, and marker bed V_2, as shown by Fig. 138. The value of any K is given by

$$K_{mn} = \frac{\cos i_{nm}}{V_n} = \frac{\sqrt{V_m^2 - V_n^2}}{V_m V_n} \quad (275)$$

Equation (274) gives the weathering correction in terms of directly measurable quantities: *i.e.*, e_s, D_s, and e_d which are given by the survey data; t_{om}, Δt_1, and Δt_2 which are given by the

weathering shot-time plot (Fig. 136 or 137); and the K's, which are given by the velocities involved [Eq. (275)].

WEATHERING CORRECTIONS FOR REFLECTION SHOOTING

In reflection shooting, the detector spread is usually close to the shot point so that the first arrivals on the reflection records can be used to calculate the weathering. The shot is nearly always placed below the surface zone. Therefore, the first arrivals reach the detectors by the dotted wave paths (Fig. 139).

Fig. 140.—Reflection weathering correction notation.

The first arrival times to the individual detectors are indicated by the crosses of the time-distance diagram of the upper part of the figure. The average straight line through these points has the slope $1/V_1$. If the dashed line parallel to this is drawn through the origin, the individual intercept times, such as t_i, will be the times above this line. These intercept times will be equal to the individual delay times D, associated with the thickness of the surface zone under the corresponding detector. Thus, if this thickness is W_d,

$$t_i = D = W_d \frac{\cos i}{V_0}$$

and

$$W_d = \frac{t_i V_0}{\cos i}$$

$$= t_i \frac{V_1 V_0}{\sqrt{V_1^2 - V_0^2}} \qquad (276)$$

As in the corrections for refraction shooting, we can make the surface zone correction in various ways. For instance, the corrections can be calculated (1) to the elevation of the surface at the shot point, (2) to the elevation of the shot, and (3) to an arbitrary datum elevation. The notation used for the various corrections is shown by Fig. 140.

Corrections to the Elevation of the Surface at the Shot Point.— For calculating the corrections by this method, we reduce the time to what it would be if the surface layer had a velocity V_1 instead of V_0. For a given detector where the weathering thickness is W_d (Fig. 140), the actual travel time in the surface layer is W_d/V_0. The desired corrected time is W_d/V_1. Therefore, the correction t_w, which must be subtracted from the measured time to take account of the surface layer, is

$$t_w = W_d \left(\frac{1}{V_0} - \frac{1}{V_1} \right) = W_d \frac{V_1 - V_0}{V_1 V_0} \qquad (277)$$

(this assumes that the reflection travels vertically through the weathered layer, which is usually a fairly close approximation). Substituting W_d from Eq. (276),

$$t_w = t_i \frac{V_1 V_0}{\sqrt{V_1^2 - V_0^2}} \cdot \left(\frac{V_1 - V_0}{V_1 V_0} \right)$$

$$= t_i \sqrt{\frac{V_1 - V_0}{V_1 + V_0}} \qquad (278)$$

$$= t_i K' \qquad (278a)$$

where

$$K' = \sqrt{\frac{V_1 - V_0}{V_1 + V_0}} \qquad (279)$$

Finally, we wish to reduce the times to what they would be if shot and detector were on a level plane at the elevation of the surface at the shot point and the velocity were V_1 downward from that plane. The other times that must be taken into account are

1. The time (to be added) that would have been taken for the wave to travel from the surface to the shot at depth D_s, which would be

$$\frac{D_s}{V_1} \qquad (280a)$$

2. The time (to be added if the surface elevation at the detector is lower than that at the shot point) required to travel the additional vertical dis-

tance corresponding to the difference in elevation between detector and shot point, which would be

$$\frac{E_s - E_d}{V_1} \tag{280b}$$

The total surface correction C_1 is the sum of all the corrections, (278a), (280a), and (280b), which is (remembering that the time t_w must be subtracted)

$$C_1 = -t_s K' + \frac{D_s}{V_1} + \frac{E_s - E_d}{V_1}$$

$$= -t_s K' + \frac{D_s - E_d + E_s}{V_1} \tag{281}$$

Depths derived from times calculated with this correction indicate the distance of the reflecting horizon below the surface of the ground at the shot point.

Corrections to the Elevation of the Shot.—In this method the corrections are calculated to reduce the times to what they would have been if the detector were at the same elevation as the shot and both shot and detector were below the surface layer. The corrections required are

1. The time (to be subtracted) required for a wave to travel from the base of the weathering to the surface. This time is

$$-\frac{W_d}{V_0} \tag{282}$$

2. The time (to be subtracted if the base of the weathering is above the shot point) required for the wave to travel from the level of the shot point to the base of the weathering. The elevation of the shot is $E_s - D_s$. The elevation of the base of the weathering is $E_d - W_d$. Therefore the time correction required is

$$-\frac{(E_d - W_d) - (E_s - D_s)}{V_1} \tag{283}$$

The total weathering, or surface correction, is the sum of the terms (282) and (283), or

$$C_2 = -\frac{W_d}{V_0} - \frac{E_d - W_d - E_s + D_s}{V_1}$$

$$= \frac{E_s - E_d - D_s}{V_1} - W_d \left(\frac{1}{V_0} - \frac{1}{V_1} \right)$$

$$= \frac{E_s - E_d - D_s}{V_1} - t_s K' \tag{284}$$

where K' is given by Eq. (279). Depths derived from times calculated with this correction are depths below the elevation of the shot (not the elevation of the surface at the shot point).

Correction to a Datum Elevation.—In this method, corrections are calculated to reduce the times to what they would be if both shot and detector were on a datum plane at an arbitrary elevation h, referred to sea level. The datum plane is below the base of the surface zone. As in the refraction shooting corrections (page 303), let

e_s = elevation above datum of surface at shot point.
e_d = elevation above datum of the detector.

Then the correction times required are the times for all parts of the wave path above the datum plane. They are all to be subtracted. Again, with the approximation that the wave paths are vertical, these times are

1. The time required for the wave to travel from the shot to the datum plane, which is

$$-\frac{e_s - D_s}{V_1} \tag{284a}$$

2. The time required for the wave to travel from the datum plane to the base of the weathering, which is

$$-\frac{e_d - W_d}{V_1} \tag{284b}$$

3. The time required for the wave to travel through the weathering, which is

$$-\frac{W_d}{V_0} \tag{284c}$$

The total correction is the sum of these terms:

$$\begin{aligned}
C_3 &= -\frac{e_s - D_s}{V_1} - \frac{e_d - W_d}{V_1} - \frac{W_d}{V_0} \\
&= \frac{D_s - e_s - e_d}{V_1} - W_d\left(\frac{1}{V_0} - \frac{1}{V_1}\right) \\
&= \frac{D_s - e_s - e_d}{V_1} - t_i K'
\end{aligned} \tag{285}$$

where, again, K' is given by Eq. (279). Depths derived from times corrected by this method are below the elevation of the datum plane.

Example of Surface Correction.—The entire process of making the surface correction is rendered quite mechanical by entering the various factors into an appropriate table. In the example on page 310, surface corrections and depths are calculated for the same set of actually observed data by each of the three methods just described.

It will be noticed that the subsea depths by method 2 are about 20 ft. greater than those by method 1 and that those by method 3 are about 40 ft. greater. The depths were all determined from the corrected time with the same "depth chart." However, the depth chart used is calculated for a velocity that increases with depth from 9,000 ft. per second at the surface to about 12,500 ft. per second at depths corresponding to times of around 1 sec. The corrected times by method 2 are less than those by method 1 by an amount corresponding to the time required for the wave to go down and back through a layer 64 ft. thick, *i.e.*, by $2 \cdot 64/9,000 = 0.014$ sec. But the calculated depth is less by the amount corresponding to this same time difference applied to a region where the velocity is 12,500 ft. per second, *i.e.*, by $12,500 \cdot 0.014/2 = 87$ ft. Therefore, the depths calculated by method 2 should come out to be $87 - 64 = 23$ ft. shallower than by method 1. By method 3 the difference at the surface is 130 ft., and a calculation of the same sort as the one above shows that the depths should come out $181 - 130 = 51$ ft. shallower than by method 1.

These differences (in this case up to about 1 per cent), however, have no particular significance. In actual practice the same method of surface corrections would always be used for a given area, and relative depths would be correct. The velocities are rarely, if ever, known accurately enough to give absolute depths correct to 1 per cent.

Corrections by Use of Fiducial Time.[1]—In this method, the corrected times are used instead of depths. The application of an assumed or measured velocity distribution and the change from directly determined times to calculated depths is made only as a final step on those times which, from correlation with other

[1] The writer is indebted to L. W. Gardner for this method.

TABLE FOR CORRECTIONS BY METHOD 1

$E_s = 1,130$ ft.; $D_s = 64$ ft.; $V_0 = 2,500$ ft./sec.; $V_1 = 9,000$ ft./sec.

E_d	Distance	T_f	T_iK'	$\dfrac{D_s - E_d}{+ E_s}$	$\dfrac{D_s - E_d + E_s}{V_1}$	C_1	T_r	T_0	Depth	Depth subsea
1,138	90	0.022	0.009	56	0.006	−0.003	0.927	0.924	4,825	3,695
1,149	300	0.046	0.008	45	0.005	−0.003	0.929	0.926	4,830	3,700
1,156	510	0.072	0.010	38	0.004	−0.006	0.932	0.926	4,825	3,695
1,161	720	0.096	0.010	33	0.004	−0.006	0.934	0.928	4,830	3,700
1,168	930	0.123	0.011	26	0.003	−0.008	0.933	0.925	4,800	3,670
1,178	1,140	0.147	0.011	16	0.002	−0.009	0.936	0.927	4,795	3,665

TABLE FOR CORRECTION BY METHOD 2

E_d	Distance	T_f	T_iK'	$\begin{array}{c}E_s - E_d\\ - D_s\end{array}$	$\dfrac{E_s - E_d - D_s}{V_1}$	C_2	T_r	T_0	Depth	Depth subsea
1,138	90	0.022	0.009	− 72	−0.008	−0.017	0.927	0.910	4,740	3,675
1,149	300	0.046	0.008	− 83	−0.009	−0.017	0.929	0.912	4,745	3,680
1,156	510	0.072	0.010	− 90	−0.010	−0.020	0 932	0.912	4,740	3,675
1,161	720	0.096	0.010	− 95	−0.011	−0.021	0.934	0.913	4,740	3,675
1,168	930	0.123	0.011	−102	−0.011	−0.022	0.933	0.911	4,720	3,655
1,178	1,140	0.147	0.011	−112	−0.013	−0.024	0.936	0.912	4,710	3,645

TABLE FOR CORRECTION BY METHOD 3

Elevation of datum = 1,000 ft.; $e_s = 130$ ft.

e_d	Distance	T_f	T_iK'	$\begin{array}{c}D_s - e_s\\ - e_d\end{array}$	$\dfrac{D_s - e_s - e_d}{V_1}$	C_3	T_r	T_0	Depth	Depth subsea
138	90	0.022	0.009	−204	−0.022	−0.031	0.927	0.896	4,655	3,655
149	300	0.046	0.008	−215	−0.024	−0.032	0.929	0.897	4,655	3,655
156	510	0.072	0.010	−222	−0.025	−0.035	0.932	0.897	4,650	3,650
161	720	0.096	0.010	−227	−0.025	−0.035	0.934	0.899	4,655	3,655
168	930	0.123	0.011	−234	−0.026	−0.037	0.933	0.896	4,625	3,625
178	1,140	0.147	0.011	−244	−0.027	−0.038	0.936	0.898	4,625	3,625

The column headings are:

Distance = horizontal distance of detector from shot point, ft.

T_f = time of first arrival, sec.

T_i = intercept time, sec.

K' = angle factor = $\sqrt{\dfrac{V_1 - V_0}{V_1 + V_0}} = \sqrt{\dfrac{9,000 - 2,500}{9,000 + 2,500}} = 0.745.$

D_s = depth of shot (= 64 ft.).

E_d = elevation of detector, ft.

E_s = elevation of surface at shot point (= 1,130 ft.).

C_1, C_2, C_3 = total correction by methods 1, 2, and 3, respectively, sec.

T_r = observed reflection time, sec.

T_0 = corrected reflection time, sec.

Depth = depth of reflection (read from depth chart), ft.

Depth subsea = depth of reflection below sea level, ft.

e_s = elevation of surface at shot point above datum level, ft.

e_d = elevation of detector above datum level, ft.

times or from general geologic information, are considered of sufficient interest to be converted to depths.

First, the surface corrections are made by the use of a datum level (method 3, page 308). These corrected reflection times for each detector trace are plotted, instead of actual depths, on the usual profile, the horizontal positions being the usual "center points" midway between shot point and detector.

The corrected times T_0 can be plotted conveniently and rapidly by use of a "fiducial time" F. This time is an arbitrary reference chosen near the average reflection time of the events being
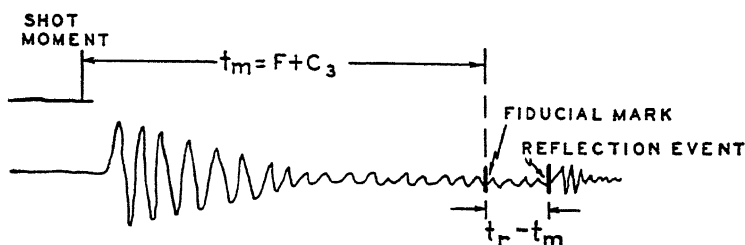
Fig. 141.—Tape markings and notation for calculating reflections by the "fiducial time" method.

mapped and for convenience is an integral number of seconds or tenth-seconds. For each detector trace (Fig. 141) a fiducial mark is placed at a time t_m given by

$$t_m = F + C_3; \qquad C_3 = t_m - F \qquad (286)$$

where C_3 is the surface correction given by Eq. (285). Then, since $T_0 = t_r - C_3$, it follows that

$$T_0 = (t_r - t_m) + F \qquad (287)$$

The time, $t_r - t_m$, can be scaled off conveniently on the record with dividers and plotted on the time profile with reference to the fiducial time F to give a plot of the corrected reflection time.

It is evident that for a given velocity distribution, the fiducial time F corresponds to a constant reference depth. Depth differences below or above that reference depth are determined from the time difference, $t_r - t_m$, multiplied by the velocity pertinent to the part of the geologic section involved. If reflections are read over a large range of reflecting times, it is convenient and desirable to use several fiducial times for reflections from different parts of the record. Total depths will be those corresponding

to the time T_0, corrected to the datum plane at elevation h, so that final depths values are referred to that plane.

The corrected reflection times plotted from the corrected times T_0 have no "angularity" correction, so the plots from detectors at different distances will give lines bowed downward with a curvature depending on the depth and velocity. For deep
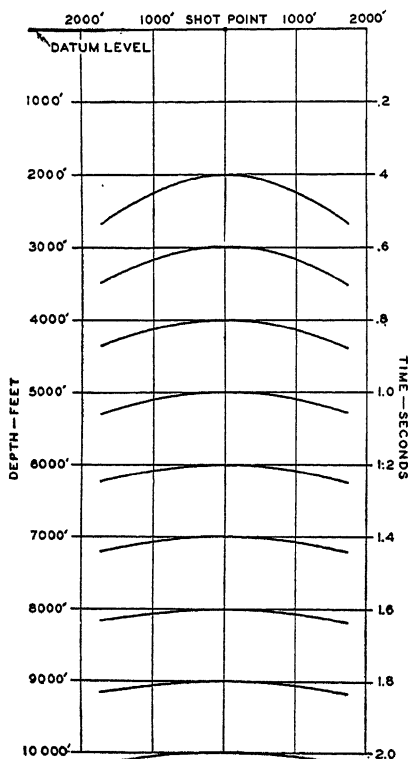
Fig. 142.—"Umbrella chart" for converting reflection times without "angularity" corrections to depths.

reflections and detector spreads that are not too wide, this curvature is not very great, and it may not be necessary to make a correction for it. If detector spreads on both sides of the shot point are used, the time for zero detector distance may be interpolated by drawing a curve between the times to detectors on both sides of the shot point. Then the depth can be calculated from whatever velocity data are available, and it is only at this

stage that any interpretation or assumption other than the times from the seismic records enters the calculations.

A chart may be calculated that gives theoretical curves, based on available velocity data or assumption, which give, for different depths, the relation between detector distance and expected reflection time. An example of such a chart for a simple case is given by Fig. 142. By comparing such curves with the actually plotted corrected times, the depths can be read directly from the chart. If the reflecting horizon is not horizontal, the dip will be indicated by the angle at which the chart has to be placed to match a calculated curve with an observed one.

It is also possible to use the fiducial time method with an "angularity correction" included. In this method the fiducial time for each trace is that calculated for the shot-detector distance and for a given velocity distribution.

Referring to Fig. 143, the depth corresponding to a vertical reflection at the fiducial time F will be
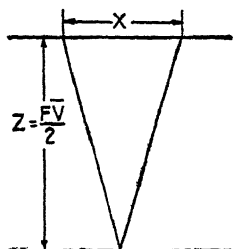
Fig. 143.—Reflection from the depth corresponding to the fiducial time.

$$Z = \frac{F\bar{V}}{2}$$

where $\bar{V}$ is the average velocity corresponding to the reflection time F. The reflection time F_x from the same level to a detector at distance x is

$$F_x = \frac{2}{V}\sqrt{\left(\frac{FV}{2}\right)^2 + \left(\frac{x}{2}\right)^2}$$
$$= F\sqrt{1 + \left(\frac{x}{FV}\right)^2} \tag{288}$$

If we mark the fiducial time as before (Eq. (286) and Fig. 141), except that now we use the time F_x, so that the mark is made at the time

$$T'_m = F_x + C_3 \tag{289}$$

the corrected times

$$T_0 = (t_r - T'_m) + F_x$$

will plot in a straight line if the average velocity used in calculating F_x [Eq. (288)] is correct.

Curved-ray Paths in Reflection Shooting.—In all the theory of corrections and depth calculation for reflection shooting, it has been assumed that the wave paths are straight lines from shot to reflecting surface and from reflecting surface to detector.
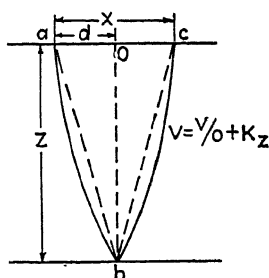
Fig. 144.—Curved reflection paths in medium with velocity increasing linearly with depth.

It has been shown (page 258) that, if the velocity increases with depth, as is commonly true, the wave paths are curved. Therefore, the assumption of straight-line wave paths is only an approximation. However, under ordinary conditions, this approximation is so very close that there is no practical advantage in using the more complex curved path theory for calculating reflection depths. This can be shown as follows:

In a medium where the velocity increases linearly with depth, the time for a wave to travel from a to b (Fig. 144) is

$$t = \frac{1}{K} \cosh^{-1} \left[1 + \frac{K^2(d^2 + Z^2)}{2V_0(V_0 + KZ)} \right]^* \tag{290}$$

The vertical time, such as would be determined by well shooting, would correspond to the time for the path ob and will be given by Eq. (290) with $d = 0$; *i.e.*,

$$t_0 = \frac{1}{K} \cosh^{-1} \left[1 + \frac{K^2 Z^2}{2V_0(V_0 + KZ)} \right] \tag{291}$$

and the average vertical velocity to the depth Z will be

$$\bar{V} = \frac{Z}{t_0} \tag{292}$$

To compare the depths calculated by the straight-line and curved paths, we can compute for given V_0 and K and for a given depth Z the true reflection time t, by Eq. (290). We can also compute the true average velocity by Eq. (292) [with the value of t_0 calculated from Eq. (291)] and compute the depth by the simple formula

$$Z' = \frac{1}{2}\sqrt{\bar{V}^2 t^2 - x^2}\dagger$$

* See, for instance, Slotnick, 1936, p. 301.
† See Eq. (253), p. 284.

A comparison of the depth thus computed with the depth assumed for calculating t gives a measure of the error introduced by assuming straight-line propagation. An example of such calculations is given by the following table, calculated for the constants,

$$K = 0.5 \text{ sec.}^{-1}; \qquad V_0 = 6,000 \text{ ft./sec.}$$

Z, feet	X, feet	t	t_0	$\bar{V}$	Z'	$Z - Z'$	Error, per cent
5,000	3,000	1.4539	1.3932	7,177.6	4,997.6	2.4'	0.05
	4,000	1.4993	1.3932	7,177.6	4,995.9	4.1'	0.08
	5,000	1.5557	1.3932	7,177.6	4,993.6	6.4'	0.13
7,000	3,000	1.8791	1.8381	7,616.4	6,997.1	2.9	0.04
	4,000	1.9103	1.8381	7,616.4	6,994.9	5.1	0.07
	5,000	1.9497	1.8381	7,616.4	6,992.3	7.3	0.11
9,000	3,000	2.2685	2.2385	8,041.2	8,996.2	3.8	0.04
	4,000	2.2916	2.2385	8,041.2	8,994.2	5.8	0.06
	5,000	2.3210	2.2385	8,041.2	8,991.3	8.7	0.10

From this table it is evident that, even for wide detector spreads, the error introduced by the assumption of linear paths will rarely be over 0.1 per cent of the depth. Other uncertainties, particularly in accurate knowledge of the actual velocity distribution, make such an error quite negligible.

CHAPTER XVII

SEISMIC APPARATUS

DEVELOPMENT OF SEISMIC FIELD EQUIPMENT

Most of the development of the field equipment for seismic prospecting has been carried out by the various competing oil and prospecting companies. It is natural, therefore, that there is no standard set of equipment that might be described. The geophysical literature contains no detailed technical description of a complete set of seismograph field equipment, which is only a natural result of the intensely competitive nature of the field activity.

Although there is great variation in detail, and constant change and improvements are being made in various parts of the field and testing equipment, the essential functions are the same in the different sets of apparatus. Therefore, the description given of the field equipment will be primarily functional rather than an attempt to describe in detail the circuits or operation of any one set of equipment.

FUNCTIONS OF SEISMIC APPARATUS

Seismic apparatus and field operations have as their one primary objective the accurate determination of wave travel times from a shot to detectors for refracted or reflected waves. The elements of the field operations and apparatus shown schematically in Fig. 145 are

1. The shot which originates the elastic wave.
2. The detectors which respond to the resulting ground motion.
3. The amplifier-filter-recorder system which makes a permanent record of certain selected components of the detector response.
4. A timing system for measuring the time between the instant of explosion and the detector response.

In the following discussion the parts of the apparatus pertaining to these four elements of the seismic procedure are treated in the order named.
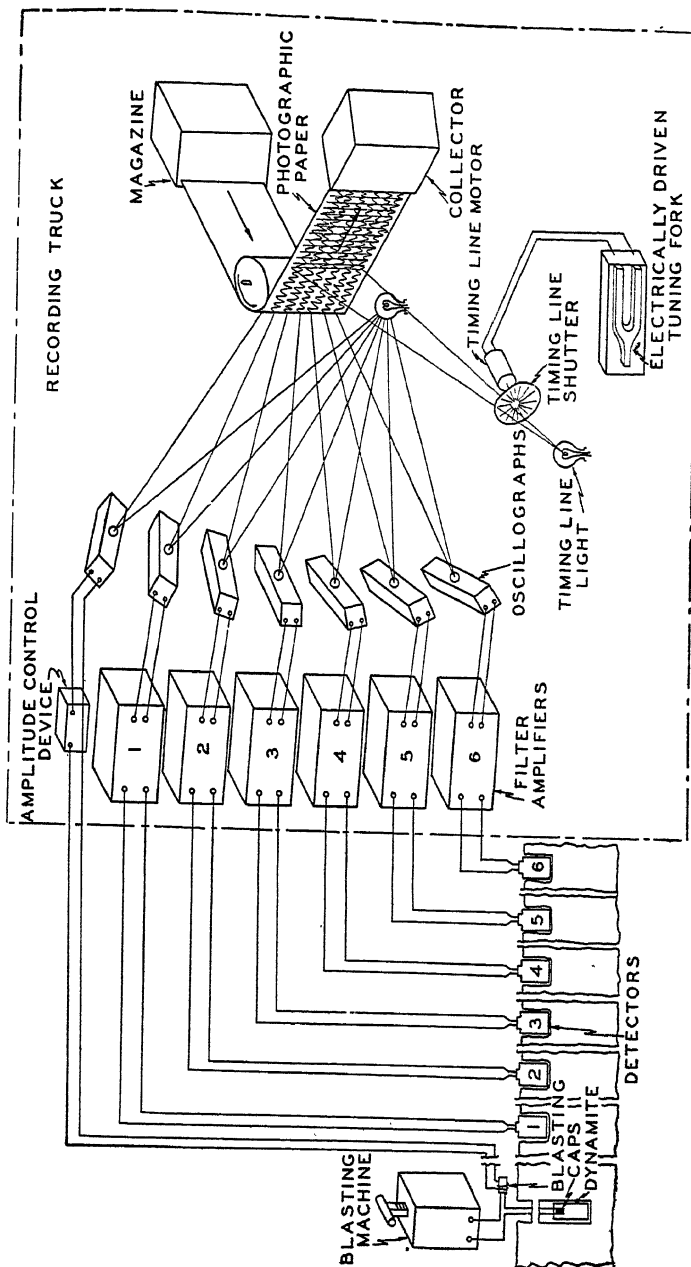
FIG. 145.—Functional diagram of essential elements of reflection seismograph field apparatus. As shown, 6 channels and reflection traces are indicated, but 8, 10, 12, or more are frequently used. Also groups of two, four, or more detectors may be used for each of the single detectors indicated. Galvanometer type oscillographs are shown, but string types are frequently used.

THE SHOT

In modern seismic prospecting, the explosive is practically always placed in a drilled hole at some distance below the surface. It was found early in the history of reflection prospecting that
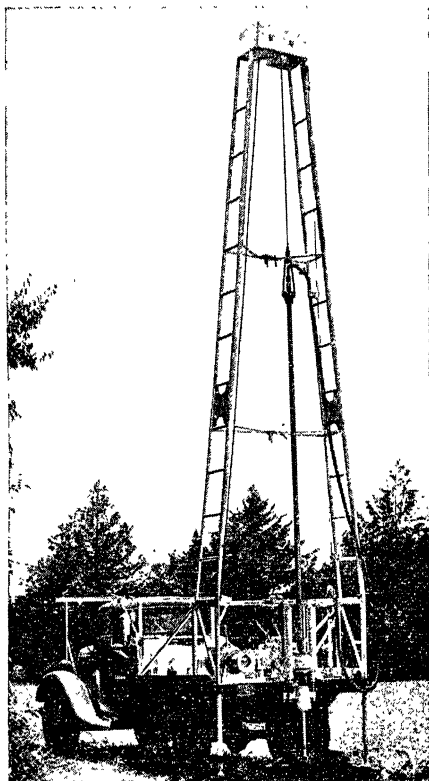
Fig. 146.—A shot hole drill.   (*Photograph courtesy G. E. Failing Supply Co.*)

very much better reflection records were obtained if the shot were placed below the low-speed surface zone.   This probably is partly because of reflection of much of the energy at the velocity boundary at the base of this zone when the shot is above it and partly because the unconsolidated near-surface material tends to absorb the energy of a shot placed within it and does not transmit wave energy efficiently to the lower, more consolidated strata.   The shot holes are usually drilled to a short distance below the surface zone.   Frequently it is found that there is a particular optimum

depth of shot hole that gives best reflections, commonly in a clay or shale layer. The average depth of shot holes is around 50 to 60 ft., but occasionally holes several hundred feet deep are used.

The Shot Hole Drill.—The shot hole drill is a complete small-scale rotary drilling outfit mounted on a heavy motor truck (Fig. 146). Special machines have been developed for this work which are capable of drilling holes to a depth of several hundred feet and can drill the ordinary shot hole quickly and economically. The usual hole is about 5 in. in diameter. Under average conditions, a modern shot hole drill will drill a 50-ft. hole in ½ to 1 hr., and a drill crew will make 6 to 10 such holes per 8-hr. day. If holes are deeper or drilling is difficult, it may be necessary to have more than one crew on the drill and work two or three shifts.

The Explosive.—The explosive is usually dynamite. The size of the charge varies enormously. Under very favorable circumstances, a charge of less than 1 lb. of dynamite will give reflections from depths of 10,000 to 15,000 ft. In another area, especially if there is soft material or loose sand at the surface, a shot of 100 lb. might be required. For refraction work the charge increases greatly with increase of shot-detector distances, and charges of many hundreds to, occasionally, one or two thousand pounds may be required. The large charges required make it almost impracticable, under ordinary circumstances, to carry out refraction work with shot-detector distances greater than about 10 miles.

The charge is usually "tamped" by filling the shot hole to the surface with water. The explosive manufacturing companies have developed special dynamites for seismograph work which will detonate uniformly under pressures up to several hundred pounds to the square inch of "tamping" fluid.

The shot is fired electrically, usually by a blasting machine (a hand-operated electric generator) which is much safer than the use of an electric battery.

The Shot Moment.—The shot moment may be indicated in one of three ways: (1) by an auxiliary electric circuit including a wire around the charge which is ruptured by the explosion, (2) by the rupture of the firing circuit itself from the explosion of the detonating cap, or (3) by a circuit which is broken by the detonation of a second cap at the surface which is electrically

connected in series with the one in the dynamite charge. The dynamite manufacturers have done considerable experimental work to produce caps of uniform characteristics, and caps are now available for which the instant of detonation is uniformly related to the firing current. Results of a detailed study of time of firing of caps have been given by Burrows.[1]

In reflection work, the shot moment usually is conveyed to the recorder by wires, as the distance from the shot to the recording truck is usually of the order of 1,000 to 3,000 ft. In refraction work, where the distance may be several miles, it is common to use radio communication. The Federal Communications Commission has allocated several frequencies for "geological stations (in the geophysical service)" which may be used for such communications by properly licensed field radio transmitters. At the present time, the frequencies assigned to such service are:

Kilocycles	Kilocycles
1,602	30,620
1,628	31,060
1,652	33,540
1,676	35,540
1,700	

SEISMIC DETECTORS

The magnitudes of the earth's movements measured in seismic prospecting are extremely small. A good seismic detector will show an appreciable response from a person stamping on the ground at a distance of 100 to 200 ft. The detectors, together with their associated amplifiers, are usually made sensitive enough so that they begin to show "microseisms." These are the continuous, very slight movements of the ground caused by the wind, especially where there are trees; by waves on a shore; or by very minute earth movements. A recent analysis[2] and measurement of modern seismic equipment indicate that ground movements with amplitudes down to the order of 10^{-8} in. can be detected. The "noise level" of these microseisms limits the maximum sensitivity of detector-amplifier systems which may be usefully employed.

[1] Burrows, 1936.
[2] Gardner, 1938.

Classification of Detectors.—All detectors contain an inertia element suspended or supported so as to permit movement between it and a frame or case connected to the ground. When the case is moved by ground motion, the inertia element tends to remain stationary so that there is relative movement between it and the case. This relative movement is either amplified mechanically and optically (now obsolete) or made to generate or control an electrical impulse of some kind. A variety of electromechanical systems has been proposed or used for seismic detectors. The nature of the mechanical-electrical coupling will determine the property of the ground movement to which a given instrument will respond. Thus, detectors may be classified according to their method of response as:

1. Displacement detectors which measure the actual movement of the ground with respect to a more or less fixed inertia mass.

2. Velocity detectors which measure the rate of movement or velocity of the ground movement with respect to a more or less fixed inertia mass.

3. Acceleration detectors which measure the force acting on a more or less fixed inertia mass.

Detectors may be further classified as tuned or untuned. A tuned detector has a natural frequency in the frequency range of ground movement most commonly useful in seismic prospecting (25 to 60 cycles per record) and is relatively undamped. In an untuned detector the natural frequency of the moving system is either much higher or much lower than that of the ground movement, and the system is more or less damped.[1]

The untuned detector will tend to give a response that is more nearly a measure of the actual ground movement than will a tuned detector. However, the usual seismic practice neither requires nor desires an actual record of the ground movement. The mechanical-electrical coupling is usually more or less complicated so that the actual response cannot be clearly classified into one of the three categories named above. Theoretically, if the mechanical and electrical characteristics of the detector and associated recording apparatus are completely known, it should be possible to derive the actual ground movement from the record,[2] but this is seldom of interest and is rarely, if ever, done in actual exploration practice.

[1] For a general discussion of seismic detectors, amplifiers, and field equipment see Heiland, 1934.

[2] Bryan, 1936, gives examples of the derivation of ground movement from

Examples of Seismic Detectors.—Brief outlines of the physical principles of a few seismic detectors are given below. The list is not complete but includes most of the types that are now used extensively or that have been used in the past.

Electromagnetic Detectors.—This type of detector (Fig. 147) depends on the voltage generated by a coil of wire moving in a magnetic field. In one form ("geophone") the coil acts as the inertia element, and the magnet is fixed to the case. In another form ("magnetophone"), the magnet is suspended and acts as
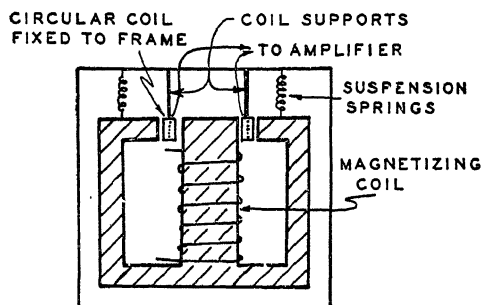
FIG. 147.—Principle of the moving coil type detector. A permanent magnet is now commonly used instead of the electromagnet indicated.

the inertia element, and the coil is fixed to the case. In either type there is relative motion between the coil and magnet when the instrument is moved. The voltage generated is proportional to the relative velocity of the parts, so the instrument may be classed as having a velocity response.

In earlier instruments of this type, the required strong magnetic field was supplied by a magnetizing coil. More recently the development of new permanent magnetic materials, such as "Alnico," has made the magnetizing coil and current unnecessary and reduced the size of detectors of this type. It is probable that the electromagnetic detector is the type most commonly used in the field at the present time.

Schweydar's Mechanical Detector.—This type of detector was used extensively in fan shooting for salt domes in the Gulf Coast

two detectors exposed to the same movement but having very different characteristics and giving records of quite different appearance. The ground movements calculated from the two different records were quite similar.

Also, see Hagiwana, 1935.

but is now quite obsolete. In principle this instrument (Fig. 148) consists essentially of a lead sphere suspended by a flat spring. A long, light aluminum cone magnifies the motion of the sphere. The top of this cone carries a bow with a thread which is wrapped around a slender spindle which carries a mirror. For any motion of the lead ball the bow is moved, and the spindle slightly rotated. A beam of light from the recording apparatus is reflected from this mirror, and any motion is recorded on a moving photographic paper or film. The instrument is made
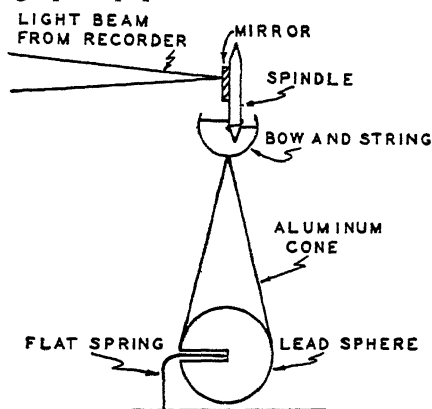
FIG. 148.—Principle of Schweydar's mechanical seismograph.

for either vertical or horizontal motion, and a combination instrument which has two elements and which measures both components simultaneously has been used in the field.

Microphone Detector.—The carbon microphone, similar to that used in an ordinary telephone transmitter, can be used as a seismograph detector. A schematic arrangement is shown in the diagram (Fig. 149). Since the microphone must be used with its face vertical, it is necessary (for a vertical seismograph) to have a mechanical arrangement by which vertical motion is changed to a horizontal motion. Microphones have not been very satisfactory, because it is difficult to make one that is stable and has a constant sensitivity; but some field seismographs have made use of them. Since the motion of the carbon microphone is extremely small, the response is proportional to the pressure on the face of the microphone unit. The microphone is therefore sensitive to the force developed by the motion and hence to the acceleration of the earth movement.

Single Carbon Contact Detector.—Figure 150 shows the principle of an ingenious arrangement by Ambronn in which a single carbon contact is the sensitive element. This contact is carried on a balance arm the other end of which carries a pair of coils arranged so that the pressure of the carbon contact can be delicately adjusted by an electric current through the two coils. This adjustment can be made from the operating control panel, and in this way a sensitive condition of the carbon contact can be assured for each setup. The coil attached to the balance arm acts as the inertia element. This instrument was designed to give sharp first arrivals for refraction work but would not be suitable for reflection work, as it does not reproduce with any accuracy the actual form of the ground movement Since the resistance of the carbon contact is proportional to the pressure, this instrument is sensitive to the acceleration of the earth's movement.

Fig. 149.—Principle of the carbon microphone detector.

Hot-wire, or Thermophone, Detector.—This detector (Fig. 151) depends upon the principle that the resistance of a heated wire
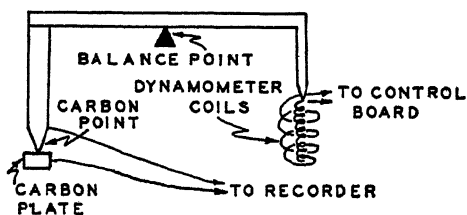
Fig. 150.—Principle of Ambronn's single carbon contact detector.

is very sensitive to the cooling effect of moving air. A grid of fine platinum wire is arranged over an opening, or throat, which connects with a very narrow air space between a fixed plate and a flexible diaphragm. The inertia element is carried on this diaphragm. Any movement of the diaphragm changes the volume of the narrow air space and causes a flow of air in or out through the throat and past the hot wire. The change of resistance is determined by a resistance bridge and is recorded on a suitable instrument. Since the change of resistance is propor-

tional to the velocity of the air through the throat and this in turn is proportional to the rate of change of the distance between the diaphragm and the fixed plate, the instrument is sensitive to the velocity of the diaphragm and therefore to the velocity of the earth's movement.
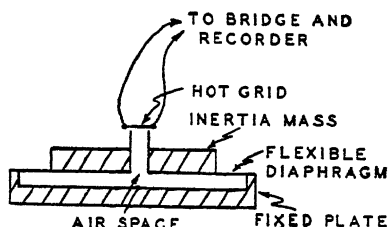
FIG. 151.—Principle of the hot-wire, or "Thermophone," detector.

Piezoelectric Detector.—This type of detector (Fig. 152) depends upon the well-known piezoelectric effect by which an electric charge is produced on the faces of a properly cut crystal of certain materials, particularly quartz and Rochelle salts, when the pressure between the crystal faces is changed. The detector is made
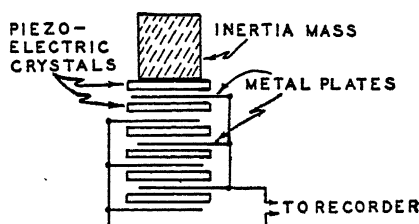
FIG. 152.—Principle of the piezoelectric detector.

of a pile of such crystals (usually quartz) with intervening metal foil to collect the charge. An inertia mass is mounted on the top of the crystal stack. The motion of the crystals is extremely small, and the effect depends upon the change of pressure and therefore on the acceleration of the ground movement.

Variable Reluctance Detector.—This type of detector depends upon the variation in the reluctance of a magnetic circuit produced by relative motion of its parts. In one type (Fig. 153) a thin iron armature is supported between the poles of permanent magnets. Movement of a mass connected to this plate causes movement of the armature which results in a change of magnetic

flux through the armature. This change in flux induces a voltage in a coil surrounding the armature. More elaborate devices of this kind have also been proposed which involve a change of reluctance in a magnetic bridge. Next to the electromagnetic type, it is probable that the variable reluctance type of detector

BALANCED ARMAT

TO AMPLIFIER

MAGNET

FLAT SPRING

INERTIA MASS
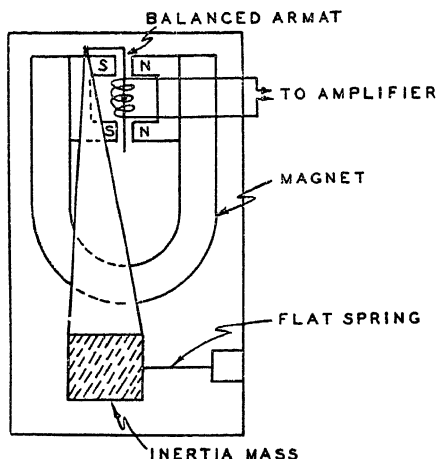
FIG. 153.—Principle of one type of variable reluctance detector.

in some form is the most commonly used in present-day seismic exploration.

THE AMPLIFIER-FILTER-RECORDER SYSTEM

The small electrical impulse from each detector (or detector group) is transmitted by a cable to an amplifier-filter. The details of the electrical system for the amplifier-filter vary greatly among different oil and prospecting companies. However, the amplifier is nearly always an arrangement of vacuum tubes, condensers, transformers, and resistors which are quite similar to the corresponding parts of the audiofrequency amplifier system of an ordinary radio receiver. The component parts from which the amplifiers are built are nearly all obtained from the radio trade. The maximum voltage gain of the amplifiers is sufficient to give a slight output from normal ground unrest, or microseisms. The over-all amplification of the system (*i.e.*, the ratio of the amplitude of the response on the record to the amplitude of the ground movement) is usually in the range 10^6 to 10^7.

The amplifier is very frequently combined with a filter. This is desirable because it is found that much clearer reflections are indicated when a selected frequency range is amplified. Usually the desirable reflections are in the range of 25 to 60 cycles per second. Lower frequencies, particularly the "ground roll," which is the result of a slow-speed surface wave, are often present and cause undesirable impulses on the records unless removed. The frequency characteristics of the reflections vary with the nature of the underground materials so that different filtering may be desirable in different areas. Therefore, some filter systems are made adjustable to pass the most favorable frequencies for each field condition. The over-all frequency characteristics of the system depend on the frequency response of the detector itself as well as the filter. Therefore, the electrical design of an efficient amplifier-filter system must take into account the electrical and mechanical characteristics of the associated detector with which it is intended to be connected. In fact, in some instruments the chief filtering action is in the detector itself, rather than in the electrical system.

Variable Gain Control.—In recent years, it has become common practice to use some sort of variable gain, or volume, control in the amplifier. The variable gain may be an "expander" by which the amplification is increased with time after the first impulse is received, to compensate for the lower amplitude of later reflections. The alternative volume control is similar to the "automatic volume control," commonly used on radio receivers to give a nearly constant output (loudness) with a widely varying strength of the received signal. Such control is desirable on the seismic amplifier so that strong impulses from shallow reflections can be read on the same record with very weak impulses from deep reflections.[1] Without such control, it may be necessary to fire several shots of different magnitude and make different records to show shallow and deep reflections.

Oscillographs.—The output of each amplifier is connected to an oscillograph, or galvanometer unit. Two types of unit have been widely used.

One type uses the principle of the string galvanometer in which a very fine wire (or metal-coated quartz fiber) is lightly stretched in a strong magnetic field. When a current passes

[1] Norman, 1939, p. 13.

through the filament, it is deflected by the magnetic field. A magnified image (shadow) of the filament is focused on the photographic recording paper. The string galvanometer permits a very compact instrument, as a number of strings, sometimes called a "harp," can be stretched in a very small space in the same magnetic field. As many as 12 strings are used in the same galvanometer.

The second type uses a tiny coil suspended between the poles of a permanent magnet. The coil carries a very small mirror from which a beam of light is reflected and focused as a fine spot on the photographic recording paper. As the variable current from the amplifier passes through the coil, it rotates slightly in the magnetic field and deflects the spot of light on the paper.

Modern recorder systems carry at least 6 and frequently 12 or more oscillograph elements, all focused on the same strip of photographic paper. One of the elements may be used separately to give the shot moment, or the shot-moment circuit may be coupled to one (or several or all) of the same oscillograph circuits that are used for recording the detector impulse.

The Camera System.—The "camera" is the mechanism for passing the sensitive photographic paper under the light beams from the oscillograph elements. It consists essentially of a magazine which holds a roll of sensitized paper, a rotating drum, and a collector in which the exposed paper is wound up. The collector is easily removable so that the exposed film can be developed immediately. The camera drum and collector are driven by a spring motor or electric motor. The paper speed is commonly around 1 ft. per second. The photographic paper usually used is 6 in. wide. The photographic supply companies have developed special papers with highly sensitive emulsions for seismograph use. Recently, some manufacturers have begun packing the rolls of paper (about 200 ft. in a roll) in hermetically sealed tin cans.

The record usually is developed immediately after exposure, either in a developing compartment in the same truck that carries the instrument or in a developing box, which is a light-tight box in which the developer manipulates the film from the outside through light-tight sleeves fitting over his arms. This assures that a satisfactory record has been made before the "spread" of detectors, connections to recorder, etc., are disturbed.

THE TIMING SYSTEM

Since the travel time of the seismic wave is the fundamental quantity measured in seismic prospecting, it is necessary to provide a reliable timing mechanism. The primary time standard is usually a carefully calibrated, electrically driven tuning fork. This fork is made to actuate a mechanism that puts timing marks of some kind on the tape.

In the earlier equipment the tuning fork actuated an oscillograph element which made a timing trace at one edge of the record. Present instruments nearly all use a timing line which goes entirely across the tape. This line is controlled by some sort of shutter or rotating disk which makes flashes of light across the tape. The shutter speed is controlled by the tuning fork, commonly through a motor that is synchronized with the fork. It is usual to provide an arrangement such that the tenth-second lines are heavier than the others, so that the counting of time intervals on the tape is facilitated. The timing lines are usually 0.01 or 0.005 sec. apart which, with a tape speed of about 1 ft. per second, makes lines about 0.1 in. apart on the tape (for a time interval of 0.01 sec.). With such tape speeds and timing lines, it is relatively easy to read time intervals on the tape to one-thousandth of a second. This is about all the precision that is useful, as other sources of error, such as weathering corrections, shot moment, and the marking of reflections, contribute variations that may total several thousandths of a second.

The timing also may be considered to include the coordination between shot and recorder. Since the total exposure of the record lasts only 3 or 4 sec., it is essential for the starting of the exposure to be controlled by the shooter or for the shot to be controlled by the recorder operator. This control may consist of verbal telephone orders, given to the shooter by the operator over the shot-moment recording circuit, the operator giving his order when his tests show all equipment ready for the shot to be fired. Actual control of the shot by the operator has been used. However, this practice is somewhat dangerous, especially if the operator cannot actually see that conditions at the shot point are clear, and has led to accidents. In usual field practice, the starting of the recording paper through the camera and the firing of

the shot are coordinated closely enough so that the record is exposed for not over about $\frac{1}{2}$ sec. before the shot moment is recorded.

THE RIEBER "SONOGRAPH"

A system of seismograph recording that is somewhat different from the common systems already described is the "sonograph" developed by Frank Rieber[1] in California. This has carried some of the technique of sound recording from the moving-picture industry to seismic prospecting.

In this system the ordinary oscillograph traces are replaced by "sound tracks" of variable transparency on a moving-picture film—10 tracks from 10 different detectors being recorded side by side on the same film. This film is then run through an "analyzer" in which beams of light pass through the individual "sound" traces and shine on a photoelectric cell which converts the variable light intensity into a variable electric current. A recording pen is actuated by this current. If the light is controlled by a single track, the pen makes a trace that would
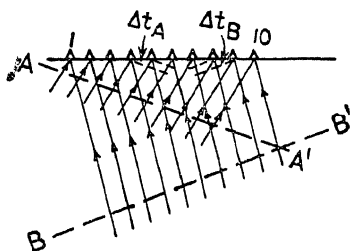
Fig. 154.—Crossed wave fronts, indicating reflections arriving simultaneously from different directions.

correspond with the ordinary oscillograph trace from a single detector. However, the analyzer is arranged so that the photoelectric cell may be actuated by the instantaneous sum of the light from all of the 10 tracks. In this way, effects that reach the various records "in phase" are added up to give a relatively large disturbance of the recording pen, whereas random effects that are not in phase tend to cancel each other.

The distinctive feature of the sonograph system is the possibility of making variable time "offsets" between the light beams passing through successive records. If there are certain regular time differences between wave arrivals at successive detectors, there will be a maximum amplitude of response of the recorder pen when the offset times are set equal to these time differences

[1] Rieber, 1936a, 1936b; 1937.
Johnson 1938.

to bring the successive responses in phase. These time intervals will correspond to a wave reaching the detectors at a certain angle with the surface. Thus, in Fig. 154 a wave front AA' will strike successive detectors at a time interval Δt_A. If the time offsets between light beams passing through successive tracks when run through the analyzer are set equal to Δt_A, the impulses will all add up in phase and give a maximum response of the recorder pen. By running a series of analyzer records, set with systematically variable offset times, the setting corresponding to maximum response can be found, and the angle at which the corresponding wave reached the detectors can be determined. A second wave front, such as BB', striking the detectors from an entirely different direction would give a maximum response at a quite different setting of the offset times, corresponding to the time Δt_B. In this way it is possible to determine the direction of separate wave fronts, even when they strike the detectors at the same time and crisscross one another, which would make a very complex and confusing pattern on an ordinary record.

The sonograph was developed for the application of reflection seismograph methods to areas of complex geology and steeply dipping beds. It should be useful for disentangling complex reflection patterns in such cases. In simple structural situations and regions of gentle to moderate dips it is doubtful if it has any great advantage over the usual methods. It is considerably slower and more expensive in the field than the conventional seismic methods, and therefore its principal utility probably will be in attempting to work out special problems that are too complex for ordinary reflection prospecting.

CHAPTER XVIII

SEISMIC FIELD OPERATIONS AND INTERPRETATION

RELATION OF RESULTS TO FIELD OPERATIONS

In seismic prospecting the interpretation and final results are closely dependent on the technical details of the field equipment and the manner of its distribution on the ground. This is quite different from the conditions in gravity and magnetic prospecting, for their interpretation requires little concern with the details of the field technique or instruments by which the data were obtained other than assurance as to the precision and the adequacy of reduction of the results. Once a gravity or magnetic survey is made, the area is permanently covered. Resurveys are required only if means and demands for higher precision are developed or closer control is desired. On the other hand, the character and utility of a given seismic record depend upon many details of the field work, such as the charge and depth of the shot, type and natural frequency of detector, filtering, volume control, spacing of detectors, multiplicity or interconnections of detectors. For this reason many areas have been shot once with only shallow or with poor or useless results, only to be reshot later when improved equipment, larger charges, deeper shot holes, or different detector spreads afforded much better or deeper records. Thus, we cannot safely say that the seismic exploration of an area is complete with a given amount of coverage at a given time because new instruments and field methods or new geological conceptions, such as deeper production possibilities, may make it desirable to reenter an area once considered thoroughly tested.

The close dependence of results on the details of the field operation requires that a seismograph field party include an interpreter to work up records daily. This permits modification of the field procedure, particularly shot depth, detector spread, and filter settings, to improve or maintain record quality. Usually at the beginning of a survey of a new area, certain preliminary

tests and experiments are required or desirable to adjust the details of field operation to give the best results.

SEISMOGRAPH FIELD PARTIES

The organization and personnel of seismograph field parties are not standard, but certain more or less regular procedures are carried out by different operating companies under similar working conditions. The general deploy of a seismograph party in the field is illustrated by Fig. 155. The approximate organization, personnel, and equipment of a field party for operation from motor trucks in areas of reasonably favorable surface conditions will be somewhat as shown in the table on page 334.

The organization outlined there totals 16 men and eight pieces of motor equipment. Such an organization, together with the supplies, dynamite, maintenance, and depreciation of equipment, etc., will cost from $7,000 to $10,000 per month to keep in the field.

Seismograph operations have been and are being conducted under a great variety of surface conditions, and seismograph equipment has been taken into almost impenetrable areas. Under such conditions the organization and equipment of the field party will differ greatly from that outlined above. For instance, in working the marsh areas of the Gulf Coast, practically all the equipment is carried on boats or barges. Special means of transportation, such as buoyant marsh buggies or wide-wheeled swamp buggies, have been developed and used in such areas. In swamps and other places where the material immediately beneath the surface is very soft, the shot hole drill may be dispensed with, and shot holes put down by "jetting." A pump driven by a small gasoline motor, such as a large-size outboard boat motor, circulates water through a pipe which is rotated slowly by hand. In some areas it is possible to put down shot holes by jetting much faster than by drilling, and holes well over 100 ft. deep have been made in this way. Also, the transportation of heavy drilling equipment is eliminated. In extremely difficult areas it may be necessary to pack all the equipment on the backs of men or mules. Under such circumstances certain redesigning and rearranging of individual units of equipment is required so that it can be divided up into small, rugged, individual units for such packing.

Personnel	Duties	Equipment
One party chief....	General charge of all operations of the field organization	One party chief's car
One permit man...	Arranging permission with landowners for entrance upon private land or in some states for operations along roads adjacent to private land	One permit man's car
One surveyor and two rodmen.	Making the necessary surveys for determining elevations and locations of all shot-point and detector positions	One surveyor's truck or car
One driller and two assistants.	Drilling shot holes. In difficult areas more than one drilling crew may be required	One shot hole drill, one driller's water truck (for providing water for drilling mud)
One shooter and one assistant.	Loading the shot holes, tamping the shots, and firing the shots on instruction from the instrument operator. Two shooters may be required if shots are made both ways to each detector spread. Assistant drives truck for water when necessary	Shooter's truck, commonly equipped with a tank; for hauling water for tamping holes, dynamite, tools, etc.
One instrument operator and one developer.	The instrument operator has general charge of the recording equipment. The developer develops the records on location so that the operator may know that a satisfactory record has been obtained before completing operations for a given detector spread	One instrument truck with two compartments, one of which contains amplifiers, oscillographs, and all recording equipment; the other, a photographic darkroom, for developing the records
One lineman and one assistant.	Laying out and picking up of detector cables, shot-moment wires, etc.	One wire truck with reels for handling detector cable, etc.
One office interpreter and one computer.	Interpretation of records currently with operations, to guide the fieldwork, make maps and reports of results, etc.	

THE DETECTOR SPREAD

The term "spread" refers to the general arrangement, on the surface, of the detectors with respect to one another and the shot point. The details of the individual detector spreads, the interval between spreads, the number of shots for each spread, and the number and connections of the detectors vary greatly from one area to another and from one prospecting organization to another. These variations are the result of a great number of experiments to attempt to improve record quality so that reflections are more easily recognized. As a result of the development of equipment and field technique, it now is possible to obtain workable reflections in areas that a few years ago gave hopelessly complex records on which reflections could not be recognized.

In a general way, detector spreads may be divided into "short spreads," in which all the detectors are within a distance of about 1,000 ft. or less from the shot point; and "long spreads," in which the detectors are in an interval of around 1,000 to 4,000 ft. or more from the shot point. Other things being equal, a short spread is preferred because less wire and detector cable is required for connecting shot-moment circuit and detectors to the recording unit. However, a long spread may have a decided advantage when there are strong surface disturbances from the shot which may be attenuated or may not reach more distant detectors before the desired reflection events. In some areas, such as the Gulf Coast, there is a low-frequency, very slow-moving, apparently surface wave, called "ground roll,"[1] which may be avoided by choosing a detector spread such that it has passed the detector (short spread) or has not yet reached the detectors (long spread) by the time the reflected events of principal interest arrive.

In many areas there is a certain degree of anisotropy in the velocities; *i.e.*, the wave velocities parallel and perpendicular to the bedding are not the same. This may lead to difficulties with long spreads which have an appreciable component of the

[1] The "ground roll" may be a Rayleigh wave or a Love wave. However, its velocity is usually very low, and it is difficult to find velocity ratios consistent with the expected theoretical ratios between Rayleigh or Love waves and the longitudinal wave velocity of the surface layer. It is possible that velocity ratios more nearly in accord with theory would be obtained by considering the longitudinal velocity of only a thin layer very near the surface.

wave path parallel to the bedding. When reasonable values for the vertical velocity are used, corrected depths or times do not come out continuous or parallel from spreads shot in opposite directions, as they should if the wave velocities were isotropic and the wave paths linear.
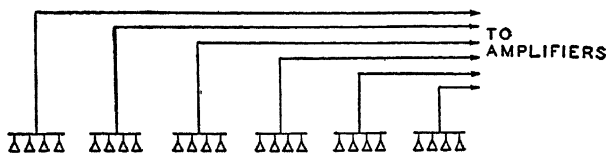
FIG. 156.—Multiple detectors—simple combination.

In recent years it has become common practice to use a number of detectors for each amplifier-recorder circuit. Such multiple detectors have the advantage of tending to combine impulses from vertically traveling waves and to cancel out impulses of horizontally traveling waves and thus to give greater amplitude to true reflection events and less to certain disturbing waves. Two different methods of connecting multiple detectors are used: "simple combination" and "overlapping combination."
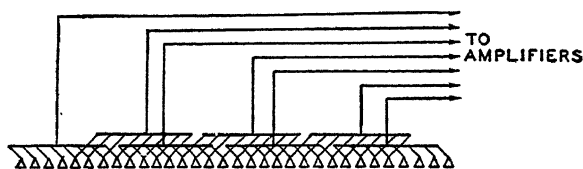
FIG. 157.—Multiple detectors—overlapping combination.

The simple combination uses separate groups of detectors, each group being connected to a single amplifier-recorder circuit (Fig. 156). Then each record trace is derived from ground movements within the zone covered by a single group of detectors.

The overlapping combination uses groups of detectors with overlapping connections (Fig. 157) so that each detector impulse contributes to more than one trace on the record. In this way each individual trace is a "running average" of the detectors to which it is connected. Since part of the energy recorded by any two adjacent traces on the record is derived from detectors that are connected to both recorder circuits, the overlapping combination tends to give a forced similarity to adjacent traces. This makes a record on which reflections stand out across the tape

from one trace to another. The degree to which overlapping should be carried is questionable. If carried too far, it may defeat its purpose, for the overlapping connections may cause a strong, erratic disturbance to give a simultaneous record on several traces and make it look like a real reflection. The real test of any special method of connecting detectors is in the quantative analysis of the results and the consistency and reliability of the subsurface geological picture produced.
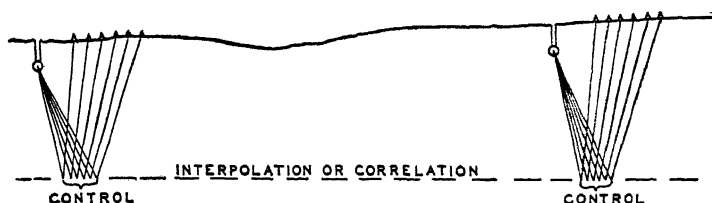
Fig. 158.—Reflection paths for single shot-detector spread.

Ground Plan of Reflection Prospecting.—The interval between successive detector spreads varies greatly, depending on the purpose of the survey and precision required, the nature of the underlying geologic section, the surface conditions controlling access to the area, and the technical policies of the operating company. In early days of reflection prospecting it was common practice
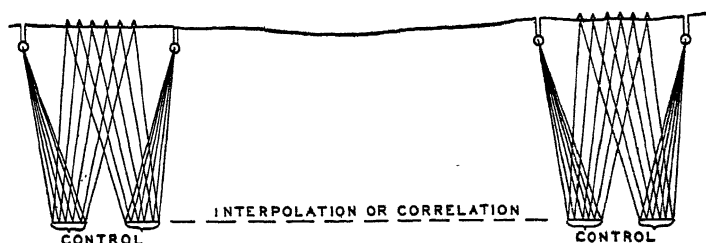
Fig. 159.—Reflection paths for single detector spread with two-way shot.

for shot points to be a mile or more apart. More recently the general tendency has been to use closer control, for experience has shown that serious errors may occur in assuming geologic continuity over large gaps in the control; also subsurface details of geologic importance may be missed. More common modern practice is to have shot points of the order of $\frac{1}{4}$ mile apart with the detector spreads covering much or all of the interval between shots.

Various different distributions of detector spreads with increasing closeness of control are diagrammatically indicated by Figs. 158 to 162. The choice of spread depends on many factors.

The "single-shot" spread (Fig. 158) can be used in "good shooting" areas where the records are simple and a few definite
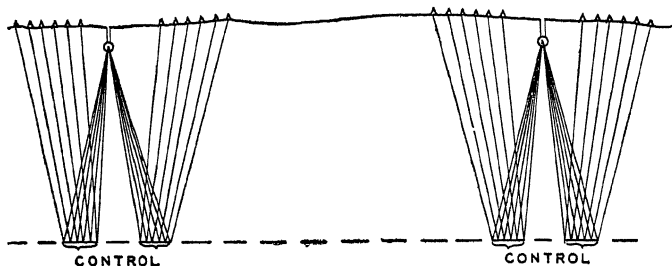
FIG. 160.—Reflection paths for single shot with two-way detector spread.

and clearly recognizable reflections are obtained, which can be correlated from one location to another. This was the general type of spread used in much of the early work in Oklahoma.

The "two-way shot" (Fig. 159) and the "two-way spread" (Fig. 160) are equivalent in the amount of subsurface control that they give. The choice between them is principally controlled by
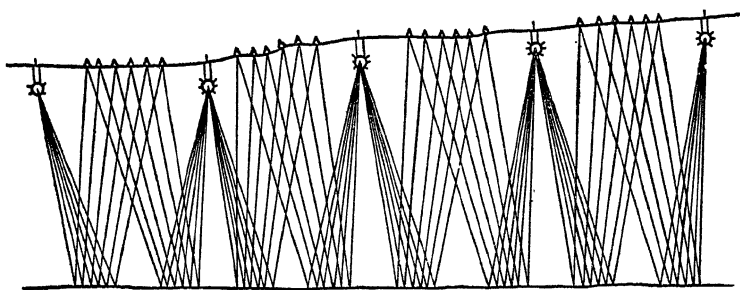
FIG. 161.—Reflection paths for continuous spread.

the relative cost of shot holes and of setting out detectors. The two-way spread is particularly adapted to operation with a double set of detectors and recording apparatus.

When correlations become somewhat uncertain, the spreads may become continuous (Fig. 161). This leaves only rather short intervals between subsurface control points, across which reflections must be correlated. This arrangement may be used either with a two-way instrument spread or with a double shooting crew, shooting toward each spread from both sides.

Finally, when maximum detail is desired or reflections are very difficult to follow from one spread to another, the shooting may be closed up to give "continuous center-point" control. One pattern for such control is shown by Fig. 162. The points of control obtained are indicated by the braces along the hypothetical reflecting horizon. For example, the brace 1-*B*
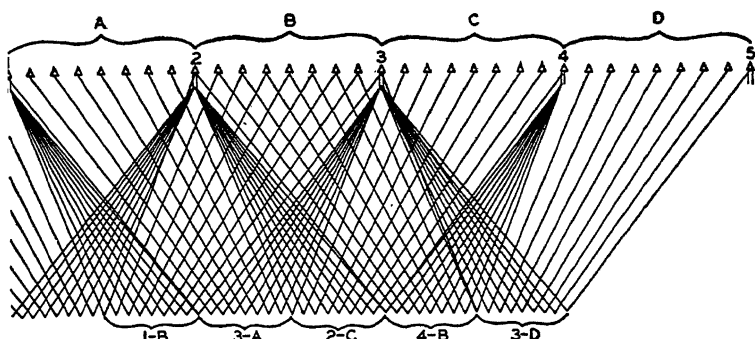
FIG. 162.—Reflection paths for continuous center-point control.

embraces the reflection points determined by wave paths from shot point 1 to detector spread *B*.

SHOT HOLES AND SURFACE VELOCITIES

There is usually an optimum practical depth at which the shot should be placed. This will depend principally on the thickness of the surface zone, or "weathering." Also, the wave velocity in the surface zone must be known to determine a value for V_0 to be used in the surface zone corrections. Therefore, it is a desirable practice on beginning exploration in a new area to carry out certain preliminary tests to determine these factors.

Tests may be made by shooting a series of shots at various depths, say at 10-ft. intervals,[1] in a hole drilled well below the surface zone (Fig. 163). If records of the waves from such shots are made by one or more detectors at the surface near the shot hole (detectors 1, 2, 3) and also by a spread of detectors at distances comparable with a normal detector spread (detectors 4, 5, 6), it is possible to. measure or determine

1. The velocity characteristics of the surface zone (from interval times of first arrivals at detectors 1, 2, and 3 for individual shallow shots).

[1] Ittner, 1939.

2. The vertical velocity of the underlying "unweathered" zone (from intervals of first arrivals at separate detectors 1, 2, or 3 for successive deeper shots).

3. The thickness of the weathering at the hole (from the break in velocity between 1 and 2).

4. The horizontal velocity of the top of the "unweathered zone (from the difference in first arrival times at detectors 4, 5, 6).

5. The optimum shot depth (from the shot depth giving best reflections at detectors 4, 5, 6).

Frequently the optimum shot depth is just below the base of the weathered layer. In some areas the best shot position is just
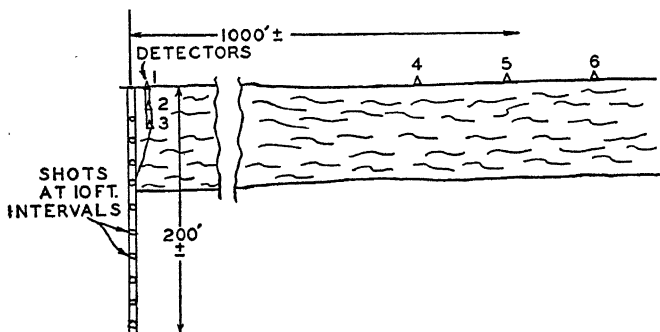
Fig. 163.—Preliminary test shooting to determine optimum shot depth and surface zone velocities.

below the ground-water table. Sometimes there is a definite bed, such as a shale or clay bed, within or just below which a shot gives best results. If such a bed can be recognized in drilling, each shot hole is drilled to that bed.

MARKING SEISMOGRAPH RECORDS

The first step in the interpretation of reflection seismograph results is the marking of the records. This may be considered to include the necessary accessory operations of marking first arrivals for weathering corrections, calculating these corrections, and marking the time scale on the timing lines. Marking reflections may be a very simple matter when records are good or a most difficult one if reflections are poor.

If records are very good, there may be a few outstanding reflection pulses[1] on all the records, the pulses having similar

[1] The term "pulse" is used to designate a small group of waves, which is considered to indicate a reflection. The pulse may consist of a single peak

character from one record to another. Then, it is necessary only to select a particular characteristic, such as the first peak or the first trough of each pulse used, and mark that point on each trace on the record (Fig. 164).

If reflections are poor, it may be difficult to find patterns that are continuous even across the traces on one record. Then it may be necessary to mark all events on each record that look like reflections by marking all peaks or valleys that appear to carry across the record. Selection of the events that probably are reasonably continuous reflections is then left until the reduced times or depths are plotted on the profile. This plot may show that reasonably good and consistent reflections are being selected, even though they do not appear very definite on the record. It also may show that events which look like good reflections are not, because they do not carry from one record to another. However, it is often possible to use reflections that appear on only one or two records, for they are true reflections from lenses or nonpersistent beds. They often give fairly satisfactory and reliable indications of dips, even if they cannot be correlated from one record to another.

Frequently, a given pulse on the record will gradually change character across the tape. For instance, a reflection pulse may appear with two maxima on the trace at one edge of the tape, and the character may gradually change so that by the time the trace at the other edge of the tape is reached the pulse contains three maxima, or it might be contracted to a single maximum. For example, Fig. 165 is marked to show a reflection for which the pulse appears with two prominent peaks with an intermediate minor peak on the first few traces. In the lower traces the same pulse has a single prominent peak, and the intermediate one has disappeared. In cases like this it is often difficult to decide which peak or valley should be marked to correspond across one tape or from one record to another. In plotting up results it may be found that the reflection times or depths are not continuous but have a small displacement. This discontinuity

---

or trough on the trace but more commonly includes two or three peaks and troughs. The detailed nature of the pulse depends in part on the physical properties, thickness, velocity contrast, etc., of the rocks causing the reflection and in part on the mechanical and electrical characteristics of the detector-amplifier system.
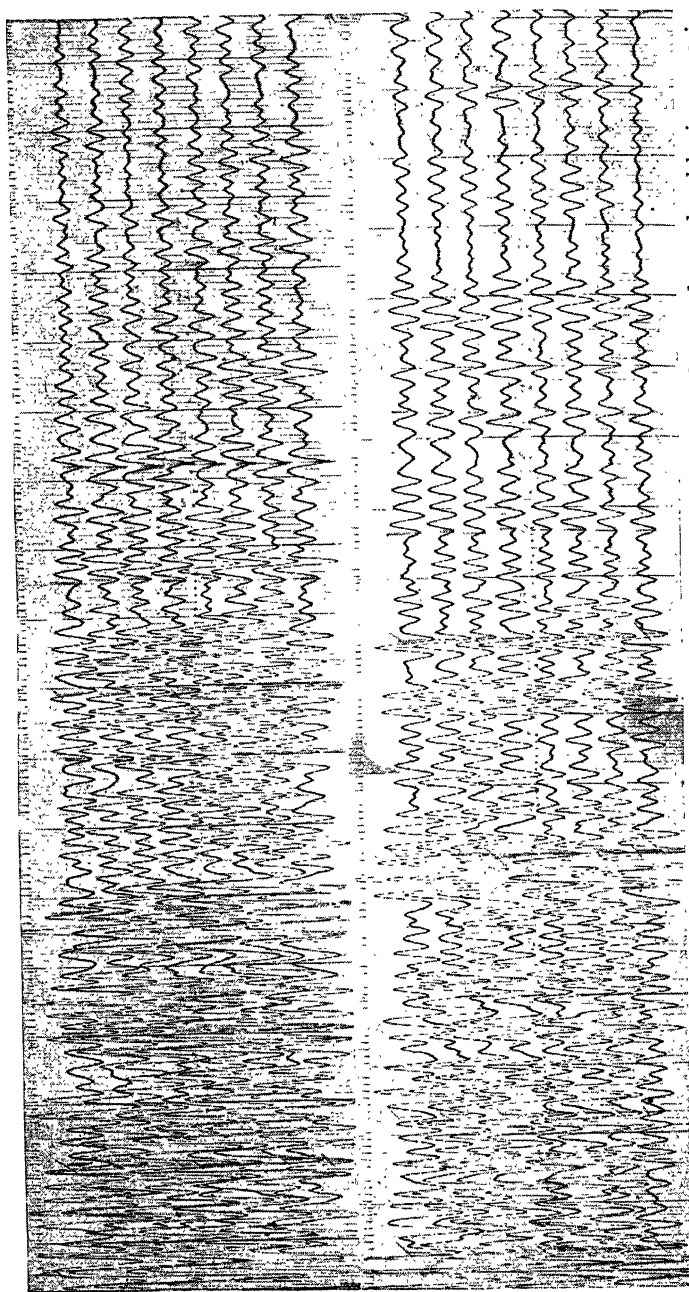
FIG. 164.—Seismograph record showing several good, easily marked reflections. The part of the record reproduced begins approximately 1 sec. after the shot moment and therefore shows reflections coming from depths below about 5,000 ft.
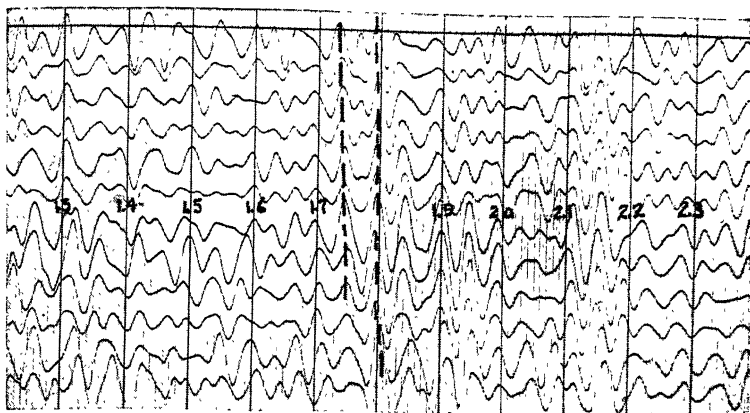
FIG. 165.—Seismograph record showing change of character.
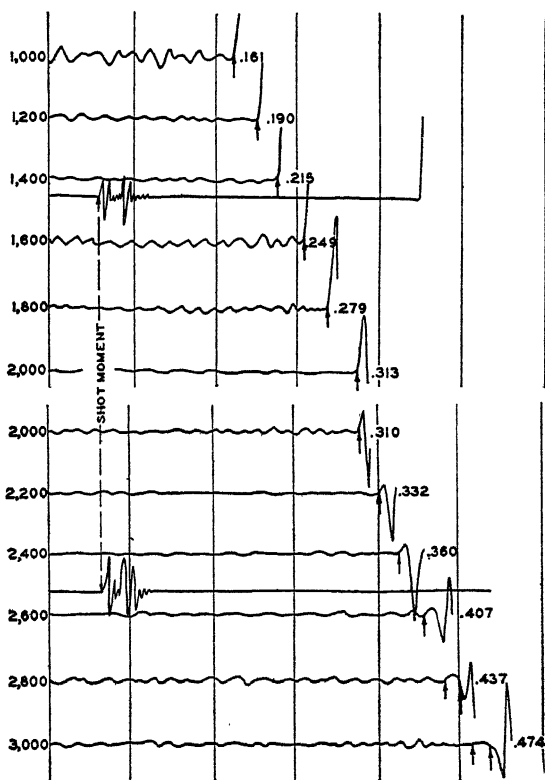
FIG. 166.—Seismograph record showing complex first arrival.

corresponds to jumping one cycle in marking the reflection and means that a wrong choice has been made in following the phase of the reflection pulse across the tape or from one record to the next. The time between cycles is commonly of the order of 0.02 to 0.04 sec. which, with a velocity of the order of 10,000 ft. per second, means that jumping one cycle will correspond to an apparent depth discontinuity of the order of 100 to 200 ft.

The marking of first arrivals, to be used for weathering corrections, is usually straightforward, as the energy in these waves is
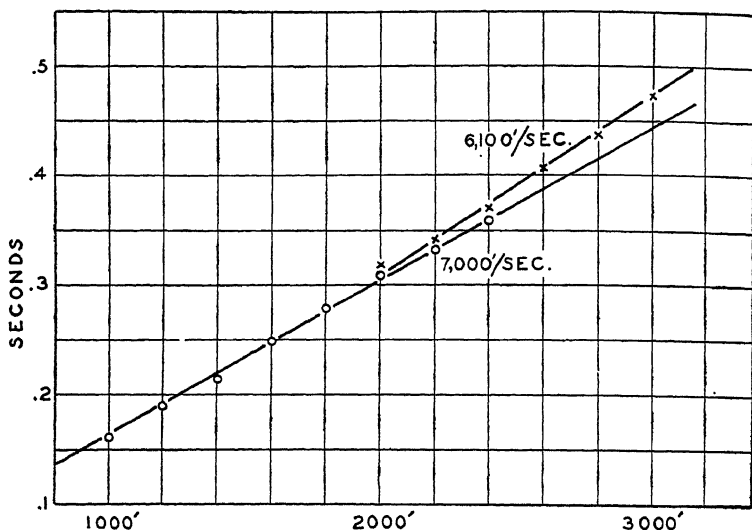
Fig. 167.—Time-distance curve for first arrivals of Fig. 166.

relatively large, and they make very definite, sharp breaks on the traces and are easily marked. However, if the detector spread is wide and the first detectors are quite near the shot, there may be a distinct change in the nature of the first arrivals. This usually means that the energy carried in the fastest event becomes too weak to be recognized and a slower but stronger wave is the first event clearly shown. Figure 166 shows part of a record that has complex first arrivals. A higher speed bed causes an upward break on the first three traces. A slower speed bed with a downward break follows about 0.01 sec. later. By the last three traces the higher speed impulse is practically unrecognizable. By plotting a time-distance curve (Fig. 167) it is evident that the higher speed is about 7,000 ft. per second

which, if the arrival persisted, would appear at the times indicated by the first arrows. From Fig. 166 the stronger later event is carried by a bed with a speed of about 6,100 ft. per second.

THE REFLECTION PROFILE

The primary basis for the interpretation of reflection results is a depth or time profile (Figs. 169, 170). This corresponds in a rough way with a geologic cross section. It is simply a plot, either of reflection times with all surface and angularity corrections properly applied or of reflection depths calculated from these times. (Once the reflection events and first arrivals are marked
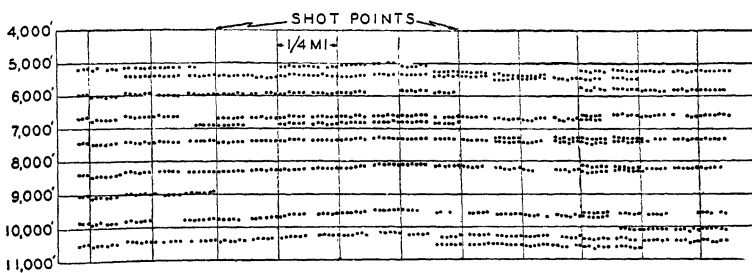
Fig. 168.—Reflection profile from continuous control. Plotted points are depths calculated for each detector position at horizontal positions midway between shot and detector, corresponding to the "center point," or reflection point, of the reflected wave. Note that some reflecting horizons are much more continuous than others, but none is continuous across the profile. This profile shows a definite structure in deeper horizons but not in upper layers, indicating a geological unconformity. Note particularly reversal in dip at about the center of the profile as shown by the reflections from around 9,500 ft. depth.

on the records, the calculation of the reflection times or depths is a straightforward, routine process, carried out by one of the reduction methods of Chap. XVI.) For each reflection event marked on each record trace, a point may be plotted on the profile. For low or moderate dips (up to several degrees) the point is plotted at a horizontal distance midway between shot point and detector (corresponding to any one of the reflection points, as shown on Figs. 158 to 162). The number of levels, or "horizons," at which reflection points are plotted, will depend on the number of "workable" reflections on the records.

The amount of control on the reflection profile will depend, of course, on the type of detector spread. This will be controlled by the reliability of the reflections and by the general geologic nature of the underground section. Where there are distinct lithologic changes between geologically continuous beds, the

same reflections with approximately the same depth or time intervals appear regularly on the records, and in such cases it may be possible to shoot separate spreads (Fig. 158, 159, or 160) a mile or more apart. Under very favorable conditions it is even possible that an experienced interpreter may recognize a particular reflection as coming from a particular geologic horizon, such as the top of the Hunton or the top of the Viola lime in Oklahoma or the Austin or Pecan gap of northeast Texas. When records are good enough so that reflections can be definitely
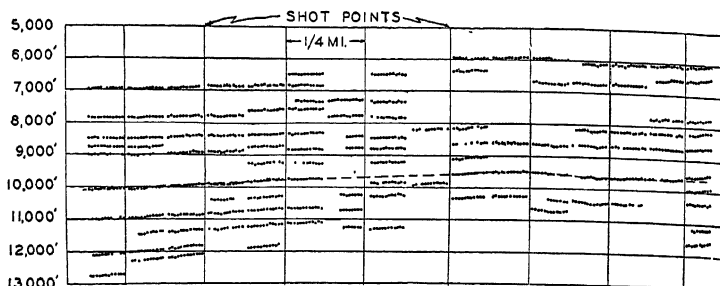
Fig. 169.—A reflection profile from the Gulf Coast. Regional south dip is shown by the general dip of reflections from right to left across the profile. Reversed, or north, dip indicating structure is shown by deeper reflections over the right-hand third of the profile. A structural reversal is clearly indicated (note phantom horizon indicated by dashed line at 9,500 to 10,000 ft. depth). Convergence (thinning of beds over structure) is shown in left third of profile, particularly by change in the interval between the reflections from about 9,000 ft. and those from about 10,000 ft.

carried and correlated from one shot point to another, the general operation is called "correlation shooting."

As reflections become less certain and the correlation from one point to another becomes questionable, it is necessary to place detector spreads closer together and use a more or less continuous spread, as shown by Fig. 161 or 162. In recent years spreads of this type have become more common than the more isolated spreads (Figs. 158 to 160) because so much reflection work has been done in areas where a few clear-cut, correlatable reflections are the exception rather than the rule. In many areas where the geologic section does not show distinct lithologic discontinuities, it is still possible to do effective reflection seismograph work because numerous reflections are recorded. Any individual reflection may not be continuous for any considerable distance; but by plotting all reflection events on the reflection profile it is

usually possible to obtain a very definite measure of the subsurface configuration. Thus, although no particular geologic horizon gives a continuous reflection, a series of reflections may indicate consistently that the beds are dipping at a certain rate. It is then possible to draw a "phantom horizon" which is a line parallel with the dips generally indicated by the reflections. This phantom horizon corresponds with no definite geologic horizon but will be quite accurately parallel to the stratification in the part of the geologic section to which it belongs. Quite frequently, it is useful to work out several phantom horizons at different depths which may or may not be parallel. Such work may be able to show convergence of beds, unconformities, etc. Under favorable conditions it may be possible to follow two separate horizons that come together to "pinch out" intervening beds. Under certain geologic circumstances such work may be very important for the possibility of locating chances of "shore line," or "stratigraphic," oil accumulation. Needless to say, such attempts require careful work, experienced marking of reflections, and close control.

MAPPING SEISMOGRAPH RESULTS

Usually the final result of a seismograph survey is a contour map. The primary basis for the map is a series of depths worked out from the reflection profile. The precision with which such a map represents the depth and configuration of the rocks is variable over wide limits.

Under favorable conditions where there are clear reflections from certain continuous beds, such as a continuous limestone under or within a thick shale section, the seismograph map may show accurately the depth to the stratum (limestone) giving a certain reflected event. Then the map may be almost as accurate as could be made by an actual contact by drilling at each detector spread.

More usually, the construction of the map is not so simple, and the results are more uncertain. More frequently than not, any particular reflection is not continuous over a wide area, and closer control with dip determinations or phantom horizons must be used to tie a picture together.

In very difficult areas, such as portions of the Gulf Coast, there are not enough reliable reflections to make even a reasonably

continuous phantom horizon. However, it is usually possible to get at least an approximate idea of the dip within one or two zones of depth at many or most of the detector spreads. The dips so indicated, of course, are the components along the line of the spread. A map may consist only of these dip indications without any attempt at construction of subsurface contours, but such dips may still give very useful indications and may be sufficient to indicate at least approximately areas of anticlinal dip reversal and therefore areas of interest. In the Gulf Coast, where over large areas the regional dip is to the south or southeast, any indication of reversed dip (*i.e.*, north or northwest dip) is a possibility of closure and therefore of interesting structure. With fair dip control it may be possible to construct an approximate contour map to give a fairly good general picture, but it cannot be taken as representative of structure at any particular depth. With only dip control it is usually impossible to determine faulting.

In most areas, it is highly desirable to have the lines of detector spreads laid out in closed traverses. Then the precision and continuity with which any particular horizon is being carried can be checked by the error of closure when the depths are carried around a closed loop. Large errors of closure indicate that the same bed has not been followed all the way around the loop or that a fault has been crossed and thus may indicate that the reflecting bed itself is not continuous. Under fair to good conditions, depths can be carried around loops of several miles circumference and closed within 100 ft.

Mapping Faults.—If correlations can be carried, and particularly if a series of reflections with approximately equal intervals is present on most of the records in a given area, faults may be clearly indicated by displacement of the pattern of reflection depths on the two sides of the fault. In unusually favorable circumstances, small faults can be recognized directly on the records by the offset of reflections.

When depths are carried by a phantom horizon or by dips, faults may not be apparent, for a fault generally will produce no change of dip except very close to the fault plane. Thus, there may be no direct indication of a fault unless, by rare chance, reflections on the same spread are received from both sides of the fault and make an actual offset on the tape. The chance of

such an observation is considerably reduced by the fact that subsurface conditions are quite likely to be irregular in the immediate vicinity of a fault so that poor or no reflections are commonly experienced in just the areas where the fault indication would be most likely. However, evidence for faulting may be given by "misclosure." If depths around a given traverse fail to close by amounts much larger than is normally expected, this misclosure may be considered as evidence of faulting, on the assumption that the fault has a substantially different displacement at the two points where crossed by the lines of the closed detector traverse. By cutting up large closed traverses with internal cross lines and by looking for direct evidence, such as zones of poor reflections, it is sometimes possible to localize faulting quite definitely, even though no correlations across the fault are possible.

The location of faults by misclosures has a natural tendency to place the fault at the points where the traverses are closed and where the misclosure becomes apparent. This is quite erroneous, for the source of the misclosure may be at a quite different point in the closing traverse. The location of the position of the fault must depend on some other indication, such as zones of poor or no reflection, or possibly (but very rarely) on an indication of the fault on the records themselves.

The detection of faults becomes more and more difficult as the records become more and more complex. When there are only one or two outstanding reflections, it is comparatively simple and straightforward to determine the displacement of such a reflection by a fault. However, when there are many reflections and they do not have a definite sequence, it is quite possible that a fault displacement may bring two reflections that are really from different beds close together so that they will be interpreted as a continuous reflection from the same bed.

PRECISION OF REFLECTION RESULTS

A number of factors may affect the precision with which depths are determined from reflection shooting.

Timing.—The actual measurement of times on the records is usually quite accurate, and the time of any particular event can be determined to within 0.001 or 0.002 sec. The tuning forks used for controlling the timing lines are usually accurate enough

so that there is no very important source of error in the placing of the timing lines on the records.

Shot Moment.—With modern blasting caps and technique of firing, the uncertainties in the instant of explosion are very small. It is probable that in usual practice the shot moment is determined within about 0.001 sec.

Weathering.—Uncertainties in weathering corrections are probably the largest single source of error in determining the times of reflection events, and they usually contribute small irregularities to the plotted results on the reflection profile. If the topography is rugged, some uncertainty is introduced in the corrections for differences in elevations, and careful consideration must be given to the velocities that are used for the surface corrections in order to avoid small errors from this source. It is probable that under average working conditions uncertainties in the weathering and surface corrections are from 0.001 to 0.005 sec. and that in areas of bad surface conditions or rugged topography they may be over 0.010 sec.

Marking Records.—Except under very favorable circumstances there is always uncertainty in consistent marking of the seismograph records. Some of the irregularities that may be shown in the reflection profile are attributable to this cause. In addition there are often changes in character of the record which make it difficult to follow the same phase continuously. These changes probably are caused by lensing or changing of thickness of beds that cause the reflections. To that extent the apparent errors in the result are indications only of the lack of continuity of the subsurface horizons, but at the same time they may contribute to errors in the depth determination of any particular horizon and lead to errors of closure on closed traverses.

Velocities.—The greatest single source of error in the calculation of the depth to a reflecting horizon is the uncertainty in the determination of the over-all velocity for the time of the reflection. If the velocities are determined from reflection spreads themselves (by the T^2x^2 method, page 285), it is almost impossible to be certain of the over-all velocities closer than a few per cent. If velocities are determined from well-placed shooting in wells, the velocity characteristics of an area may be fairly accurately determined. If the velocities are reasonably uniform, and similar velocities are indicated by shooting in wells over a con-

siderable area, it may be possible to determine the over-a velocity and the depths to the reflecting horizons within a pr cision of 1 per cent or less. In some areas there are very consierable local changes in velocity so that major corrections seismograph maps may be required to take care of these change This has proven particularly troublesome in California whe velocity variations corresponding to depth corrections of as muc as 100 to 150 ft. per mile sometimes occur.[1]

Relative Depth.—In most of the applications of the reflectic seismograph method it is relative depths rather than absolu depths that are important. Thus, if a seismograph map shov a structure with 100 ft. of closure at a depth of several thousan feet, it is much more important to know that the closure present than to know exactly the depth of the horizon giving th reflections on which the closure is mapped. Under fair to goo operating conditions it is possible to determine relative deptl closely enough so that broad structures with closures of onl 100 or 200 ft. and areas of several square miles can be fairl definitely determined, although it would be impossible to dete mine the absolute depth within anywhere near this precision.

At least an approximate idea and sometimes a fairly definit measure of the actual depth of the reflecting horizons become important in cases where there are unconformities in the geologi section. For instance, if a large unconformity is present abov which the sediments are flat and below which they might b deformed to make an interesting structure, it is important if th seismograph indicates flat beds to know whether or not they ar above the unconformity. If they are definitely below the uncor formity, the flat indication would condemn an area; but above, it would not.

INTERPRETATION OF REFRACTION RESULTS

The interpretation of refraction shooting is not nearly s straightforward as reflection shooting, and the details of the inter pretation technique will depend a great deal upon the shot detector pattern as laid out on the ground. In some cases, suc as simple fan shooting, the interpretation is extremely simple an consists only of determining the time leads and indicating locall irregular areas by the simple process outlined in Chap. XI

[1] Pratley, 1939.

(page 278). In extensive profile shooting by refraction methods, the results are indicated on some sort of plotted profile or cross section on which the depths and dips of refracting beds are shown. Such profiles also may show the time-distance curves and the geometry of the inferred minimum time wave paths. Before such data can be plotted, it is necessary to calculate surface corrections (usually from special correction shots near the detector spread) time intercepts, etc., so that depths can be calculated. The number of variables is greater than in the interpretation of reflection results, particularly in that more than one set of wave paths may account for the observed travel times. The refraction time is always made up of parts at both ends of the wave trajectory; the intercept time is made up of the "down time" at the shot end and the "up time" at the detector end; and the measured intercept time interval gives the sum of these two. Therefore, if differences in depth are to be determined, it is necessary that the two parts be separated. This can be done by use of the delay time (or intercept time) as indicated in Chap. XIV [Eq. (223) and example, page 266; also Eq. (249)].

COMPARISON OF REFLECTION AND REFRACTION RESULTS

The obvious advantages of the reflection method are so great that the question may be raised as to why the refraction method should ever be used; the reflection method maps many beds, but the refraction method usually maps only one; the reflection method uses much smaller charges and shorter detector spreads and is therefore very much cheaper in the field than is the refraction method. However, in some areas it is almost impossible to get useful and reliable reflections. This is particularly true in areas where there is a thick cover of alluvial or glacial material through which it is impractical to drill shot holes. In such areas it may still be possible to get definite first arrivals on refraction records and to map a velocity discontinuity which will give useful subsurface information. Also, refraction work may be applicable to areas of steep dips and, particularly, of more or less vertical discontinuities such as faults or flanks of salt domes where reflection results become of questionable utility. The refraction method also may provide a useful reconnaissance exploration method, as isolated refraction profiles can give velocities and depths to velocity discontinuities that quite possibly may be

correlated with definite major changes in the geologic column, such as unconformities, tops of heavy limestone beds, depth to granite basement. The determination of velocities helps in such a problem, as the velocity may serve to identify the geological formation being followed. Thus refraction work at widely spaced points may give useful information on the general geology of an area, such as regional dips and thickness of sediments. It would rarely be possible to gain such information from a few scattered reflection spreads, as the correlation of even very clear reflections from widely spaced areas would rarely be reliable.

LIMITATIONS OF SEISMOGRAPH MAPPING

In difficult areas the making of a seismograph map from depths or dips calculated from the records may call for a great deal of skill and judgment and for a very considerable amount of experience. It is at this stage that the seismic interpreter has to become a geologist. A man with a purely physical background may be inclined to feel that reflections are very real things and that there must be corresponding dips or relative depths in the underground strata. With such ideas, he may come out with a map that a geologist will say is unreasonable or does not conform to the geological habit of the area. On the other hand, a man with a purely geological background is naturally inclined to disregard certain indications that do not fit his ideas of the kind of geological picture that should be reasonable. These differences in viewpoint have led to many arguments, for geophysical exploration and interpretation have brought geologists and physicists into contact with each other as they never have been before. Even after all the years that geophysical exploration has been conducted, it is rare for a geologist really to understand the physical background of geophysical prospecting or for a physicist to become a really competent geologist. It does not seem feasible to have the details of the construction of a seismic map worked out in cooperation between a geologist on one hand and a physicist or engineer on the other. The best results seem to be obtained by one's learning the fundamentals of the other's science. Good geophysical interpreters may start out as either physicists or geologists. Perhaps another generation will see a truly hybrid offspring of the union of geology and physics which is being attempted in some of our educational institutions.

The details of the process by which energy reaches a detector from the explosion of a dynamite charge are far from completely understood. The initial disturbance is probably a steep-front transient compressional disturbance and not a "wave" in the ordinary periodic or cyclic sense of wave phenomena. In traveling through the earth, the disturbance apparently acquires a periodic character in that it becomes a short "pulse," or damped wave train. By the very fact of its being highly damped, it cannot have a single frequency. The physical properties of the transmitting medium must control, to a certain extent, the character of the wave that comes back to the surface after penetrating thousands of feet of rock. Perhaps some thin rock layers actually oscillate physically to impose their period on the reflected or transmitted waves. For instance, hard surface beds, such as the Caliche (surface limestone) of West Texas, apparently vibrate as a drumhead and impose a troublesome high-frequency response on the detectors. Also, it seems probable that reflections from successive strata or from the top and bottom of the same stratum give a periodic aspect to an otherwise sharp transient compressional pulse. Perhaps multiple reflections occur to give waves coming in at times that would be interpreted as coming from strata twice as deep as their actual origin.

It should always be kept in mind that the trace on the record is rarely, if ever, even an approximate picture of the actual ground movement at the detector. The record is modified by the mechanical characteristics of the detector, by the frequency selectivity of the amplifier, and by the mechanical characteristics of the oscillograph. Each element of the system impresses its characteristics on the final record. Thus, the frequency dominating the record is quite possibly the primary frequency of the detector or filter rather than the dominant frequency of the actual ground movement. The same reflection from the same shot may look quite different if recorded by different detector-amplifier systems.

APPENDIX

DERIVATION OF EQUATIONS FOR EQUAL TIME CIRCLES

By an integration similar to that giving Eq. (213) (page 259) the time for a wave to travel from O to P (Fig. 170) is

$$T = \frac{1}{K}\left(\cosh^{-1}\frac{V_m}{V_0} - \cosh^{-1}\frac{V_m}{V}\right) \tag{293}$$

where V is the velocity at a depth z. From the figure,
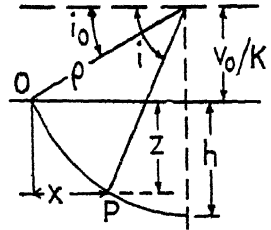
$$x = \rho(\cos i_0 - \cos i)$$

$$= \rho\left[\sqrt{1 - \left(\frac{V_0}{V_m}\right)^2} - \sqrt{1 - \left(\frac{V}{V_m}\right)^2}\right] \tag{294}$$

But from Eq. (208) (page 258),

$$\rho = \frac{V_m}{K}$$

so that Eq. (294) becomes

$$x = \frac{V_m}{K}\left[\sqrt{1 - \left(\frac{V_0}{V_m}\right)^2} - \sqrt{1 - \left(\frac{V}{V_m}\right)^2}\right] \tag{295}$$

$$x^2 = \frac{V_m^2}{K^2}\left[1 - \left(\frac{V_0}{V_m}\right)^2 + 1 - \left(\frac{V}{V_m}\right)^2 - 2\sqrt{1 - \left(\frac{V_0}{V_m}\right)^2}\cdot\sqrt{1 - \left(\frac{V}{V_m}\right)^2}\right]$$

$$= \frac{V_m^2}{K^2}\cdot\frac{V_0 V}{V_m^2}\left[2\frac{V_m^2}{V_0 V} - \frac{V_0^2}{V_0 V} - \frac{V^2}{V_0 V}\right.$$

$$\left. - 2\frac{V_m^2}{V_0 V}\sqrt{1 - \left(\frac{V_0}{V_m}\right)^2}\cdot\sqrt{1 - \left(\frac{V}{V_m}\right)^2}\right]$$

$$\frac{x^2}{2} = \frac{V_0 V}{K^2}\left(\frac{V_m^2}{V_0 V} - \frac{V_0^2 + V^2}{2V_0 V} - \sqrt{\frac{V_m^2}{V_0^2} - 1}\cdot\sqrt{\frac{V_m^2}{V^2} - 1}\right) \tag{296}$$

$$\frac{K^2 x^2}{2V_0 V} + \frac{V_0^2 + V^2}{2V_0 V} = \frac{V_m^2}{V_0 V} - \sqrt{\frac{V_m^2}{V_0^2} - 1}\cdot\sqrt{\frac{V_m^2}{V^2} - 1} \tag{297}$$

It can be shown[1] that

$$\cosh^{-1} a - \cosh^{-1} b = \cosh^{-1}(ab - \sqrt{a^2-1}\cdot\sqrt{b^2-1}) \quad (298)$$

From (298), if we let $a = V_m/V_0$; $b = V_m/V$, we can write (293) as

$$T = \frac{1}{K}\cosh^{-1}\left[\frac{V_m^2}{V_0V} - \sqrt{\left(\frac{V_m}{V_0}\right)^2 - 1}\cdot\sqrt{\left(\frac{V_m}{V}\right) - 1}\right] \quad (299)$$

Substituting from Eq. (297) in Eq. (299),

$$T = \frac{1}{K}\cosh^{-1}\left(\frac{K^2x^2 + V_0^2 + V^2}{2V_0V}\right) \quad (300)$$

But

$$\frac{K^2x^2 + V_0^2 + V^2}{2V_0V} = \frac{K^2x^2 + (V_0 - V)^2 + 2V_0V}{2V_0V} = 1 + \frac{K^2x^2}{2V_0V} + \frac{(V_0-V)^2}{2V_0V}$$

and, since $V = V_0 + Kz$,

$$z = \frac{V - V_0}{K}$$

and

$$\frac{K^2x^2 + V_0^2 + V^2}{2V_0V} = 1 + \frac{K^2(x^2 + z^2)}{2V_0V}$$

So we can write Eq. (300) as

$$T = \frac{1}{K}\cosh^{-1}\left[1 + \frac{K^2(x^2 + z^2)}{2V_0V}\right]$$

$$= \frac{1}{K}\cosh^{-1}\left[1 + \frac{K^2(x^2 + z^2)}{2V_0(V_0 + Kz)}\right] \quad (301)$$

which is Eq. (215) (page 259).

Also,

$$\cosh KT = 1 + \frac{K^2(x^2 + z^2)}{2V_0(V_0 + Kz)}$$

---

[1] Let

$$\cosh^{-1} a - \cosh^{-1} b = \cosh^{-1} q$$

and let

$$A = \cosh^{-1} a; \quad B = \cosh^{-1} b$$

Then

$$A - B = \cosh^{-1} q$$
$$\cosh(A - B) = q = \cosh A \cosh B - \sinh A \sinh B$$
$$\sinh A = \sqrt{\cosh^2 A - 1} = \sqrt{a^2 - 1}; \quad \sinh B = \sqrt{b^2 - 1}$$
$$q = ab - \sqrt{a^2 - 1}\cdot\sqrt{b^2 - 1}$$
$$\cosh^{-1} a - \cosh^{-1} b = \cosh^{-1}(ab - \sqrt{a^2 - 1}\cdot\sqrt{b^2 - 1})$$

Therefore,

$$x^2 + z^2 = \frac{2V_0(V_0 + Kz)}{K^2}\,(\cosh KT - 1)$$

and

$$x^2 + z^2 - \frac{2V_0Kz}{K^2}\,(\cosh KT - 1) = \frac{2V_0^2}{K^2}\,(\cosh KT - 1)$$

Add $(V_0^2/K^2)(\cosh KT - 1)^2$ to both sides:

$$x^2 + z^2 - \frac{2V_0z}{K}\,(\cosh KT - 1) + \frac{V_0^2}{K^2}\,(\cosh KT - 1)^2$$

$$= \frac{V_0^2}{K^2}\,(\cosh KT - 1)^2 + \frac{2V_0^2}{K^2}\,(\cosh KT - 1)$$

$$x^2 + \left[z - \frac{V_0}{K}\,(\cosh KT - 1)\right]^2 = \frac{V_0^2}{K^2}\,[(\cosh KT - 1)^2 + 2(\cosh KT - 1)]$$

$$= \frac{V_0^2}{K^2}\,(\cosh^2 KT - 1)$$

$$= \frac{V_0^2}{K^2}\,\sinh^2 KT \tag{302}$$

Then Eq. (302) can be written

$$r^2 = x^2 + (z - \lambda)^2 \tag{303}$$

Equation (303) describes a circle of radius r, centered at a distance λ below the surface. Thus, the equal time circles can be drawn as circles of radius

$$r = \frac{V_0}{K}\,\sinh KT \text{ [Eq. (217) of page 260]}$$

centered at a depth

$$\lambda = \frac{V_0}{K}\,(\cosh KT - 1) \text{ [Eq. (216) of page 260]}$$

below the surface.

BIBLIOGRAPHY

1917

FESSENDEN, R. A.: Methods and Apparatus for Locating Ore Bodies, U.S. Patent 1,240,328, Sept. 18, 1917.

1929

BARTON, D. C.: The Seismic Method of Mapping Geologic Structure, "Geophysical Prospecting, 1929," *Trans. Am. Inst. Min. Met. Eng.*, vol. 81, pp. 572–624.

1930

MEISSER, O. and H. MARTIN: "Luft- und Bodenseismik" in "Handbuch der Experimentalphysik," ed. by W. Wien and F. Harms, Band XXV, Teil 3, pp. 209–302, Akademische Verlagsgesellschaft m.b.H., Leipzig.

MINTROP, L.: "On the History of the Seismic Method for the Investigation of Underground Formations and Mineral Deposits," Pt. II, Seismic G.m.b.H., Hannover (128 pages).

REICH, H.: "Geologische Unterlagen der angewandten Geophysik," in "Handbuch der Experimentalphysik," ed. by W. Wien and F. Harms, Band XXV, Teil 3, pp. 1–46, Akademische Verlagsgesellschaft m.b.H., Leipzig.

THORNBURGH, H. R.: Wave-front Diagrams in Seismic Interpretation, *Bull. Am. Assoc. Petroleum Geologists*, vol. 14, No. 2, pp. 185–200, February, 1930.

1931

BROUGHTON EDGE, A. B., and T. H. LABY: "The Principles and Practice of Geophysical Prospecting," Cambridge University Press, London.

1932

EWING, M., and L. D. LEET: Seismic Propagation Paths, "Geophysical Prospecting, 1932," *Trans. Am. Inst. Min. Met. Eng.*, vol. 97, pp. 245–260.

LEET, L. DON, and W. MAURICE EWING: Velocity of Elastic Waves in Granite, *Physics*, vol. 2, No. 3, pp. 160–173, March, 1932.

LESTER, O. C., JR.: Seismic Weathered or Aerated Surface Layer, *Bull. Am. Assoc. Petroleum Geologists*, vol. 16, No. 12, pp. 1230–1234, December,

1933

JONES, J. H.: A Seismic Method of Mapping Anticlinal Structures, *Proc. World Petroleum Cong., London, July* 19–25, 1933, vol. 1, pp. 169–172. London, 1934.

MUSKAT, M.: The Theory of Refraction Shooting, *Physics*, vol. 4, No. 1, pp. 14–28, January, 1933.

1934

EWING, MAURICE, A. P. CRARY, and J. M. LOHSE: Seismological Observations on Quarry-blasting, *Trans. Am. Geophys. Union*, 15th annual meeting, pp. 91–94.

HEILAND, C. A.: Certain Instrument Problems in Reflection Seismology, "Geophysical Prospecting, 1934," *Trans. Am. Inst. Min. Met. Eng.*, vol. 110, pp. 411–454.

ROSAIRE, E. E., and JOSEPH L. ADLER: Applications and Limitations of Dip Shooting, *Bull. Am. Assoc. Petroleum Geologists*, vol. 18, No. 1, pp. 119–132, January, 1934.

WEATHERBY, B. B., W. T. BORN, and R. L. HARDING: Granite and Limestone Velocity Determinations in Arbuckle Mountains, Oklahoma, *Bull. Am. Assoc. Petroleum Geologists*, vol. 18, No. 1, pp. 106–118, January, 1934.

1935

HAGIWARA, TAKAHIRO: A Comparison of the Displacement, the Velocity, and the Acceleration Seismograms, *Bull. Earthquake Research Inst. Tokyo*, vol. 13, Pt. 1, pp. 138–145.

1936

BRYAN, A. B.: True Ground Motion from Mechanical Seismograph Records, *Geophysics*, vol. 1, No. 3, pp. 340–346, October, 1936.

BURROWS, L. A.: Relation between Firing Current and Performance in Seismograph Caps, *Geophysics*, vol. 1, No. 2, pp. 219–227, June, 1936.

GUTENBERG, B.: On Some Problems Concerning the Seismic Field Methods, *Beitr. angew. Geophysik*, vol. 6, pp. 125–140, 1936–1937.

MACELWANE, J. B.: "Introduction to Theoretical Seismology, Part I, Geodynamics," John Wiley & Sons, Inc., New York.

a. RIEBER, F.: A New Reflection System with Controlled Directional Sensitivity, *Geophysics*, vol. 1, No. 1, pp. 97–106, January, 1936.

b. RIEBER, F.: Visual Presentations of Elastic Wave Patterns under Various Structural Conditions, *Geophysics*, vol. 1, No. 3, pp. 196–218, June 1936.

SLOTNICK, M. M.: On Seismic Computations, with Applications, I, *Geophysics*, vol. 1, No. 1, pp. 9–22, January, 1936; II, *Geophysics*, vol. 1, No. 3, pp. 299–305, October, 1936.

WOLF, A.: The Amplitude and Character of Refraction Waves, *Geophysics*, vol. 1, No. 3, pp. 319–326, October, 1936.

1937

MUSKAT, M.: A Note on the Propagation of Seismic Waves, *Geophysics*, vol. 2, No. 4, pp. 319–328, October, 1937.

PIRSON, SYLVAIN J.: The Correlation Method of Seismographing for Oil, *Oil Weekly*, vol. 87, No. 2, pp. 24–44, Sept, 20, 1937.

RIEBER, F.: Complex Reflection Patterns and their Geologic Sources, *Geophysics*, vol. 2, No. 2, pp. 132–160, March, 1937.

1938

GARDNER, D. H.: Measurement of Relative Ground Motion in Reflection Recording, *Geophysics*, vol. 3, No. 1, pp. 40–45, January, 1938.

JOHNSON, CURTIS H.: Locating and Detailing Fault Formations by Means of the Geo-sonograph, *Geophysics*, vol. 3, No. 3, pp. 273–291, July, 1938.

LAWLOR, REED: Nomogram for Dip Computations, *Geophysics*, vol. 3, No. 4, pp. 349–357, October, 1938.

LEET, L. D.: "Practical Seismology and Seismic Prospecting," D. Appleton-Century Company, Inc.

MUSKAT, M.: The Reflection of Longitudinal Wave Pulses from Plane Parallel Plates, *Geophysics*, vol. 3, No. 3, pp. 198–218, July, 1938.

ROCK, S. M.: Three Dimensional Reflection Control, *Geophysics*, vol. 3, No. 4, pp. 340–348, October, 1938.

1939

a. GARDNER, L. W.: An Areal Plan of Mapping Subsurface Structure by Refraction Shooting, *Geophysics*, vol. 4, pp. 247–259.

b. GARDNER, L. W.: Seismograph Prospecting, U.S. Patent 2,153,920, Apr. 11, 1939.

ITTNER, FRANK: Seismograph Field Operations, *Am. Inst. Min. Met. Eng. Tech. Pub.* 1059, pp. 15–21.

KELLY, P. C.: Determining Geologic Structure from Seismograph Records, *Am. Inst. Min. Met. Eng. Tech. Pub.* 1059, pp. 21–29.

NORMAN, ARTHUR: Instruments for Reflection Seismograph Prospecting, *Am. Inst. Min. Met. Eng. Tech. Pub.* 1059, pp. 9–15.

PRATLEY, H. HART: Reflection Seismograph Work in California, *Mines Mag.*, vol. 29, No. 6, p. 281, June, 1939, Colorado School of Mines.

TRACY, WILLARD H.: Theory of Reflection Seismograph Prospecting, *Am. Inst. Min. Met. Eng. Tech. Pub.* 1059, pp. 2–9.

1940

a. MUSKAT, M., and M. W. MERES: Reflection and Transmission Coefficients for Plane Waves in Elastic Media, *Geophysics*, vol. 5, pp. 115–148.

b. MUSKAT, M., and M. W. MERES: The Seismic Wave Energy Reflected from Various Types of Stratified Horizons, *Geophysics*, vol. 5, pp. 149–155.

PART IV

ELECTRICAL AND MISCELLANEOUS METHODS AND MEASUREMENTS IN DRILL HOLES

CHAPTER XIX

ELECTRICAL PROSPECTING METHODS

INTRODUCTION

There are a number of ways in which electrical principles have been applied to the elucidation of underground conditions. In fact, the history of electrical prospecting is older than that of most of the other methods of geophysical exploration, as some attempts to apply electrical principles to determine underground conditions were made over a hundred years ago.[1]

The modern developments of electrical prospecting methods have been largely in comparatively shallow applications, and most of this development has been made by the mining rather than the oil industry; but the very attractive possibility that electrical methods might be used for the detection of oil itself has kept a certain amount of development along these lines underway more or less continuously. However, there are inherent limits to the depth of penetration that it is feasible to obtain by electrical prospecting schemes, and these depths are so shallow that the utility of most of the ordinary electrical methods for oil prospecting is doubtful. The number of electrical prospecting parties in the field has never been large and is almost negligible in comparison with the other methods.

The continued interest in electrical methods that has been manifest by the oil industry is sufficient to justify the inclusion here of a limited discussion of the physical principles underlying the various schemes of electrical prospecting. Also, certain modifications of electrical methods have very important applications in the exploration of bore holes and the determination of properties of the strata penetrated by the hole, particularly the porosity and indications of oil or gas.

The theory of electrical methods is relatively complicated, and there is a voluminous periodical literature treating of their various phases and applications. In fact, in spite of the com-

[1] For a brief history of electrical prospecting methods, see Rust, 1938.

paratively limited commercial application that these methods have had in the oil industry, the volume of literature on electrical methods is quite comparable with that on any of the other geophysical prospecting principles.

CLASSIFICATION OF ELECTRICAL PROSPECTING METHODS

The electrical methods may be classified as:

1. Natural current methods.
   Local currents.
   Telluric currents.
2. Artificial current methods.
   Conductive methods.
   Direct-current measurements.
   Alternating-current measurements.
   Inductive methods.
   Transient methods.

Most of the methods listed have been developed and applied by the metal-mining industry, and much of the literature is in the publications of that industry.[1] Because of their limited application to oil prospecting the discussions here will be confined to brief statements of the physical principles involved.

NATURAL CURRENT METHODS

Local Currents.—Local natural earth currents depend on the fact that certain ores, particularly sulphide ores, are electrochemically active so that they behave like the elements of a battery. The battery action depends on the oxidation of the end of the ore body nearer the surface, within the range of surface water. The upper end thus becomes negative; the lower, positive; and electrical current tends to flow downward within the ore body. The return current in the surrounding rock flows upward and toward the upper end. The exploration methods depend

---

[1] Much of the American literature on electrical prospecting methods is contained in the publications of the American Institute of Mining and Metallurgical Engineers, particularly the special volumes "Geophysical Prospecting, 1929" (*Trans.*, vol. 81), "Geophysical Prospecting, 1932" (*Trans.*, vol. 97), and "Geophysical Prospecting, 1934" (*Trans.*, vol. 110).

Also, see Eve and Keys, "Applied Geophysics," Cambridge University Press, 2d ed. (1933) or 3d ed. (1938), pp. 63–171; or Broughton Edge and Laby, "The Principles and Practice of Geophysical Prospecting," Cambridge University Press, pp. 9–134 and 236–298, 1931.

upon measuring differences in potential between points on the surface of the ground. By mapping the potential differences it is possible to infer the directions of current flow in the ground and their source, which in turn will give indications of the location of bodies responsible for the currents.

Since an ordinary metal electrode in contact with the ground is apt to have a self-potential of its own with respect to the ground, it is necessary that special precautions be taken in making the electrical contact through which the differences in potential are measured. This is done by the use of "nonpolarizing" electrodes which commonly consist of a porous clay pot filled with a saturated solution of copper·sulphate and an excess of copper sulphate crystals. The measurements are carried out by simply measuring the difference in potential between pairs of such pots located at points along profiles or in a more or less regular grid over the area surveyed.

These methods have no application in prospecting for oil.

Telluric Currents.—A quite different type of natural current method depends on the measurement of "telluric" currents. These are irregular natural currents on a large scale within the earth which are intimately related to diurnal magnetic variations and have corresponding diurnal and also short-period variations. They are particularly active at the time of magnetic storms.

Measurements are made by comparing the potential differences between two pairs of electrodes set along perpendicular lines at a fixed station with potential differences between similar sets of electrodes at a mobile station.[1] It is found that the time variations of potential difference at points many miles apart are very similar in form, but the amplitudes are variable with position. The variations in amplitude are governed, to a certain extent, by variations in electrical resistance of the earth's crust (in a manner somewhat analogous to that in which an obstruction to its flow can govern the course of a stream). Mapping of the amplitude variations or the ratios of the potential at the mobile stations to the simultaneous potential at the fixed station may permit deductions as to the presence or absence of relatively conducting or nonconducting rocks in large units and thus indicate large geologic features. For instance, a sedimentary basin would have less resistance to the telluric currents than an area

[1] Schlumberger, 1939.

of shallow granite. The testing of this scheme is very meager as yet, but it appears possible that it may be capable of indicating large-scale geologic features at great depth in simple geologic situations.

ARTIFICIAL CURRENT METHODS

All the various artificial current methods apply an electrical current or radiation of some kind to the ground. The electrical impulse may be applied directly, by means of electrodes inserted into the ground (conductive methods), or the current may flow in the ground by electromagnetic induction from alternating currents in lines or loops or coils at or above the surface of the ground (inductive methods). Measurements are made either of the difference in potential or of the electromagnetic field set up by the ground currents.
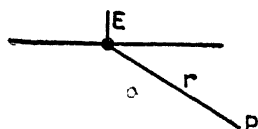
FIG. 171.—Potential about a point.

Conductive Methods. *Direct Currents.*—In the conductive methods the electric current is applied to the ground through two electrodes which make electrical contact with the ground. The potential difference is usually measured between two other electrodes. The quantity that is determined by such measurements is primarily the conductivity of the ground. Various configurations of electrodes may be employed.

Consider an electric current I, entering a homogeneous ground of resistivity or specific resistance ρ* at an electrode E (Fig. 171). The potential V, at a point P, distant r from the current source, is

$$V = \frac{\rho I\dagger}{2\pi r} \qquad = \frac{\rho I}{2\pi a} \qquad (304)$$

For any given configuration of electrodes the potential difference between two measuring electrodes may be calculated (on

* Specific resistance (for a homogeneous, isotropic medium) ρ is defined by the relation $R = \rho L/A$, where R is the resistance of a sample of material of length L and cross section A. If L and A are unity, then ρ becomes the resistance across two opposite faces of a cube of unit dimensions. The unit used is usually the centimeter, and ρ is then the resistance in ohms across a 1-cm. cube expressed as ohms per centimeter cube and with the dimensions ohms × centimeters (not, as sometimes said, ohms per cubic centimeter).

† Ehrenburg and Watson, 1932, p. 427.

the assumption of homogeneous conductivity) by simply considering the differences of potential at the two potential electrodes that arise from the points at which the current enters and leaves the ground.

For example, a very common electrode system is the "Wenner" configuration (Fig. 172) in which four electrodes are equally spaced at an interval a along a straight line.

The potential at P_1 due to current entering the ground at E_1 is $\rho I/2\pi a$, and that due to the current leaving the ground at E_2 is $-\rho I/2\pi \cdot 2a$, so that the total potential at P_1 is

$$V_1 = \frac{\rho I}{2\pi}\left(\frac{1}{a} - \frac{1}{2a}\right) = \frac{\rho I}{2\pi}\left(\frac{1}{2a}\right)$$

FIG. 172.—Wenner electrode configuration.

Similarly, the potential at P_2 is

$$V_2 = \frac{\rho I}{2\pi}\left(-\frac{1}{a} + \frac{1}{2a}\right) = -\frac{\rho I}{2\pi}\left(\frac{1}{2a}\right)$$

so that the potential difference measured between P_1 and P_2 is

$$V = V_1 - V_2 = \frac{\rho I}{2\pi a} \tag{305}$$

Thus, for this electrode system the ground resistivity is given by

$$\rho = \frac{V}{I} \cdot 2\pi a \tag{306}$$

Expressions for determination of resistivity for other electrode configurations can be derived by similar applications of the fundamental relation of Eq. (304).

The value of resistivity determined by an expression such as Eq. (306) applies to a volume of ground that depends on the electrode spacing. As the spacing is increased, the current penetrates more deeply into the ground. For a homogeneous earth, it can be shown that at a vertical plane midway between the two electrodes, just half the current flows at a depth greater than half the electrode spacing, and half flows at shallower depth. This depth is indicated by the dotted line of Fig. 173.

When the ground resistivity is not homogeneous, the resistivity value given by an expression such as Eq. (306) is an "effective" resistivity which is a weighted average of whatever resistivity

may exist in the region within which the current flows. As the electrode spacing is increased, part of the current spreads out to greater and greater depths, and the resistivities of deeper and deeper beds have an appreciable effect on the measured "effective" resistivity. Thus, if values of resistivity are determined for successively wider spreads of the electrode configuration, a curve of apparent resistivity plotted against spread (*e.g.*, the distance *a* of the Wenner configuration) will show varying values as the current reaches deeper beds of varying resistivity. By proper interpretation of such apparent resistivity curves, inferences may be drawn as to the depths of beds of varying resistivity
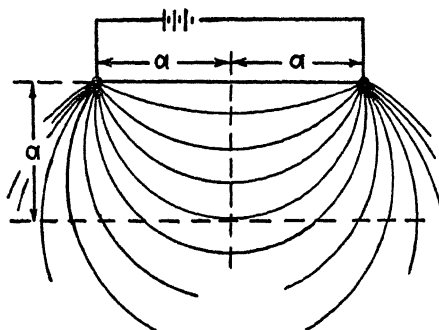
Fig. 173.—Current distribution between electrodes in a homogeneous earth.

which in turn may be interpreted as indications of certain geological conditions.

Methods of Measurement.—The conductive methods may be applied with various sources of electric current. Direct currents from batteries have been used to a limited extent, but their use is often unsatisfactory because of polarization effects. The polarization arises because of electrolytic action which takes place in the vicinity of the ground electrode and tends to produce a counter electromotive force so that the current changes with time. This effect can be overcome to a certain extent by the use of nonpolarizing electrodes, and such electrodes are essential for the use of simple direct-current sources.

A simple scheme for overcoming the polarization difficulty is the Gish-Rooney[1] method. A battery is used for the source of current, but the current is supplied to the ground through a

[1] Gish and Rooney, 1925.

commutator which reverses the direction of current flow at each revolution (Fig. 174). A second commutator on the same shaft reverses the connections to the potentiometer or voltmeter at the same time that the current to the ground is reversed. Thus, the current and voltage are measured by ordinary direct-current methods just as if a simple direct current were applied to the ground, but the current in the ground is reversed in direction with each half revolution of the commutator. The commutator is arranged to be turned by hand at a rate that is not at all critical but that gives alterations of the current in the ground at the rate of some thirty times per second.
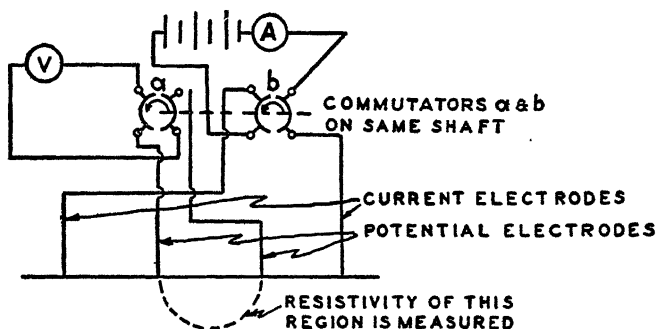
FIG. 174.—Circuit for the Gish-Rooney method of measuring ground resistance.

The "Megger" system is similar in principle to the Gish-Rooney system. However, instead of a battery, a hand-operated generator is used. The shaft of the generator carries a double commutator similar to that of the Gish-Rooney system. The instrument contains an indicator similar to an ordinary electric meter except that the position of the needle depends upon two coils, one of which carries the current being sent into the ground and the other a current that is a measure of the voltage between the potential electrodes. The indicator is so related to the coils that the position of the needle is a measure of the ratio of voltage to current and therefore is a direct measure of resistance.

A modification of the conductive electric methods which has had some application to prospecting for oil structures is the process of "continuous electrical profiling" as developed by Jakosky.[1] The current applied to the ground is a low-frequency

[1] Jakosky, 1938.

alternating current of a special wave form. One current electrode and two potential electrodes are kept fixed and in line; the other current electrode is moved continuously outward along the same line. Variations in the potential are read as the current electrode is moved. The operation is facilitated by having the outer electrode consist of a motor truck with special metal rear wheels which make a continuous electrical contact with the ground. Changes in potential are interpreted in terms of changes in resistivity in the zone between the moving electrode and the other current electrode.

Alternating-current Measurements.—No clear theoretical distinction is usually made between direct-current and alternating-current methods using grounded electrodes as long as low-frequency alternating current is used. This is because, for low frequency, the current distribution in the ground is substantially the same as for direct current. The choice of whether direct or low-frequency alternating current is used is governed primarily by ease of measurement and the difficulties from polarization and self-potential disturbances to direct-current measurements. Thus, the Gish-Rooney system uses a direct-current energy supply and measuring instruments but applies an alternating current to the ground. The same results should be obtained by using a low-frequency, alternating-current energy supply and alternating-current measuring instruments, without the use of the double commutator. The equivalence of alternating- and direct-current measurements breaks down when the frequency becomes high enough so that the current distribution in the ground is materially changed or appreciable current is induced in the ground or measuring circuits or appreciable phase changes occur between current supply and measuring circuits. The frequency at which such effects become appreciable is a complicated function of the distribution of ground resistivity and electrode spacing.[1]

Inductive Methods.—There is a considerable variety of electrical prospecting methods which depend upon currents induced in the ground by a primary alternating current and the measurement of the resulting electromagnetic field at the surface. The theory of all these methods depends upon the fact that the electric or magnetic field in the space around the primary current

[1] See p. 377.

depends upon the currents that are induced in any subsurface conductors. If the subsurface material were homogeneous, these fields would have a certain form. By measuring the actual phase and direction of the magnetic vector it is possible, from the differences between the measured pattern and that which would be expected for a homogeneous subsurface, to infer something of the nature of any changes in conductivity of the subsurface material. Such measurements are influenced particularly by horizontal changes in conductivity, and therefore the inductive methods have been applied (in oil prospecting) principally for locating faults.

Two different systems of induction are used. One of these employs some sort of current loop or coil of relatively small dimensions so that at a distance the effect is essentially that of an oscillating dipole at the coil. The other uses an insulated cable laid out on the ground and measures the field in the immediate region of this cable, usually in a series of short traverses perpendicular to the cable.[1] The theory of the alternating-current methods is quite complicated and becomes increasingly so if the interpretation is carried to the consideration of more than two or three conducting layers. Certain empirical charts and schemes of interpretation are used that facilitate the determination of changes in conductivity from the rather complicated measurements of the magnitude, direction, and time phase of the magnetic field.

The penetration of induced electric currents in the ground is a function of their frequency and of the electric conductivity and specific inductive capacity of the ground. Within the range of frequencies used for electrical prospecting the conductivity rather than the specific inductive capacity is the principal factor that determines the penetration and influences the results. For the specific case of induction from an oscillating dipole (which corresponds to induction from a small closed loop or coil) it has been shown that, for conductivities within the range of earth materials, the optimum frequency for depths of penetration of the order of 1,000 ft. or more becomes very low (less than 10 cycles per second).[2] For induction from a long horizontal wire the optimum frequency is as low as can be used and meas-

[1] Zuschlag, 1932.
[2] Peters and Bardeen, 1932, p. 116.

ured.[1] These restrictions make the application of certain electromagnetic methods to deep prospecting very difficult, as serious technical problems arise in connection with the generation and measurement of alternating currents of such low frequency.[2]

ELECTRICAL TRANSIENT METHOD

A special development in electrical methods which has been made by the oil industry rather than the mining industry is the electrical transient, or so-called "eltran," method. The original development of this method seems to have been based on the idea that it would provide a means by which electrical prospecting could be extended to greater depths.[3]

The transient methods depend either upon the introduction into the ground of a sharp current pulse, such as may be made by suddenly closing or opening an electrical circuit connected to grounded electrodes, or upon impressing an electric current of a certain wave form on the ground. Measurements are made either of the form of the current or more commonly of the form of the resulting potential. The electrode system used has usually con-

---

[1] *Ibid.*, p. 118.

[2] For a plane wave, of frequency f, transmitted through a medium with conductivity σ, permeability μ, and specific inductive capacity S (in rational e.m.u.) the real amplitude of the magnetic vector H_y at a penetration z into the medium is

$$H_y = H_0 e^{-2\pi f K z}$$

where

$$K^2 = \frac{\mu}{2}\left(\sqrt{S^2 + \frac{\sigma^2}{\omega^2}} - S\right)$$

and

$$\omega = 2\pi f$$

When, as is usually true for earth materials, $\sigma/f >> S$,

$$K^2 = \frac{\mu\sigma}{2\omega}$$

and

$$H_y = H_0 e^{-z\sqrt{\frac{\omega\mu\sigma}{2}}}$$

For the above expressions (in slightly different units) and numerical examples of attenuation and penetration calculated therefrom, see Eve, 1932, pp. 161–162.

[3] Karcher and McDermott, 1935.

sisted of four electrodes in line, with the two potential electrodes outside the two current electrodes (Fig. 175).

The interpretation of the results depends upon determining in some way the time constants, such as the rate of build-up or of die-down of the potential. Variations in this rate are expected to correlate with variations in the electrical properties of the subsurface. In some of the earlier proposals it was expected that sharp nicks or irregularities in the curves would be found which would result from penetration of the current to conductors at different depths.[1] However, in the later developments this principle seems to have been abandoned, and the interpretation of results is based on measurements of the time constants.
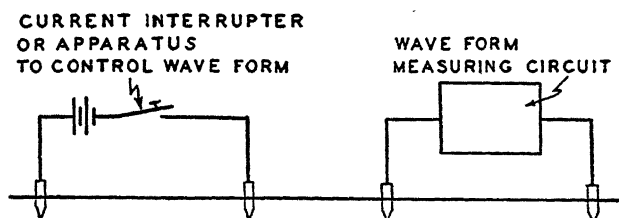
Fig. 175.—Electrode configuration and schematic principle of the eltran system.

The time constants have been measured in two different ways. In the first work, measurements were made of the actual form of the recorded transient voltage. Another system measured the resultant transient from two symmetrical and oppositely disposed current sources.[2] In these measurements the variations in ground characteristics were correlated with variations in the time required for the current to build up or to die down to a certain fraction of its final value. A later method, which has been called "sawtran,"[3] applies a square wave to the ground. The resulting voltage between the potential electrodes is then run through a distorting electrical network by which the voltage is restored to the same square wave form as the impressed current. The distorting network then compensates for the amount of distortion produced in the part of the circuit that flows underground. A numerical value for the amount of distortion can be obtained from the values of the electrical variables used in the

[1] Blau, 1933.
[2] Statham, 1936.
[3] Klipsch, 1939.

distorting network. This method removes the necessity for actual measurements of the wave form on a photographic record and is considerably more rapid in use in the field.

There is considerable conflict at present as to the real value of the electrical transient methods. Some tests[1] have indicated that the underground characteristics measured by the eltran method are substantially the same as are measured by ordinary resistivity determinations with similar electrode spreads and, therefore, that the eltran survey does not penetrate to appreciably greater depths than ordinary electrical prospecting methods. On the other hand, claims have been made of very definite determination of oil itself at depths much greater than would be expected by ordinary electrical prospecting. The uses and interpretations of the method are still almost entirely empirical, and there is no theory to support the claims that great depths or the detection of oil in place should be possible.

The future utility of these methods is difficult to evaluate. The intensive development has made the application of the more complicated transient measurements comparatively straightforward, simple, and rapid in the field so that the measurements are actually carried out more rapidly than the simpler resistivity determinations. At present it seems very probable that the method has no greater depth penetration than other electrical methods but that it may have useful application because of the fact that apparently there often are shallow secondary indications of geological structure at greater depths[2] and that electrical measurements may indicate these variations. Whether or not the eltran method would be superior to the simpler electrical measurements for this purpose is still a debatable point.

DEPTHS REACHED BY ELECTRICAL METHODS

There are certain limitations on the depths that may be explored by electrical methods. Since these limitations are the principal reason why such methods are not more extensively used in oil prospecting; the background for them will be examined.

The depths attainable depend on the methods used. The entire question of depths attainable is somewhat controversial, as there is considerable disagreement between the expectations of

[1] Blondeau, 1939.
[2] Rosaire, 1938.

theory and the claims of practice. The controversy arises principally because the rather simple subsurface conditions assumed for the theory (particularly horizontal continuity) are not generally met in practice.

Comparatively small, shallow, horizontal discontinuities in the electrical properties of the ground may have a greater effect on the electrical measurements than much greater discontinuities at depth. Unless these are recognized as such, they may be misinterpreted as indications of deep or vertical changes. From theoretical considerations, no sharp changes of electrical effects measured at the surface can be expected to result from deep contrasts in electrical properties. Therefore, all sharp nicks or kinks in curves of electrical properties plotted as a function of horizontal variables, such as electrode spacing or position of the electrode spread or assembly, are much more probably the result of superficial irregularities rather than manifestations of significant geologic contacts or irregularities at depths substantially greater than the horizontal dimensions of the nicks or kinks involved.

Direct-current Methods.—For direct currents applied to a homogeneous medium, the depth to which the current penetrates depends only on the horizontal spread of the electrodes at which the current is applied. Thus there is no theoretical limit to the depth that may be reached. In fact, measurements have been made in France[1] using long telephone lines to apply currents between electrodes as much as 150 miles apart to measure resistivities at depths of some tens of miles.

Theoretical investigations of the distribution of electrical current in the ground are nearly all based on the assumption that the layers are horizontal and homogeneous in a horizontal plane. Under the further assumption that the ground is homogeneous vertically, it can be demonstrated readily that just half the current will flow across the vertical plane midway between the electrodes above a depth equal to half the electrode spacing; the other half will flow at a greater depth (Fig 173).

If the subsurface is stratified with layers of different resistivity, it is evident that as the electrode spacing is increased, layers at successively greater depths will carry some of the current, and measurements made on the surface will begin to be affected by

[1] Schlumberger. 1932.

the electrical characteristics of these deeper layers. However, some of the current is still being carried by the shallow layers. There is no sudden change in current distribution as the electrode spacing is increased but only a gradual change as deeper layers have increasing "weight" or proportional influence on the current distribution. For any given system of electrodes it is possible to calculate a "weight curve" which shows the relative influence that parts of the section at different depths have on the quantities measurable at the surface.[1] Thus, as the electrode spacing is increased, a sharp discontinuity in resistivity will gradually begin to influence the measurements, will have a maximum influence at a certain spacing, and will have less influence again at still larger spacings. No matter how sharp the discontinuity, the effect on a curve of effect versus spacing will be smooth. The situation is quite similar to the magnetic and gravity effects of a body at depth; for no matter how sharp its boundaries, its effects will be smoothed out and cannot make sharply changing curves. Such considerations are the basis of the statement previously made that sharp breaks in resistivity curves cannot be interpreted as the effects of sharp resistivity discontinuities at depth but rather must be interpreted in terms of longitudinal (*i.e.,* horizontal) variations of resistivity at shallow depths.

Rules have been developed from which estimates of depth are made from changes in resistivity as the electrode spacing is changed. For instance, with the Wenner electrode configuration and the Gish-Rooney measurements, an empirical rule used is that the depth to a resistivity change is equal to the electrode interval at the point on the curve of resistivity versus electrode spacing at which the change occurs.[2] Curves have been calculated for various assumed resistivity distributions to assist in the interpretation of more complex situations.[3] Such rules and curves are usually empirical and have no definite theoretical basis except for assumed conditions that are simpler than actual conditions met in nature. This follows from the fact that the theoretical relations between quantities that should be measured

[1] Evjen, 1938.
[2] Eve and Keys, 1938, pp. 102–107.
[3] Tagg, 1934.
Pirson, 1934.
Wetzel and McMurray, 1937.

and the electrode spacing vary with the distribution of resistivity below the surface. Therefore, a depth rule that would be applicable to one resistivity distribution would not apply to another.

The foregoing does not mean that the empirical depth rules are of no value. If a rule can be established for a given known resistivity situation in a given area, such as might be established by making electrical measurements over an area where the resistivity contacts are known from drilling, then the same rule may be reasonably applied to determine unknown depths to resistivity contacts in a similar situation or in the same general area. However, the empirical nature of such rules should not be forgotten, and the application of a rule derived in one area to another where the subsurface resistivity distribution is quite different might lead to grossly erroneous results.

Alternating-current Methods.—The discussion of depths and depth rules as applied to direct-current methods is also applicable to low-frequency, alternating-current methods but with certain important limitations. In all alternating-current methods the depth of penetration of the current that might be expected is dependent upon the frequency and upon the conductivity of the ground.[1] For inductive methods there is an optimum frequency for a given conductivity of the ground which should be used for investigations at a given depth, and this frequency decreases with the depth. As pointed out above (page 371), deep penetration requires the use of very low frequencies. However, the difficulty of generating and measuring alternating currents increases greatly at low frequencies, so that this makes a rather definite limitation on the depths that can be reached by alternating-current induction methods. It is probable that practically useful results are not obtained by any of the alternating-current inductive methods at depths greater than around 2,000 ft.

For conductive methods, using alternating current, the situation is more complicated. In geophysical work with alternating currents (or with reversed direct current as in Gish-Rooney or

---

[1] The current distribution in the ground also depends to a certain extent upon the dielectric constant. However, the relative effect of the dielectric constant decreases with the frequency, and for frequencies and conductivities that are used in electrical prospecting the effect of the dielectric constant is usually practically negligible. See Peters and Bardeen, 1932, p. 113; also Slichter, 1932, p. 447.

Megger measurements) it is usual, when any theory is applied, to use the simple direct-current theory. For alternating currents, the current distribution in the ground will depart from that of direct current for two reasons: (1) The "skin effect," or mutual reaction of the current upon itself, will tend to make more of the current flow at shallower depths than the direct-current distribution; and (2) a certain amount of current will be induced in the ground by the surface wire carrying current to the ground electrodes. These effects will increase with increase in frequency and also for increase in conductivity.

An exact quantitative statement of the change in current distribution and the resulting change in apparent resistivity resulting from the use of alternating currents is not possible, as the theoretical problem involved does not seem to have been solved. From consideration of a somewhat similar but not identical problem which arises in connection with the mutual impedance and interference between power circuits and telephone lines, it is probable that, for small-scale work (as in ore prospecting) and for ordinary ground conductivities, there will be little practical difference between alternating- and direct-current resistivities for frequencies up to around 100 to 200 cycles but that there may be very material differences for frequencies around 1,000 cycles or higher.[1]

Although an exact theory for calculating the details of the alternating-current distribution in the ground is not available for the electrode systems and circuits of ordinary electrical prospecting, we can make some approximate guesses from the theory for other cases. In general, theory indicates that assuming unit permeability (which is quite closely true for earth materials) and neglecting displacement currents (which are quite negligible for earth conductivities and for frequencies below radiofrequency (see footnote, page 377), the amplitude of current at a depth h should depend on the factors $h\sqrt{f/\rho}$. An exact attenuation factor cannot be given, as the current distribution is inferred indirectly from the theory for other effects, such as the mutual impedance of grounded circuits. However, there are certain empirical criteria, based on different estimates of the value of $h\sqrt{f/\rho}$ at which the current is "small" or "negligible," and calculation of these estimates gives at least a useful approxima-

[1] Railroad Commission of the State of California, 1919, p. 158.

tion to alternating-current penetration. In the following examples the numerical values are given for h in meters, f in cycles per second, and ρ in ohm-centimeters.

1. From the theory of the "skin effect"[1] the amplitude is reduced by a factor $1/e$ when

$$h\sqrt{\frac{2\pi\mu f}{\rho}} = 1$$

For the units chosen, this is equivalent to saying that (for $\mu = 1$) the current is reduced to 36.7 per cent of its initial value when

$$h\sqrt{\frac{f}{\rho}} = 50.3$$

2. For a long, grounded line (current flow parallel to the surface) Radley and Josephs[2] give the criterion that "a negligible part of the current flows at a depth such that $10^6 h\sqrt{\sigma f} > 800$." This criterion is a rather arbitrary choice, based on theoretical curves for mutual impedance. In the units chosen, this becomes

$$h\sqrt{\frac{f}{\rho}} \geqslant 25.3$$

3. Haberland[3] gives a semiempirical criterion based on a similar situation and also depending on the theory for impedance of grounded circuits. In the units chosen, this becomes

$$h\sqrt{\frac{f}{\rho}} = 36$$

4. Slichter[4] has suggested a somewhat lower value, partly as an empirical value which seems to work out fairly well in geophysical experience. In the units chosen it is

$$h\sqrt{\frac{f}{\rho}} = 13$$

[1] Jeans, 1933, p. 479.

[2] Radley and Josephs, 1937, p. 102.

[3] Haberland, 1926, p. 371.

[4] L. B. Slichter, personal communication.

Using the criteria given, we can calculate the maximum frequencies to give penetration to given depths as follows:

h, meters	ρ, ohm-cm.	f (Slichter)	f (Radley)	f (Haberland)	f (skin effect)
100	10^3	16.9	64	130	250
	10^4	169	640	1,300	2,500
	10^5	1,690	6,400	13,000	25,000
316	10^3	1.7	6.4	13	25
	10^4	16.9	64	130	250
	10^5	169	640	1,300	2,500
1,000	10^3	0.17	0.64	1.3	2.5
	10^4	1.69	6.4	13	25
	10^5	16.9	64	130	250

Although the different criteria give widely varying frequency figures, it is evident that very low frequencies are required to penetrate considerable depths, especially with the lower resistivity values. (These figures involve the assumption that the electrode spacing is wide enough so that the current flow is essentially parallel with the surface.)

Some attention has been given to the applications of radio-frequency currents to prospecting. Theory indicates that there is little hope that such currents would be useful except for very shallow exploration. The attenuation of current increases so much for high frequency that, for ordinary ground conductivities, radiofrequency currents would not be expected to have an appreciable part of their energy penetrate more than a few hundred feet.[1]

To summarize, it appears that present electrical methods, employing measurements made on the surface, are limited by theoretical and practical difficulties to comparatively shallow exploration. Therefore, their application to oil prospecting appears limited to the detection of relatively shallow secondary manifestations of deeper underlying structure. There seems to be no present application of electrical principles that will indicate

[1] Eve, 1932.
Also see footnote 2, p. 372.

rectly the presence or absence of oil at usual producing depths, sed on the modification of electrical properties of the rock by e insulating or other properties of oil itself.   On the other hand, ctrical methods have many useful applications for indicating inerals, ground water, etc., and in engineering applications, ch as indicating depth to bedrock in connection with proposed nstruction, such as dams, bridges, or tunnels.

CHAPTER XX

ELECTRICAL WELL LOGGING

ELECTRICAL MEASUREMENTS IN WELLS

A special application of electrical measurements which has become of great importance to the oil industry is made for the exploration of wells. The process of electric well logging is essentially a resistivity measurement "turned on end" with the electrodes disposed vertically in a well instead of horizontally along the surface of the ground. A resistivity measurement is made using apparatus similar in principle to that of the Gish-Rooney system. The resistance measured is that of the rock in the walls of the drill hole to a distance back from the hole depending on the spacing of the electrodes.

The electric well logging methods have been developed principally by two French brothers, C. and M. Schlumberger.[1] Electrical measurements in wells were first tried in the Pechelbron field in France in 1929. Shortly thereafter they began to be used extensively in the U.S.S.R. and later in Rumania and in the Lake Maracaibo fields in Venezuela. Within the last few years they have been used considerably in this country and are now being applied extensively and, in some areas, have become almost as much a part of drilling wells as mechanical coring or catching samples of cuttings.

MEASUREMENT OF SPECIFIC RESISTANCE

The measurements are made by running into the well a long assembly containing three electrodes which are connected to the surface by a specially designed three-conductor cable. The cable passes over a measuring pulley and on to a large drum. Electrical connections to the three conductors are made through

[1] For a good general discussion of electrical coring, see C. Schlumberger, 1938. For somewhat more detailed discussion of the theory see C. and M. Schlumberger and Leonardon, 1934a, 1934b.

For a critical study of the uses and interpretation of electric well logging, see Houston Geological Society, 1939.

contact rings on the drum. The arrangement is shown schematically in Fig. 176.

An approximate theory for the three-electrode system used by Schlumberger can be set up very simply.

The upper two potential electrodes, M and N (Fig. 176), are relatively close together. The lower, or current, electrode A
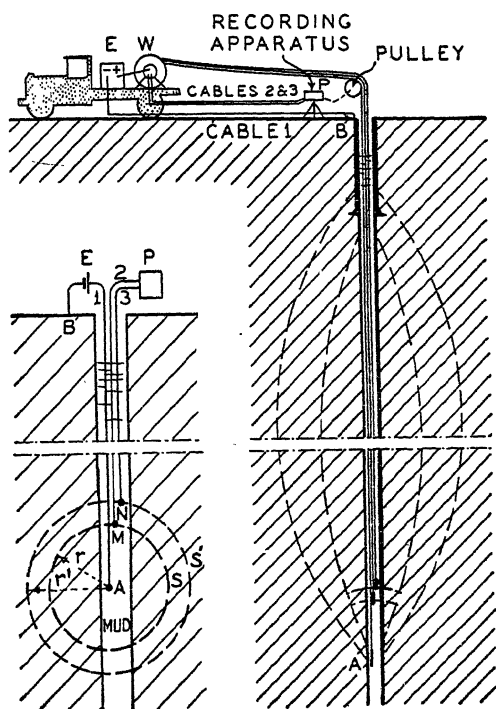
FIG. 176.—Principle and electrode system for electric well logging. (*After Schlumberger, 1934a.*)

is a short distance farther down the hole. An electric current, either direct or low-frequency alternating, is passed from electrode A through the ground to a grounded point, commonly the well casing. The current from A may be considered as flowing out equally in all directions so that it passes through successive spherical shells around A. The points M and N may be considered as representative of two such shells, and the potential difference between them is a product of the current I flowing from A and the resistance R between the two shells. If this

potential difference is ΔV, then

$$\Delta V = RI \text{ and } R = \frac{\Delta V}{I} \tag{307}$$

If the rock around A is considered to be homogeneous with a specific resistance ρ, the resistance across a thin shell of thickness Δr will be

$$\Delta R = \frac{\rho \, \Delta r}{A} = \frac{\rho \, \Delta r}{4\pi r^2}$$

and the total resistance between shells of radius r_1 and r_2 will be

$$R = \frac{\rho}{4\pi} \int_{r_1}^{r_2} \frac{\Delta r}{r^2} = -\frac{\rho}{4\pi}\left(\frac{1}{r_2} - \frac{1}{r_1}\right)$$

$$= \frac{\rho}{4\pi} \frac{r_2 - r_1}{r_1 r_2} \tag{308}$$

By equating (307) and (308),

$$\frac{\Delta V}{I} = \frac{\rho}{4\pi} \frac{r_2 - r_1}{r_1 r_2}$$

$$\rho = 4\pi \frac{\Delta V}{I} \frac{r_1 r_2}{r_2 - r_1} \tag{309}$$

Thus, from measurements of the current to electrode A and the difference in potential between the two electrodes M and N, together with the known spacing of the electrodes, the specific resistance of the rock opposite the two electrodes M and N can be computed.

It might seem that the mud in the drill hole would influence the measurements. It does to a certain extent. However, if the distance apart of M and N is a few times the diameter of the hole, the influence of the mud is small, and the resistivity measured is principally that of the rock in the part of the section between M and N. However, the mud is an essential element of the system, as it forms the electrical contact between the electrodes and the rock in the walls of the hole. Therefore, electrical well logs are always run with mud or water in the hole.

The electrical conductivity of rocks depends almost entirely on the electrolytic fluids that they contain, since the rock minerals themselves (except for metallic minerals) are very good insulators. Therefore, the measured resistivity will vary

greatly, depending on the porosity of the rocks and the nature of the fluids that they contain and particularly the salt content of the fluid. A given rock filled with salt water has a low resistance; if filled with fresh water, a high resistance; and if filled with oil, a still higher resistance. The specific resistance of different rocks under different conditions of water content, etc., may vary over a very wide range.

ELECTRICAL INDICATIONS OF POROSITY

Early in the history of the practical application of resistivity measurements in drill holes it was noticed that there is a self-potential in the hole; *i.e.*, a potential was indicated when no current was applied. It has been found that this potential is closely related to the porosity of the beds opposite the electrode. The potential is explained as arising in two ways: (1) by electrofiltration and (2) by electroosmosis.

Electrofiltration.—It can be shown that, if a liquid is forced through a porous dielectric medium (such as water passing through sand in a glass tube), a difference in potential is set up, apparently from friction of the fluid on the dielectric. The magnitude of the potential set up is proportional to the rate of flow of the liquid and, therefore, will depend on the pressure gradient causing the flow and the permeability of the dielectric medium. The pressure of the liquid in a drill hole will, in general, be different (usually higher) from the natural pressure of the rock. Therefore, there will, in general, be a flow of fluid, usually from the hole to the rock. This flow sets up a difference in potential which can be expressed as

$$E = K\rho(P' - P)^*.$$

* Schlumberger, 1934a, p. 258, gives the expression

$$E = m\frac{R}{V}P$$

where m is a constant, R is the resistivity of the fluid, P is the "pressure of the liquid" (really the differential pressure causing the flow), and V is the viscosity of the liquid. However, when the e.m.f. is measured in laboratory experiments with water flowing through sand, it is found that it becomes negligible when liquids having salt content as high and resistivities as low as those of oil field waters are used. Thus, it appears that, although there undoubtedly is a real potential associated with the flow of fluids through

where P' is the pressure of the drilling fluid, P is the rock pressure, ρ is the resistivity of the liquid, and K is a constant. The measurement of E is made simply by measuring the potential difference (in millivolts) between an electrode lowered in the well and another electrode grounded at the surface. If fluid flow is into the rock, the electrode in the well is negative with respect to that at the surface.

Electroosmosis.—When two electrolytes are in contact, an electromotive force is observed which is

$$D' = K' \log \frac{\rho_1}{\rho}^*$$

i.e., the electromotive force is proportional to the logarithm of the ratio of the resistivities of the two electrolytes. In a drill hole, the two fluids, *i.e.*, the drilling mud and the natural fluid in the rock, form the two electrolytes. Usually the rock fluids are more salty and have lower resistance than the drilling fluid. Under this condition the potential is negative.

Permeability Measurements.—When an electrode is put in the well, the actual potential measured is presumably a combination of the two effects just mentioned. The two can be studied separately to some extent, for by changing the pressure of the fluid the electrofiltration component should change, whereas changing the salinity of the mud should change the electroosmosis component. The exact contribution of each effect has not been completely determined, but apparently[1] the electrofiltration component is considerably the larger of the two.

The measurements, of course, must be made in open holes where the rocks are in direct contact with the well fluid. A well

---

porous material in wells, the simple theory usually given is far from complete and much is yet to be learned about the details of the origin of this potential.

* Schlumberger, 1934b, p. 278. It is probable that this relation also is oversimplified. Since the two electrodes, one in the well and one at the surface, are far apart, the potential measured probably is affected by differences in resistivity of electrolytes throughout the geologic section. However, the principal variation may come from variations in the immediate vicinity of the lower electrode. The relationship of this concentration potential to the porosity is probably not very simple, but usually there apparently is a correlation between the two so that an empirically useful relation results.

[1] Schlumberger, 1938, p. 354.

casing is such a perfect electrical shield that properties of rocks outside the casing cannot be determined by electrical measurements inside.

ELECTRICAL WELL LOGGING EQUIPMENT AND OPERATION

In the actual application of the principles outlined above, the resistivity and self-potential are measured simultaneously. An alternating-current circuit and potentiometer measure the resistivity; a direct-current potentiometer measures the self-potential. The resulting values (resistivity in ohm meters, self-potential in millivolts) are plotted side by side against the depth in the hole.

The apparatus is now highly developed. Special cables are used which are very strong (tensile strength up to 8 tons[1]) and have very good insulation between the three conductors (several megohms per kilometer).[1] A special winch for holding 10,000 ft. or more of cable is mounted on a heavy truck. Measurements are made while pulling the weighted electrode assembly up the hole. A measuring wheel, turned by the cable, operates the paper on which the resistivity and porosity values are plotted by potentiometers which are kept balanced by keeping a needle at a fixed point, thus continuously compensating for the variable resistivity and potential. Measurements are made at a rate of about 1,000 ft. per hour. More recent apparatus uses completely automatic recording to increase the rate and reliability at which holes are measured.

A very recent development has been that of a method of making electrical well logging measurements simultaneously with drilling operations.[2] This involves the use of special drill pipe carrying an electric cable and with joints so made that when sections of pipe are screwed together, an electric connection is made to carry the current from one joint of pipe to the next. Also, special bakelite sections of drill pipe are used just above the bit to insulate the metallic sections that serve as electrodes.

In the last few years there has been a development to complicate the resistivity measurements by the addition of a "second curve," a "third curve," etc. These are resistivity curves made with different electrode spacings. This makes the analogy with

[1] *Ibid.*, p. 355.
[2] Reed, 1939.

surface electrical prospecting somewhat closer, for the differen
resistivity values correspond with different electrode spacin
and therefore with different depths of penetration of the measur
ing current into the rock back from the drill hole.   The principa
utility of these curves seems to be in evaluating and eliminatin
the disturbing effects on the resistivity that are caused by con
tamination of the natural rock fluids by drilling fluid penetratin
into the rock.   Also, the differences between the curves fo
different electrode spacings indicate corresponding differences ir
the degree to which drilling mud penetrates the formation fron
which an indication of porosity is obtained that is independen
of the self-potential measurement.

INTERPRETATION OF ELECTRIC WELL LOGS

The interpretation of electric well logs is largely empirical and
a matter of practical experience in the general area and geologic
section in which they are made.   The general principles observed,
however, are as follows:

1. A high resistivity means either
   a. A nonporous formation containing relatively little conducting
      fluid (*i.e.*, salt water).
   b. A porous formation containing a nonconducting fluid, such as oil
      or gas.
2. A low resistivity means a porous formation containing a conducting
   fluid (*i.e.*, salt water).
3. A high self-potential (millivolt) value means a permeable formation.

Different combinations of resistivity and potential may be
interpreted roughly as

1. Low resistivity, low potential.   This should indicate a formation con-
taining enough salt water to be a relatively good conductor but of low
permeability, which usually will be interpreted as a shale.
2. Low resistivity, high potential.   This should indicate a formation con-
taining salt water to make it a good conductor and high permeability, which
may be interpreted as a water sand.
3. High resistivity, low potential.   This should indicate a formation con-
taining little or no salt water and having low permeability, which may be
interpreted as a tight limestone, salt, gypsum, coal, etc.
4. High resistivity, high potential.   This should indicate a formation con-
taining little or no conducting liquid but permeable, which may be inter-
preted as an oil or gas sand, since oil and gas are not electrical conductors.

From the foregoing, it may appear that the interpretation of
an electrical well log is very simple and positive and that the

application of a few elementary rules should lead to definite and unambiguous results. However, electric well logging partakes of many of the uncertainties of geophysical prospecting from the surface. There are complicating factors and uncertainties in underground conditions which lead to border-line cases, and it is not always possible to divide up the parts of an electric log into clear-cut categories, such as have been indicated. To mention only one source of confusion, some oil sands contain connate water which renders them almost as conducting as some salt-water sands. On the other hand, more information than is indicated by the simple outline above may be gained from a proper control of the well logging conditions and measurements and study of the resulting curves. For instance, the degree of saturation of an oil sand and its potential productivity are determinable from electrical resistivity measurements, together with other field and laboratory data.[1]

APPLICATIONS OF ELECTRIC WELL LOGGING

Electric logs are used for several different purposes, depending on local geologic conditions and problems. Many examples of electric logs and their uses are given in the literature, particularly the papers by Schlumberger.[2]

Correlation.—Correlation may be made by matching up characteristic resistivity or potential indications from one well to another. In some cases given geologic markers give characteristic responses on the electric logs. In others, electric logs show characteristic indications that cannot be identified with any known lithologic changes but that can be recognized from one well to another. In some cases, where the geologic section contains thick members with definite lithologic differences, the correlations can be carried for long distances, even many miles, or from one field to another. For instance in West Texas the lime and anhydrite sections have characteristic high resistivities which can be recognized over large distances (50 miles).[3] In other areas, correlations cannot be carried safely over large distances but may give detailed structural information on a field.

[1] Martin *et al.*, 1938.
[2] See particularly Schlumberger, 1938, and Houston Geological Society Study Group, 1939.
[3] Gillingham and Stewart, 1938.

Schlumberger[1] gives an example where faults and other structural details of a field that had not been known from geologic correlations were recognized from a study of electric logs.   Faults may be shown up clearly by changes in interval between certain clear-cut characteristics of the electric logs.[2]   A very detailed correlation of electric logs across the Tepetate field shows many correlatable horizons and includes a fault.[3]

Indications of Oil Sands.—In many cases, oil sands may be indicated by electric logs where they were not indicated by oil shows in drilling.   It is claimed that a number of new fields have been discovered from wells which, when tested by electric logs, gave indications of oil sands even though the well otherwise might have been abandoned without a production test because of the absence of shows.

Details of an Oil Zone.—Minor variations within a producing zone may be indicated by changes of resistivity, either horizontally or vertically.   For example, a sudden decrease of resistivity in going downward in a well, together with a continuous high porosity may indicate the water-oil contact in the producing sand.   Thus, electric logs may give indications of points for casing perforations, plug back jobs, etc.   Decreasing resistance from well to well laterally may indicate an increasing water content with the oil.   An example of this from Venezuela is given by Schlumberger.[4]

Unfavorable Results.—Good results are not always obtained, and electric logging may not always give the simple and definite indications that might be expected from all the examples cited above.   Just like surface geophysical methods, it works much better in some areas than in others.   For instance, some details have been given[5] of an instance in California where the electrical indications apparently were not reliable and the well did not perform at all according to expectations from the electrical indications.

[1] Schlumberger and Leonardon, 1934*b*, pp. 282–283.

[2] Schlumberger, 1938, p. 359.

[3] Bornhauser and Bates, 1938, p. 297.

[4] Schlumberger, 1938, p. 361.

[5] Jensen, 1937, pp. 64–66.

CHAPTER XXI

MISCELLANEOUS PROSPECTING METHODS AND OPERATIONS IN WELLS

There are a few principles of geophysical prospecting in limited use at present that do not come under the classifications of gravitational, magnetic, or electric. Also, a number of technical operations carried out in connection with the drilling or operation of oil wells are distinctly exploratory in nature and have been developed as by-products of geophysical technique. This chapter outlines the principles of those methods and operations which are considered of probable interest to exploration geophysicists.

SOIL ANALYSIS OR CHEMICAL PROSPECTING

A type of geophysical prospecting based essentially on chemical analysis for surface indications of oil has developed rather rapidly within the past few years. This is an attempt to find a method that will give a direct indication of the actual presence of oil itself rather than the indirect indications which are all that are given by any of the geophysical methods.

The original idea on which the chemical method of prospecting began to develop was that gases associated with oil would, to a certain extent, penetrate and spread upward through the overlying formations and that these gases should be present in sufficient quantity over oil fields to be detected by appropriate methods of analysis. The idea was that the concentration of gases directly related to oil should be greater immediately over an oil deposit than in surrounding areas. There are some hydrocarbon gases, particularly methane, that occur naturally from decomposition of vegetation as well as in connection with oil deposits. However, certain heavier hydrocarbons, particularly ethane and propane, are found naturally only in connection with oil deposits. Therefore, it was thought that an analysis which

would show very small concentrations of ethane and heavier hydrocarbons might be capable of detecting the presence of oil.

Apparently the first exploitation of this idea was made in the U.S.S.R. in 1929 to 1930. In that work samples of gas were drawn from the soil and later analyzed for their various hydrocarbon constituents.

The method of analysis for the hydrocarbon constituents that seems to have been most successful, both in the early work and in later developments in this country, is that based on the different vapor pressure characteristics of the different gases. If a mixture of hydrocarbon gases is cooled to liquid-air temperatures and then allowed to warm up, the different constituents vaporize at different temperatures. The different temperature-vapor pressure characteristics of the different gases serve to separate the various constituents, and the relative quantities may be determined by chemical analysis. Methods are developed for determining extremely small fractions of certain constituents, such as detecting 1 part in 10^9 of ethane.

The first work, using soil gas drawn from shallow holes, apparently had some slight success in Russia; but results were erratic, and the method did not appear very promising on early tests in this country. This led to attempts to use other constituents of the surface soil rather than the gas itself, and the present chemical prospecting methods are based on the analysis of a sample of the soil itself rather than the gases drawn from the ground.

The use of the soil sample is based on the assumption that, as hydrocarbon gases percolate up to the surface from buried oil deposits, certain chemical changes occur at the surface where they are exposed to sunlight and air. These changes are supposed to result in the formation of certain much heavier hydrocarbons or waxes which are accumulated and concentrated in the surface soil.[1] Also, gases might be expected to be occluded on the soil particles. Naturally, the accumulation would be expected to be greater over an oil deposit than in other areas.

The characteristic materials are extracted from the soil sample for analysis by pumping off occluded gases and by treating the sample with certain solvents. A rather involved chemical process of extraction and analysis is carried out, the details of

[1] Horvitz, 1939, p. 222.

which are not publicly available. Finally, the concentrations of certain constituents are determined for each sample.

Field Procedure.—The field procedure is very simple and consists essentially of taking samples of the soil at rather close intervals along profiles. Commonly the samples are taken at intervals of about $\frac{1}{10}$ mile. They are immediately sealed up in suitable containers, such as ordinary glass fruit jars, and are sent to a laboratory for analysis.

Interpretation.—The numerical values resulting from the soil sample are plotted on a map at locations corresponding to those at which the samples were taken. Several maps may be made, each one giving the proportions of a different constituent as indicated by the analysis. The final interpretation or selection of areas of interest is based on a comparison of the various maps.

From experience in testing the chemical methods on known oil fields, it seems more or less generally true in American experience that there is a tendency for the chemical constituents associated with oil to be more concentrated around the periphery of the oil-bearing area so that, when mapped, the area of concentration forms a "halo" surrounding the oil area. The interpretation of the results consist principally in recognizing these halos from the maps of the concentration of hydrocarbon, heavy mineral, or other constituents of the soil samples. The halo pattern does not seem to have been recognized in the rather extensive Russian experience.[1]

After the halo had been indicated by field experience, an explanation for it was sought. The explanation now given is that the uplift of structure and the mineralization from percolating ground waters tend to reduce the porosity of the strata immediately overlying the structure.[2] This is presumed to result partially from cementation and partially from chemical processes associated with migrating gas. In any event it is assumed that there is a tendency toward the formation of a more or less impervious cap in the area vertically above the oil deposit. Thus, the upward migration of gas is presumed to be more restricted in this impervious area, and therefore less gas reaches the surface

[1] Sokolov is definite on this point and says "It can only be stated positively that the area of maximum indices will be within the outline of the deposit"; Sokolov, 1936, p. 246.

[2] Rosaire, 1938b.

in the area directly above the oil deposit than in the immediately surrounding area, thus leading to the formation of the halo.

Some of the maps[1] that have been published by the soil-gas prospecting companies appear quite convincing. On the other hand, the range of individual values on which these maps are based is very large, and, in general, there seems to be a distinct tendency for very wide scattering of the values. This erratic variation of values, together with the questions as to the fundamental chemical and physical processes responsible for the concentration of the substances indicated by the chemical analysis, leaves much skepticism regarding the objective relation between the soil-gas measurements and underlying oil deposits.[2] A really complete statistical analysis of a large volume of soil analysis data, including surveys over areas where oil is not expected, would be very desirable for testing the premises on which the expectations of the present chemical prospecting methods are based.

TEMPERATURE MEASUREMENTS IN WELLS AND GEOTHERMAL PROSPECTING

Electrical resistance thermometers have been used for measuring temperatures in wells. Apparatus has been developed by which a continuous record of temperature, to a small fraction of a degree, can be obtained. A number of economically and scientifically useful applications can be made of such measurements.

It is sometimes of interest and importance to know, in cementing a well, how far the cement that has been pumped down through the casing has been forced up in the annular space between the casing and the walls of the hole. This can be determined by making temperature measurements at the proper time after the cement has been put in place. The heat of setting of the cement causes a rise in temperature which begins at the top of the cement and can thus be used to determine its position behind the casing.[3]

Temperature measurements may be used for locating the source of gas flowing into a well. The expanding gas cools the formations so that by making temperature logs at properly

[1] See, for example, the maps by Horvitz, 1939.
[2] See discussion by Teplitz and reply by author, Horvitz, *op. cit.*, pp. 225–228.
[3] Deussen and Guyod, 1937.

chosen time intervals the changes in temperature indicated can be used to determine the level at which the gas flow occurs. This has been used to indicate the level at which pipe should be set to reduce gas-oil ratios.[1] The indications of such temperature measurements are somewhat more definite when used in connection with resistivity and porosity curves, as the combination gives more definite and diagnostic information than either would separately.

Variations in underground temperature have been suggested as a means of geological correlation.[2] This would depend upon identifying irregularities in the temperature curves from one location to another.

Another possible use of temperature measurements is as a means of geophysical prospecting. It is known, for instance, that the ground temperature over salt domes is slightly higher than normal because the thermal conductivity of salt is higher than that of the surrounding sediments. It has been proposed that temperature measurements in comparatively shallow or core drill holes could be used for locating areas that lie over deeply buried salt intrusions, and tests over known structures seem to have indicated that the method has some possibility of giving useful indications. Since the expected temperature differences are small, it would seem necessary in making such tests to give careful attention to the temperature disturbances that may be caused by drilling and production over known structures.

Underground temperature measurements are of interest in connection with the history and age of the earth. Calculations of the age of the earth can be made on certain assumptions that involve the average temperature gradient near the surface. The reciprocal gradient varies over a range from around 20 to 200 ft. per so Fahrenheit, degree the determination of a representative average is very difficult.[3] On the other hand, the variations themselves have been the basis for some speculations as to the geologic history of surface deformations. In general, gradients are higher over structure than in undisturbed areas, so a high gradient value may be indicative of local structure. Estimates of the time since the last glacial age have been based on calcula-

[1] Gillingham and Stewart, 1938, pp. 84–91.
[2] Deussen and Guyod, 1937, p. 804.
[3] Van Orstrand. 1935.

tions to fit detailed rock temperature measurements in deep mines.[1]

Temperature measurements have to be made and interpreted with some care, because the results depend upon the history of the well immediately before the measurements are made. The heat from drilling and the disturbance that may be set up by circulation of fluid from the surface can affect the temperature locally so that, if a true measure of the natural temperature conditions of the rock is to be obtained, it is necessary to wait for some time after drilling operations before truly representative temperatures can be measured. Since such waiting is expensive, it is probable that comparatively few measurements made in deep wells are as accurately representative of the true rock temperature as might be desired.

RADIOACTIVE PROSPECTING[2]

Some years ago there was considerable interest in the measurement of radioactivity as a method of geophysical prospecting. The basis of this interest was the expectation that the percolation of ground waters or gases would have a tendency to bring radioactive materials to the surface of the earth. By measuring the radioactivity of soil gas, it was expected that zones of greater circulation could be detected and that the method should be particularly useful for locating faults.

Considerable testing of this idea was carried out. The tests were made either by passing gases, drawn from shallow holes, through an electroscope or by testing soil samples in a special electroscope. In either case, variation in the rate of discharge of the electroscope indicated variation in the amount of radioactive material (*i.e.*, the radioactive gas radon) in the air or in the soil.

Tests indicated the presence of readily measurable quantities of radioactive material in the soil gas and much variation in their magnitude. There is no systematic increase in radon content of soil gas with depth of the sample below the surface.[3] There is a rather definite relation between the radon content of soil gas and the heavy mineral content of the soil,[4] and radioactivity

[1] Ingersoll, 1932.
[2] Ambronn, 1928, pp. 107–133.
  Eve and Keys, 1938, pp. 238–247.
[3] Botset and Weaver, 1932.
[4] Clark and Botset, 1932.

measurements should be able to indicate changes in geologic formations when the changes are accompanied by changes in heavy mineral content, as is often the case. Thus such measurements might be used to locate formation contacts under alluvial cover or should detect faults that bring formations of very different heavy mineral content into juxtaposition. However, in general, any real correlation of radioactivity with deep geologic disturbances is so badly mixed up with variations from extraneous causes that the method has not developed into a useful prospecting tool.

RADIOACTIVITY MEASUREMENTS IN WELLS

It would be desirable in many areas or oil fields to be able to determine the nature of the rock in a well behind the casing. For instance, the problem of correlating old wells may come up in connection with later development or deeper drilling. Also, it would be useful to be able to detect oil sands for locating points for gun perforating. One attack on this problem has been made by measuring in a well the penetrating radiation (gamma rays) given off by radioactive minerals. Gamma rays are sufficiently penetrating to be detected through well casing.

A device for such measurements has been developed by Howell and Frosch.[1] It consists essentially of two Geiger counters. The pulse rates of the counters are proportional to the rate at which radioactive radiations reach them. By measuring these rates with a frequency meter and galvanometer, a determination is made of the relative quantity of radioactive material in the rock opposite the device, and logs of radioactivity are obtained. It is stated that reasonably satisfactory measurements can be made at a rate of about 25 ft. per minute.

The radioactive logs appear to be rather closely related to electric logs. Sands are found to be less radioactive than shales. Oil sands are not more radioactive than other sands. The method appears to offer a definite possibility of correlating geologic formations behind casing. The method has not yet had sufficient application to determine just how useful it will be, but it seems at present that its utility will be limited to rather special applications and that it probably will not develop to a degree comparable with electric logging.

[1] Howell and Frosch, 1939b.

A special application of the gamma-ray technique has been made for the detection of cement behind casing.[1] This is accomplished by mixing a radioactive mineral with the cement before pumping it into the well. The gamma-ray detector is then run into the well, and the relatively strong radioactivity of the cement serves to tell its position behind casing or even behind old cement.

FLUID-LEVEL MEASUREMENT

A problem that arises in connection with the operation of pumping wells is the determination of the height of the fluid under which the pump operates. The problem is that of determining the distance from the top of the well down to the surface of the fluid in the annular space between the well casing and the tubing through which fluid is pumped to the surface. This problem has been solved by the application of the same principle as that of reflection prospecting. A sound wave is sent down the well in the annular space between the tubing and casing, and the time is measured which a wave reflected from the surface of the fluid requires to come back to the surface of the ground.[2]

A special fitting is connected to the well which usually has two branches; one of these branches contains the wave-generating mechanism, and the other a suitable detector which is responsive to the sound waves in the well.

Waves may be generated by the use of an explosive, for which shotgun shells or dynamite blasting caps are used. When an explosive is used, it is necessary to insert a flame arrester between the explosive chamber and the well to prevent the ignition of gas that may be in the well. Also, the wave may be set up by the injection into the well of a charge of gas at comparatively high pressure.

The detector may be either an ordinary telephone-type carbon microphone or a diaphragm that mechanically actuates a small mirror from which a recording light beam is reflected. The detector must be constructed to withstand the pressure of gas in the well to which it is connected and at least moderate pressure changes.

[1] *Ibid.*
[2] Walker, 1937.
Jakosky, 1939.

The control and recording apparatus is similar in a general way to that used for seismic prospecting. If a microphone is used, the output is amplified and connected to an oscillograph making a photographic record on a moving tape. If a mechanically actuated mirror is used, a record may be made without intermediate amplification. A recently developed apparatus has a recording pen so that the result of a measurement becomes available immediately with no waiting for the development of a photographic record. The firing of the shot is controlled electrically and is coordinated with the recording so that the shot is fired shortly after the photographic tape is started through the camera. Some systems use a special valve in front of the detector which is opened at a predetermined time after the shot is fired to protect the detector from the immediate effects of the wave generating explosion.

The velocity of transmission of the sound wave varies over a considerable range because of the variable nature of the gas in the well. If a well is producing gas, so that it is flushed out by the flow, the gas content will be quite uniform, and the wave velocity uniform. This wave velocity may be determined by a separate measurement of travel time on a sample of gas drawn into a special pipe or tubing of known length, using the same apparatus that is used on the well.

Frequently the wave velocity is quite variable between the top and the bottom of the well. This occurs in wells that are not making any appreciable volume of gas. However, the space above the oil contains certain gases that are evaporated from the oil, and these may be heavy (for instance, propane) and have a wave velocity lower than that of air. As the fluid level rises and falls, owing to changes in the pumping rate, the gas becomes partially mixed with air so that the space may contain mostly air at the top and mostly heavy gas at the bottom. Figure 177 shows wave velocities calculated from measurements in a well in which the velocity varied from about 1,060 ft. per second (mostly air) at the top of the well to about 715 ft. per second (probably mostly heavy gas) at the bottom of the well.

There are always other reflections observed besides the one from the surface of the fluid. These come from other mechanical discontinuities in the space in which the sound wave travels. These can be used to determine wave velocity so that accurate

depth measurements can be made even when the velocity is quite variable. The most useful of these is the series of reflections that come from the collars or connectors by which the successive sections of tubing are joined. If the lengths of the joints of tubing are known, it is then necessary only to count the total number of tubing joint reflections arriving before the reflection coming from the surface of the fluid and calculate the depth to the fluid directly from the number of sections and fraction of a section of tubing between the surface and the top of the
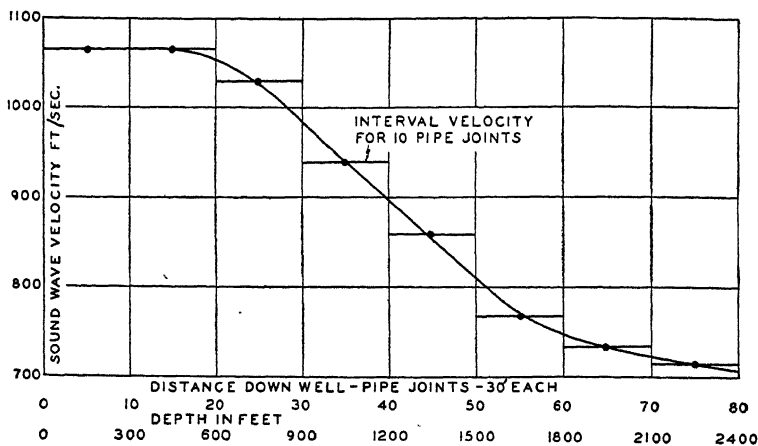
Fig. 177.—Velocity curve for sound waves in an oil well.

fluid. In other cases a definite reflection from the tubing catcher or some other obstruction in the well may be identified. If such a reflection comes from a depth not too far above the surface of the fluid, the depth to the fluid can be calculated from the ratio of the travel time of the wave from the reflection-forming obstruction at known depth to the travel time of the wave from the surface of the fluid. In some cases, special reflectors are inserted in the well to facilitate the fluid-level measurements.

The determination of fluid level by sound reflections has now reached a well-developed stage, and the method is being applied regularly in connection with the operation of pumping equipment on wells.[1] The process has been approved as a legal method of measuring fluid level in connection with determinations of well potentials for proration allowables of production.

[1] Simons, 1939.
Strang, 1939.

DETERMINATION OF SOURCE OF WATER

A problem that frequently arises in connection with the operation of oil wells is the determination of the source of water that may be produced with the oil. If the exact level at which the water is coming in is known, it may be possible to shut it off by cementing, plugging back, or setting casing.

One possible method of detecting water is to make resistivity measurements[1] of a conditioned mud in the hole. This can be done by a measurement similar to that for electric logging, except that the electrode spacing is closer so that the resistivity measured is principally that of the fluid in the well rather than that of the adjacent rock. Where water comes in, the resistivity will be changed (usually decreased, by the inflowing salt water), and the depth of the water source will be indicated by the resistivity curve.

A more recent and apparently more promising method of accomplishing the same result is the Dale photoelectric method.[2] This uses a device containing a source of light shining through windows across a gap on to a photoelectric cell. The apparatus is arranged so that as it is raised through the well, the fluid in the well passes through the gap across which the light passes. Variation in the amount of light transmitted across the gap is indicated by variation in the photocell current which thus measures the relative opacity of the fluid. The mud is first conditioned or dyed to be relatively opaque. Where clear formation water comes into the well, the fluid is diluted, becomes less opaque, and lets more light fall on the photoelectric cell. A continuous measure of the photocell current is made at the surface by connection through a suitable electric cable to surface apparatus, which gives a curve of the opacity of the fluid. Several curves are made at varying times after first conditioning the well by circulating the opaque mud and reducing the pressure to allow the formation water to come into the well. The progress of development of relatively transparent regions, caused by inflowing clear formation water, can be determined by comparing successive curves, and thus the depth of the source and direction of movement (*i.e.*, either up or down) of the water may be inferred. This

[1] Schlumberger, 1934*a*, p. 266.
[2] See, for instance, Gillingham and Stewart, 1938, p. 91.

method has one definite advantage over the resistivity measurement in that it can be used in cased wells and thus may be used to show water that may be entering through broken casing.

WELL SURVEYING[1]

In drilling holes by the rotary method, it is seldom, if ever, that a hole is perfectly straight. The long string of drill pipe used to turn the drill is really very flexible, especially when its length becomes several thousand times its diameter. If excess weight is put on the bit or if dipping strata of different hardness are encountered, the hole may be deflected to a surprising degree. Inclination of holes of up to 20 deg. from the vertical is not uncommon, and in extreme cases inclinations as high as 60 to 70 deg. have been found. It is quite possible for the bottom of a hole 6,000 or 8,000 ft. deep to be displaced as much as $\frac{1}{2}$ mile laterally from a position vertically below the surface location. In other cases wells are deflected intentionally in order to drill into zones that, for one reason or another, are inaccessible from a point directly above. A spectacular instance of controlled directional drilling is that in which deflected wells have been drilled to intersect the bottom of a well that is out of control, cratered, or on fire, so that mud can be pumped down in the control well to kill the flow of oil or gas from the wild well. Any of these circumstances may make it desirable to know with some precision the true course of a well and the location of the bottom with respect to its surface location.

To determine the course of a well underground it is necessary to determine the deflection of the hole from the vertical and the azimuth of the direction of the deflection at successive intervals down the hole. This involves (1) the determination of the magnitude and direction of the departure of the course of the hole from the vertical and (2) the determination of a reference azimuth to which the direction of the departure from the vertical is referred. Several methods are used for each of these factors.

One method of determining departure from the vertical is by the use of free-swinging pendulums or plumb bobs of different sorts. These all depend upon a mass hanging freely so that its position is vertical. A registration of its position with respect

[1] For a general discussion of the methods and apparatus for well surveying up to about ten years ago, see Haddock, 1931.

to some fixed element of the instrument is made either photographically or by a pinprick which is marked by a magnetically actuated mechanism that raises a recording disk against a sharp point at the bottom of the pendulum.

A spherical level is also used. This is a refinement of the ordinary "bull's-eye" level and consists of a glass curved to an approximately spherical shape with a series of concentric rings etched on the glass and with a small bubble in the liquid under the glass. If the device is tilted, the bubble will be displaced from the center to a degree that is indicated by its position with respect to the rings and in a direction that is indicated by the line through the bubble and the center of the rings.

Direction Indicators.—The simplest manner of obtaining the reference direction is the use of a magnetic compass needle, the position of which may be recorded either photographically or by means of a magnetically operated pinpricking mechanism similar to that used for marking the position of the pendulum. The compass method is subject to magnetic disturbances produced by the drill pipe or tools to which it is connected. Also, there may be very slight disturbances due to magnetic properties of the rocks themselves. The method cannot be used inside the pipe of a cased hole.

Another method which is not open to the aforementioned objections is the use of oriented drill pipe. This depends upon recording or correcting all twists of the drill pipe as it is let down into the hole, so that the orientation of a given reference mark in the well-surveying instrument at the bottom of the string of drill pipe is preserved from the surface down. As each section of pipe is lowered into the well, a careful determination of any twist that occurs is made by the use of special instruments which clamp on the pipe and sight on a reference point. It is claimed that the orientation can be preserved to 1 deg. or less of angle by this method. There is some question as to how much twist may be introduced by the curving of the pipe in a very crooked hole, but apparently these sources of uncertainty are not enough to interfere seriously with accurate well surveying depending on this method.

The third method is the use of a gyroscope for maintaining the reference direction. A small gyroscope powered by dry batteries is driven at a speed of 10,000 to 14,000 r.p.m. The precision

with which the gyroscopically maintained reference direction is preserved can be checked by comparing its position at the beginning of a run and when the instrument is returned to the surface at the end of a run.   Sample data indicate checks in the direction as close as 10 min. of arc or better after runs of $2\frac{1}{2}$ to $5\frac{1}{2}$ hr. The instrument can be run on either wire line or drill pipe.

The Schlumberger "electromagnetic teleclinometer"[1] determines magnitude and direction of inclination by electromagnetic induction.   A small coil is rotated by a motor about an axis parallel with the well bore.   The resulting induced voltage is measured at the surface through a multiconductor cable which also supplies power and controls other operations within the apparatus.   The coil is just below an electromagnetic pendulum. If the device is vertical, the coil occupies a symmetrical position in the field of the electromagnetic pendulum, and the induced voltage is zero.   If the apparatus is inclined, a voltage is induced that is proportional to the degree of inclination.   In a second operation the current to the electromagnetic pendulum is turned off; the coil acts as an earth inductor; and the induced voltage is proportional to the earth's field.   By determining the relative phase of the voltage induced from the earth's field and that from the electromagnetic pendulum, the azimuth of the direction of displacement of the pendulum with respect to the magnetic meridian is determined.   Thus, the apparatus determines both magnitude and direction of the inclination.

All the well-surveying devices are arranged to make a series of readings that are either controlled from the surface or take place automatically at prearranged time intervals.   In either case this provides a means of determining the depth at which the deflection readings are made.

The principles of the better known well-surveying systems are as follows:

The "Driftmeter" uses oriented drill pipe and a free-swinging pendulum.

The Alexander Anderson system uses oriented drill pipe and a special multiple pendulum.

The Surwell "Clinograph" (of the Sperry Sun Company) uses a gyroscope and spherical level with a photographic record made on 16-mm. moving-picture film which includes a photo-

[1] Schlumberger and Doll, 1937.

graph of a small watch by which the depth is determined from correlation with a synchronized depth-time record made at the surface.

The Eastman "single-shot" survey uses a magnetic compass and a special pendulum with a mechanical recording system. The "multiple-shot" survey uses automatic photographic recording. This is also used in connection with oriented drill pipe, so that the magnetic and orientation indications can check one another.

The Lane-Wells Company uses the Anderson system in cased holes and a magnetic direction indication in uncased holes.

CORE ORIENTATION

In connection with the drilling of exploratory wells it is frequently of great economic importance to know the direction of dip. For instance, if tests in a well indicate that it is near the edge of an oil field and cores show that the strata are dipping, it is of great importance to know which direction from the well is up dip, as that would be the direction toward the center of the possible structure in the area. This could be ascertained if it were possible to determine the strike and dip of the formations cut by the drill, by determining the orientation that the core had before it was broken loose from the surrounding rock.

Mechanical methods of orienting cores have been developed and used to a certain extent,[1] but such methods take special tools and considerable care in their operation and require the cutting of special cores for orientation. Therefore, it would be very desirable if the orientation of cores cut during the ordinary course of drilling could be determined by measurements made on them at the surface.

The Herrick-Lynton method of core orientation depends upon measuring the residual magnetism of the cores.[2]

The essential feature of Lynton's apparatus is a carefully shielded sensitive astatic magnetometer. The core is first prepared by cutting to an accurate cylindrical form with square ends and is carefully treated to avoid contamination by iron particles or to remove any surface iron particles that may have become

[1] Macready, 1930.
Haddock, 1931.
[2] Lynton, 1937; 1938.

attached to the core from the drilling tools or drilling mud. The core is then slowly rotated near one end of the lower magnet of the magnetometer, and the deflection of the magnetometer recorded as the core is rotated through 360 deg. The process is repeated with the core turned end for end and rotated in the opposite direction. The difference of the two curves is a measure of the permanent magnetization or polarization of the core perpendicular to the axis of rotation.

Lynton's method should be capable of determining the azimuth and relative magnitude of the component of polarization perpendicular to the axis of rotation. It does not determine the component parallel to the axis.

If the axis of the core were not vertical when cut (*i.e.*, if the well deviates materially from the vertical), it is necessary to know both the amount and the direction of the departure of the hole from the vertical in order that the true strike and dip of the bedding planes in the core may be determined from their inclination with respect to the core axis and the orientation of the core.

Once the direction of magnetization of a core has been determined, the problem of reconstructing the position that the core occupied underground is intimately connected with the history of the process by which the core became magnetized. Lynton first assumed[1] that the magnetization occurred at the time of deposition of the sediments. The magnetization is supposed to have been caused by the orientation in the earth's field of minute particles of magnetized material as they settle through quiet water. If this assumption is correct, the magnetization should be substantially in the direction of the field at the time of deposition. A tendency for the magnetization to be somewhat nearer the horizontal than the direction of the field might be expected because any flattened particles of magnetized material would tend to assume a horizontal position in settling through the water. However, the horizontal component of the mass of magnetized material should be in the direction of the horizontal component of the earth's field at the time of deposition.

The assumption of magnetization in the direction of the field at the time of deposition is qualitatively consistent with the results of the work by McNish and Johnson,[2] who made careful

[1] Lynton, 1937, p. 585.
[2] McNish and Johnson, 1938.

measurements of the direction of polarization of varved clays. These indicated variation of some 20 deg. in the direction of the horizontal component over the period of some hundreds of years during which the successive clay layers were deposited and a maximum departure of about 35 deg. from the direction of the present earth's field. Large changes in the direction of the earth's magnetic field also have been suggested by studies of the polarization of lava flows which are presumed to have become magnetized during cooling and to have retained their polarization to the present time.

If, as seems probable, large changes in the direction of the earth's magnetic field have occurred during geologic time, and if the polarization acquired by the sediments at the time of deposition is retained to the present, the determination of the position of an underground core would be very questionable because of the unknown direction of the field at the time of magnetization. Also, any geologic tilting of the beds would change the direction of magnetization, since the original vertical component would contribute to the radial magnetization of the core. (To work back from the measurements of dip and direction of present magnetization of the core to the conditions at the time of magnetization would require measurement of the vertical component of the sample which is not included in Lynton's measurements.)

In spite of the difficulties of interpretation and the unknown origin of the magnetization of sedimentary cores, the orientation of cores from determination of the direction of the radial component of polarization seems to have given useful results. This seems to indicate that the direction of magnetization of many sediments is essentially that of the present earth's field and that therefore these sediments probably have not preserved a direction of magnetization acquired at the time of deposition. Perhaps the magnetization of the sedimentary sample is materially modified at the time of drilling by the mechanical shock and vibration of the core bit, so that at the time of cutting the core becomes remagnetized in the direction of the present earth's field. If this could be established, it would add much confidence to the utility of orienting cores by their magnetic polarization.

A proposal that would eliminate the uncertainties in the magnetic history has been made by Vacquier.[1] This involves drill-

[1] Vacquier. 1939.

ing a pilot hole into the bottom of the well and inserting into this hole a fluid cement containing highly magnetized small particles which would be oriented by the earth's field while the cement is still liquid. After the cement is set, a core is cut in the usual way, a core that would now contain the magnetized plug of cement. The orientation then could be readily determined with a magnetometer. Actual application of this method in a well has not yet been attempted.

DETERMINATION OF DIP BY ELECTRICAL MEASUREMENTS

Systems have been devised for the determination of the direction of dip of underground strata by electrical measurements in wells.

The Doll system[1] depends upon the same principle that is used to give porosity determinations in electrical well logging. The apparatus contains three electrodes spaced 120 deg. apart around the vertical axis and held near the sides of the drill hole. A separate curve of self-potential versus depth is made from each electrode. If there is a sharp stratigraphic change at which a definite change in the self-potential occurs, this change would appear on the three electrodes at the same depth if the boundary were perpendicular to the axis of the hole but would appear at slightly different depths if this boundary were inclined. From the differences in depth of the three indications, the magnitude and direction of the dip, with respect to the electrode system, of the plane at which the electrical indication occurs can be determined. An attachment to the apparatus contains a level bubble and compass which are photographed to determine the azimuth and inclination of the instrument at the time the electrical measurements are made so that the direction and absolute magnitude of the dip of the inclined plane can be determined.

Another electrical system[2] depends on the anisotropy of electric conductivity in stratified deposits. A potential distribution around a well is set up by passing current from an electrode in a well to one at the surface. A long cylindrical apparatus is let into the well which contains four external electrodes, spaced 90 deg. apart. Differences in potential are measured between diametrically opposite pairs of electrodes through wires leading

[1] Doll, 1939.
[2] Schlumberger and Doll, 1937.

to the surface. If the strata are dipping, the equipotential surface will tend to be parallel with the bedding places on account of the anisotropic conductivity, and this dip will be indicated by a difference in potential between electrodes on opposite sides of the hole. By measuring the potential between two pairs of electrodes, the two components of dip will be indicated, and thus the direction of dip with respect to the position of the electrodes can be determined. The magnitude of dip cannot be measured with much precision because the equipotential surface is not necessarily closely parallel with the bedding. Any inclination of the hole and its direction is determined by an "electromagnetic teleclinometer" (see page 404) in the lower part of the same apparatus. It is claimed that the apparatus can determine the direction of dip satisfactorily when dip angles are greater than about 5 deg. and is particularly good for steep dips. It is stated that the apparatus has been used in the principal oil countries of the world.

THE SEISMIC-ELECTRIC EFFECT

If two electrodes are inserted in the ground and an electric current passed between them, there will be a periodic change in the current when a seismic wave passes through the region between the electrodes. The frequency and form of the variation in electric current are similar in some respects to the seismic wave forms recorded by mechanical detectors. This change of current is a manifestation of the "seismic-electric" effect. It has been proposed[1] that this effect could be used as a basis for the detection of seismic waves. Within the past few years there has been considerable interest both in the fundamental phenomena involved and in its practical application to geophysical prospecting.

An extensive experimental study of the seismic-electric effect was made in Germany[2] for the purpose of determining the fundamental cause of the change in current. The work included a study of the effect of variation of voltage, current, electrolyte, electrolytic conductivity, etc., on the magnitude of the seismic-electric effect. From this work the conclusion was reached that the source of the effect is in polarization phenomena at the surface of separation between the electrodes and the earth.

[1] Blau and Statham, 1936.
[2] Thyssen, Hummel, and Rülke, 1937; 1938.

An attempt to use the seismic-electric effect for geophysical prospecting was made by Belluigi[1] in Ethiopia. Belluigi used a circuit similar to that used for ordinary electric conductivity measurements in that he supplied the current to the ground through two outer electrodes and measured the effect of seismic waves on the variation of potential between two inner electrodes.

From Thompson's[2] experiments in this country, there is evidence that the source of the seismic-electric effect is, to a considerable extent, in the body of earth material through which the current flows rather than principally at the electrodes, as the German work indicated. Thompson used a circuit similar to that of Belluigi but used three instead of only two potential electrodes.

More recently, an attempt to use the effect for practical prospecting was made by British investigators.[3] The results were not particularly encouraging for the practical utility of the seismic-electric effect as a substitute for seismic detectors. The method is less sensitive than mechanical-electrical detectors; the electric changes do not give a true reproduction of the ground movement; and the results are considerably affected by weather conditions.

At the present time, the utility of the seismic-electric effect in practical geophysical prospecting is in a controversial state. It is possible that it may become a useful aid to geophysical exploration, but at present the indications are that its promise is not great enough to justify the extensive development that probably would be required to secure a system comparable with or better than present seismic detectors.

[1] Belluigi, 1937.

[2] Thompson, 1936; 1939.

[3] Waters and Wen-Po, 1939.

BIBLIOGRAPHY

1919

"Inductive Interference between Electric Power and Communication Circuits," Selected Technical Reports, Railroad Commission of the State of California, San Francisco, California State Printing Office, San Francisco, Apr. 1, 1919 (1,160 pages).

1925

GISH, O. H., and W. J. ROONEY: Measurement of Resistivity of Large Masses of Undisturbed Earth, *Terr. Mag. Atmos. Elec.*, vol. 30, pp. 161–188.

1926

HABERLAND, G.: Theorie der Leitung von Wechselstrom durch die Erde, *Zeitschr. f. angew. Mathematik*, Band VI, Heft 5, pp. 366–379, October, 1926.

1928

AMBRONN, RICHARD: "Elements of Geophysics," trans. by Margaret C. Cobb, McGraw-Hill Book Company, Inc.

1930

MACREADY, GEORGE A.: Orientation of Cores, *Bull. Am. Assoc. Petroleum Geologists*, vol. 14, No. 5, pp. 559–578, May, 1930.

1931

HADDOCK, M. H.: "Deep Borehole Surveys and Problems," McGraw-Hill Book Company, Inc., New York.

1932

BOTSET, HOLBROOK G., and PAUL WEAVER: Radon Content of Soil Gas, *Physics*, vol. 2, No. 5, pp. 376–385, May, 1932.

CLARK, R. W., and HOLBROOK G. BOTSET: Correlation between Radon and Heavy Mineral Content of Soils, *Bull. Am. Assoc. Petroleum Geologists*, vol. 16, No. 12, pp. 1349–1356, December, 1932.

EHRENBURG, D. O., and R. J. WATSON: Mathematical Theory of Electrical Flow in Stratified Media with Horizontal, Homogeneous and Isotropic Layers, "Geophysical Prospecting, 1932," *Trans. Am. Inst. Min. Met. Eng.*, vol. 97, pp. 423–442.

EVE, A. S.: Absorption of Electromagnetic Induction and Radiation by Rocks, "Geophysical Prospecting, 1932," *Trans. Am. Inst. Min. Met. Eng.*, vol. 97, pp. 160–168.

INGERSOLL, L. R.: Geothermal Gradient Determinations in the Lake Superior Copper Mines, *Physics*, vol. 2, No. 3, pp. 154–159, March, 1932.

PETERS, LEO J., and JOHN BARDEEN: Some Aspects of Electrical Prospecting Applied in Locating Oil Structures, *Physics*, vol. 2, No. 3, pp. 103–122, March, 1932.

SCHLUMBERGER, CONRAD, and MARCEL SCHLUMBERGER: Electrical Studies of the Earth's Crust at Great Depths, "Geophysical Prospecting, 1932," *Trans. Am. Inst. Min. Met. Eng.*, vol. 97, pp. 134–140.

SLICHTER, L. B.: Observed and Theoretical Electromagnetic Model Response of Conducting Spheres, "Geophysical Prospecting, 1932," *Trans. Am. Inst. Min. Met. Eng.*, vol. 97, pp. 443–459.

ZUSCHLAG, THEODOR: Mapping Oil Structures by the Sundberg Method, "Geophysical Prospecting, 1932," *Trans. Am. Inst. Min. Met. Eng.*, vol. 97, pp. 144–159.

1933

BLAU, L. W.: Method and Apparatus for Geophysical Prospecting, U.S. Patent 1,911,137, May 23, 1933.

JEANS, SIR JAMES: "The Mathematical Theory of Electricity and Magnetism," 5th ed., Cambridge University Press, London.

1934

PIRSON, SYLVAIN J.: Interpretation of Three-layer Resistivity Curves, "Geophysical Prospecting, 1934," *Trans. Am. Inst. Min. Met. Eng.*, vol. 110, pp. 148–158.

a. SCHLUMBERGER, C., M. SCHLUMBERGER, and E. G. LEONARDON: Electrical Coring; a Method of Determining Bottom-hole Data by Electrical Measurements, "Geophysical Prospecting, 1934," *Trans. Am. Inst. Min. Met. Eng.*, vol. 110, pp. 237–272; also *Tech. Pub.* 462.

b. SCHLUMBERGER, C., M. SCHLUMBERGER, and E. G. LEONARDON: A New Contribution to Subsurface Studies by Means of Electrical Measurements in Drill Holes, "Geophysical Prospecting, 1934," *Trans. Am. Inst. Min. Met. Eng.*, vol. 110, pp. 273–289; also *Tech. Pub.* 505.

TAGG, G. F.: Interpretation of Resistivity Measurements, "Geophysical Prospecting, 1934," *Trans. Am. Inst. Min. Met. Eng.*, vol. 110, pp. 135–147.

1935

KARCHER, J. C., and EUGENE McDERMOTT: Deep Electrical Prospecting, *Bull. Am. Assoc. Petroleum Geologists*, vol. 19, No. 1, pp. 64–77, January, 1935.

VAN ORSTRAND, C. E.: Normal Geothermal Gradient in the United States, *Bull. Am. Assoc. Petroleum Geologists*, vol. 19, No. 1, pp. 78–115, January, 1935.

1936

BLAU, L. W., and LOUIS STATHAM: Method and Apparatus for Seismic Electric Prospecting, U.S. Patent 2,054,067, Sept. 15, 1936.

SOKOLOV, V. A.: "Gas Surveying," published in Russia by ONTI NKTP SSSR; 1936, Glavnaya Redaktsiya Gorno-Toplivnoi Literatury, Moscow, Leningrad; English translation by and published by A. A. Boehtlingk, Berkeley, Calif., December, 1939.

STATHAM, LOUIS: Electric Earth Transients in Geophysical Prospecting, *Geophysics*, vol. 1, No. 2, pp. 271–277, June, 1936.

THOMPSON, R. R.: The Seismic Electric Effect, *Geophysics*, vol. 1, No. 3, pp. 327–335, October, 1936.

1937

BELLUIGI, A.: Seismic-electric Effects of the Soil and Seismic-electric Prospecting, *Oil Weekly*, vol. 87, No. 12, pp. 38–42, Nov. 29, 1937.

DEUSSEN, ALEXANDER, and HUBERT GUYOD: Use of Temperature Measurements for Cementation Control and Correlations in Drill Holes, *Bull. Am. Assoc. Petroleum Geologists*, vol. 21, No. 6, pp. 789–805, June, 1937.

JENSEN, JOSEPH: Recent Developments Related to Petroleum Engineering, *Trans. Am. Inst. Min. Met. Eng.*, vol. 123, pp. 63–68.

LYNTON, EDWARD D.: Laboratory Orientation of Well Cores by their Magnetic Polarity, *Bull. Am. Assoc. Petroleum Geologists*, vol. 21, No. 5, pp. 580–615, May, 1937.

RADLEY, W. G., and H. J. JOSEPHS: Mutual Impedance of Circuits with Return in a Horizontally Stratified Earth, *Jour. Inst. Electrical Eng.*, vol. 80, pp. 99–103, January, 1937.

SCHLUMBERGER, C., M. SCHLUMBERGER, and H. G. DOLL: Le pendagemètre électromagnétique et la détermination de l'orientation du pendage des couches sédimentaires recoupés par les sondages, *Rev. industrie minérale*, No. 392, pp. 193–200, Apr. 15, 1937.

THYSSEN, ST. V., J. N. HUMMEL, and O. RÜLKE: Die Ursachen des seismisch-elektrischen Effektes, *Zeitschr. f. Geophysik*, vol. 13, pp. 112–119.

WALKER, C. P.: Determination of Fluid Level in Oil Wells by the Pressure Wave Echo Method, *Trans. Am. Inst. Min. Met. Eng.*, vol. 123, pp. 33–43.

WETZEL, W. W., and HOWARD V. McMURRAY: A Set of Curves to Assist in the Interpretation of the Three Layer Resistivity Problem, *Geophysics*, vol. 2, No. 4, pp. 329–341, October, 1937.

1938

BORNHAUSER, MAX, and FRED W. BATES: Geology of Tepetate Oil Field, *Bull. Am. Assoc. Petroleum Geologists*, vol. 22, No. 3, pp. 285–305, March, 1938.

EVE, A. S., and D. A. KEYS: "Applied Geophysics in the Search for Minerals," 3d ed., Cambridge University Press, London.

EVJEN, H. M.: Depth Factors and Resolving Power of Electrical Measurements, *Geophysics*, vol. 3, No. 2, pp. 78–95, March, 1938.

GILLINGHAM, W. J., and W. B. STEWART: Application of Electrical Logging Methods to West Texas Problems, Pt. 1, *Petroleum Eng.*, vol. 9, No. 7, pp. 52–55, April, 1938; Pt. 2, *Petroleum Eng.*, vol. 9, No. 8, pp. 84–91, May, 1938.

JAKOSKY, J. J.: Continuous Electrical Profiling, *Geophysics*, vol. 3, No. 2, pp. 130–153, March, 1938.

LYNTON, EDWARD D.: Recent Developments in Laboratory Orientation of Cores by their Magnetic Polarity, *Geophysics*, vol. 3, No. 2, pp. 122–129, March, 1938.

MARTIN, M., G. H. MURRAY, and W. J. GILLINGHAM: Determination of the Potential Productivity of Oil-bearing Formations by Resistivity Measurements, *Geophysics*, vol. 3, No. 3, pp. 258–272, July, 1938.

McNISH, A. G., and E. A. JOHNSON: Magnetization of Unmetamorphosed Varves and Marine Sediments, *Terr. Mag. Atmos. Elec.*, vol. 43, No. 4, pp. 393–406, December, 1938.

ROSAIRE, E. E.: Shallow Stratigraphic Variations over Gulf Coast Structures, *Geophysics*, vol. 3, No. 2, pp. 96–121, March, 1938.

RUST, W. M., JR.: A Historical Review of Electrical Prospecting Methods, *Geophysics*, vol. 3, No. 1, pp. 1–6, January, 1938.

SCHLUMBERGER, C.: "Electrical Coring," in "The Science of Petroleum," ed. by A. E. Dunstan, Vol. I, pp. 351–363, Oxford University Press, London.

THYSSEN, ST. V., J. N. HUMMEL, and O. RÜLKE: Über das Wesen des seismisch-elektrischen Effektes, *Beitr. angew. Geophysik*, vol. 7, pp. 209–217.

1939

BLONDEAU, E. E.: Shallow Resistivity Survey at South Elton, La., *Geophysics*, vol. 4, No. 4, pp. 271–278, October, 1939.

DOLL, H. G.: Method and Arrangement for Determining the Direction and the Value of the Dip of Beds Cut by a Bore Hole, U.S. Patent 2,176,169, Oct. 17, 1939.

HORVITZ, LEO: On Geochemical Prospecting—I, *Geophysics*, vol. 4, No. 3, pp. 210–228, July, 1939.

HOUSTON GEOLOGICAL SOCIETY STUDY GROUP: Electrical Well Logging, *Bull. Am. Assoc. Petroleum Geologists*, vol. 23, No. 9, pp. 1287–1313, September, 1939.

a. HOWELL, LYNN G., and ALEX FROSCH: Detection of Radioactive Cement in Cased Wells (abstract only), *Oil Weekly*, vol. 95, No. 5, p. 32, Oct. 9, 1939.

b. HOWELL, LYNN G., and ALEX FROSCH: Gamma-ray Well-logging, *Geophysics*, vol. 4, No. 2, pp. 106–114, March, 1939.

JAKOSKY, J. J.: Bottom-hole Measurements in Pumping Wells, *Am. Inst. Min. Met. Eng.*, *Tech. Pub.* 1058.

KLIPSCH, PAUL W.: Recent Developments in Eltran Prospecting, *Geophysics*, vol. 4, No. 4, pp. 283–291, October, 1939.

REED, PAUL: Simultaneous Electrical Logging and Drilling, *Oil and Gas Jour.*, vol. 38, No. 27, p. 93, Nov. 17, 1939.

SCHLUMBERGER, MARCEL: The Application of Telluric Currents to Surface Prospecting, *Trans. Am. Geophys. Union*, 20th annual meeting, pp. 271–277.

SIMONS, HARRY F.: Bemis Potential Obtained by Productivity Index, *Oil and Gas Jour.*, vol. 37, No. 42, pp. 49–50, Mar. 2, 1939.

STRANG, W. H.: Reaction to Draw-down Methods of Determination both Favorable and Adverse, *Oil Weekly*, vol. 93, No. 13, pp. 31–38, June 5, 1939.

THOMPSON, R. R.: A Note on the Seismic-electric Effect, *Geophysics*, vol. 4, No. 2, pp. 102–105, March, 1939.

VACQUIER, VICTOR: A Proposed Geophysical Method for Orienting Cores, *Geophysics*, vol. 4, No. 4, pp. 292–299, October, 1939.

WATERS, K. H., and W. WEN-PO: An Investigation of the Seismic-electric Effect, *Beitr. angew. Geophysik*, vol. 7, pp. 337–346.

PART V
GEOPHYSICAL INTERPRETATION

CHAPTER XXII

GEOPHYSICAL INTERPRETATION

THE IMPORTANCE OF THE GEOPHYSICAL MAP

The final result of a geophysical survey is nearly always a map. The values, contours, or perhaps only nebulous outlines of one or more "areas of interest" on such a map are the basis of decisions affecting leasing, drilling, or perhaps more geophysical work. In any case these decisions will usually involve at least a few thousand and not infrequently many thousand or even hundreds of thousands of dollars. The geophysical map is generally accompanied by a written report. The text of the report may give technical details of the geophysical field operations, the interpretation methods and calculations or the geology of the area; but when the decisions are made, it is probably the map that receives the final study and closest attention. In many cases, the loss of a geophysical report would not be serious if the loss did not include the map.

The nature of the geophysical map will depend on the geophysical method or methods from which it is derived. If it is a gravity or magnetic map, it probably will show measured values and contours with reductions for various known effects and disturbances. Perhaps there will be more than one map showing different stages of reduction. Local anomalies will be indicated, and the associated area of interest may be designated by suitable outlines, trend lines, centers, or other notations. A seismograph map usually has contours that presumably represent the attitude of geologic horizons at more or less definite depths. If data are sparse or inconclusive, more than one map may be shown with alternative interpretations or sets of contours. If results are very indefinite, or control very open, the map may show only dip indications. The clarity with which the underground picture may be read depends greatly upon the number and variety of the methods and upon the nature of the earth media intervening between the surface of the ground on which the measurements

are made and the underground surface on which the information is desired.[1]

The Interpreter's Commitments and Reservations.—The interpreter may have many "ifs," "ands," "buts," and especially "maybes" with which he would like to qualify his statements and conclusions. However, the man who has to decide whether or not to spend the money is likely to be typified by the executive who pokes his finger into the ribs of an interpreter studying a nebulous gravity minimum and, in the attitude of a thug committing a holdup, demands: "Is it a dome or isn't it a dome?" The interpreter, especially if his background of training is that of a physicist or engineer accustomed to reach decisions through orderly processes of a high degree of certainty, may feel that he would as soon be the victim of a holdup as be forced to make a commitment on the basis of the geophysical information at hand. Later in his experience he may come to treat the prospecting for oil as the great gamble that it is. Then his commitments will be based on probabilities, and the boundary between his "yes" or "no" is a rather intangible factor of probability. If the various facts and factors that determine this boundary are properly weighed and balanced against one another, his answers, on the average and in the long run, should be on the winning side.

THE COMBINATION OF PHYSICS AND GEOLOGY

Geophysical interpretation must of necessity combine physics and geology. Up to the present time geophysical interpreters are either physicists who have learned some geology or geologists who have learned some physics. The two sciences do not mix easily, for the physicist trained in an exact science, controlled by experiment and by well-established laws, may stand aghast at the geologist who, figuratively, pushes on a pad of paper until it buckles in the middle and seems to consider the experiment a justification for a theory of the mechanics of the formation of the Appalachian Mountain system. On the other hand, many a physicist whom geophysics has brought into contact and cooperation with good geologists has gained a great deal of respect for the breadth of vision that brings order into a tumbled mass of

[1] Paul Weaver, Relation of Geophysics to Geology, *Bull. Am. Assoc. Petroleum Geologists*, vol. 18, No. 1, pp. 3–12, January, 1934.

mountain scenery; builds up a complex history of advancing and receding seas over millions of years of time from observations of fossil bugs, size of sand grains, and the chemical nature of very dull-looking and superficially nondescript chunks of rock; or guesses that an important geological disturbance lies beneath an area because of some very nebulous and apparently unimportant and insignificant variation in the surface material.[1]

The differences in background have led to some conflict between geologists and geophysicists and not a little blaming of one another for faults of commission and omission.[2]

There has been some debate in geological and geophysical journals on the question of geophysical interpretation in terms of a geologically "acceptable," or perhaps more properly "natural," underground picture.[3] The geologist has felt that the geophysicist is presumptuous,[4] and the geophysicist has felt that the geologist is too conservative[5] in recognizing departure from recognized type geologic situations. Detailed plans have been set forth[6] for a geophysical organization that will insure proper cross-checking of geophysical results so that the various geological and geophysical factors will receive proper consideration. It is the variation in judgment and weighing of the several geophysical and geological elements involved—which in the final analysis is a matter of probability—that has led to accusations and a certain amount of antagonism between geologists and geophysicists.

[1] Ludwig W. Blau, The Interpretation of Geophysical Data (with discussion by A. Deussen, O. L. Brace, and D. C. Barton), *Geophysics*, vol. 2, No. 2, pp. 95–113, March, 1937.

[2] O. L. Brace, The Interrelationship of Geology and Geophysics, *Bull. Am. Assoc. Petroleum Geologists*, vol. 21, No. 2, pp. 197–211, February, 1937.

E. E. Rosaire, Review of "The Interrelation of Geology and Geophysics," by O. L. Brace, *Bull. Am. Assoc. Petroleum Geologists*, vol. 21, No. 2, pp. 197–211, February, 1937; *Geophysics*, vol. 2, No. 1, pp. 63–67, January, 1937.

D. C. Barton, Discussion of a review by E. E. Rosaire (Geophysics, Vol. II, No. 1, January, 1937, pp. 63–67); *Geophysics*, vol. 2, No. 2, pp. 166–167, March, 1937.

[3] See p. 110 of the discussion by Brace in the reference in footnote 1 above.

[4] Brace, *op. cit.*, p. 197.

[5] Rosaire, *op. cit.*, p. 65.

Blau, *op. cit.*

[6] B. B. Weatherby, The Organization of an Effective Exploration Department, *Geophysics*, vol. 1, No. 2, pp. 179–188, June, 1936.

Better geophysical maps will be made by geophysicists, and better use of them by geologists will come about, when the two sciences attain more complete coordination. We may even hope for the day when a really competent combination of geologist and physicist will emerge in the same man who will be truly a "geo-physicist" in all that that combined title implies.

THE JUDGMENT AND WEIGHING OF GEOPHYSICAL RESULTS

Let us now look at the making of a geophysical map with a view toward its final utility, *i.e.*, its economic value in the finding of oil reserves.

Test Surveys over Known Structure.—One of the most useful aids in the interpretation of geophysical results is a test survey of an area where subsurface structure is more or less accurately known. Such a test gives a reasonable basis for estimating the expected geophysical effect over another similar geologic situation. It may go even further and give definite values for the physical constants of the earth materials that produce the geophysical effect. For example, a gravity survey over a known structure may provide the basis for a quantitative estimate of the density contrasts that are responsible for the gravity effect. A seismograph survey will give definite information on the velocity distribution and may, in favorable circumstances, serve definitely to correlate a given reflection pattern or reflection character with certain geologic horizons. A test survey in the case of the magnetometric method requires more careful choice, since commercial exploitation of an oil field seriously interferes with the determination of the true magnetic effect because of the magnetic disturbance resulting from buried casing as well as steel derricks, pipe, and other magnetic materials on the surface. Thus, if a reliable magnetic picture of a known structure is desired, it should precede and anticipate the extensive development by which the structure will become known. The single wildcat discovery well, which proves the existence of a structure or the first few wells following it, will not greatly disturb the picture, so that in the very early stages a reasonably satisfactory magnetic survey can be obtained. Then as the field development proceeds and the structural picture develops, a reliable basis for determining the magnetic effect of that particular structure will

become available and may serve as a means of estimating expected effects from other structures in similar situations.

There is always a tendency to use the analogy of a geophysical picture over a known area for the interpretation of an unknown prospect. This is true particularly in magnetic and gravity surveys where we are mapping force fields rather than the actual structural surface, as in seismograph work. If a new geophysical picture turns out to be similar to one previously obtained over a known and important structure or oil field, there is naturally an inclination to attribute the new picture to a similar and therefore interesting cause. In general, this procedure is justified. However, it must be applied with caution and reservation. In many instances a geophysical effect cannot be explained in terms of the known magnitudes and probable physical properties of the sedimentary rocks involved in a known structure. Then, the gravity or magnetic picture may be attributed to differences in density or in magnetic polarization below the sedimentary section. In such cases the geological connection between the probable cause of the geophysically measured effects and the sedimentary structure may be obscure. For instance, an intrusion of one type of igneous rock within another might give a gravity or magnetic anomaly or both, but the question of whether or not a structure in the overlying sediments is to be expected will depend on the nature and time of the geologic processes by which the intrusion took place. In cases of this type the use of analogy in applying the interpretation of a known area to an unknown one may be grossly misleading, as the indefinite and unknown geological relations between the inferred deeper disturbance and the actual sedimentary structure either may not be real in the "known" case or may not similarly exist in the unknown area.

Calculations to Control Interpretation.—A certain amount of calculation is often desirable to understand the cause of geophysical effects. Rather detailed calculations of gravity or magnetic tests over known structures are definitely valuable, as they will indicate the magnitude of the geophysical disturbance that may be expected from such a feature, assuming reasonable contrasts in the physical constants of the rocks involved. Such calculations may then lead to a definite basis for estimating which part

of the geophysical picture is local (*i.e.*, due to the disturbance in the immediate area of the structure) and which part is regional. On the other hand, highly precise or detailed calculations are not of value in an area of unknown subsurface conditions, because the physical properties and depths of the physical contrasts responsible for the geophysical effects are not known, and unknown and undeterminable variations in these factors may vitiate any but qualitative estimates. In such cases it is nevertheless very useful to control estimates by approximate calculations, such as those based on assumed regular geometric forms like spheres, cylinders, and simple faults, as they will test the order of magnitude and reasonableness of suggested causes of observed geophysical magnitudes.

An example of useless calculation is one in which an interpreter calculated an overhang for a salt dome many thousand feet deep on the basis of a none too accurate torsion balance picture. The details in the surface gravity effect that would result from the overhang would be so smoothed out as to be entirely unmeasurable. Furthermore, a quite different dome form could be worked out which also would give calculated effects in close agreement with those observed. Thus, any one of several calculated pictures might fit the observed effect very closely. About all that could be said regarding the value of the calculation is that the customer's desire for a definite picture was satisfied.

Combining Different Geophysical Methods.—In many cases a combination of geophysical pictures is valuable in interpretation. This is more particularly true of gravity and magnetic pictures than of seismograph, although there are cases where indefinite seismograph pictures may have their interpretation guided to a certain extent to be consistent with a gravity or magnetic anomaly. However, the latter statement applies only when the seismograph results are extremely unsatisfactory, for, in general, a good seismograph picture implies an interpretation sufficiently unambiguous to preclude the introduction of major modifications based upon information derived from other geophysical methods.

The combination of gravity and magnetic surveys may be useful in separating gravity anomalies that are primarily of basement origin from those which probably are caused principally by density contrasts within the sediments. For instance, if a broad

and strong gravity anomaly is more or less coincident with a strong magnetic anomaly, it is quite certain that the origin of both is in the basement rocks below the sediments. It is then a question of the geological history of the area to decide whether or not the basement disturbance has caused a structure in the overlying sediments. On the other hand, if a gravity anomaly of quantitatively reasonable relief and breadth is unaccompanied by a magnetic disturbance, it is a reasonable, although not necessarily certain, inference that the gravity effect comes from within the sedimentary section.

The combination of geophysical methods and their economics should be considered carefully in the broad planning of a geophysical campaign. Thus, relatively cheap magnetic and gravimeter surveys are expected to serve as guides pointing to comparatively local areas of possible structure to be tested and more definitely located and detailed by the more expensive seismograph method. Whether gravity or magnetics or both should be used will depend upon a careful consideration of the geologic disturbances one hopes to find and the physical properties of the rocks involved. In completely new areas, this may have to be learned by preliminary testing and experience gained with all methods of geophysical attack.

Reconciling Geological and Geophysical Indications.—The final interpretation of geophysical maps generally involves the problem of reconciling the geophysical indications with geology. As mentioned earlier, there has been considerable wrangling between geologists and geophysicists as to what is an "acceptable" geophysical picture.

Some have contended that the geophysical quantities should be worked out quite independently of any geological considerations[1] and that the interpreter of any one set of geophysical measurements should be unfamiliar with geological expectations or of any other information that might influence his interpretation. There are arguments in favor of this attitude, as it should tend to set out the geophysical factors clearly by themselves. Also, a purely geophysical consideration may lead to interpretations which are geologically "unorthodox" but which, if properly appreciated and followed up, could lead to new and eventually proved and useful geologic conceptions.

[1] Blau, *op. cit.*, p. 102.

The opposite viewpoint would have the interpreter use all information available. Some definite geologic guides have no geophysical reaction. Thus many markers useful to the geologist have no physical contrasts that can be measured by geophysical methods, as, for example, changes in color or paleontological markers. Also, there are geophysical contrasts that may have no particular corresponding geological identity, such as many of the reflecting horizons used in unconsolidated sediments. Moreover the physical contrasts may not be parallel with the geological stratification, although, in general, this probably is not often an important source of difficulty. Also, a great deal of useless speculation or calculation may be avoided by a comparatively small amount of geological control. Thus, a single well on a salt dome, drilled through cap rock into salt, will permit a fairly definite calculation of the form and position of the entire dome from an adequate gravity survey, but no amount of calculation could give a definite and unambiguous subsurface picture without any subsurface control.

Which of the foregoing points of view will lead to the most useful results depends on the physical, personal, and psychological factors involved. A geophysical map made by a physicist unfamiliar with the general geology of an area may give a picture that a geologist would at once reject as extremely improbable or entirely impossible. On the other hand, the geophysical indications may suggest interpretations which are unorthodox to the geologist and which he therefore may hesitate to accept. A certain amount of compromise is necessary on both sides, and it seems clear that the final map should be made by a true geophysicist, competent to consider the proper weighing of all pertinent factors, geophysical and geological, and to exercise careful judgment as to which are important and acceptable and which should be rejected. The final result should be a picture that is a most probable compromise among all these factors. Since the final use of this picture is essentially geological, the final geophysical map should be one that a geologist is able to use.

The ultimate purpose of a geophysical map is to locate a well to be drilled in the hope of finding oil. The measure of the success of the geophysical survey is the increased probability of finding oil which results from its use. This measure is difficult to evaluate, and it is even more difficult to divide credit for eventual

success or failure among the various geophysical, geological, economic, personal, and simple chance factors that may have contributed to the selection of a drilling location. However, the very substantial new oil reserves developed as a more or less direct result of geophysical surveys are concrete evidence of the ultimate value of geophysical exploration. It is almost certain that carefully planned, executed, and interpreted geophysical surveys will have an important part in the search for new oil reserves as long as the limited proved supply is being rapidly depleted.

INDEX

A

Abbott, 232

Acceleration, unit of, 15

Acceleration detectors, 321

Accumulation of oil, 2

Adler, Joseph L., 359

Age of earth, from temperature measurements, 395

Airplane, for gravimeter transport, 42

Airy theory of isostasy, 130

Alabama, 203

Allegheny River, 60

Alternating-current conductive methods, current penetration, 377

Alternating-current measurements, 370

Alternating-current methods, depths reached by, 377

Amarillo Mountains, magnetic survey over, 225

Ambiguity, of gravity interpretation, 120

of magnetic interpretation, 205

Ambronn, Richard, 188, 226, 324, 396, 411

American Askania Corporation, 75, 152, 228

American Institute of Mining and Metallurgical Engineers, 364

Amplification ratio, 326

Amplifier-filter-recorder system, the, 326

Amplitude of current at depth, factors controlling, 378

Analysis of weathering shot data, 299

Anderson system of well surveying, 404

Aneroid barometer for elevation measurements, 55

Anglo Persian Oil Company, 275

Angularity correction, 312, 313

for fiducial time, 313

Anisotropy of electric conductivity, 408

"Anomaly" field of the earth, 168

Apparatus, seismic, 316

Apparent velocity, variation of, with dip, 268

Applications of electric well logging, 389

Arc shooting, 275

Artificial current methods, 366

Askania, 179, 193

Askania gravimeter, 30

Askania Werke, 177

Athy, L. F., 101, 151, 221, 226

Auxiliary function for calculating delay time, 263

Avers, Henry G., 97, 152

B

Bardeen, John, 412

Barrett, William M., 204, 219, 227, 228

Barsch, O., 40, 153

Bartels, J., 168, 226

Barton, Donald C., 97, 101, 116, 127, 128, 150, 153, 271, 279, 358, 421

Barton and White, 37, 39

Basement magnetization, 222

Bates, Fred W., 413

Belluigi, A., 410, 413

Berroth, A., 43, 150

Bibliography, electrical and miscellaneous methods, 411

gravitational methods, 149